THE UNIVERSITY OF HULL

Development a Portable System for Monitoring Chemicals Pollutants in Environmental River Water Samples

being a Thesis submitted for the Degree of Doctor of Philosophy in the University of Hull

by

Zeid Osama Oiaidha

BSc (King Abdulaziz University)

MSc (Loughborough University)

August 2016

Abstract

Environmental pollution has become a serious problem around the world that influences all living organisms directly and indirectly. The growing world population is accompanied by developments in several fields including industry, agriculture and technology. All of this leads to increase in the rate of pollution of air, soil and water and these needs to be monitored. The detection of pollutants in the environmental sample is challenging due to the complex sample matrix and often trace level concentration of the analytes. Currently, the analysis is commonly carried out by high-cost sophisticated instrumentation and therefore the development of portable systems capable of detecting chemical pollutants in environmental samples with high selectivity and sensitivity has become urgent. This work aimed to develop a microfluidic system that combined pre – concentration and detection of a mixture of organic pollutants in river water sample.

The pre – concentration step utilised solid phase extraction (SPE), in which a modified silica monolith column by octadecyl carbon chain (C_{18}) acted as the sorbent. The silica monolith was selected due to its bimodal structure that offered high surface area while ensuring a low backpressure when liquids were pumped into it. In addition, the silica surface could be easily modified, with a suitable functional group such as (C_{18}) that increase the interaction between the analytes and sorbent surface. In addition, the silica monolith offered high stability with several organic solvents.

In this work the silica monolith was modified by octadecyl silane C_{18} (reverse- phase) to pre – concentrate the mixture of organic compounds involved (progesterone, estradiol and benzo (a) pyrene) from river water samples. The pre - concentration process of the mixture of analytes were determined in river water sample with HPLC-UV detection where the concentration of the sample (100 mL) at loading step was 1 µg mL^{-1} and after complete the elution step (1 mL) the concentration of analytes were jumped to 51, 62 and

60 µg mL^{-1} for estradiol, progesterone and benzo (a) pyrene respectively. The effective of extraction and pre – concentration process of organic pollutants from river water sample is improved the limit of detection (LOD) and avoided of interference of the detection method.

To achieve high selectivity, an immunoassay was evaluated with both electrochemistry and chemiluminescence detection. These detection methods were selected due to their high sensitivity, selectivity and the simple instrumentation required. A heterogeneous assay was carried out with an antibody that was modified with a ferrocenecarboxaldehyde tag. The antibody was immobilised onto an indium tin oxide (ITO) electrode using electrochemistry through a phenylamine group on the ITO electrode surface. A fast and sensitive multiplexed detection method was developed with square wave voltammetry (SWV) with limits of detection (LOD) of 28.74, 68.53 and 60.48 pg mL^{-1} for progesterone, estradiol and benzo (a) pyrene respectively in river water matrix. With luminol chemiluminescence detection the LODs values were decreased, where this technique achieved LOD at 20.5, 12.95 and 13.97 pg mL^{-1} for progesterone, estradiol and benzo (a) pyrene respectively also in river water matrix.

Two different designs of microfluidic system device were then fabricated with the aim of combining all the steps in one device, Cyclic olefin copolymer (COC) polymer was used to make the first design, while the second design was made from glass.

Acknowledgements

First and foremost I would like to express my profound thanks to Almighty Allah and his greatest prophet Muhammad peace be upon him, for giving me the strength, patience, inspiration and opportunity during every moment in all my life.

Secondly, I would like to express my deepest gratitude to my supervisor Professor Gillian Greenway for her marvellous support, patience and motivation throughout my PhD period. I could not think this work would be done without her encouragement and vast knowledge. I was astonishingly fortunate to have her as a supervisor to guide me throughout my research. Besides my supervisor, I would like to thank other supervisors who contributed to this thesis. I am deeply grateful to Professor Nicole Pamme for her valuable practical advice and helped to overcome the challenges faced in my projects. I also would like to thank Dr Jay Wadhawan for his advice and constructive comments on the electrochemical experimental work through the period I worked with him.

Also, my thanks to Dr Nathan Brown, Dr Mohammed Nasr Esfahani and Dr Alex Iles for microfluidic device manufacture, and Mr Tony Sinclair for SEM images of the monolith. In addition, much appreciation goes to my friends who became part of this PhD experience and spent a lot of time listening and sharing both the happiness and sadness; thank you.

Finally, I would like to mention an important person in my life who has passed away in my second year of my PhD; is my father, Osama. He inspired me since I was a child to seek knowledge and respect what I learn. He was always with me in every moment of my life. I would also like to thank the second important person in my life my Mother Samira, which was the first teacher for me in this life. In addition, I want to thank her for all her support and patient while I am away from her and all my life. Thanks also go to my lovely

children Osama, Aus and Nasser for their patience when I am away from them and I have not had enough time with them. Last, but not least, I would like to express my immense thank to my amazing wife Nedaa for her encouragement and brightening my life in the last eleven years. This thesis would not have been possible without her standing by me. She provided me through my life with love, inspiration, motivation and optimism. I could not thank her enough and find any words to describe her supports through my life.

Abbreviation

APTMS	3-aminopropyl-trimthoxysilane
BET	Brunauer-Emmett-Teller
C_{18}	Octadecyl carbon chain
CDMOS	chlorodimethyl octadecyl silane
CL	Chemiluminescence
COC	cyclic olefin copolymer
CV	Cyclic voltammetry
EDC	endocrine-disrupting compound
EDC	N-(3-dimethylaminopropyl)-N-ethylcarbodiimide hydrochloride
EDX	Energy dispersive X-ray spectroscopy
ELISA	Enzyme-linked immunosorbent assays
Fc-CHO	Ferrocenecarboxaldehyde
g	Gram
GC-FID	Gas chromatography – Flame ionisation detector
GC-MS	Gas chromatography – Mass spectrometry
GPTMS	3-glycidyloxypropyl-trimethoxysilane
HCl	Hydrochloric acid
HETP	Height equivalent to theoretical plate
HPLC	High performance liquid chromatography

HRP	Horseradish peroxidase
ITO	Indium tin oxide
LLE	Liquid – liquid extraction
LLOQ	Lower limit of quantification
LOD	Limit of detection
µm	Micrometre
m	Meter
M	Molar
µTAS	Micro total analytical system
min	Minute
ml	Millilitres
N_2	Nitrogen gas
NaOH	Sodium hydroxide
NHS	N-Hydroxysulfosuccinimide
nm	Nanometre
PBS	Phosphate buffered saline
pg	Picogram
PDMS	Polydimethylsiloxane
PEEK	polyetheretherketone

PMMA	Polymethyl methacrylate
ppm	Part per million
R^2	Correlation of determination
RLU	Relative light unit
RSD	Relative standard deviation
SEM	Scanning electron microscopy
SPE	Solid-phase extraction
SSHs	Steroid sex hormones
SWV	Square wave voltammetry
STD	Standard deviation
Sulfo-NHS	N-hydroxysulfosuccinimide sodium
TEOS	Tetraethyl orthosilicate
THF	Tetrahydrofuran
TMOS	Tetramethyl orthosilicate
UV	Ultraviolet
UV-Vis	Ultraviolet-visible spectroscopy
λ	Wavelength
^oC	Degree Celsius

Table of contents

ABSTRACT I

ACKNOWLEDGEMENTS III

ABBREVIATION V

TABLE OF CONTENTS VIII

LIST OF FIGURES XII

LIST OF TABLES XX

CHAPTER 1. INTRODUCTION 1

1.1 ENVIRONMENT POLLUTION 1
1.1.1 AIR POLLUTION 1
1.1.2 SOIL POLLUTION 2
1.1.3 WATER POLLUTION 3
1.1.4 CHEMICAL POLLUTANTS 4
1.1.5 ANALYSIS OF CHEMICAL POLLUTANTS 9
1.2 SAMPLE PREPARATION 10
1.2.1 LIQUID – LIQUID EXTRACTION (LLE) 11
1.2.2 SOLID PHASE EXTRACTION (SPE) 13
1.3 SPE SORBENT 18
1.3.1 PARTICULATE MATERIALS AS SORBENT 19
1.3.2 MONOLITHIC MATERIALS AS SORBENTS 20
1.4 ORGANIC POLYMER MONOLITHIC 22
1.4.1 FABRICATION OF THE ORGANIC POLYMER MONOLITH 23
1.5 INORGANIC SILICA MONOLITHIC 24
1.5.1 FABRICATION OF THE INORGANIC SILICA MONOLITH 25
1.5.2 DRYING AND CALCINATION 31
1.6 COMPARISON BETWEEN THE POLYMER MONOLITH AND SILICA MONOLITH 31
1.7 MODIFICATION OF THE MONOLITHIC SILICA SURFACE WITH A FUNCTIONAL GROUP. 33
1.8 CHARACTERISATION OF MODIFYING STATIONARY PHASE 34
1.8.1 NITROGEN PHYSISORPTION METHOD 35
1.8.2 SCANNING ELECTRON MICROSCOPY - ENERGY DISPERSIVE X-RAY SPECTROSCOPY (SEM – EDX) 37
1.8.3 EXTRACTION PERFORMANCE 37
1.9 DETECTING OF ORGANIC POLLUTANTS IN THE ENVIRONMENTAL WATER SAMPLE. 39
1.10 ANTIBODIES AND IMMUNOASSAY DETECTION 40
1.10.1 ANTIBODIES 40
1.10.2 MONOCLONAL AND POLYCLONAL ANTIBODIES 41
1.11 IMMUNOASSAY 42
1.11.1 HOMOGENEOUS IMMUNOASSAY 43
1.11.2 HETEROGENEOUS IMMUNOASSAY 43
1.11.3 COMPETITIVE AND NON – COMPETITIVE IMMUNOASSAY 44

1.11.4 Detection methods used immunoassay system 47
1.11.5 Immobilization the antibody onto solid support surface 49
1.11.6 Plastic substrates for antibody immobilisation 49
1.11.7 Glass substrates for antibody immobilisation 52
1.11.8 Other types of substrate used for antibody immobilisation 56
1.11.9 Antibody modification 58
1.12 Microfluidics 60
1.12.1 Microfabrication 61
1.12.2 On-chip fluid manipulation 63
1.13 Microfluidic device for environmental analysis 65
1.13.1 Spectroscopic detection 67
1.13.2 Luminescence detection 68
1.13.3 Electrochemistry 78
1.14 Aim of PhD 84

CHAPTER 2. EXPERIMENTAL 86

2.1 Reagents 86
2.2 Equipment 89
2.3 Instruments 90
2.4 Fabrication of silica monolithic rod 90
2.4.1 Preparation of silica monolithic rod for a flow system 92
2.4.2 Surface modification of silica monolithic rod with C18 93
2.5 Monolithic materials characterisation 93
2.5.1 SEM analysis 93
2.5.2 Brunauer-Emmett-Teller (BET) analysis 93
2.5.3 EDX analysis 94
2.6 Evaluation of extraction of silica monolith modified surface 94
2.6.1 Preliminary experiment to pre - concentrate the organic pollutants from the C18 silica monolith 94
2.6.2 HPLC method for characterisation of silica monolith 96
2.6.3 Evaluation of the ability of both types of silica monolith rods to pre – concentrate. 97
2.6.4 Progesterone pre – concentration 97
2.6.5 Organic pollutants extraction and pre – concentration 98
2.6.6 Optimisation of the HPLC 99
2.6.7 Organic pollutants pre – concentration 100
2.6.8 Analytical figures of merit 100
2.7 Detection of organic pollutants 102
2.7.1 Optimisation of chemiluminescence reagent 102
2.7.2 Chemical silanisation of solid support surface 104
2.7.3 Antibody immobilisation on the silanised glass surface. 105
2.7.4 Characterisation of antibody immobilisation 105
2.7.5 Electrochemistry detection. 107
2.7.6 Modification of the solid support surface by electrochemistry. 107
2.7.7 Labelling and immobilisation of the antibodies with ferrocene carboxaldehyde. 110
2.7.8 Evaluation of the electrochemical method for antibody immobilisation. 111
2.7.9 Oxidisation of antibody ferrocene tag (Ab – Fc) onto the surface. 111
2.7.10 Optimisation of incubation time for antibody - antigen reaction 112
2.7.11 Evaluation of interferences effects on organic pollutant detection 112

2.7.12 Evaluation of the stability of ferrocene tags 113
2.7.13 Effect of the analyte concentration on the CL emission signal 114
2.7.14 Preparation of calibration curve for analytes 114
2.8 Microfluidic chip fabrication 115
2.8.1 Polymer chip fabrication 115
2.8.2 Glass microfluidic fabrication 118
2.9 Conclusion 123

CHAPTER 3. DEVELOPMENT OF SILICA MONOLITH FOR SAMPLE PREPARATION 125

3.1 Fabrication of silica monolith 125
3.1.1 Hydrothermal treatment of the silica monolith by ammonia 127
3.1.2 Comparison between TMOS and TEOS 129
3.1.3 Impact of the porogen size on the synthesis of the silica monolith 130
3.2 Modification of the silica monolith by C18 132
3.2.1 EDX analysis 136
3.3 Solid phase extraction 137
3.3.1 Preliminary experiment to pre – concentrate the organic pollutants 137
3.3.2 Compare the extraction efficiency between TMOS and TEOS 141
3.3.3 Optimising the flow rate 143
3.4 Pre – concentration of the analytes 145
3.4.1 Figure of merit for the progesterone calibration curve 145
3.4.2 Pre – contraction of the progesterone 146
3.4.3 Pre – concentration of the progesterone from river water sample 148
3.5 Multi - analyte extraction and pre – concentration 150
3.5.1 Optimisation of HPLC 150
3.5.2 Figure of merit for calibration curves of estradiol, progesterone and benzo (a) pyrene. 154
3.5.3 Pre – concentrate the mixture of organic pollutants 156
3.5.4 Pre – concentrate mixture of non – polar organic pollutants from river water 159
3.6 Conclusion 162

CHAPTER 4. ANTIBODY IMMOBILISATION 163

4.1 Chemiluminescence immunoassay detection 164
4.1.1 Optimisation the reagent of chemiluminescence reaction 164
4.1.2 Optimisation of HRP concentration 164
4.1.3 Optimisation of luminol concentration 165
4.1.4 Optimisation of hydrogen peroxide concentration 166
4.2 Chemical silanisation of glass surface 167
4.2.1 Assessment of surface modification using contact angle measurements 168
4.2.2 Evaluation of success of the chemical immobilisation of antibody by chemiluminescence 171
4.3 Electro method for modification the ITO electrode 176
4.3.1 Labelling the antibody with ferrocenecarboxaldehyde (Fc – CHO) 177
4.3.2 Modification of the ITO electrode 178
4.3.3 Immobilisation of antibody labelled with ferrocene onto ITO electrode 181
4.4 Characterisation of the antibody immobilised onto the ITO electrode surface 182
4.4.1 Effect of the different concentration of the analyte on the labelled antibody 184

4.4.2 Optimisation of the incubation time 186
4.4.3 Figure of merit for calibration curves of estradiol, progesterone and benzo (a) pyrene by SWV. 188
4.4.4 Determination of interference of analytes by square wave voltammetry 190
4.5 Conclusion 193

CHAPTER 5. ORGANIC POLLUTANTS DETECTION 194

5.1 Oxidation of labelled ferrocene on the antibody 194
5.1.1 Evaluated the stability of ferrocene tags 198
5.1.2 Chemiluminescence detection of analytes 199
5.1.3 Optimise the incubation time of antibody antigen interaction 200
5.1.4 Optimisation the exposure time 202
5.1.5 Interference studies for the analyte 203
5.2 Calibration curve for each analyte by chemiluminescence immunoassay technique. 205
5.3 Development of pre – concentrate the analytes from a river water sample followed by CL immunoassay 207
5.4 Environmental pollutants analysis in chip 210
5.4.1 Polymer chip 210
5.4.2 Glass chip 214
5.5 Conclusion 217

CHAPTER 6. CONCLUSION AND FUTURE WORK 218

6.1 Development of the silica monolith for chemical pollutants extraction and pre – concentration. 218
6.2 Chemical pollutants extraction and pre – concentration 219
6.3 Method of immobilisation of the antibody 220
6.4 Detection of chemical pollutants from environmental water sample 221
6.5 Combine the pre – concentration method with detection of the chemical pollutants of river water. 222
6.6 Microfluidic device and future work 222

CHAPTER 7. REFERENCES 224

List of figures

Figure 1-1: Diagram of chemicals pollutions types. 5
Figure 1-2: Liquid – liquid extraction process using a separation funnel, (A) before extraction where 100 % of analyte in the aqueous layer, (B) after extraction most of the analyte moved to organic solvent layer. 12
Figure 1-3: The main step of solid phase extraction involve (conditioning, loading, washing and elution). 15
Figure 1-4: Interaction between polar analyte (phenylamine) and polar sorbent silica via hydrogen bond [48]. 16
Figure 1-5: Interaction between non – polar analyte and non – polar sorbent bonded silica via Van der Waals forces [48]. 17
Figure 1-6: Ion exchange interaction, (A) strong cation exchange sorbent, (B) strong anion exchange sorbent [48] 18
Figure 1-7: Scanning electron image of the (A) packed particles column and (B) monolithic column [54]. 21
Figure 1-8: Schemes reaction of hydrolysis and condensation reaction in sol-gel process [77b]. 28
Figure 1-9: Scanning electron microscope electron image of (A) silica monolith made with 100 % of 10,000 MW PEO, (B) silica monolith made with 50 % of 10,000 MW PEO with 50 % of 100,000 MW PEO and (C) Silica monolith made with 100,000 MW PEO [84] 30
Figure 1-10: Scanning electron microscope image show the difference in morphological structure between (A) silica monolithic and (B) polymer monolithic 33
Figure 1-11: Six different shapes of sorption isotherm as IUPAC classified types (I – VI) [102]. 37
Figure 1-12: Antibody structure [114] 42
Figure 1-13: Heterogeneous non – competitive immunoassay [127] 46
Figure 1-14: Heterogeneous competitive immunoassay [127] 47
Figure 1-15: The ways of immobilisation the antibodies onto the solid support surface, (A) random orientation and (B) ideal orientation. 59
Figure 1-16: the process the fabrication of a glass microfluidic device. 63
Figure 1-17 movement of the solution inside the microfluidic channel,(A) a pressure flow of the solution movements in the centre of a channel and (B) the plug

flow where the same velocity is exhibited for all molecules except for those very close to the internal surface wall when an electrical field is applied [184]. 66
Figure 1-18: Diagram of the chip that use in the experiment [189].....67
Figure 1-19: Beaton et al. LOC system for in suit analysis of nitrate and nitrite in natural water [191]. 68
Figure 1-20: Jablonski diagram to explain the luminescence process [194] 70
Figure 1-21: The two types of chemiluminescence reaction (direct and indirect reaction) [196]. 73
Figure 1-22: Mechanism for the chemiluminescent reaction of luminol with hydrogen peroxide [197]. 75
Figure 1-23: Operation of a CCD based on a 2 x 2 pixel chip, where the yellow circles represent photoelectrons that are stored within the pixels [197]. 77
Figure 1-24: cyclic voltammetry waveform[212].....80
Figure 1-25: Example of reversible cyclic voltammotogrm, Where E_{pc} = peak cathodic potential; i_{pc} = peak cathodic current; E_{pa}= peak anodic potential, and i_{pa}=peak anodic current [213].....81
Figure 1-26: Diagram of the square wave waveform where a staircase waveform and square wave waveform are combined to show the overall square wave voltammetric waveform [217]. 83
Figure 2-1: Silica monolith rods sealed in heat shrinkable tube with borosilicate tube for connection. 92
Figure 2-2: CCD image of two Eppendorf tubes with chemiluminescence reagents where the (A) is the blank (PBS + 20 mM of mixture luminol + H_2O_2, (B) is a sample well included HRP + 20 mM (luminol + H_2O_2).....102
Figure 2-3: An array biochip array holder (RANDOX), which enable of multiple detections on glass slides and plastic slides, cell holder was aligned under the CCD camera inside the box for CL detection. 106
Figure 2-4: Schematic showing the general experimental set up for the chemiluminescence detection.....106
Figure 2-5: The ITO electrode used in electrochemistry modification.....107
Figure 2-6: Set up of the electrochemical cell with, three electrodes dipping into an aqueous ethanol solution 108
Figure 2-7: A scheme of polymer microfluidic device fabrication.....114
Figure 2-8: Dimensions of the top and bottom layers of the polymer chip 115

Figure 2-9: Assembly of the polymer microfluidic parts.....116
Figure 2-10: COC polymer microfluidic device with the ITO electrode and tubing....116
Figure 2-11: Schematic showing the experimental set up for the microfluidic device with the chemiluminescence detection.....117
Figure 2-12: Dimensions of the top and bottom layers of the glass chip.....118
Figure 2-13: The top and bottom layer of the glass chip 119
Figure 2-14: Assembly of the top and bottom layers of glass chip.....120
Figure 2-15: Redesign of the ITO glass electrode 120
Figure 2-16: The design of top and bottom layer of clamps.....121
Figure 2-17: Glass chip with ITO electrode.....122
Figure 3-1: Image of white and crack-free silica monolithic rods prepared by using the sol gel method. 124
Figure 3-2: SEM images of the Internal structure of silica monolith rods consisting of TMOS + PEO (200K) + 1 M Acetic acid(A) before 1 M NH_4OH treatment, (B) after 1 M NH_4OH treatment.....125
Figure 3-3: BET isotherm curves for TMOS monolithic silica. Isotherm (A) is for TMOS monolithic silica before hydrothermal treatment, and isotherm (B) is for TMOS monolithic silica after hydrothermal treatment. 126
Figure 3-4: SEM image of (A & B) TEOS , (C & D) TMOS the scale bar for (A & C) are 10 µm with low magnification and the scale bar for (B & D) are 1 µm with high magnification. 128
Figure 3-5: Formation of octadecyl – silica (C18 – silica) on the silica monolith surface. 131
Figure 3-6: SEM image for TMOS, (A) shows the internal structure of non-modified monolith and (B) shows the internal structure of C18 modified monolith. 132
Figure 3-7: EDX spectra for non – modified TMOS silica monolith 134
Figure 3-8: EDX spectra for modified TMOS silica monolith 134
Figure 3-9: UV – Vis spectra scan of 10 µg ml^{-1} of progesterone. 135
Figure 3-10: Calibration curve for progesterone with use UV – Vis spectrophotometer at 250 nm, (n = 3). The error bar indicates one standard deviation. 136
Figure 3-11: pre -concentration of the progesterone sample (1 µg ml^{-1}) using methanol and acetonitrile for elution step, (n = 3). The error bar indicates one standard deviation. 137
Figure 3-12: HPLC chromatogram of extraction of the target analyte by the C18 TMOS modified column, where (A) standard solution of progesterone (10 µg mL^{-1})

was directly inject in the HPLC system, (B) Loading fraction, (C) washing fraction and (D) elution fraction. 139
Figure 3-13: The extraction efficiency of progesterone using C18 modified column (TMOS & TEOS), (n = 3). The error bar indicates one standard deviation. 140
Figure 3-14: Effect of the flow rate on the extraction efficiency of 10 µg mL^{-1} of progesterone by TMOS and TEOS C18 modified monolith (n=3). The error bar indicates one standard deviation. 141
Figure 3-15: Calibration curve of progesterone standard solutions with peak area plotted against concentration (µg mL^{-1}), (n = 3). The error bar indicates one standard deviation. 143
Figure 3-16: HPLC chromatogram of pre - concentrate the target analyte by C18 - TMOS modified column, where (A) Loading fraction, (B) elution fraction. 144
Figure 3-17: The pre-concentrated profile for progesterone, (n=3). The error bar indicates one standard deviation. 145
Figure 3-18: HPLC chromatogram of pre - concentrate the target analyte in river water sample by C18 TMOS modified column, where (A) Loading fraction, (B) elution fraction. 146
Figure 3-19: The pre-concentrated profile for progesterone from river water sample. (n=3). The error bar indicates one standard deviation. 147
Figure 3-20: HPLC chromatogram for mixture of (benzo (a) pyrene, progesterone, β-estradiol with mobile phase composition (acetonitrile: water, 75, 25) to optimise the absorbance wavelength where, (A) shows the chromatogram of the organic compounds mixture at 250 nm, (B) shows the HPLC chromatogram of mixture at 240 nm, (C) present the HPLC chromatogram of mixture at 230 nm and (D) shows the HPLC chromatogram of mixture at 230 nm. 148
Figure 3-21: HPLC chromatogram for the mixture (benzo (a) pyrene, progesterone and β-estradiol with mobile phase composition (acetonitrile: water, 80, 20) at 230 nm. 150
Figure 3-22: Calibration curve of the estradiol (orange line), progesterone (blue line) and benzo (a) pyrene (grey line) standard solution with peak area plotted against their concentration, (n = 3). The error bar indicate one standard deviation. 152

Figure 3-23: HPLC chromatogram of pre – concentrate standard mixture of organic pollutant through TMOS – C18 modified column where, (A) shows the standard of mixture (1 µg mL^{-1}, (B) shows the chromatogram of loading fraction, (C) shows the chromatogram of the washing fraction and (D) represent the chromatogram of the elution fraction. 154
Figure 3-24: The pre – concentration efficiency of 1 µg mL^{-1} of estradiol, progesterone and benzo (a) pyrene using TMOS C18 modified column. The average recovery was obtained from three consecutive experiment, (n = 3). The error bar indicates one standard deviation. 155
Figure 3-25: HPLC chromatogram of pre – concentrate river water sample spiked with estradiol, progesterone and benzo (a) pyrene at (1 µg mL^{-1}) by using TMOS – C18 modified column where, (A) shows the river water sample before pre – concentration process, (B) shows the chromatogram of loading fraction, (C) shows the chromatogram of the washing fraction and (D) represent the chromatogram of the elution fraction. 157
Figure 3-26: The pre – concentration efficiency of river water sample spiked with 1 µg mL^{-1} of estradiol, progesterone and benzo (a) pyrene using TMOS C18 modified column. The average recovery was obtained from three consecutive experiment and the error bar indicates one standard deviation. 158
Figure 4-1: Effects of the changing progesterone - HRP concentration on the CL emission intensity, (n = 3). The error bar indicates one standard deviation 162
Figure 4-2 Effect of the luminol concentration on the signal intensity of CL detection, (n = 3). The error bar indicates one standard deviation 163
Figure 4-3: Effects of the H_2O_2 concentration on the signal intensity of CL detection, (n = 3). The error bar indicates one standard deviation 164
Figure 4-4: Process of silanisation of glass support surface [151]. 165
Figure 4-5: Contact angle measurement for variousconcentration of APTES and GPTMS, (n = 3). The error bar indicates one standard deviation 166
Figure 4-6: Photographs of water droplet at various interaction times for silanisation process where, (A) shows the contact angle of pure glass, (B) 30 min of silanisation process, (C) 60 min of silanisation process, (D) 90 min silanisation process and (E) 120 min silanisation process. 167
Figure 4-7: Effect of the time interaction between the glass slide and APTES on the contact angle measurement, (n = 3). The error bar indicates one standard deviation 168

Figure 4-8: Mechanism of immobilisation of the antibody on the APTES modified glass surface by using activation buffer of EDC and sulfo – NHS. 169
Figure 4-9: Two examples of a CCD image of the CL emission signal emitting from progesterone - HRP attached to an immobilised antibody on the surface of microscope slides (0.8 × 0.8 cm). The glass surface was chemically modified using APTES, the scale bar 0.5 cm. 170
Figure 4-10: Two examples of a CCD image of CL signal emitting from progesterone - HRP attached to an immobilised antibody on the surface of microscope slides (0.8 × 0.8 cm). The glass surface was chemically modified using APTES, where the red circle line showed place of the antibodies were spotted and they found to be spread over the surface, the scale bar 0.5 cm. 171
Figure 4-11: Two examples of a CCD image of CL signal emitting from progesterone - HRP attached to an immobilised antibody on the surface of microscope slides (0.8 × 0.8 cm). The glass surface was chemically modified using GPTES, where the red circle line showed place of the antibodies were spotted and the antibodies were found to be spread over the surface, the scale bar 0.5 cm. 172
Figure 4-12: Theoretical concept for the electrochemical protocol for antibody immobilisation the arrows are representative of the transfer of an electron through a molecular wire [227]. 174
Figure 4-13: Reaction schemes for labelling of antibody with Fc-CHO [228] 175
Figure 4-14: Schematic of the modification process of the ITO electrode. 176
Figure 4-15: Cyclic voltogramm of the reduction process of the nitrobenzene diazonium onto the ITO electrode surface in the degassed solution of 4-nitrobenzenediazonium and TBAP in acetonitrile. The cyclic voltammetry started at +0.7 V scanning down to -0.4 V and with a return sweep to +0.7 V performed over four scans with a scan rate of 10 mV s^{-1} at room temperature. 177
Figure 4-16: Reduction of nitrobenzene on the ITO electrode in degassed 0.1 M KCl-ethanol (90:10, v: v) by cyclic voltammetry. The peak potential is at -1.0 V and scan rate 0.1 V s^{-1} at room temperature. 178
Figure 4-17: Electrochemical oxidation and reduction mechanism of nitrobenzene at the modified ITO electrode [231]. 179

Figure 4-18: The reaction of immobilisation of labelled antibody (Ab – Fc) onto ITO electrode surface.....180
Figure 4-19: Cyclic voltammograms of blank ITO electrode surface and ITO electrode surface in percent of labelled antibody. The san rate was 100 mV s^{-1}, and all the scan carried out in 10 mM of PBS at pH 7.5.....181
Figure 4-20: Cyclic voltammograms of labelled antibody on the ITO electrode surface with scan rates from 10 mV s^{-1} rising to 1000 mV s^{-1}. 182
Figure 4-21: Cyclic voltammogram of (A) ITO electrode with labelled anti – progesterone used as blank, (B) ITO electrode with labelled anti – progesterone after adding progesterone. The scan rate was 100 mV s^{-1} and all scan carried out in PBS buffer at pH 7.5.....183
Figure 4-22: Cyclic voltammograms for different concentration of progesterone. The scan rate was 100 mV s^{-1} and all scan carried out in the PBS buffer at pH 7.5.....184
Figure 4-23: Square wave voltammograms of labelled anti – progesterone of blank and after added progesterone 100 pg mL^{-1}at various incubation time. Frequency 25 Hz, amplitude 1 mV, all scan carried out in the PBS buffer at pH 7.5. .185
Figure 4-24: Square wave voltammograms for different concentration of progesterone, frequency 25 Hz, amplitude 1 mV all scan carried out in the PBS buffer at pH 7.5.....186
Figure 4-25: Calibration curve of the estradiol (blue line), progesterone (orange line) and benzo (a) pyrene (grey line) standard solution with Δ peak current plotted against their concentration, (n = 3). The error bar indicates one standard deviation. 187
Figure 4-26: Square wave voltammogram of labelled anti – benzo (a) pyrene, where the blue line present is the blank and the orange line present with mixture Frequency 25 Hz, amplitude 1 mV, all scan carried out in the PBS buffer at pH 7.5.....189
Figure 4-27: Square wave voltammogram of labelled anti – estradiol, where the blue line present is the blank and the orange line present with mixture Frequency 25 Hz, amplitude 1 mV, all scan carried out in the PBS buffer at pH 7.5. .189
Figure 4-28: Square wave voltammogram of labelled anti – progesterone, where the blue line present is the blank and the orange line present with mixture Frequency 25 Hz, amplitude 1 mV, all scan carried out in the PBS buffer at pH 7.5.....190

Figure 5-1: cyclic voltammogram of ferrocene labelled of antibody oxidisation at the scan rate of 10 mV s^{-1} 193
Figure 5-2: Oxidation process of the ferrocene labelled of antibody. 194
Figure 5-3: (A) the ITO electrode prepared with copper foil and separate for three places by circle adhesive tape for immobilisation the labelled antibody, (B) image of chemiluminescence emission light from the places of immobilised anti – progesterone upon addition of luminol and H_2O_2. 195
Figure 5-4: chemiluminescence image for anti – progesterone, where (A) represent the ferrocene molecule labelled antibody, (B) immediate after oxidised the ferrocene, (C) after 1 day of oxidised the ferrocene and (D) after 3 days of oxidised the ferrocene. 197
Figure 5-5: chemiluminescence image for immobilised anti - progesterone onto ITO electrode upon addition of luminol and H_2O_2 (A) blank, (B) 100 ng mL^{-1} of progesterone. 198
Figure 5-6: Example of chemiluminescence image for anti - progesterone and 1 µg mL^{-1} of progesterone reaction at different incubation times at room temperature. 199
Figure 5-7: graph show the influence of the incubation time for anti – progesterone and 1 µg mL^{-1} progesterone interaction on the chemiluminescence intensity (RLU), (n = 3). The error bar indicates one standard deviation. 200
Figure 5-8: Graph of influence of exposure time of the image taken to get the CL emission intensity, (n = 3). The error bar indicates one standard deviation. 201
Figure 5-9: Example of interference study of the effect of 100 ng mL^{-1} progesterone on chemiluminescence signal of three different antibodies, (A) is showed the blank of the ITO electrode where the each spot present different type of antibody, and (B) showed the effected of added the analyte (progesterone 100 ng mL^{-1}) onto three spots. 202
Figure 5-10: Results of CL emission signal for interference investigated for each antibody, where the blue bar present the blank, the orange bar present the effect of progesterone standard, the grey bar show the effect of estradiol standard and the yellow bar present the influence of the benzo (a) pyrene standard. The error bar indicates one standard deviation. 203

Figure 5-11: CL immunoassay calibration curves for benzo (a) pyrene (yellow line), estradiol (blue line) and progesterone (grey line) for concentration ranges from 100 to 0.05 pg mL^{-1}. The error bar indicates one standard deviation. 205
Figure 5-12: chemiluminescence image of (A) blank ITO electrode and (B) the same ITO electrode after addition of the SPE elution fraction. 207
Figure 5-13: The chip was aligned under the CCD camera enclosed in a light-proof box before injecting the reagents. 209
Figure 5-14: Chemiluminescence image upon addition of 20 mM luminol and H_2O_2 for immobilised anti - progesterone on the ITO electrode within the chip. The image was taken under stop –flow conditions. 209
Figure 5-15: chemiluminescence image upon addition of 30 mM luminol and H2O2 for immobilised anti - progesterone on the ITO electrode within the chip. The image was taken under stop - flow conditions. 210
Figure 5-16: Chemiluminescence image upon addition of 30 mM luminol and H_2O_2 for immobilised anti - progesterone on the ITO electrode within the chip. The image was taken under stop – flow conditions. 211
Figure 5-17: chemiluminescence image upon addition of 20 mM luminol and H_2O_2 for three immobilised antibodies on the cut ITO electrode. 212
Figure 5-18: Chemiluminescence image upon addition of 20 mM luminol and H_2O_2 for immobilised three types of antibodies on the reshaped ITO electrode inside the glass chip. The image was taken under stop - flow conditions. 213
Figure 5-19: Chemiluminescence image upon addition of 30 mM luminol and H_2O_2 for immobilised three types of antibodies on the reshaped ITO electrode inside the glass chip. The image was taken under stop - flow conditions. 214
Figure 6-1: The preliminary design of the chip that will use in future work 222

List of tables

Table 1-1: Example of priority pollutants of PAH 6
Table 2-1: Reagents..... 86
Table 2-2: Materials used..... 89
Table 2-3: Instruments 90
Table 2-4: The process to evaluate the ability of TMOS to pre – concentrate the analyte 96
Table 2-5 : Chemical structure of the organic pollutants analytes targets in this study.. 98
Table 3-1: The physical properties of the internal structure of TMOS and TEOS monoliths..... 129
Table 3-2: The physical properties of TMOS silica monolith before and after modification 132
Table 3-3: The retention time and peak area of the triple organic pollutants mixture (estradiol, progesterone and benzo (a) pyrene) 100 µg mL^{-1} that injected directly into the HPLC, (n = 3). 149
Table 3-4: Analytical figure of merit of estradiol, progesterone and benzo (a) pyrene 152
Table 3-5: The concentration of each analytes after pre – concentration process of standard mixture of (estradiol, progesterone and benzo (a) pyrene), (n = 3). 155
Table 3-6: Concentration of each fraction of pre – concentration of river water sample spiked with non – polar organic compounds procedure, (n = 3)..... 158
Table 4-1: Analytical figure of merit of estradiol, progesterone and benzo (a) pyrene 188
Table 5-1: Precision of immobilisation of labelled antibody on the ITO electrode surface. 196
Table 5-2: Result obtained for interference studies for all types of antibodies 203
Table 5-3: Analytical figures of merit for estradiol, progesterone and benzo (a) pyrene by using chemiluminescence immunoassay detection. 205
Table 5-4: The Δ CL emission intensity value and the concentration of three analytes that spiked with river water at concentration 1 pg mL^{-1} and pre – concentrated by using C18 TMOS monolith column 207

Chapter 1. Introduction

1.1 Environment pollution

The human population has dramatically increased around the world in the last decades, which has significantly affected the balance of the natural environment [1]. There are many definitions of environmental pollution, and all of these definitions revolve around the same meaning. One definition widely used to describe pollution was written by Holdgate: "The introduction by man into the environment of substances or energy liable to cause hazards to human health, harm to living resources and ecological system, damage to structure or amenity, or interferences with the legitimate use of the environment" [2]. In this definition, humans play a significant role in the changing of the ecosystem because it is a comparatively recent improvement in the planet's history. In the 19th century, the Industrial revolution began, and industrialisation spread around the globe; pollution has spread with it. Examples of human activity are present in the percentage change of the concentration of the atmospheric greenhouse gas, carbon dioxide, and in the percentage of fresh water used [3].

The environmental pollution issue has become a dangerous problem that directly affects all organisms and ecosystems in the world. The impact of pollution on the ecosystem includes all sources that the natural world gives to people, such as food (crops and water purification) and the climate, including temperature and precipitation [4]. There are three main types of environmental pollution: water pollution, soil pollution and air pollution.

1.1.1 Air pollution

Air pollution occurs when the gases, dust, fumes or odours that are in the air in harmful amounts directly affect organism's health. According to the National Ambient Air Quality Standards (NAAQS), there are six types of air pollutants [5]. The chemical reaction

between nitrogen oxides in sunlight and volatile organic compound (VOC) influence on the ground-level ozone that is an air pollutant. VOC and nitrogen oxides are emitted from factories, motor vehicle exhausts and chemical solvents. Breathing this ozone can lead to respiratory problems, especially in children and the elderly [6]. The second air pollutant is carbon monoxide (CO), which is a colourless, odourless gas produced as a result of combustion processes. CO is harmful, reducing the delivery process of oxygen to the body's organs; high concentrations can cause death [7]. Sulphur dioxide (SO_2) is an air pollutant from fossil fuel combustion emission and nitrogen dioxide (NO_2 is a pollutant emitted from the burning fuel of cars, trucks and buses. These are highly reactive gases and are the primary causes of acid rain [8]. Also, these gases react with soil or dust particles, metals and organic chemicals to form particulate matter, which is an air pollutant because it can affect hearts and lungs if inhaled [6]. The final source of air pollution is lead, which was previously used in vehicle gasoline; however, now its primary source is aircraft operating with leaded aviation gasoline [6].

1.1.2 Soil pollution

The soil is a key component of the earth, influencing all organisms. Soil pollution occurs when toxic chemicals (organic or inorganic) are in the soil at levels that affect organisms [9]. The main cause of soil pollution is a human activity that directly affects the land, such as industrial expansion, especially mining. If the products of this industry are not disposed of safely, the soil surface becomes unsafe in the long term. Another source of soil pollution is the expanding agriculture activities needed to supply enough food for people. Various pesticides, chemicals and fertilisers have been used so much they have become part of the soil and have negatively influenced people's health. Oil leaks are considered sources of soil pollution. Leaks can happen during the storage or transport of chemicals. These leaks can also affect groundwater [10].

1.1.3 Water pollution

The earth's surface is covered by over two - thirds of water. Increased population has put more pressure on water sources [11]. Human activity in the seas, oceans, rivers and other inland waters have reduced the water sources and have affected water quality [12]. Water pollution occurs when one or more substances build up in the water and cause problems for organisms. There are two types of water on the earth: surface water and groundwater. Surface water comprises around 95.5 % of all the water on the earth; it includes oceans, seas, rivers and lakes. Groundwater comprises around 4.5% of the earth's water. Drinkable water is no more than 3.5% of the total amount of water [13].

1.1.3.1 Source of water pollution

Water pollution has many different causes, which makes it difficult to control. Water pollution sources can be classfied into two types: indirect sources and direct sources [14].

1.1.3.2 Indirect source

Indirect sources involve all of the pollution sources that affect the environment vicariously; this includes urban development. When a population grows, the demand for housing grows, which means increase and expanded in number of cities and towns. This results in growths in construction activities, additional landfills for more garbage, inappropriate sewer collection and treatment, and a increase in chemicals production from industries. Also, global warming is an indirect source of water pollution, increasing the water temperature; this leads to the deaths of marine organisms. During rain, landfills might leak and cause groundwater pollution. Rain can also propel animal waste to rivers and lakes [14-15].

1.1.3.3 Direct source

Direct sources of water pollution are similar to the sources that cause air and soil pollutions. Industrial waste usually contains many organic and inorganic compounds, and, in some places in the world, this waste goes directly to the surface water. The same process occurs with sewage and wastewater, which are often treated in sewage treatment plants; the product of this process goes into the surface water. Another source causing surface water pollution is burning fossil fuel as coal and oil. The ash, which contains highly toxic chemicals, may end up in the water. A large amount of pesticides, chemicals and fertilisers (mentioned in 1.1.2) affect the surface water, especially lakes and rivers [16]. Mining is a source of pollution because it uses harmful chemicals that end up in the groundwater. Also, leaks from sewer lines affect the groundwater [15].

Water pollution can be categorised into different types. One type is biological water pollution, which can occur naturally or by human activity. This occurs when the water is contaminated with various kinds of bacteria, viruses and parasites, such as Escherichia coli **(**E. coli) and typhoid. Another type of water pollution is oxygen depletion, which is decreased oxygen levels in the water. However, the primary cause of water pollution is a result of chemical compounds (organic or inorganic)[17].

1.1.4 Chemical pollutants

Chemical pollution happens when natural chemicals or synthetic chemicals are reachs to toxic levels in the environment, threatening human health, degrading ecosystem functions and decreasing wildlife numbers [18]. The chemical pollutants can be divided as shown in Figure 1-1.

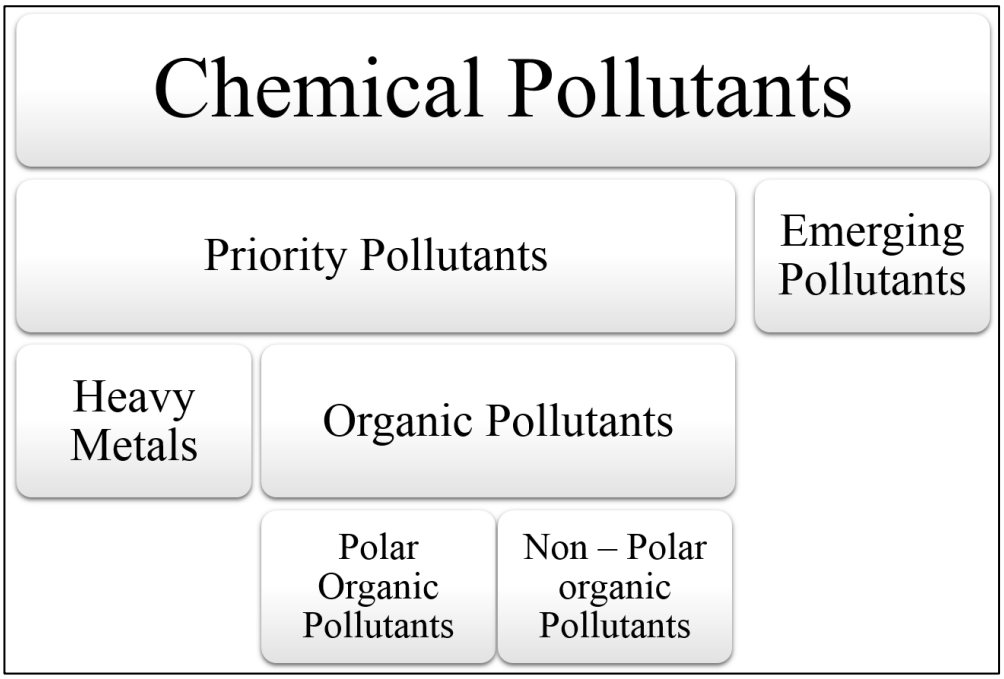

Figure 1-1: Diagram of chemicals pollutions types.

1.1.4.1 Priority pollutants

In 2014, the Environment Protection Agency (EPA) in the United States published a list of 126 priority chemicals that contaminate water. This list including metals, biocides, plant protection products, selected existing chemicals and other groups, for example polycyclic aromatic hydrocarbons (PAHs) that are mostly incineration by-products and polybrominated diphenyl ethers (PBDEs) [19]. All of these chemicals negatively affect the ecosystem; however, one of the most harmful groups is PAHs, which involves over 100 different chemical compounds [20].

1.1.4.2 Polycyclic aromatic hydrocarbons (PAHs)

PAHs is a group of compounds created from the incomplete burning of materials that consist of carbon, such as garbage, gas, oil, coal, wood or other organic substances [21]. PAHs are formed when two or more benzene rings are fused together by a pair of carbon atoms (covalent bond) [22]. Over 100 PAHs are known to occur naturally, but the EPA selected 16 candidates as priority pollutants. Table 1-1 shows examples of these priority compounds based on the number of benzene rings [23].

Table 1-1: Example of priority pollutants of PAH [24]

Name of Compound	Number of benzene rings	Solubility in water	Structure	Toxicity
Naphthalene	2	31.6 mg/L (25 °C)	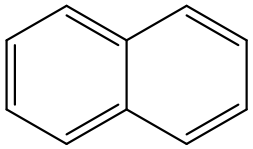	damage or destroy red blood cell possibly carcinogenic to humans and animals
Phenanthrene	3	1.6 mg/L	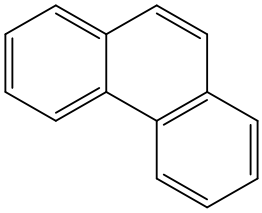	found in cigarette smoking and cause a cancer
Benzo(a)pyrene	5	0.2 to 6.2 µg/L	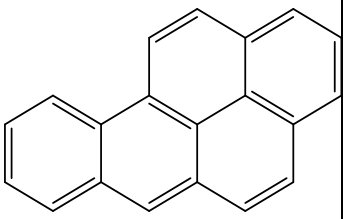	Effect directly on nerves system, immune system, reproductive system and cause cancer
Dibenz(a,h)anthracene	5	0.24 µg/L (25 °C)	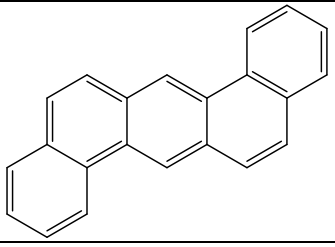	Interaction with DNA that causes mutations.

PAHs are non-polar compounds, which indicates that they do not ionise in water phase (hydrophobic compounds). Therefore, PAH compounds are insoluble in water; they are always found at very low concentrations in environmental water samples. However, the degree of PAHs' solubility in water depends on the molecular weight of compounds, as the solubility decreases when the molecular weight increase, also a rise in temperature up to 30°C enhances the solubility of PAH compounds in water [20].

PAH compounds that consist of fewer than four rings are semi-volatile, whereas compounds composed of four or more rings are non-volatile. PAHs compounds have a hydrophobic nature, thus they exhibit a high affinity for suspended particles when entering an aquatic environment. These particles tend to sink, leading to them settling on the sediments. Thus, the concentration of PAHs in the water usually depends on their concentration in sediments [25].

PAH compounds can reach humans through the air (breathing), contact with skin or drinking the water. How PAHs specifically impact individual health depends on the extent of exposure (length of time) and the amount of PAHs to which the person was exposed (concentration)[26]. When PAH compounds enter the body, they are rapidly distributed to many different tissues in the liver, trachea, stomach, kidney and oesophagus. Experiments that have been conducted on laboratory animals show that breathing air containing PAHs caused lung cancer, eating food containing PAHs caused stomach cancer and applying PAHs to skin caused skin cancer [24].

Benzo (a) pyrene has been shown to be a potent chemical carcinogen, because when it reaches to the cells is undergoes metabolic activation by the cytochrome P450-dependent monooxygenase system and is converted to reactive, toxic metabolites that bind covalently to cellular elements such as DNA [27]. The World Health Organisation (WHO) has specified the concentration of benzo(a)pyrene to be between 0.2 µg L^{-1} to 0.7 µg L^{-1} in drinking water [28].

1.1.4.3 Emerging pollutants

In the last 20 years, several researchers have mentioned the existence of new chemical compounds, called emerging compounds, in wastewater soil, air and aquatic environments [29]. “Emerging pollutants can be broadly defined as any synthetic or naturally occurring chemical or any microorganism that is not commonly monitored in the environment but has the potential to enter the environment and cause known or

suspected adverse ecological and/or human health effects". These kind of pollutants have occurred for a long time, but the detection methods for the chemicals compounds have been developed in the last 20 years, which lead to recognising the influence of emerging chemical or microbial pollutants to the environment. Also, with developments in many fields in science, new chemicals could create a new source of emerging pollutants [30].

Emerging contaminants arise from a several types of product and contain a wide range of chemical compounds which are involved in a variety of human and veterinary medicine, such as antibiotics and anti-parasitic agents [31]. Human personal care products are classified as a source of emerging pollutants, including fragrances, essential oils and similar synthetic and natural hormones, such as oestrogens and androgens [32]. Some microorganisms, such as fungi and bacteria, naturally produce toxic compounds that enter the environment; these are also sources of emerging pollutants [29]. In addition, because of developments in different science fields, there are new compounds that have been produced, such as nanomaterials, which might enter the environment and affect human health or the ecosystem [33].

An endocrine-disrupting compound (EDC) is defined as "an exogenous substance that causes adverse health effects in an intact organism, or its progeny, consequent to changes in endocrine function". The first report mentioning the incomplete removal of steroids in the wastewater treatment procedure was at the end of the 1960s [34]. After that, many works presented several human hormones in wastewater that showed incomplete removal in the treatment process [35]. A preliminary list of priority compounds that have been mentioned of EDC characteristics includes the oestrogens ethynyl, estradiol, oestrone and progesterone. The EDCs fall into two main categories: those that occur naturally and those that are man-made [36].

Estradiol (17β estradiol) (E2) is a natural steroid hormone and is the prevailing sex hormone in females and it is only produced in 3 out of the 30 days of the cycle [36].

Progesterone is a 21-carbon skeleton (C21) steroid; it is a natural steroid hormone secreted by the ovaries and placenta. These hormones work by coupling with oestrogen for present the female sex characteristics and the repair of the menstrual cycle [37]. In general, the effects of steroid sex hormones (SSHs) in the environment has been became under focusing, as there is a continuous increase in the prevalence of anthropogenic substances in the environment [38]. The negative impact of SSHs on the environment is illustrated dramatically in fish, where it affects reproductive behaviour as fish produced fewer numbers of eggs or in some cases no eggs at all, and this occurs after only a few weeks of exposure to either of the two different kinds of synthetic SSHs at concntration in the rang 4 – 0.7 ng L^{-1} for that hormones found in female reproductive drugs, [39].

The main sources of SSHs are drugs utilised for the treatment of hormonal disorders, as birth control pills and analogous drugs, and cosmetic industries. The addition of progesterone and other types of sex hormones to cosmetics products has been widely added since they have several advantages, such as eliminating wrinkles, enhancing hair growth and increasing skin elasticity [40]. In addition, steroid hormones from these sources are excreted from humans and animals, and they can enter the environment since sewage treatment plants do not completely remove hormones [38]. The progesterone and estradiol uses widely in this products also they produce from female mammals, for that both of them were selected to apply in this work as example of emerging pollutants

1.1.5 Analysis of chemical pollutants

The analysis of chemical pollutants in environmental water samples at very low trace concentration has greatly increased and a range of different instruments have been developed[41]. All PAH compounds should be analysed using highly sensitive and selective analytical techniques; research efforts have focused on developing new techniques or on improving methods for contaminant analysis. Common techniques used to analyse PAH compounds with high precision are gas chromatography/flame ionisation

detector (GC-FID), GC–mass spectrometry (GC–MS), high-performance liquid chromatography/ultraviolet (HPLC/UV) and HPLC tandem MS (HPLC MS/MS); these methods provide highly accurate results. However, these techniques require highly-qualified technicians, expensive equipment and a special site in the laboratory [42].

The analysis of sex hormone compounds in environmental water samples is a challenging process due to the concentration of compounds usually at very low levels (0.1– 4 ng L^{-1}) and complexity of the environmental matrices [39]. The typical procedure for analysing SSHs involves diverse sample preparation steps, such as filtration, derivatisation, extraction, evaporation, pre-concentration and purification. The most common techniques used for analysis are GC–MS and HPLC, which has become the most popular; different types of extraction methods were also applied such as liquid liquid extraction (LLE) and solid phase extraction (SPE) [43].

1.2 Sample preparation

Any analytical process has a number of steps starting with sample collection, transport and storage, followed by the extraction of the analyte and selection of a suitable technique for identification and quantification and finally writing up and reporting the result. The analytical methodology is usually based on the kind of sample and the target of the analysis, but the extraction of the analyte can be considered to be one of the most vital steps in the analysis process because usually, it is one major source of inaccuracy in the analysis procedure [44].

Analytical instrumentation has massively developed in recent years with GC and HPLC combined with very sensitive detectors. However, environmental water samples may still not be directly analysed on account of the complexity of the samples that include many different species of contaminants including organic and inorganic compounds which may also lead damage to the instruments [44].

The extraction of the target analytes is a critical step to achieving the correct result in the analysis process by removing potential interfering compounds. However, up to 30 % of the total analysis error can be caused by this stage. Most errors in sample preparation occur in the elution step where the elution solvent is not efficient [45]. The elution step can be used to pre – concentrate the target analyte at very low concentration before analysis which improves the detection capability. This is achieved by either extracting a miniscule volume of eluent or by evaporating the solvent [45].

In general, the extraction and pre – concentration of the target analyte in environmental water samples can be time and chemicals consuming, requiring complex processes as well as being a source of contamination. The most common extraction techniques used with environment samples are liquid – liquid extraction (LLE) and solid phase extraction (SPE) [45]. A suitable extraction process should be rapid, reproducible, straightforward and achieve acceptable extraction recovery for the target analyte.

1.2.1 Liquid – Liquid Extraction (LLE)

Liquid – liquid extraction is classified as the oldest and standard method to extract and purify target analytes from environmental water samples. The Principle of LLE depends on the distribution of analyte between two immiscible liquids in that the compounds matrixes have a different solubility, usually using organic solvent and another phase is water. The distribution of analyte between two phases depends on the polarity of compounds where polar hydrophilic compounds tend to be used in the aqueous phase and non – polar hydrophobic compounds for the organic solvent. The organic solvent is the key factor in LLE technique where some point should be taken in considering, such as solubility in the aqueous phase, purity and should it be appropriate for the instrument use [45].

The calculation of the distribution coefficient is required to evaluate the LLE method. The distribution coefficient (K_D) can be defined as "the ratio of the concentration of the analytes in two immiscible liquids phases at equilibrium", where Equation 1-1 can be used to calculate it.

$$K_D = \frac{C_{org}}{C_{aq}}$$ Equation 1-1[45]

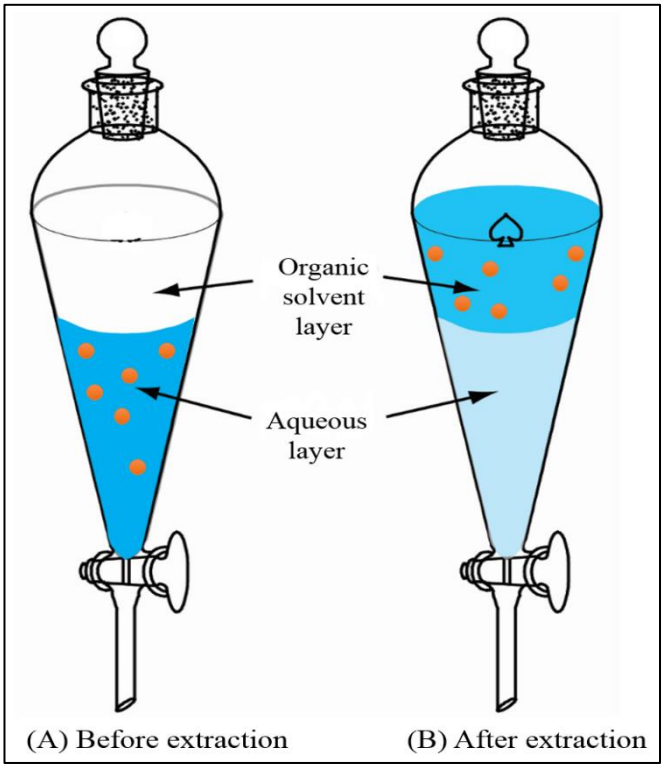

Figure 1-2: Separation funnel used for liquid – liquid extraction, where (A) shows the funnel before extraction with 100 % of the target analyte in the aqueous phase, (B) shows after completion the extraction process where the majority of the target analyte moved to an organic phase.

Tavakoli, *et al.* [46] used the LLE technique to extract and pre – concentrate the mixture of PAHs compounds (benzo (a) pyrene, acenaphthylene, chrysene, acenaphthene, anthracene, fluorene, phenanthrene, flouranthene, and naphthalene) from water samples by using a ternary component system consisting of water, methanol and chloroform. The process was carried out with 2.5 mL of sample solution including (100 µg L^{-1} of PAHs

mixture + 25 µL of 10 mg L^{-1} of biphenyl) which used as an internal standard, and the extraction solvent was made up from (1.2 mL of methanol with 60 µL of chloroform). Both of mixture was mixed in one tube and gently shaken, then used the centrifuge to separate the mixture. The mixture of the analytes was injected to GC – FID where the LOD was in the range 0.1 – 0.03 µg L^{-1}.

Barber *et al.* extracted oestrogen from wastewater by liquid –liquid extraction using methylene chloride. The extract was analysed by GC-MS in both selected ion monitoring mode and full scan mode, and the LOD was around 60 ng mL^{-1} [47].

As any analytical technique, LLE can offer some advantages such as offered acceptable extraction recovery, a large sample capacity, acceptable reproducibility and it is useful to remove the matrix. On another hand, there are some significant disadvantages with this technique, it is time-consuming, and uses a lot of hazardous organic solvent requirements and it is hard to automate. Also, in the process of the LLE is not so good at pre – concentration the analyte and some interferences in the sample matrix can cause emulsion formation [45].

1.2.2 Solid phase extraction (SPE)

The principle of SPE is similar to liquid – liquid extraction where the process of isolating the analyte from a mixture compounds dissolved in the liquid phase depends on their physical and chemical properties. This method is used for pre - concentration and extraction of volatile or non – volatile compounds by an interaction of the analyte with either a solid phase or sorbent [45].

SPE first appeared in 1970 as an alternative technique to LLE that was faster and used less hazardous solvents. The first disposable columns contained silica sorbent and were produced by Waters Corporation in 1977 which led to a rapid increasing use of SPE and it has become critical for extraction and pre – concentration for a trace amount of analyte

for various application involving environmental, industrial, pharmaceutical and biological analysis [48] [45].

SPE have been used widely in the environmental analysis for both chemicals on the priority pollutant list and emerging pollutants and several types of sorbent have been used. In general, the advantage of using SPE is makes the sample preparation stage reproducible, faster and highly accurate. In addition, the efficiency of the extraction became higher leading to increased recovery. Also, the volume of solvent consuming reduce when comparing with LLE. However, there are few disadvantages of the SPE procedure including restricted capacity, high cost and blockages of the SPE cartridge by the complex leading to high backpressures in the flow system. These drawbacks did not prevent SPE becoming widely used particularly since a significant advantage of SPE is that it can be connected online directly to HPLC or GC. This online integration allows automation of the sample preparation and prevents loss or contamination of the sample by reducing the handling between the sample preparation and analysis step.

1.2.2.1 Solid phase extraction technique process

The SPE procedure depends on the solid sorbent held in the cartridge which is responsible for extraction and / or pre – concentration of the analyte from the matrix. The extraction process has four steps as shown in Figure 1-3. In the first step the sorbent is conditioned by utilising a suitable organic solvent to equilibrate, activate and wet it, also to remove any impurities. The second step involves loading the sample solution into the SPE system. In this step, the target analytes are trapped on the sorbent, and undesirable compounds flow through to waste. In the third step, the sorbent with the trapped analyte is usually washed with an appropriate solvent that will not elute the target analyte but will ensure all the interfering compounds are washed out. Finally, an appropriate solvent is used to elute the target analytes from the sorbent and collected for further analysis [45].

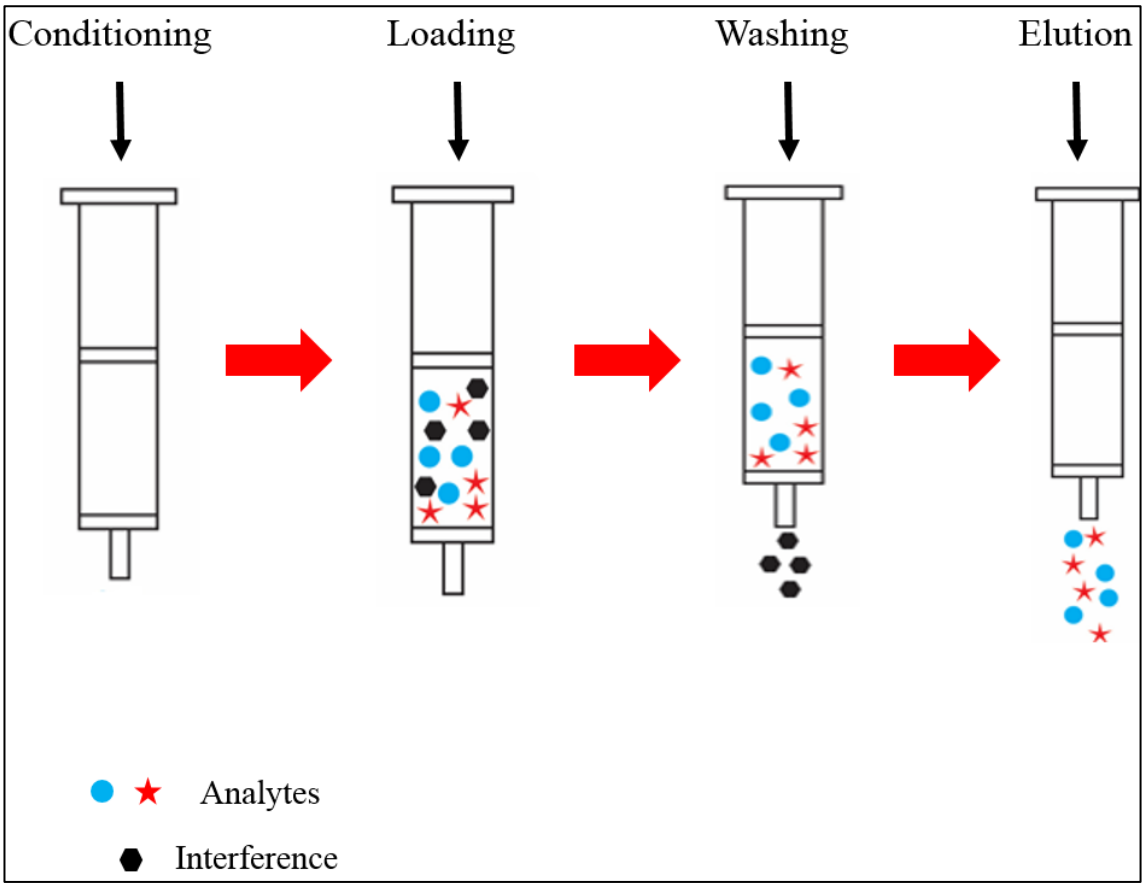

Figure 1-3: The stages of solid phase extraction involve (conditioning, loading, washing and elution).

The pre – concentration process is the same as extraction, but the volume of elution is selected to be much less, than the volume of sample loaded on the cartridge. The mechanisms of SPE extraction based on the type of the interaction between the active site on the surface of the sorbent and the analytes. The SPE process can be completed depending on gravity or by using a pumping system; however, the flow rate needs to be adjusted during loading, washing and eluting stages because it necessary to achieved the optima flow rate for each step that led to increase the efficiency of extraction. The SPE sorbents can be classified into three main types; ion exchange, normal phase and reverse - phase [49].

1.2.2.2 Normal phase extraction

The stationary phase in the normal phase extraction is polar for example alumina (Al_2O_3) or silica $(SiO_2)_x$, or the silica sorbent surface is modified with polar functional groups, for example, cyano or amino. In normal phase SPE, interactions occur between the polar group of the target analyte in a non – polar sample matrix and the polar group on the sorbent surface. These interactions can be dipole – dipole interaction or hydrogen bond as shown in Figure 1-4 [45].

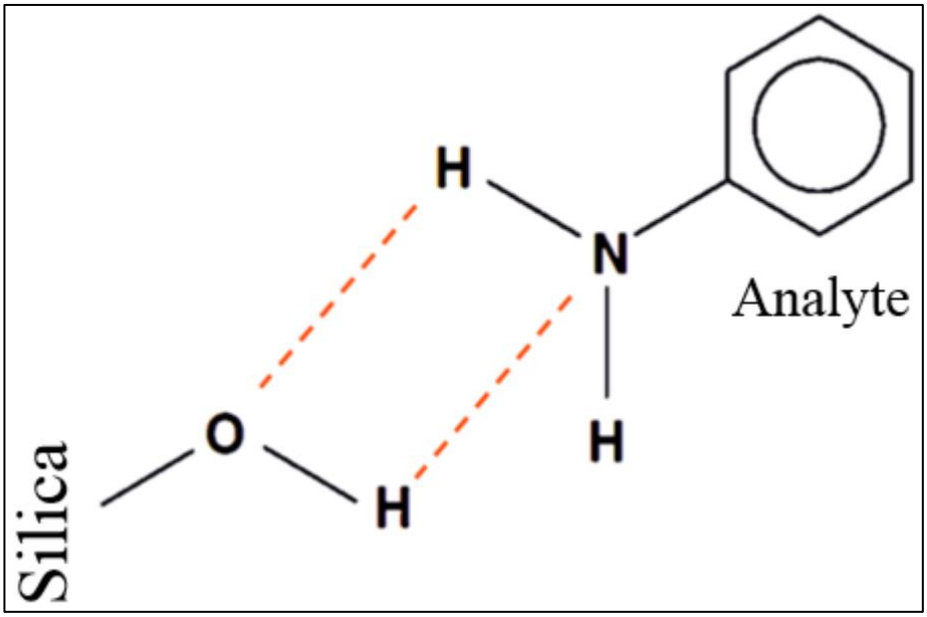

Figure 1-4: Interaction between polar sorbent silica and polar analyte (phenylamine) *via* hydrogen bonding [50].

1.2.2.3 Reverse - phase extraction

Reverse - phase extraction is the method based on the characterisation of the surface for the non – polar sorbent (stationary phase). A non – polar group such as phenyl, octyl, octadecyl or butyl that interacts with non – polar functional groups on the target analyte, where this method is the opposite of normal phase. This interaction can be dispersion or van der Waals forces, London dispersion forces or π – π interaction as shown in Figure 1-5, in the elution stage a non – polar solvent is usually used to release the target analyte from the sorbent surface [45].

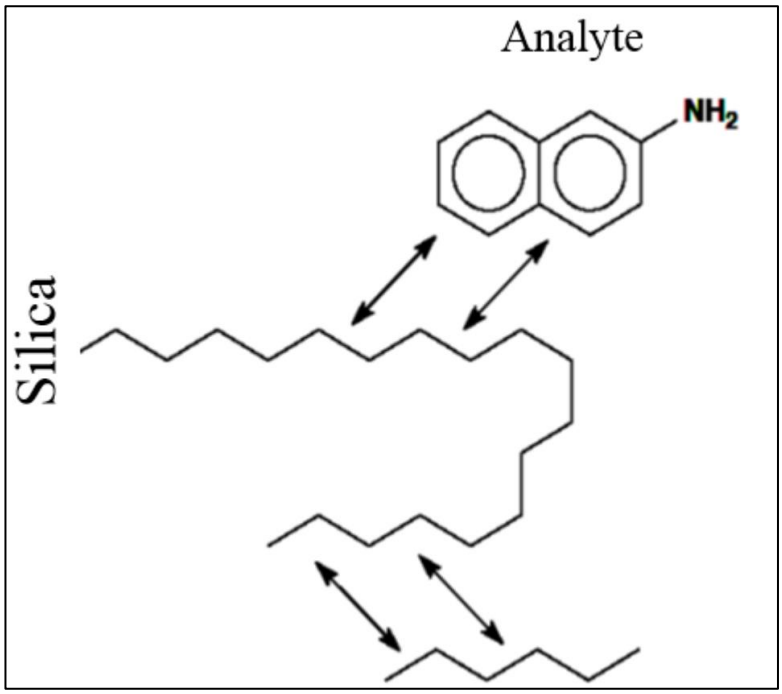

Figure 1-5: Interaction between non – polar sorbent and non – polar analyte bonded silica *via* Van der Waals forces [50].

1.2.2.4 Ion exchange extraction

In the ion-exchange extraction, the sorbent backbone such as silica have normally composed the sorbents that attached to a carbon chain terminated by positively or negatively charged functional groups. In this process, an ion exchange resins are used, and interaction depends on the preferential electrostatic attraction between the charge on the sorbent surface and the opposite charge of a functional group of the target analyte. Mainly, the ion-exchange resins can be divided to three types; the first type is the cation exchange, where the sorbents are negatively charged and interact with positively charged analytes (cations) such as use a resins that a cross-linked with an aliphatic sulfonic acid (- SO_3 H) functional group as shown in Figure 1-6. Also, an ionizable functional group such as amine or carboxylic acid (COOH) can be used for weaker exchange as shown in Figure 1-6. The second type is an anion exchange, where in this case the sorbents are positively charged similar the analyte carries a negative charge, where an aliphatic quaternary amine group (-$N^+(CH_3)_3$) are commonly used. [50]. In zwitterion-exchange, the

silica backbone contains molecules which can be negatively or positively charged; therefore the functional group can attach to it[49].

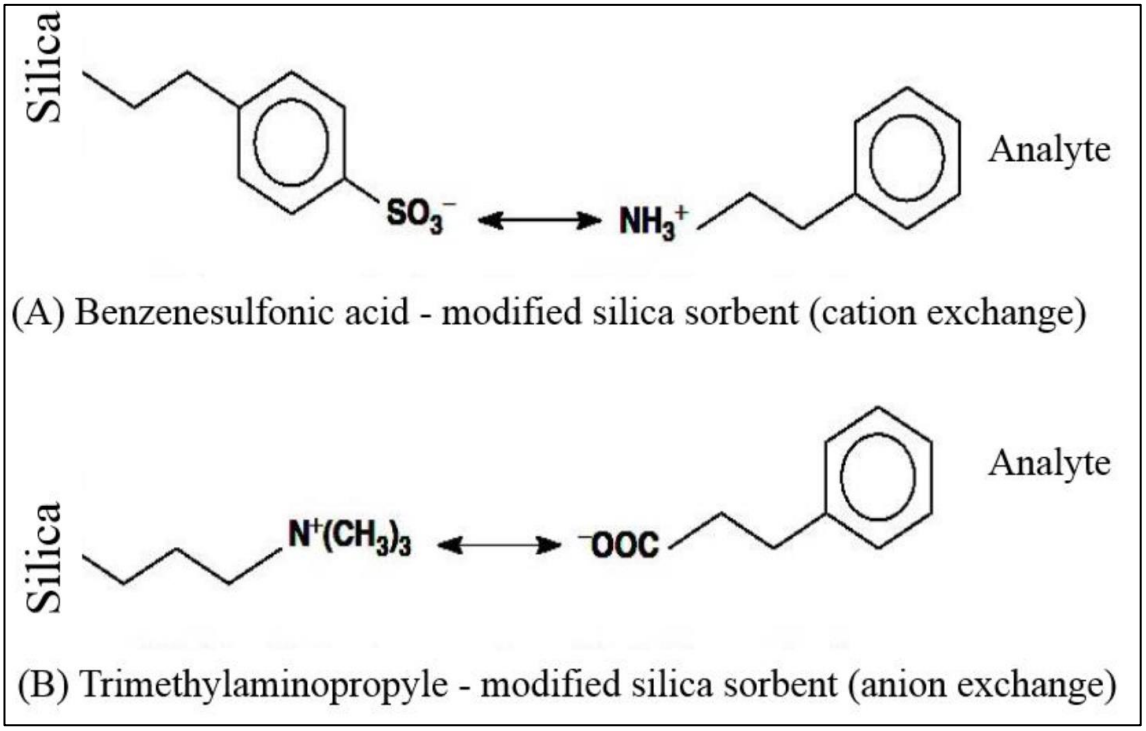

Figure 1-6: Ion exchange interaction, (A) strong cation exchange sorbent, (B) strong anion exchange sorbent [50].

1.3 SPE sorbent

As seen from the previous discussion SPE sorbents can be prepared from several types of materials, the perfect sorbent material must have a high stability for chemicals for the solvent through all the extraction stages process. The material also needs to be physically stable for extended periods under any ambient climatic condition. As well as this consideration there are two important properties which should be considered when choosing a suitable sorbent. The first requirement being a high surface area which increases the possibility of interaction between the active site on the sorbent surface and the target analyte. The second feature is a good permeability to allow a large volume of the sample to be loaded at a high flow rate without back pressure [51].

The most popular materials used for SPE sorbent are organic polymers and silica. However, a drawback of both materials is the requirement to use solvent for conditioned through the extraction procedure, and they must be wet all the time until the analyte have been loaded [52]. A new generation of polymer sorbent such as styrene – divinylbenzen copolymer (PS – DVB) has been modified to be hydrophobic, acid, basic and neutral which make them suitable to extract a wide range of analytes using simple procedure without a conditioning step. The modified polymer sorbent surface is better to use with aqueous samples because it usually provides a high surface area that enhances the loading capacity and extraction efficiency. Also, the silica modified surface sorbent has been become widely used in a large range of analysis applications that include the environment analysis [49].

1.3.1 Particulate materials as sorbent

In SPE the cartridges are filled with particulate organic polymer or silica as previously mentioned. The diameters of particles in the range between 1 to 10 µm place between two porous frits have been widely used to fill the packed cartridges. Using these small particles sizes provides a high surface area to volume ratio leading to a high efficiency for the extraction. As example of that, a typical cartridge packed with 5 µm diameter particles provides a surface area around 120 $m^2 g^{-1}$ whereas cartridge packed with 2.7 µm diameter particles provide 230 $m^2 g^{-1}$ surface area [53]. Although this reduction in particle size gives improved the extraction efficiency, it leads to an increase in the resistance to flow of the solvent which generates a higher back pressure, because pores are blocking for complex sample. The decrease in the size of the particles diameter is directly proportional to the increase in backpressure. To reduce the effect of back pressure, the length of column can be decreased, but this causes a reduction the opportunities of interaction site on the sorbent surface, which reduces the extraction efficiency [54].

Monolithic materials have been investigated to overcome the problem of backpressure and surface area.

1.3.2 Monolithic materials as sorbents

In the last 25 years, new materials with a monolithic structure have been developed to overcome the problem of backpressure in the particles columns. The word "monolith" comes originally from the Greek language and is derived from two words merged into one "mono" which means one and "lithos" which means stone. In the analytical chemistry context, a monolith structure can be defined as "an interconnected skeletal structure of a continuous macro – porous (through pore) that can be built up from polymer or silica" [55].

The advantage of using the monolithic column compared with the packed column is clear to see in Figure 1-7, which show the differences between two conventional chromatographic columns. Figure 1-7 compares the internal structure of (A) a column packed with particles and (B) a monolithic column fabricated from a single piece of porous solid that provide a comparatively big channel for continuous flow through the structure and higher number of through pore channels penetrating compared with packed column [56].

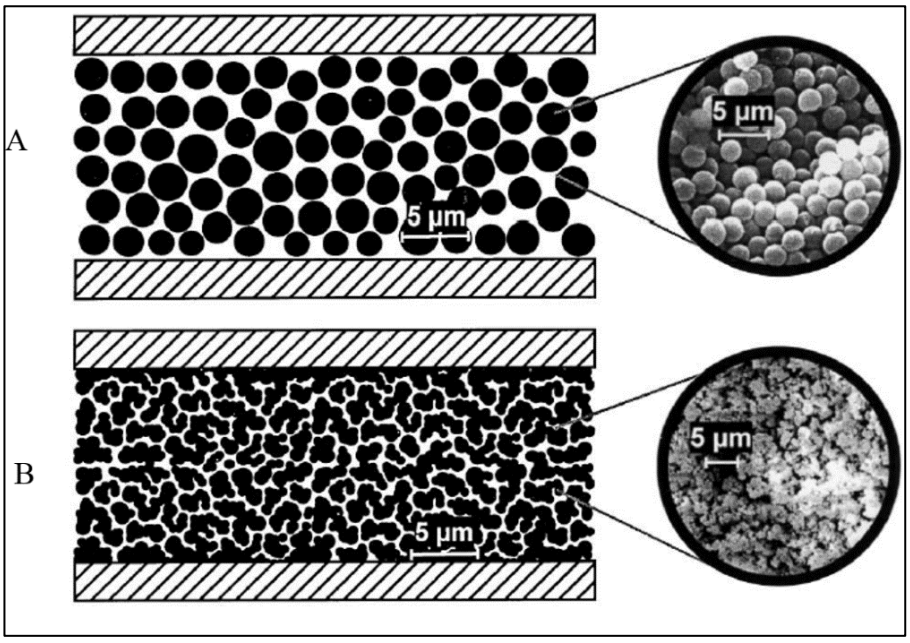

Figure 1-7: Scanning electron image of the (A) packed particles column and (B) monolithic column [56].

The process of movement of the mobile phase inside the column was described by van Deemter in 1956 relating it to the separation efficiency regarding the height equivalent theoretical plates (HETP) of the column. The main factors contributing to (HETP) are shown in Equation 1-2. A higher efficiency of extraction or separation corresponds to lower plate height values. Kobayashi *et al.* repeated the influence of structure on the kinetic performance of monolithic and packed columns [57].

$$HETP = A + \frac{B}{u} + Cu \qquad \text{Equation 1-2 [57]}$$

Where A: eddy diffusion, B: axial diffusion, C: mass transfer and u: linear velocity

The eddy diffusion (A) term represents the motion of the solute molecule in the mobile phase through the stationary phase in the column using different paths, which is relating to band broadening. The various paths for the solute molecule into column are generated by the through – pore structure in the monolithic column and the packed column through inter – particle spaces. In the packed column the movement of the solute molecule based on the particle size, while in the column packed with the large particle, the movement of

the solute molecule through the column takes the different circuitous path which means it take a long time to leave the column, and this led to large band broadening. The travel time of the solute molecule inside the packed column is therefore related to the particles size, so in the packed column decreasing the particles size led to a reduction in the travelling time inside the column, and as a result of this, the band broadening peak of the analyte is decreased. Using a small particle size and choosing the suitable well-packed column can minimise the eddy diffusion [58].

In the silica monolith column, the large through pores in the structure network offer high external porosity and reduce the diffusion path length. This led to the majority of solute molecules moving smoothly through pores with a simple resistance in the path, which led to a small band broadening [59].

The mass transfer term (C) describes the flow of the solute molecule through the column between the mobile phase and the elution phase or stationary phase. Fast transfer kinetics happen, when the difference in time between the solute molecule in the stationary phase and the mobile phase is low and the time will be short. Conversely, slow transfer kinetics occur when the difference between them is high and the time will be longer. In the packed column reducing the depth of mesopore on the monolith or the particle size which is response of the effect of mass transfer between the stationary phase and the analyte, which would lead to minimised the effect of the mass transfer [58-59].

The longitudinal diffusion (B) refer to diffusion along the column and relates to the flow of the solute molecule when introducing into the column. In general, the diffusion of the molecules undergoes symmetrically around the centre of the column, so the flow of the mobile phase in the pass inside the column is inversely proportion to the longitudinal diffusion. The contribution of the longitudinal diffusion in solid phase extraction is small, because generally the movement of the solution through the column based on the method

of introduce it such as by using syringe pump of electrical filed or depend on the gravity [58].

1.4 Organic polymer monolith

The monolithic material was reported in 1989 by Hjerten *et al.* [60] and was based on polyacrylamide polymer. It was successfully used in the chromatographic separation of proteins. A continuous medium depends on rigid macroporous polymer monoliths that used a simple moulding process for forming it was reported by Svec *et al.*[61]. This work enhanced the possibility to use the monolithic media as a chromatographic stationary phase. Then, different organic polymers were used to fabricate monoliths such as polyacrylamide, polymethacrylate and polystyrene [62]. There are many advantages to using polymeric monolithic beds; they can be prepared in one polymerisation step, and their shape and position can be controlled by using masks and UV radiation for initialisation of polymerisation. These polymeric monoliths are widely used in chromatographic separation of macromolecules such as proteins and lipids, and it shows high stability at different pH values [63]. However the polymeric monoliths have a low mechanical strength because of shrinking or swelling with organic solvents, and their surface area is relatively low making separation of low molecular mass compounds challenging [64].

1.4.1 Fabrication of the organic polymer monolith

As mentioned previously in 1.3.2 polymer monoliths are prepared simply for a moulding process. For polymer monolith fabrication there are many organic polymers that have been used as monomers, but some of the organic polymers were widely used as polymethacrylate, polystyrene and polyacrylamide [62].

To prepare the polymeric monolith from monomers, the organic solvents and free radicals are uses as an initiator to start the polymerisation process to form the monolith structure.

The polymerisation process is based on three stages; the initiation step is the first stage where the free radicals produce from decomposes the initiator to react with the monomer. The second stage is the propagation process. In this step, the chain is formed by addition of the monomer units constantly. After the chains grow, the micro globules form because the chain is precipitated as nuclei, for that, any un- polymerised monomers will be polymerised with nuclei during continues polymerisation process. The network structure formed of the growing nuclei, where the porogen system are occupied the macroporous of the monolith. When two free radicals react together, the polymerisation reaction will stop as no catalyst is available to complete the polymerisation, this step called termination [65]. The photoinitiation and thermal initiation can be used as an initiator for a polymerisation reaction and microchip, glass and fused silica capillary can be used as a transparent mould.

Xie *et al.* presented the use of organic porous polymer monoliths for SPE in 1998. This investigation focused on the influence of the initiator concentration on the size of the pore in polymer monolith, which was concluded to a smaller pore formation as a result of using a high concentration of the initiator as azobisisobutyronitrile, which led to increasing the number of free radicals, therefore, enhance the number of nuclei [66]. Then, Schley *et al.* published the work of pre – concentration and separation of seven different proteins by using a poly (styrene-co-divinylbenzene) monolith [67]. After that, a many articles have been published using the polymer monolith as a sorbent for extraction and pre – concentration especially with biomacromolecules such as proteins and DNA but few publication mentioned the use of polymer monolith with small molecules [64, 68].

1.5 Inorganic silica monoliths

Another type of monolithic materials that created instead of polymeric monolithic was based on the inorganic materials such as silica. Where in 1992 Nakanishi and Soga [69] successful prepared monolithic rods (mesoporous and macroporous) using the inorganic silica – bed materials. The sol-gel reaction used to prepare the silica monolithic rod column is considered to be the start of modern monolithic materials [70].

Depending on the pore size the monolith can be categorised by macropores (< 2 nm) and mesopores (usually in the range 2 -50 nm). The organic polymer monolith contains only macrospores, for that it usually uses to extract and separate the large molecules such as a protein. However, for small molecules such as organic pollutants, it not recommended for use [71]. To extract and separate small molecules it is required to use monolithic that offer pore size in the range between 8 to 10 nm of mesoporous and pore size greater than 50 nm of macropores [72]. The silica monolithic internal structure is characterised by the macropores that are a small diffusion pore that give a high surface area and (macropores) which is a bimodal pore size distribution include of a big through pores for large permeability. The silica monolith internal pore structure offers the surface of the monolith to react with different size of molecules through the mesopores and macropores respectively[62]. Also, the extraction efficiency in the silica monolith become high as a result of the large surface area of that offer maximises analyte retention. Also, reducing of backpressure of passing the solvent through the column with different velocity and increase the mass transfer kinetics it possible by controlling the size of the macropores. Inorganic silica monolithic materials show a high stability with several of organic solvent [73].

1.5.1 Fabrication of the inorganic silica monolith

The preliminary study of the permeability and chromatographic application of a continuous silica monolith column with reversed – phase HPLC condition was carried out by Fields *et al*. in 1996 [74]. A potassium silicate solution was introduced to a 0.32 mm i.d. × 13 cm long fuse tube and thermally cured at 100 °C for 1 h. Helium was then used to dry the column for 24 hours at 120 °C. The silica column produced as a result of this process was modified to be reverse phase by flowing through 10 % solvent of dimethyloctadecylchlorosilane. As a result of this process, a high permeability continuous silica monolith column was easily prepared. The drawback of this method was the internal morphology of the monolith was not homogenous, because of the use of emulsion and aerosol techniques during synthesis, and it had a relatively low mechanical strength.

An alternative method to prepare a silica monolith was described by Minakuchi in1998 [73a] and that depend on sol – gel technology. That method had the advantages of producing the silica monolith with good homogeneity and mechanical strength. This process also produced a silica monolith with the required double pore structure with micrometre sizes of continuous through pores and mesopores with nanometre size on the silica skeletons giving a high surface area where the macroporous provide high permeability. In addition, the resulting of t combining of macroporous and mesoporous dimensionality in the structure of the silica monolithic provides a high diffusion rate of extraction, separation and catalysis application. This sol-gel method was therefore used for silica monolith fabrication in this project. This method of preparation includes four stages (hydrolysis of precursor sol-gel formation, gelation with aging and drying with calcination.

1.5.1.1 Hydrolysis of precursor materials

The hydrolysis and condensation of the precursor are the primary processes to form the sol. To prepare the silica monolithic structure several types of precursor have been used,

but the most common precursors used are the low molecular weight alkoxysilanes such as tetraethylorthosilicate (TEOS) and tetramethylorthosilicate (TMOS) [75]. A porogen acts to forms the micropores and macropores in the silica gel, where it should be a water – soluble polymer such as polyethylene oxide (PEO). The catalyst used can be a basic catalyst such as N-methylimidazole or dimethylaminopyridine or an acidic catalyst such as acetic acid or nitric acid [76].

The catalyst in the sol-gel procedure increases the rate of the hydrolysis reaction. In the hydrolysis reaction, the alkoxide (-OR) replaces the hydroxyl groups (-OH) and alcohol molecules (ROH) are released. In the group of Si-OH or Si-OR, the oxygen atom is protonated to complete the hydrolysis process, and H-OR or H-OH are good leaving groups [77] [78].

Figure 1-8 (Scheme 1) shows the first stage in the reaction of the hydrolysis of the water with the liquid alkoxide. The silanol group (Si-OH) formed as the result of the hydrolysis process, that flow with condensation process when all these silanol group interactions together and this led to producing polycondensed species including two silane molecules linkages with siloxane (Si-O-Si) as shown in Figure 1-8 (Schema 2 and 3). The viscosity of the solution dramatically increases as a result of the continuous reaction of the polycondensation to convert the sol into the gel by a formation of alcohol or an oxide bridged network [79].

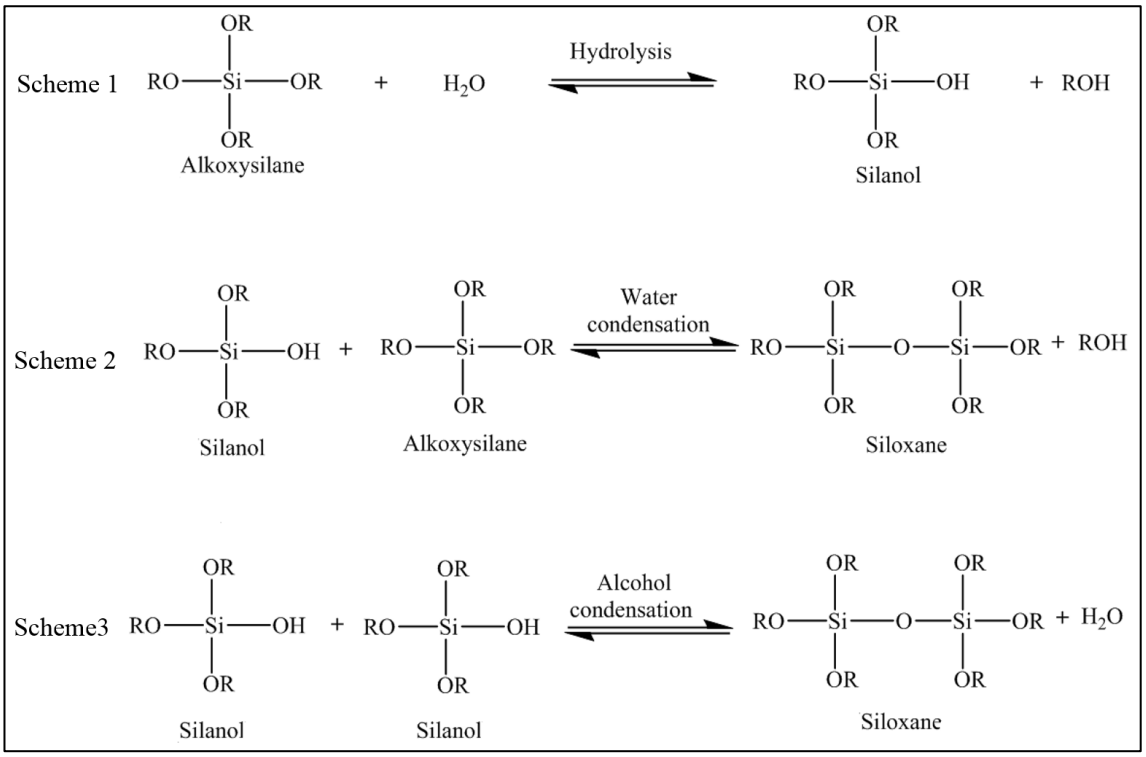

Figure 1-8: Mechanism of the reaction of hydrolysis and condensation reaction in sol-gel procedure [80].

The hydrolysis process for TEOS, the catalyst used is a strong acid such as nitric acid. Whereas a weak acid such as acetic acid was selected to use as a catalyst for TMOS because the TMOS undergoes the hydrolysis process faster than TEOS due to the stability of the ethyl group higher than methyl group [81].

Before the viscosity of the partially polymerised solution becomes very high, the solution is poured into a suitable mould. There are many factors effected in the casting process such as the shape of the mould used (to prevent any reaction between the solution and the mould) and the shape of the mould [80]. In this project, a plastic syringe (Becton Dickinson Polypropylene Hypodermic BD, 1 mL) was utilised as the mould to fabricate the silica monolith rod.

A range of parameters can influence the hydrolysis and condensation reaction processing such as pH, precursor concentration, catalyst and solvent. Also, the type of precursor can directly affect the reaction rate depending on the reactivity with water, Metal alkoxides

such as aluminium or titanium are more reactive with water compared with silicon alkoxide because they have higher Lewis acidity and lower electronegativity [82].

For the sol-gel process, the silicon alkoxides have been widely used compared with other types of alkoxides because of the reaction between the water and alkoxysilanes produce a good homogeneity solution. Also, the hydrolysis and the condensation process is affected by the ratio of water and silicon alkoxides. A slow hydrolysis process is seen with a small amount of the water due to a decrease in reactant concentration, but a large amount of water also leads to slow hydrolysis because the reactant (silicon alkoxides) is diluted. The condensation process is completely dependent on the pH in the alkaline conditions the mesoporous gel has pore sizes of 50 – 2 nm but in acidic conditions a dense structure forms with an increase in micropore (pore size < 2nm) [83] [84].

To get a good silica monolith column many researchers have used different chemicals composition and investigated the effect of the physical parameter during the gel formation procedure on the internal structure of the silica monolith [85].

1.5.1.2 Gelation

The gelation process occurs when the silica oligomers linking together to build a three-dimensional network produce a semi-solid wet gel material, the time to complete this process is defined as the gelation time. The viscosity of the solution is increased through the gelation procedure because the condensation reaction produces particles which make clusters [86].

1.5.1.3 Aging and hydrothermal treatment

In the aging stage the silica skeleton with a continuous network of the through pores in the skeleton surface is generated as result of the polycondensation reaction of the silica in the existence of the porogen (such as polyethylene oxide, PEO) soluble in the water and the phase separation between the silica – PEO system and water. In addition to

creating the macropores, the porogen is used to solubilise the alkoxysilane reagent. The molecular weight of the PEO should be high as it is required to stabilise the oligomers against phase separation [73b].

A change in the porogen concentration and molecular weight can lead to controlling the size of the through pore and skeletons. A study with various molecular weights of porogen (PEO 10,000 and 100,000) was carried out by Shrinivasan et al. [87]. Figure 1-9 illustrates the change in the structure of the silica monoliths made with different molecular weights of PEO. The silica monolith made from 10,000 MW PEO gave through the pore with diameters in the range of 5 to 7 µm, while the surface area was on average 40 m^2 g^{-1} as shown in (A). The second silica monolith was made from 50 % 100,000 and 50 % 10,000 MW PEO as shown in (B) where the mixture gave through pore sizes between 2 to 4 µm and the surface area was on the average 380 m^2 g^{-1}. The third silica monolith was made with 100,000 MW PEO, which gave through pores of less than 1 µm with a surface area on average 520 m^2 g^{-1} as shown in (C).

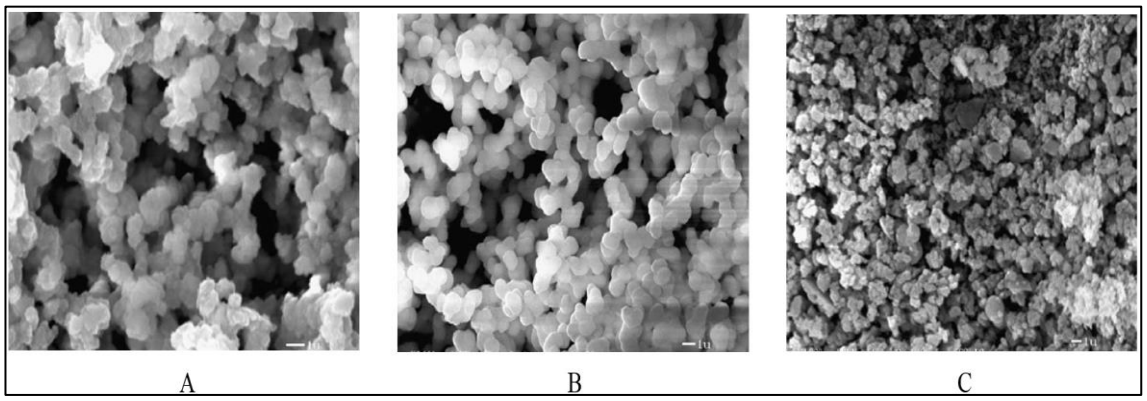

Figure 1-9: SEM image of (A) silica monolith form with 100 % of 10,000 MW PEO, (B) silica monolith made with 50 % of 10,000 MW PEO with 50 % of 100,000 MW PEO and (C) silica monolith form with 100,000 MW PEO [87].

This study showed that the increasing in the PEO molecular weight produced smaller through pore size and made the morphological structure more condensed which meant less permeability. Also, the high PEO molecular weight in the starting mixture lead to an

increase in the surface area. Another study using a different molecular weight of the PEO was carried out by Fletcher *et al.* [88] and used various concentration of large molecular weight of PEO (100,000 and 200,000). The result of the study found a growth in the surface area, and reduction of the through pore size occurred with increasing molecular weight of PEO. However, when using a very high molecular weight of PEO (300,000) to prepare the silica monolith, the monolith did not form [88].

The phase separation about the sol-gel formation is delayed when the molecular weight and the concentration of the PEO increases, which leads to the growth of a greater silica network in the gelation process before the structure of the silica monolith, become frozen. Also, the strength and thickness of the skeleton structure increases as a result of increasing the molecular weight and the concentration of PEO, but this leads to decreasing porosity and permeability of the silica monolith. During the aging process, the silica monolith shrinks enabling it to be removed easily from the mould [54, 89].

As the increasing of the surface area of the monolithic silica is an important step, the silica monolith is then treated in alkaline media that is produced by thermal decomposition of ammonium hydroxide (NH_4OH) at 100 °C to tailor the mesoporous structure. The dissolution and reprecipitation procedure is applied to tailor the mesopores inside the silica skeleton [90]. The reprecipitation occurs on the concave surface by adjusting the temperature and pH, where the dissolution process occurs on the convex surface of the silica [91].

The influence of parameters such as time of hydrothermal treatment, pH, chromatographic performance of monolith materials and temperature have been investigated with a many of studies [82, 92]. As a result of all these studies, increasing in the mesopore size and volume of distribution are related to increasing the pH and hydrothermal temperature. The hydrothermal treatment increase the mechanical strength of the monolith structure which contribute to increase the surface area [90-91, 93].

1.5.2 Drying and calcination

The drying stage is applied to the wet gel monolith to remove the majority of the solvent used in preparation (mainly water and alcohol) by an air – circulating oven, where the temperature is set between 40 to 80 °C depending on the type of solvent used. Subsequently, the monolith undergoes calcination when it is placed in a furnace at a high temperature between 500 to 650 °C to remove the organic residues without affecting the monolith structure. The calcination process increases the mechanical stability of the monolith while the surface area and pore volume decrease [79, 88]. The liquid – vapour meniscus inside the pore created from the evaporation of liquid from the pore structure, generates capillary pressures which led to more shrinking in the internal structure [94].

1.6 Comparison between the polymer monolith and silica monolith

Both types of the monolith have disadvantages and advantages; however, the main variance between silica monolith and polymer monolith is in their porous properties. Where the internal structure of the polymeric monolith contain only the macroporous, therefore polymer monolithic provide a low surface (100 – 400 $m^2 g^{-1}$) area which reduces the accessibility to interacting sites between the analytes and the surface [62]. As reducing in the interaction between the analytes and the sorbent surface this influence on the extraction efficiency, whereas the majority interacting is site accessible by short diffusion which provides by mesoporous space in the thin skeleton. On another hand, the silica monolith has a typical bimodal pore size distribution which involves mesoporous (2 – 50 nm) on the surface and macroporous (> 50 nm) which called as well by through-pore that allows the mobile phase passes through the column [95]. The advantage of the presence of mesoporous space in the silica skeleton provides a high surface area (200 – 800 $m^2 g^{-1}$) which reflected on increasing the opportunities for the interaction between the sorbent and the analyte, where the increasing in the macroporous provides the material with a

high hydrodynamic permeability [52]. Also, the mesoporous structure increases the chances of interaction between the internal surface of silica column surface and a small molecules and makes increase the diffusion rates of small particles inside the silica column more than for macro-molecules. In addition, the thin structure provides a highly efficient separation of a small molecule as it allows the trans-channel diffusion of analytes through the mesoporous. Because of the pores structure of the monolithic silica, the efficiency of the extraction, separation and pre – concentration improve with increasing the surface area as well [96] [97].

Figure 1-10 shows the internal structure of the silica monolithic where it contains mecropores and mesopores. However, the polymer monolith (glycerol dimethacrylate) includes only the macroporous and the globular structure clearly see in polymer monolith [62, 98].

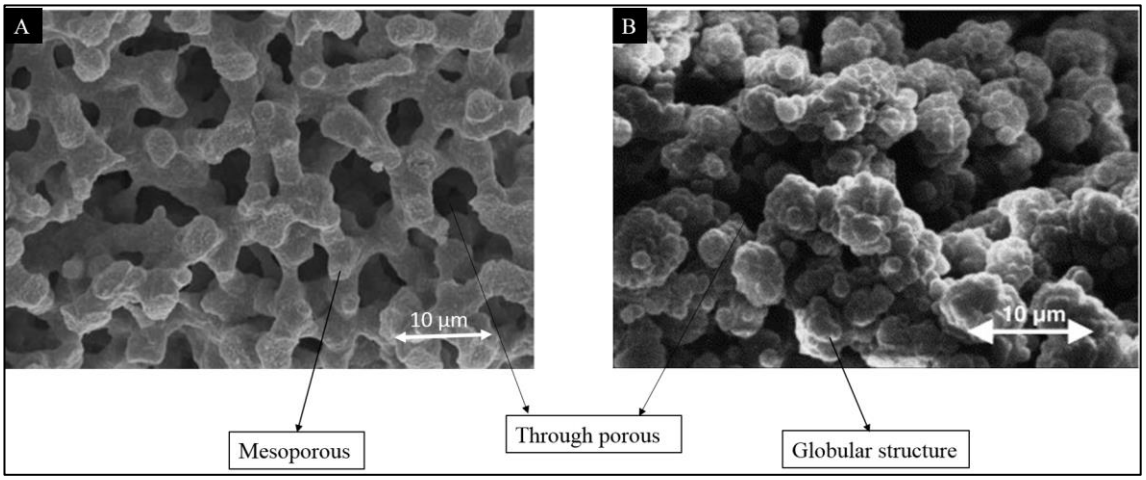

Figure 1-10: Scanning electron microscope image shows the difference in morphological structure between (A) silica monolithic and (B) polymer monolithic

Both types of monolith are simple to prepare, where the polymer monolith takes a short time and single step where the silica monolith adopts an extended time with several steps [62, 99]. However the silica monolith show high permeability, mechanical strength and relative high chemical stability but it not stable with high pH [62, 100]. Where the polymer monolith shows moderate permeability and effecting by temperature [101], also the organic

solvent causes shrinking or swelling of the monolithic structure but it is stable with a wide range of pH value [102].

The modification of the silica monolith surface can be readily derivatised with different functional types which led to further selectivity and efficiency while this process takes hours to reach equilibrium on the surface of polymer monolith as they have a huge number of crosslinking bonds [100a]. However, to fabricate the polymer monolith inside the microchip it is an easy process due to photoinitiation (light) which can an initiate a polymerisation reaction. In the case of silica monolith, these step would be a difficult process, because of the fabrication of silica monolith depends on using thermal initiation [64, 103].

The extraction applications, polymer monoliths are applied for biomacromolecules or high molecular weight, such as DNA and proteins, conversely the silica monoliths are applied for medium or low molecular weight compounds. For that, the silica monolith selected for the extraction and pre-concentrate of organic environmental pollutants will be used.

1.7 Modification of the monolithic silica surface with a functional group.

The oxygen atoms linked with silicon atoms by siloxane bonds (Si – O – Si) are the core of the silica monolith structure. The hydroxyl groups are present on the surface of silica that gives it polar properties. The most common chemical modification used with the silica surface are organosilanisation providing surface linkage esterification (Si – O –Si – C), which give surface linkage Si – O – C and chlorination give surface linkage Si – Cl. Reactions with silane reagent let to form a Si – O – Si bond on the silica surface; this bond is stable in a range of pH compared with Si – O –C bonds. For this reason, silanisation reactions are used widely based on the organosilanisation linkages [52].

Alkoxysilanes and chlorosilanes are most commonly used, and they have a different reaction rate [49].

$$R\text{-}Si(OCH2CH_3)_3 < \quad R\text{-}Si(OCH_3)_3 < R\text{-}SiCl_3$$

The alkoxysilane is less reactivity than chlorosilanes, which can react immediately on contact with a reactive group. The type of substitution on the silane is affected significantly by the generated bonded phase [52]. The most common types of chlorosilanes used for modification are dichlorosilanes, monochlorosilanes and trichlorosilanes. The dichlorosilanes and trichlorosilanes are not widely used with silica monolith because both of them consist of a high number of reactive groups and this can cause cross – linking with other chlorosilanes leading to the formation of multilayers which decreases the permeability of the silica monolith. Monochlorosilanes are widely utilised for the silica surface modification with octylsilane C8 or octadecylsilane C_{18} phases to end - capping the active sites [49].

C_{18} phase modification of silica monolith columns is commonly carried out applying monochlorosilanes, for example, chlorodimethyloctadecylsilane. This method is simple to apply under mild reaction as described by Xie *et al.* [104]. For that, the monochlorosilanes were used for modification of the silica monolith with the C_{18} in this project [105].

1.8 Characterisation of monoliths

There are many methods used to characterise stationary phases. The evaluation of the extraction efficiency (percentage of recovery of the analytes) and chromatographic performance (retention time) are the most common method applied. There however other techniques that can be used to study the morphological, chemical and physical properties such as nitrogen physisorption analysis and scanning electron microscopy - energy

dispersive X-ray spectroscopy (SEM – EDX). In considering the extraction process, it is vital to link between the morphology and extraction efficiency.

1.8.1 Nitrogen physisorption method

The physisorption technique is used to determine the physical characteristics of a silica monoliths such as the surface area and the pore size. This technique depends on the adsorption of nitrogen gas by the monolith at a constant temperature. To measure the surface area of the monolithic silica, structure a combination of vacuum, flowing gas and heat are applied to remove adsorbed contaminants acquired maybe from water vapour or carbon dioxide from the atmosphere. The vacuum is used to cool the solid sample at – 195 °C and liquid nitrogen is usually used in this process. After each amount of gas is adsorbed, the pressure is allowed the system to equilibrate, and then calculate the quantity adsorbed. The definition of the quantity adsorbed at each temperature and pressure is "an adsorption isotherm, from which the quantity of gas required to form a monolayer over the external surface of the solid, is determined". The known the area covered by adsorbed gas molecule use to calculate the surface area [106].

In the adsorption process, the reversible changes are usually producing according to van der walls forces. The applied pressure is controlling the amount of gas adsorbed on the surface, so the quantity of adsorbed gas uses to calculate the surface area of the silica monolith. The equilibrium pressure (P) occur when the pressure of the gas adsorption process stops and the amount of desorbed molecules is equal to the amount of adsorbed molecules and these applied in the calculation to find out the surface area of the silica monolith by physical adsorption of gas molecules. The isotherm measurement in the range from 0 to 1 can calculate at the relative equilibrium pressure (P/P_0), where P_0 represent the saturation pressure of the adsorptive gas which is nitrogen. Plotting the relative pressure (P/P_0) against the amount of adsorptive give the measurement of the isotherm curve, which is a function of pore size and pore volume [100b]. The International

Union of Pure and Applied Chemistry (IUPAC) is classified the isotherm curves to six types as illustrated in Figure 1-11.

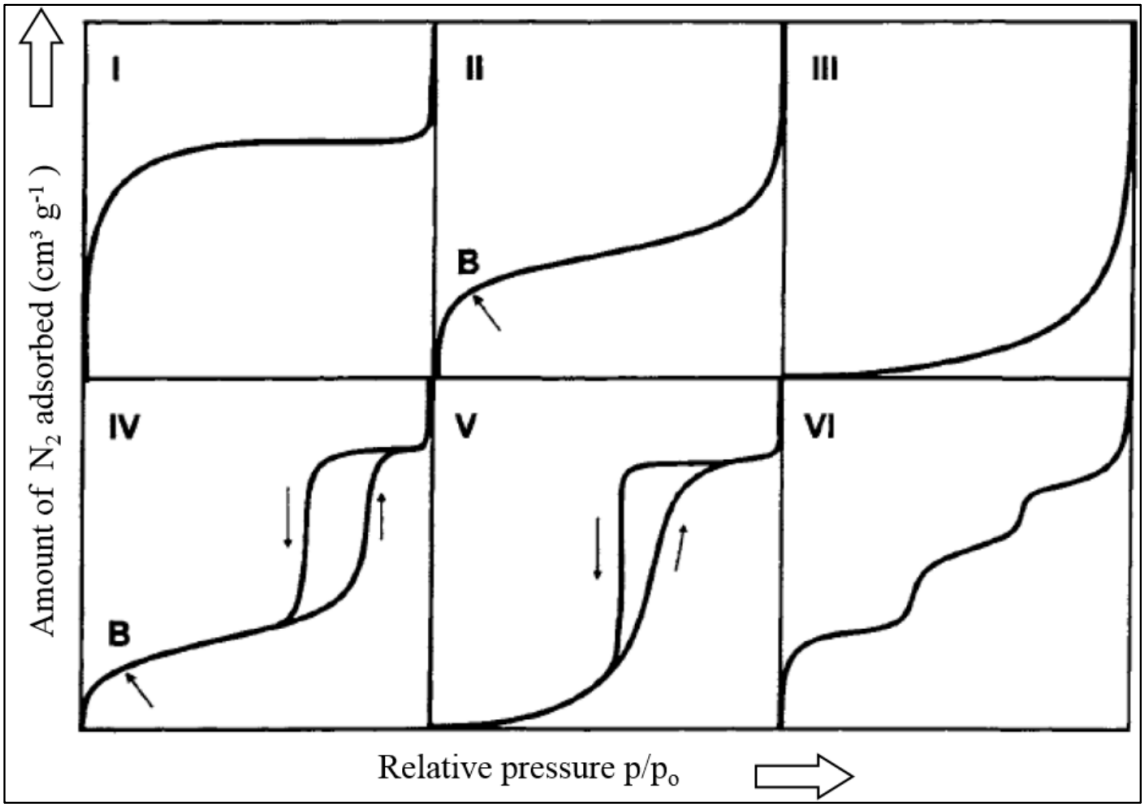

Figure 1-11: Six different shapes of sorption isotherm as IUPAC classified types (I – VI) [107].

Figure 1-11 shows the types of the isotherms, the types I isotherm curve shows a fast increase in the quantity of gas adsorption with growing the pressure until the saturation pressure. These gave for the adsorption of gas at solid containing a very small pore structure (pore size < 2) or is restricted to a monolayer such as microporous material [107]. Type II of the isotherm shows unrestricted monolayer – multilayer adsorption which is characteristic of macroporous (pore size > 50 nm) or non – porous absorbents as the result of a strong adsorption interactions. In Figure 1-11, point B indicates complete coverage of the monolayer and the beginning of adsorption in multilayer [107]. Type III isotherms are obtained as the result of a feeble adsorption interaction for non – pours forms. Type V isotherm can provide information about the presence of mesopores because of hysteresis loop where adsorption interaction is shown in the curve of this type. Type IV

isotherm shows a strong adsorption interaction because present of the mesoporous materials (pore size between 2 to 50 nm). The isotherm of type IV shows a hysteresis loop because of the existence of the mesopores and a limited uptake above the extent of relatively high pressure (P/P_0). The monolayer and multilayer cause the first point in type IV is similar to type II isotherm shape of the surface area which given adsorptive on the similar of non – porous adsorbent [107-108].

1.8.2 Scanning electron microscopy - energy dispersive X-ray spectroscopy (SEM – EDX)

SEM is considered as the most important method to study the structure of morphological for the silica monolith. SEM, also provide a determination of the homogeneity of the silica monolith structure and the size of the through pore. This technique can be connected with (EDX) to become a very powerful technique to analyse the elemental composition of the monolithic silica.

EDX is a technique which depends on the interaction between the X-ray source and sample. The characterisation of this method has a unique atomic structure that gives specific X-ray emission spectrum for each element. The x-ray beam focused on the sample which led to exciting the electron in an inner shell; therefore, ejecting it from the shell which creating the electron hole. Another electron from outer shell moves to fill the place in the inner shell and the different in energy between higher and lower shells is released to form of an X-ray emitted. In general, sample preparation requires the destruction of the column or solid sample for SEM – EDX analysis [109].

1.8.3 Extraction performance

The determination of the changing in the extraction efficiency is one of the simplest methods to study the influence of the modification process without required to shatter the monolithic structure. The modification procedure on the solid surface will change the

extraction behaviour of the materials monolith. As explained previously, when the silica monolith surface is modified with C_{18} it shifts from normal to reversed phase to give more hydrophobic interactions with the analytes [50].

Perez – Fernandez *et al.*[110] evaluated a C_{18} monolithic silica sorbent synthesised by mixing TEOS with poly (ethylene glycol) - block – poly (propylene glycol) – block – poly (ethylenene glycol) in acidic media. This sorbent used to extract and pre – concentrate the mixture for seven compounds of steroid hormones in a milk sample. The HPLC – DAD, was used as detection methods in this study. The extraction efficiency for each compound was determined based on the calibration curve for each compound which it was in the range between 88% to 108%), and this method achieved linearity (R^2 > 0.994 for 0.03 – 0.42 µg mL^{-1}).

Galan-Cono *et al.* [111] evaluated the pre – concentration of a mixture of PAHs compounds using methacrylate base monolithic column that was prepared in a 6 cm × 0.32 mm i.d. fused capillary column. GC system equipped with mass spectrometry detection (quadrupole mass analysis) applied as the detection system in this study. The methods to calculate the pre – concentration was dependent on the calibration curve for each analyte that prepared from standards concentration ranging from 2.8 ng L^{-1} to 11.5 ng L^{-1} with linearity reached to R^2 0.99 with some analytes.

In this project, HPLC was used to evaluate the performance of the monolithic silica modified with C_{18}. The extracted sample did not need further treatment when using HPLC compare with GC, as the mobile phase can be used to elute the analyte and this reduces the backgrounds noise in the chromatogram that would use as blank.

In the HPLC system, optimise the separation process factor are required to achieve a good separation result. The composition of mobile phase and the optimum wavelength are the main factors in HPLC – UV system, as used in this project.

Equation 1-3 can be used to calculate the extraction recovery as reported by Miyazaki *et al.* [112].

$$Extraction\ recovery\ (\%) = \frac{I_{elute}}{I_{total}} \times 100 \qquad \text{Equation 1-3}$$

Where I_{elute} is the quantity of analyte eluted from the sorbent with a suitable solvent and I_{total} the quantity of analyte introduced in the sorbent. The value of extraction recovery can be found from the calibration curve of the analyte that obtained by HPLC for serial known standards of analyte [111].

1.9 Detecting organic pollutants in environmental water samples.

As mentioned in section 1.1.5 the analysis of the trace level of pollutants requires highly sensitive and selective sophisticated analytical techniques, such as GC/FID, GC/MS, HPLC/UV, HPLC MS/MS and ICP – MS, as these methods provide highly accurate and precise results. However, these techniques require highly qualified technicians, expensive equipment, and a laboratory [42]. In the last 25 years, many publications have focused on the development of an alternative method to analyse the pollutants in water, aiming to improve the sensitivity, the analysis time; accuracy and selectivity because the environmental water sample usually contain matrices. To completely remove all the matrix from samples especially at trace level, is very hard even using modern sample preparation techniques. To overcome this selectivity issue immunoassays have been used. These are an analytical technique which exploits the interaction between antibodies and an antigen *via* the well-established "lock and key" mechanism, which means the antibody interact only with a certain antigen, this is ideal for applications where selectivity is paramount. Immunoassay as an analytical technique is vastly used in most of the analysis fields, because of its offered many features such as high selectivity, rapid procedure, high

sensitivity, and possible analysis of difficult complex without extensive pre-treatment [113] [11].

1.10 Antibodies and Immunoassay detection

The first immunoassay as a detection method to appear was in the 1950s when Yalow *et al.* used it to detect human insulin in pictogram (pg/L) concentrations in blood sample [114] and since then it has been widely used in clinical chemistry. Using the immunoassay technique for environmental applications began in the 1970s [115], after that the number of publications on the development and application of immunoassay for environmental analysis has rapidly increased [42].

For analysis of a mixture of chemicals organic pollutants such as benzo (a) pyrene, progesterone and β-estradiol successfully in a water sample at the trace level found without chromatographic separation, a specific technique is needed. Immunoassays are suitable for this aim.

1.10.1 Antibodies

Antibodies are specific proteins, known as immunoglobulins, which are generated by human and animal bodies in response to pathogens. Antibodies, like all proteins, have amine and carboxylic acid groups, which are produced in B-cells as part of the immune system [116]. The antibodies can be classified into different kinds depending on their role and response in destroying pathogens. They are two main classes of immunoglobulins, IgG which are major components of the immune system as they are found in blood, and are the most abundant of all the immunoglobulins. Also, the antibodies are the heaviest with weight beginning at 150 kDa. The second type is IgM which is physically the largest antibodies, and are the first to appear in response to initial exposure to antigens; the three other classes are indicated to as IgE, IgD and IgA [117]. In this work, only IgG antibodies were used because they are the most abundant of all the immunoglobulins and present in

all bodily fluids, for that they are commonly used in immunoassays. The antibodies have a Y – shape, with two similar light chains and two similar heavy chains. The heavy chains are formed with nearly 450 polypeptide residues, while the light chains have approximately 210 polypeptide residues, where the disulphide bond connecting the chains together as shown in Figure 1-12 [118].

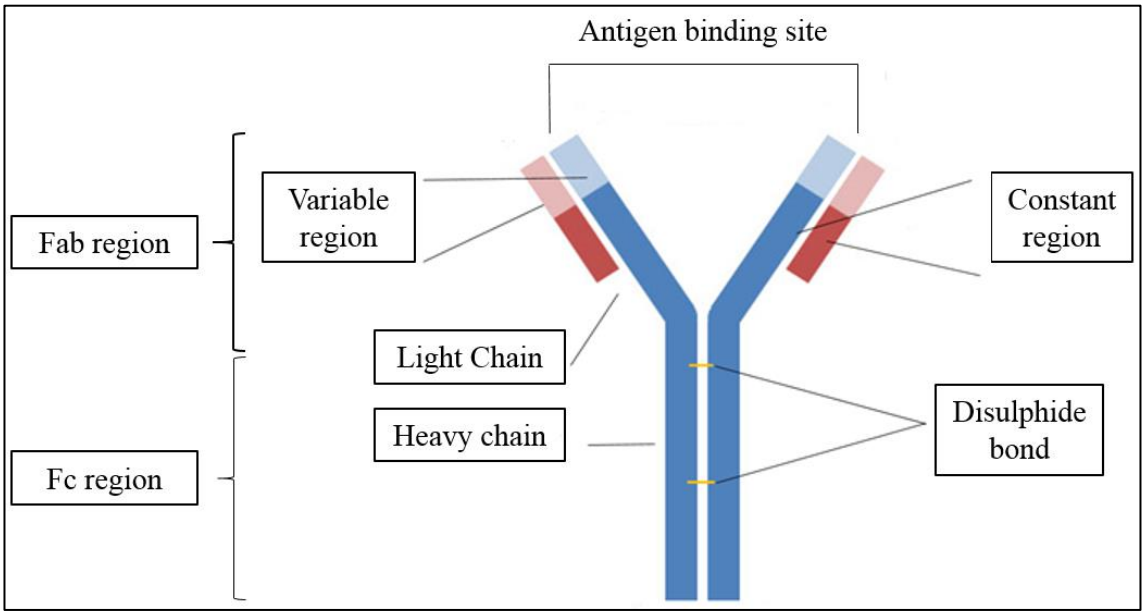

Figure 1-12: Antibody structure [118]

The general structure of the antibody shows two main regions, fragment antigen binding (Fab) and fragment crystallisation (Fc). Fab region is located at the top of antibody, which contains the both light and heavy chain. In this region the antigen becomes bound to the antibody due to the paratope is placed in this area. The paratope is the part of the antibody which it responsible for recognises the epitope of the target antigen, as a lock and key. The region of Fc is responsible for the antibody produce the suitable immune response through binding certain Fc receptors [119]. As any protein chain include amino acids, the acid groups are located at Fc region (C-terminal), wherein Fab region the amino group present (N-terminal). Therefore the antibody has different side chain that placed all over the structure [120].

1.10.2 Monoclonal and polyclonal antibodies

The different sites that antibodies can bind to the target antigen are called epitopes. Based on these, the antibodies can be classified into two types of antibody target, where the polyclonal antibodies which are a mixture of all the various antibody that can attack the different of epitopes on the antigen. While another type is monoclonal antibodies which target specific epitopes.

In nature, the monoclonal antibodies do not exist in humans, due to the human body produce several of antibodies during an infection occur to attack the pathogen and bind to all the epitopes. Nevertheless, the monoclonal antibodies are preferred to use in experimental work because they provide increasing the selectivity, thereby increasing the sensitivity and improve the reproducibility. In contrast, the polyclonal antibodies produce a different batch; therefore, it becomes very difficult to achieve a good reproducibility. In addition, it required a high sensitivity between each batch. In the mid-seventies, Kohler *et al.* were the first work to produce monoclonal antibody [121]. The disadvantage to using the monoclonal antibodies is they are more expensive because they are more specific which make the production process complex. However, the monoclonal antibodies are the most popular to use in the laboratory as the monoclonal antibody reacts with only one antigen, which makes it simply to identify [119].

1.11 Immunoassay

Immunoassays are a specific type of biochemical test based on the principle of the antibody – antigen reaction when the antibody binds to a specific antigen [122]. There are many types of biochemical interactions between antibodies and antigens. The stability of antibody – antigen interaction depends on the hydrogen bond, and other weak interactions such as electrostatic forces, hydrophobic interactions and van der Waals forces which also play a significant role in the interaction between the antibody and the

antigen regions [123]. Immunoassays are used for quantitative or qualitative analysis of small molecules in a many various fields, such as biological research, proteomics, environmental studies, pharmaceutical research and medical diagnostics. The major Investigation of immunoassays based on tags (either on the antibody or the antigen) such as fluorescent, enzyme or radio tags to produce a measurable signal [124]. However, the detection methods as surface plasmon resonance can be tag free [125]. Immunoassays can be classified into two major types – heterogeneous and homogeneous.

1.11.1 Homogeneous immunoassay

In a homogeneous immunoassay, the assay is carried out in solution, where both the antibody or antigen carry a tag and chemical or physical change arises from antibody – antigen complex. The feature of this method is that separation of the free antigen from the antibody-antigen bound complex are not required [126]. However, measuring the immunoassay response for multiplexing at the same time is challenging using this method. Chen *et al.* [127] analysed two different type of viruses (Enterovirus 71 and Coxsackievirus B3), where the antibodies were labelled using quantum dots to change the fluorescence response from the antibodies by emitting the light at a different wavelength and use this emission to quantify.

This method has some disadvantage as the sample matrix will still be existing and might causes interference for the result in complex detection systems as this shown in the work that done by Akhavan-Tafti et al.[126] In this work, the chemiluminescence homogeneous immunoassay through a sandwich immunoassay was successfully developed, where one type of the antibody that ladled with horseradish peroxidase (HRP) and the second antibody contained an acridan based label. In this works interleukin-8 (IL-8) successfully detected and achieved a LOD of 0.64 pg mL-1. The systems work with a “trigger solution” that contains hydrogen peroxide and p-hydroxycinnamic acid, a combination of this solution along with HRP and an acridan complex is needed to give the CL signal. It was

reasoned that the high sensitivity was achieved because as an immunological complex the acridan and HRP were in close proximity and thus in larger concentrations relative to each other compared to the bulk solution. However, this work not suitable for multiplexing analysis, which needs to be a way of generating different responses from each of the hormone-antigen complexes. For that, is difficult and time consuming to apply this technique for measuring a mixture of organic chemicals in polluted water.

1.11.2 Heterogeneous immunoassay

Heterogeneous immunoassay involves the immobilisation of the antibodies onto the solid support surface, where the antigen then reacts with the antibody at a boundary layer [124]. Once the process to antibody immobilisation on the solid support surface is complete, the surface is washed to remove any unbounded antibodies from the surface. Also when the sample added, the antigen need times to completion the interaction with the antibody (incubation time) the surfaced washed again to remove unbounded antigen or residues species [128]. Blocking the surface in the area where the antibodies are not bound important step to ensure the antigen does not adsorb onto the surface. Detection can be achieved with a wide range of laboratory equipment or also smartphone cameras allowing the potential of spatial resolution [129]. The advantage of this technique is increasing a sensitivity and selectivity towards its target as reduce the possibility of interference occur on the solid support surface [130]. Based on this advantages the heterogeneous immunoassay used in this project.

1.11.3 Competitive and non – competitive immunoassay

The heterogeneous immunoassay can also be classified into competitive and non – competitive immunoassay. Non – competitive immunoassay is often in the form of enzyme-linked assays (ELISA) as shown in Figure 1-13, where the sample is added to the immobilised antibodies on the solid support surface and interacts for some time to complete the incubate process to form the antibody – antigen complex. After that, a

second antibody labelled with an enzyme such as horseradish peroxidase (HRP) is added and binds to antibody – antigen complex to form which known as "sandwich format" and this step required time to complete the incubation step. The surface is then washed to remove unbounded secondary antibodies and finally, the substrate is added and the signal detected. The concentration of the analyte in this method based on the intensity of response to signal, which means the signal intensity increase with increasing the analyte concentration[131]. This method is consuming time because it required completing the incubation process twice, also with uses second antibody which mean extra cost.

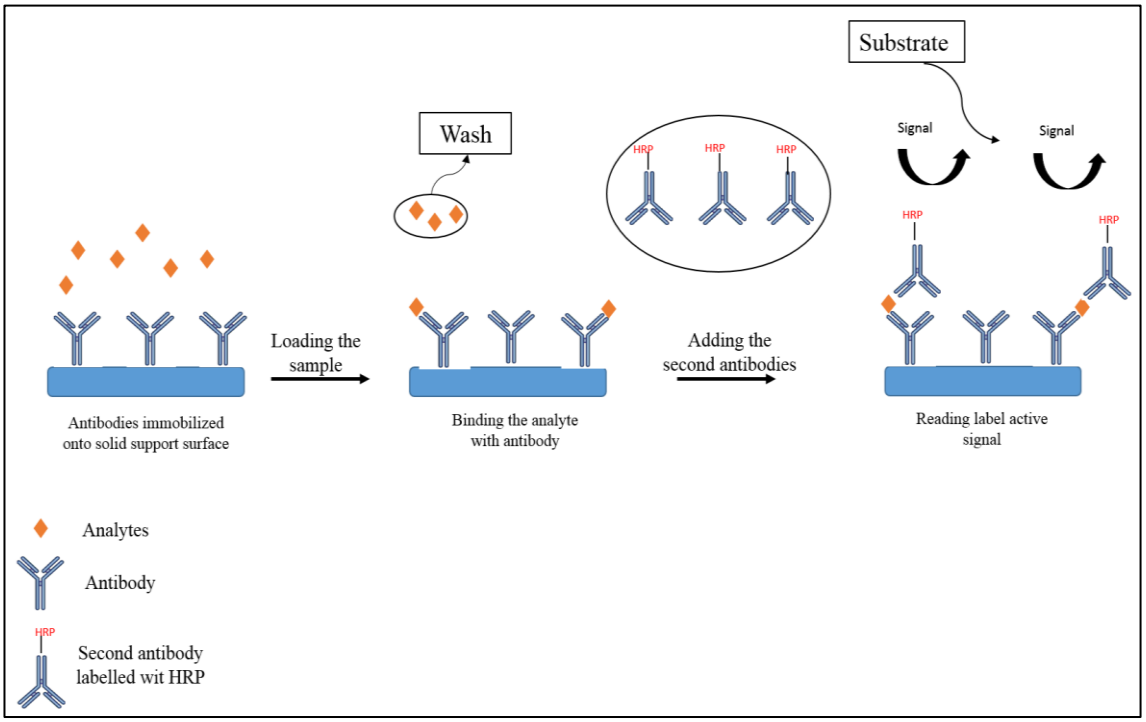

Figure 1-13: Heterogeneous non – competitive immunoassay [131]

In a heterogeneous competitive immunoassay the antibody is immobilised onto the solid support surface, then a mixture of the analyte (unlabelled antigen) and labelled antigen (HRP) that is in known amounts is added to the antibodies as explained in Figure 1-14. The complete process occurs between and the analyte from the sample and the tagged analyte version of the similar analyte during the incubation time. After a suitable time, the solid support surface is washed with a buffer to remove unbound antigen and finally, a substrate such as luminol and hydrogen peroxide is added to measure the signal.

Depending on the intensity of the signal detected the concentration of the analyte can determine [131].

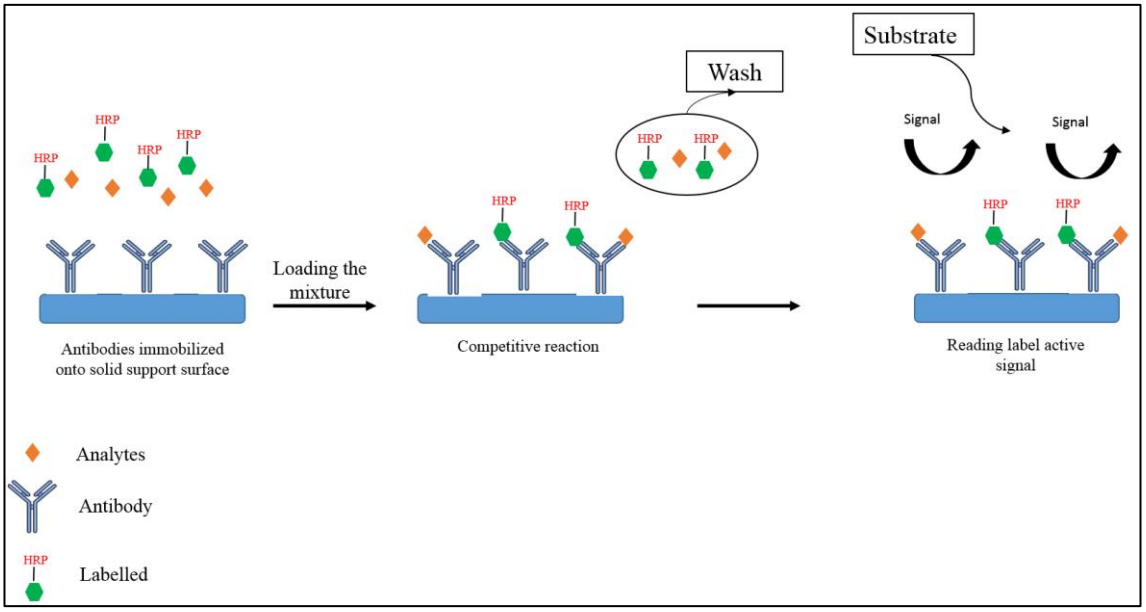

Figure 1-14: Heterogeneous competitive immunoassay [131]

The most widely used method to analyse progesterone and β-estradiol is enzyme-linked immunosorbent assay (ELISA), where Hou *et al*. were used this technique combine with chemluminescence detection to analysis of these hormones in drinking water, where LOD for analytes were in the range 58.09 – 84.96 pg mL^{-1}[132]. Also Pechenitza et al. were used the ELISA to determine the benzo (a) pyrene in vegetable oil and applied the molecular imprinted polymer (MIP) for sample preparation, this method determanied the benzo(a) pyrene at ng mL^{-1} level [133]. ELISA technique usually occurred in 96 – well microtire plate where this method is working by tagging the antigen or antibody with catalysing which usually be an enzyme to enhance the reaction to give rise signal that is measured. This process required four successive steps involved delivery of analyte and antibody, mixing, incubation followed by washing to remove unbound antibodies or analyte and detection. Measurements of the analyte concentration in the sample or attest presence the analyte in the sample can be achieved with using this technique. However, the drawbacks of this method are a labour-intensive and very time-consuming because of the long-time

of the incubation, due to the analyte particles have to spread across long distances before they encounter antibodies on the surface[134].

1.11.4 Detection methods used immunoassay system

Many detection applications which can be used with immunoassays, which have already been mentioned. In the last few years, most of the works focused on the detecting of the points of antibody antigen reaction happens. In general, the traditional way based on added the chemical species to the antibody or antigen to produce the signal that can be detected. Fluorescence, electrochemical, chemiluminescence and radiolabels are the most common label used with immunoassay system.

1.11.4.1 Label-free immunoassay

The main label-free techniques are surface plasmon resonance (SPR). This SPR technique relies on the measuring any changes to the surface interface. Usually, a gold surface is used to immobilise the antibodies and light are emitted to the surface, and it is refracted to a detector before and after loaded the analyte. Any interaction is occurring between the antibody and antigen lead to a change in the surface; the detector measures the difference in the change of the refracted light. The SPR being widely used in laboratories, but this technique is not applied extensively in the environmental analysis field, on account of the long-time procedure and the background signal that observed uncontrollable resulting of non-specific binding [135].

1.11.4.2 Labelled immunoassay

Many different tags have been used to give a measurable response when binding between the antibodies or antigens has occurred. The radioimmunoassay labels were used to perform sensitive immunoassays that include the labelling the antibody or antigen with a radiolabel. Tritium (H^3) or Iodine 125 (I^{125}) are the most common tags uses, as their half-lives are 12.26 years, 60 days consecutively. To measuring the radiation emitted, a

scintillation counter is widely used. The principle of working for this method by replacing any iodine species into the I^{125} isotope, therefore the antigen is largely unchanged; this converted species is of known concentration. It then competes with the same antigen in an unknown sample, and any unbound antigen is washed away with the radiation emitted measured. Stronger radiations with a higher number of tagged bound antibodies indicates a lower concentration in the sample. The method works very well, but working with radioactive material is dangerous, and the possibility of radiation damage to the sample is very high [136]. Based on these disadvantages the fluorescence labels have become the most common labels used.

A fluorescent dye can be used as the label with the antibody or antigen. Radiation is emitted by using a strong light source to irradiate the label as a laser. This method is used with both homogeneous and heterogeneous immunoassays where the tagged antigen competes with an untagged antigen, and the fluorescent intensity is measured and compared to determine either the concentration or the presence of the antigen. The disadvantage of this method is required to use powerful external light source for a to achieved high sensitivity [137]. Also the fluorescent not suitable for portable system device because it need special site to get accurate result. Electrochemical and chemiluminescent labels have been widely used to overcome this disadvantage.

Electrochemistry labels depend on a redox active species which is used as a tag for the antibody, antigen or even the analyte. An electrochemical cell is required to measure the reduction and oxidation activity of the label. The redox species is oxidised or reduce when a potential is usually applied to the electrode on which the antibody is immobilised, and this lead to changing in current, where this changing measured to find out the concentration of an analyte. The several redox species tags can be used such as ferrocene, [138] copper and ruthenium[139].

Chemiluminescence provides an extremely sensitive labelling method. Horseradish peroxidase (HRP) is a very common label used in chemiluminescence that can catalyse the breakdown of peroxide. HRP found in horseradish and has high sensitivity, and it is widely available tagged with antibodies [118]. When this label is used with luminol and hydrogen peroxide light is emitted which can be measured with no requirement for an external light source as will explain in section 1.13.2.1. Another tag involved to utilise of gold nanoparticles or any combination of these to assist multiplexing [140].

1.11.5 Immobilization the antibody onto solid support surface

In order to achieve a successful heterogeneous immunoassay, the antibody needs to be immobilised onto a solid support surface. The easiest way to immobilise the antibody on a surface is physical adsorption through intermolecular forces such as hydrogen bond interaction or electrostatic, van der Waals forces. These types of interaction are reversible where the environmental condition plays a vital role, for example, pH, temperature, and surface condition [141]. The problem is the antibody can be easily removed from the surface because the interaction is weak, so this approach is not usually suitable for analysis because this would affect the sensitivity of the result. [142].

When using the antibodies for analysis, they are usually attached to the solid support surface through a covalent bond using a reactive surface and the binding is usually irreversible. The amino acid residues on the antibody can interact with the active surface to make the irreversible linkage, where the end of spacer molecule is connected to the activated surface through covalent bond and after that, the antibody is connected to the other end of the spacer which is depend on the type of the surface use [143].

There are many types of the substrates that can be used to immobilize the antibody on it that including metal, plastic, magnets and glass. For glass, the most common technique

used to immobilise the antibody onto the surface involves the use of an organosilane reagent that use as crosslinker between the surface and the antibody[144].

1.11.6 Plastic substrates for antibody immobilisation

Most of the work carried out in the plastic are based on the physical adsorption which requires the antibodies to be prepared in a coating buffer. Many types of plastic have been used as substrates for antibody immobilisation. Polystyrene is widely used as explained previously in 1.11.3 where routine immunoassay work currently is carried out in polystyrene 96 well plate through an ELISA.

Many parameters should be taken an account for passive adsorption of the antibodies onto the solid support surface. These parameters that effect adsorption involved pH, temperature, the natural hydrophobicity of the antibody and it is concentration [118]. Dixit *et al.* described the use of polymethylmethacrylate (PMMA) and cyclic olefin copolymer (COC) to immobilise the antibody through covalent bond and compare both types with polystyrene. The result of this experiment showed a successful method to immobilise the antibody in all three types through a covalent bond. Also, their result concluded that the results were different between each substrate. In this method, a bottomless 96 well plate was used and the bottom consisted of a polymer was used which under investigation. Each well was washed with ethanol and then added 1 % w/v KOH at 37 °C for 1 hour to form OH groups on the polymer surface. Each surface was then modified with 2 % v/v of 3-aminopropyl-triethoxysilane (APTMS) for 1 hour at 80 °C. After that, the plate was washed with buffer and the solution of antibodies were added using 1-ethyl-3-(3-dimethylamonipropyl) carbodiimide (EDC) and sulfo - N-hydroxysuccinimide (sulfo – NHS as linker) [145].

The process of immobilisation of the antibody onto the polystyrene surface was explained clearly by Shi-Qi where the results showed the total time taken to completion the process

of the first addition of the antibodies into the well until analysis can carry out which was three days, which is a very long time required [146]. Polystyrene is preferable for use with 96 well plates, in spite of it not being appropriate to use for microfluidic devices. Also, Young *et al.*[147] reported the complex fabrication techniques needed. Moreover, polystyrene is also susceptible to leaching of bioactive materials, so the polystyrene not suitable for lab work and all the another work were focused on using anther types of the polymer as cyclic olefin copolymer (COC) and poly (methyl methacrylate) (PMMA).

In the field fabrication of microfluidic devices, PMMA is widely used as it easy to fabricate and cheap to produce. Also, the surface modification is easy with several different methods that led to antibody immobilisation. Various methods to modify PMMA surface were discussed by Goddard *et al*. including using 3 M sulphuric acid or 10 M sodium hydroxide to hydrolysis ester group on the surface to the formation of a carboxylic acid group in the surface [148]. This type of modification was used be Yang *et al.* to immobilisation based on activated the acid groups with an NHS to form NHS ester [149]. Also Brown *et al.* and Goddard *et al.* explained the method that used ethylene diamine (1 M) in dimethyl sulfoxide to amination of the surface directly [148, 150].

Goddard discussed the most common methods for activation of a polymer surface by using plasma surface treatment, where the process of the plasma depend on using oxygen under a large voltage [148]. This method is based on making the surface hydrophilic by forming (OH^-) groups on the surface. This method can be used widely with the different type of plastics, and it avoided to use any chemicals, but the drawback of this technique is required observance of many parameters to enable the surface to be modified for immobilisation of the antibody. Also, the stability of PMMA with an organic solvent is feeble, which means it not suitable to use in this work as an organic solvent is used to introduce the sample onto the chip.

COC is a popular polymer used for lab on a chip formats. But the surface of this polymer is free of any functional groups for immobilisation the antibody *via* covalent binding, and several approaches have been taken to find the best way to modify the polymer surface. One of this method was described by Diaz-Quijada *et al.* it depends on activation the surface by using an ozonolysis process, where the chip placed in an ozone generator for one hour as a result of this the carboxylic acid groups are formed successfully on the surface which made the surface ready for immobilisation of antibody using activation buffer with EDC and NHS [151]. Raj *et al.* used an oxygen plasma to activate the COC surface by exposing it to the oxygen plasma for 15 minutes at 150 W. After that the COC slides were modified with APTMS (3 %) in methanol: water (95:5), after that the succinimidyl-4-(N-maleimidomethyl) cyclohexane-1-carboxylate (sulfo-SMCC) which was utilised as a linker to bind the antibodies onto the polymer surface. Where the amide bond was formed as the result of interaction between the amine groups on the antibody and ester group in the sulfo – SMCC [152]. As mention previously with PMMA the parameters of the process to treatment the surface of the COC by oxygen plasma need to monitor to avoid damage the COC surface, however, COC showed high stability with an organic solvent, for this reason, is used in this project.

1.11.7 Glass substrates for antibody immobilisation

The process of antibody immobilisation onto glass has been had inducted to be difficult, because of During the immobilisation procedure, many factors have to be considered when selecting the appropriate method for an antibody, in this work the IgG form of antibodies used. [153].

1.11.7.1 Commercialised functional group slides

Commercial glass slides offered the range of glass surface already contain the desired functional groups such as maleimide groups, and alkyne groups are commercially available through many of companies. Zheng *et al.* used epoxide derivatized glass slides

(USArroy®, USA). A sandwich immunoassay was successfully carried out, where 500 µg mL^{-1} of antibodies was immobilised onto a surface [154]. This type of glass surface has been tested under a good condition which makes the immobilisation producer simpler, but all this comes at an additional expense, also in this project a specifically designed substrate was required.

1.11.7.2 Silanising reagents

The hydroxyl group (OH) is naturally present in the glass surfaces that makes the surface hydrophilic. Modifying the glass surface to present the appropriate functional groups on the surface that allow to immobilising the antibody on the surface is required to changing the surface to become hydrophobic which stops the antibody spreading. This target can be carried out by using silane reagent, and the glass surface needs to be sufficiently cleaned before the start in silanization process to increase the possibility of interaction of the silane reagent with the surface to form a uniform monolayer on the surface. There are many methods applied to clean the glass surface. However the method of cleaning the glass microscope slides was repeated by Crass *et al.* to prepare it for silanization, where they used a mixture of hydrochloric acid and methanol for washing, followed by submersion in concentrated sulphuric acid to ensure remove any surface contaminants effectively[155].

To immobilise the antibody on glass surface, there are many silanizing reagents which can be utilised, and the majority of silanizing methods based on a cross-linker to link the antibody onto the surface. Successful immobilisation of antibodies on the surface has been reported by using thiol, epoxy and amino terminal silane reagents such as 3-aminopropyl-triethoxysilane (APTMS), mercaptopropyltrimethoxysilane (MTS) and 3-glycidoxyproply-trimethoxysilane (GPTMS). The silanisation protocol is easily affected by the quantity of water existing in the system and it quite difficult to form a high-quality monolayer [144].

1.11.7.3 3-aminopropyl-trimethoxysilane (APTMS)

The hydroxyl functional group on glass surface bind to APTMS through an amine functional group, the proteins make covalent linkage at the other end of APTMS. There are many of solvent have utilised to insert APTES onto a glass surface such as acetone [156], toluene [157] and ethanol [158].

This method depends on immersing the glass slide into APTMS solution, and after that curing the glass slid in an oven at a temperature between 80 °C and 110 °C. The original solvent is used to wash the glass slide to remove unbound reagent. After finishing the surface modification process, crosslinking reagents are used to facilitate the process of antibody immobilisation. The common crosslinking reagent has used 1-ethyl-3-(3-dimethylamonipropyl) carbodiimide (EDC), glutaraldehyde and N-hydroxysuccinimide (NHS), and [154].

Glutaraldehyde is a bis – aldehyde compound utilised as a cross-linker with two amino group, where one of this group interact with silanised surface and the other group interact with the amino group in the antibody. However, Lake *et al.* described the disadvantage of this method, where it shows high variations in the number of cell immobilisation between batches and the reproducibility of the results have been shown to be the effect when stored because of the compound can self-polymerise. Therefore, this cross – linker not suitable for this work [159].

The most common cross-linkers that have been used to immobilise the antibody onto an APTMS surface recently are NHS and EDC. EDC is a carbodiimide that uses to activate the carboxylic acid (COOH) in the antibody to form an o – acylisourea ester. This ester can interact with an amine group on the surface to form an amide bond. NHS and EDC or its sulphinate derivative are soluble in the water, which led to directly used with the antibody in the aqueous buffer. The drawback of use EDC is the reaction of o – acylisourea ester with amines is too slow where it can hydrolyse in the aqueous solution

[160]. To overcome this issue usually added the NHS or sulphated derivative that led to creating an NHS ester, then the antibody can react with the amino derivatized surface to make the amide bond [159]. Akkoyn et al. used this reagent to active the carboxymethyl group on the silnised surface to immobilise dextran and the same reagent was used again to activate the antibody to immobilise dextran. There is incubation time before adding the antibody to the glass slide to allow the activation to occur, wherein Akkoyan *et al.* method to immobilise the antibody in 7 minutes was applied to an 80/20 mM solution of EDC and NHS before starting the process [157]. There are several of ways have been used based on this principle. The method depend on using only NHS ester was repeated by Mendoza *et al.* to interact the amino group on the antibody with the amino group on the surface to form linkage and this method was achieved by using bis – sulfo – succinimidyl substrate [158].

1.11.7.4 3-glycidoxyproply-trimethoxysilane (GPTMS)

The nature of glass surface would change to hydrophilic with using GPTMS as cover the surface with an epoxide group, and the amino group in the antibody can then be immobilised on the surface at alkaline pH [161]. For example of the use of this cross-linker, cancer biomarkers in an immunoassay were detected on a glass substrate by Mathias *et al.*, where the glass slides were immersed in a mixture solution containing 2.5 % GPTMS and10 mM glacial acetic acid in ethanol for 1 hour. Then the ethanol was used to washing the glass slide and dried by nitrogen gas. The immobilisation of the antibodies on the glass slides were carried out under glycerol buffer which consisted of 5 % glycerol in phosphate buffer saline (PBS) and left at 4 °C for overnight. Finally, the glass chip was ready to use without further steps, required and the advantage of this method was it did not need to use any linkers [162]. Another advantage of use this method is the protocol not complicated, stable at neutral pH range and easy to forms strong bond the antibody.

However, this method required a high concentration of epoxide and additional functional group to increase the antibody immobilisation opportunity [142].

1.11.7.5 Mercaptopropyltrimethoxysilane (MPTS)

MPTS forms thiol groups on the glass surface which lead to the formation of disulphide linkage between the glass surface and the sulphur group on the antibody. A chemical reduction step is required in this immobilisation procedure to cleave the disulphide bridge in the hinge region of antibody. These yields fragment with both light and heavy chains containing free thiol groups, where the fragmentation procedure is produced by either proteolytic enzymes or decreasing agents as tris (2-carboxyethyl) phosphine hydrochloride (TCEP)) and 2-mercaptoethylamine (2-MEA). The low molecular fragments are isolated from native antibodies after complete fragmentation process through using a nitrocellulose membrane or column chromatography [160-161].

Kusenezow *et al.* reported the use of a different silanizing procedure with MPTS. The glass slides were made up with 1 % MPTS and a solution of acetic acid 10 mM in ethanol was used to wash the glass slide as well. This procedure was applied using a linker and also without it, where the linker that was used was a maleimido-R-N-succinimidylesters where the R here represent the different functional group. The results showed the high reproducibility obtained when R = $(CH_2)_2NHCO(C_6H_{10})CH_3$ in linker used compared to the results achieved when R group was propyl, ethyl or cyclohexyl group due to a different in the structures. Also, when no linker was used poorer result was obtained [163].

Neves – Peterson *et al.* reported the advantage of using this procedure for immobilisation of the antibody where it can control the orientation of the antibody. However, the significant disadvantage comes from the process of splitting the antibody which is required in this procedure [161].

1.11.8 Other types of substrate used for antibody immobilisation

Other types of substrates have been used for heterogeneous immunoassays; gold is one of the materials that has worked very well for antibody immobilisation by adsorption *via* it native thiol groups. This interaction on a gold surface is known to be very stable due to the affinity of the thiol group of the antibody to the gold surface which achieved through present of a thiol group and using a bifunctional linker with it. Alternatively, the gold surface can be used directly to immobilise the antibody without any preparation of the surface, but this method requires the antibody to be split in half to generate free thiol groups. This approach hasn't been widely used because of the sensitivity of the antibody would be loss as the result of the process to complications in splitting the antibody [164].

Another method applied to immobilisation of the antibodies on a gold surface was carried out by Vashist, where the gold surface was modified with APTMS and sulfo – NHS with EDC were used as linker [165]. In this method, surface plasmon resonance was used as the detection technique that is favored as a detection method for gold substrates. However as mentioned previously in section 1.11.4.1 the SPR is not suitable for environmental analysis and the gold electrode is expensive which mean using the gold in the environmental analysis economically inefficient [164].

Electrochemistry is another detection technique used for immunoassays with a gold substrate, where the measurement of this method based on a shift in current or potential, which is an effect of adding the antigen. The gold electrode was used by Dou *et al.* were modified its surface to make a layer of free amino groups on the surface and after that, the activation buffer made up by EDC and sulfo – NHS was used as a linker for antibody [138]. In this process, the antibody was modified as well to label with ferrocene to provide the electrochemistry response. Changing in the current was observed by a voltammetric measurements which were made to determine the effect of adding the antigen. This

method achieved strong reproducibility and high sensitivity with LOD of 23 pg^{-1} mL^{-1} for detected of a creatine kinase protein.

Magnetic particles have also been used as a substrate for heterogeneous immunoassay. The magnetic particles usually include a magnetic core with a polystyrene coating; these particles are commercially available with a various functional group. The advantage of using these particles is their spatial position can be controlled with a magnet that has a great benefit in microfluidic systems where the particles can be held inside the channel of the microfluidic device and not affected by the flow. Zhang *et al.* [166] was used magnetic particles made up with chitosan / Fe_3O_4 to generate an immunosensor by, where chitosan / Fe_3O_4 magnetic particles were used with glutaraldehyde as cross-linker, detection was achieved by electrogenerated chemiluminescence with quantum dot labels. This drawback with approach is that it is hard to analysis for several species at once.

Another material used for antibody immobilisation is silicon; Yakoleva *et al*. used three different type of reagents that include the APTES, 3 – glycidoxypropyltrimethoxysilane (GOPS) and linear polyethylenimine (LPEI) to silanised a silicon microchip. The glutaraldehyde was utilised as a cross-linker to covalent immobilisation of the antibody on the surface [167].

1.11.9 Antibody orientation

There is much discussion about how the orientation of the antibody on the substrate surface affects performance. The Fab region of the antibody is contain the epitope region, so with random antibody immobilisation as see in Figure 1-15 (A) the antibody-antigen interaction will not be consistent and this will influence the sensitivity and the reproducibility of the analysis process as it is never clear how many of the antibodies are orientated in a way that will interact with the sample. Therefore there has been extensive

work into looking at ways into how to orientate antibodies in a way that will enable all antibodies present to interact with the sample as shown in Figure 1-15 (B).

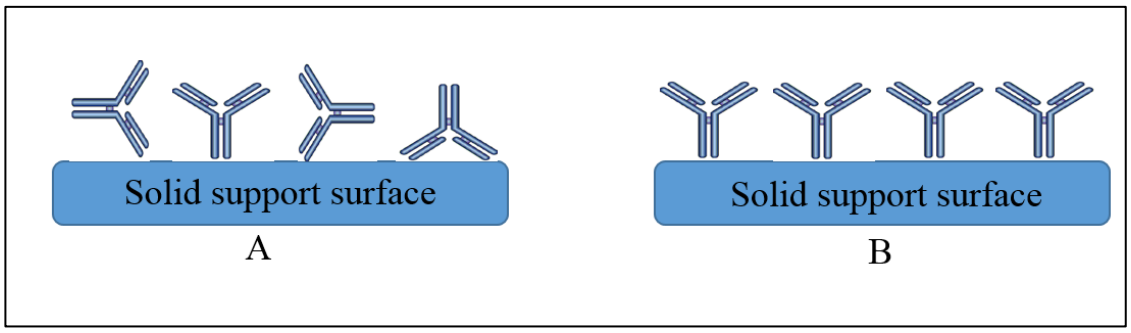

Figure 1-15: The ways of immobilisation the antibodies onto the solid support surface, (A) random orientation and (B) ideal orientation.

To guarantee the ideal orientation of the antibody on the solid support surface a commercial company (ThermoScientific ™) claims to provide a procedure to overcome all the problem of antibody orientation. This protocol depends on modification the sulphur group to lead the binding to occur through it. A maleimide cross-linker was used in this method, as it can interact with the thiol group in the antibody, where this method based on obtaining the thiol group through reducing the disulfide bonds. The procedure of this method depends on breaking the disulfide bridges which bind the two part of the antibody together with 2-mercaptoethylamine used to form the corresponding thiol, where this idea taken from the bioconjugate techniques [168]. The antibodies need to be used promptly to avoid reduce the reformation of the disulfide bonds. This technique can provide to control the orientation of the antibody as an advantage. However, a significant disadvantage is the antibody apart required to break, which reduces the activity of the antibody which reflecting on the sensitivity of the immunoassay, for that this method is not suitable to use in this project.

Another method used to improve the orientation of the antibody was to modify the carbohydrate moieties on the antibody. Gerin et al. presented this method where the substrate was a glass modified with an epoxysilane, after that the surface under an acidic

condition to increase a diol. In order to form an aldehyde functional group, the periodic acid was used to treat the diol to allow it reacted with adipic acid dihydrazide to obtain a free hydrazide group that interacted with the antibody. To prevent any interaction between any unreacted aldehyde groups on the surface and any exposed hydrazide group the sodium borohydride was used. To modify the antibody, the solution made up of 10 mM periodic acid, 150 mM NaCl and 20 mM sodium acetate buffer pH 5.0 was used to agitate it, and the ethylene glycol was added to stop the reaction. Purification of the antibodies was carried out through dialysis. Finally, two modified glass slides used to contained the antibodies at 4 ˚C [169].

The advantage of this method remains the antibody intact and allow to immobilised onto the surface, and remaining the activity and the sensitivity of it intact. Nevertheless this method requires extra care during the chemical modification of the antibody, because if any mistake occurs during the process, this can alter the antibodies and effect on its ability to operate. All of this reasons make this method not a widely used as antibodies are expensive material, and it is not desired to attempt to modify them in any way if other methods are possible.

The ferrocene tagged was used to improve the orientation of immobilisation for antibody on the gold disc electrode. Dou et al. developed this method where the gold disc electrode modified with polyaniline by electrochemical reduction of the diazonium salt. The antibody was chemically modified with ferrocene to allow the antibody bind to the surface through the activated carboxylic acid groups. This method achieved a high reproducibility with good sensitivity, and for this reason, it chose to use in this project [138].

1.12 Microfluidics

Microfluidics can be described as the process to handling of a small volume of liquid (10^{-6} to 10^{-15} L) in a network of channels with micrometre dimensions. Manz *et al.* were the first group introduced the term lab – on – a – chip in the early 1990s to explained the integration of multiple analytical processes on a single device, as sample preparation and detection [170]. As the result of the many advantages associated with use microfluidics, research in several different areas have applied this technique such as chemical or biological analysis [171], environmental analysis [172] and medical diagnostics [170-172].

Miniaturisation of analytical procedures into a small chip format include low fluid volume and has many features involving decrease in reagent and sample consumption, portability, low risk of sample contamination or loss, rapid analysis time and low cost [173]. However, the field of the microfluidic device still needs to more development to reach a practical real analysis value. The main reason for the difficulty in realising this is achieving a low – cost, sensitive, reproducible portable detection system in microfluidic device [174]. Despite this, lab-on-a-chip devices provide a great potential for the improvement of chemical pollutants in environmental application [175].

1.12.1 Microfabrication

Since first appearing microfluidic systems have been utilised extensively in many application [173], the characteristic of the material used in fabrication should be commensurate of the application to obtain the success result, for that a wide range of substrate materials have been developed [176]. Glass and silicon were the earliest materials used for microfluidic device, as both are easy to fabricate using standard methods such as photolithography with wet etching and their physiochemical properties. Furthermore, glass has high optical transparency and high chemical stability while the silicon has high thermal conductivity [177].

The glass and silicon are the most substrate use for fabrication the microfluidic device, where the method based on the photolithography with wet etching is widely applied with this substrate. The procedure of this technique depends on using a chromium metallic layer that a photoresist is a spin coated to covering the glass or silicon with over, and final step put a mask which contains the design of the channels as described by McCreedy [178]. The channel design firstly imprints onto the surface of the device rely on the UV light which penetrates the photoresist layer. After the channels are etched into the substrate surface, the chromium layer is then removed using a metal etch (typically hydrofluoric acid). The spin coating layer of sodium silicate used as adhesive to bond the cover plate onto the chip with heating the chip to complete the chip bonding [178]. The etching process is vital in the glass for that: it should note this processing is isotropic which make the walls not being parallel because it based on the etch solution that causes etching of the glass wall resulting in a non-uniform width across the channel. This fabrication technique has an accuracy of a few microns [179]. The procedure of this technique shown in Figure 1-16.

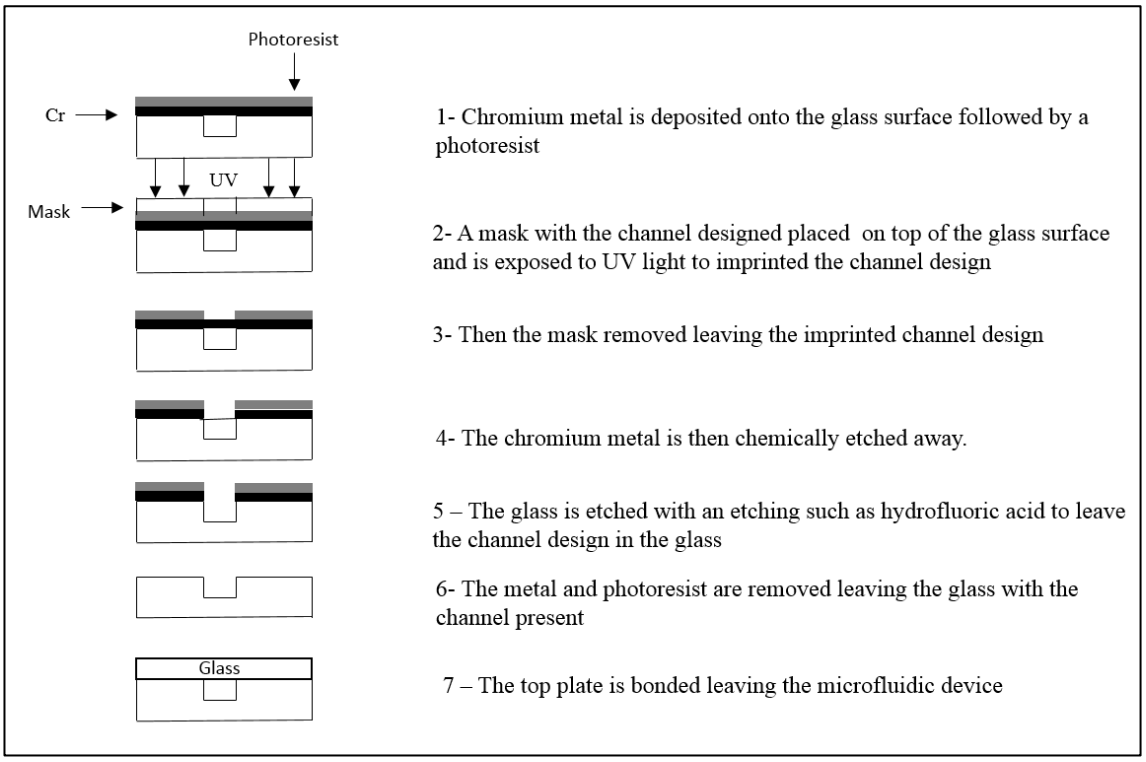

Figure 1-16: the process the fabrication of a glass microfluidic device.

There is some disadvantage using silicon and glass to make the microfluidic device, both types have low flexibilities and need harsh and chemical reagents as (HF) during etching. Also, glass microchips are breakable, and high temperatures are required for bonding (≤ 650 ºC) and there is a high cost of fabrication [180].

Polymeric materials can be used as alternatives of glass and silicon such as polymethyl methacrylate (PMMA), polydimethyalsiloxane (PDMS), polyetheretherketone (PEEK) and cycloolefin copolymer (COC). These have good advantages having optical transparency, are not easy to break, do not need cleanrooms to fabricate, have good mechanical flexibility, are easily processed and biocompatible [176]. Additionally, the low cost of the polymeric materials and the use of inexpensive techniques to fabricate such as hot embossing or injection moulding led to disposable devices [181].

Hot embossing is a technique which is based on the use of thermoplastic substrates such as COC and PMMS to form the flat sheets. In this process of this technique, a master

stamp is patterned against substrates using pressure and heat. This technique is simple and at their glass transition temperature (Tg) the thermoplastic can be reshaped [182]. However, the embossing stamp has to be prepared which is time – consuming, expensive, and specialised vacuum presses are required in embossing in order to remove air bubbles stuck between the stamp and the substrate because it can effect on the reproducibility of fabrication. The replication of embossing is poor when compare with the injection moulding [183].

The process of the injection moulding is based on the pre – polymerised pellets of a thermoplastic where the polymeric material is melted and after that injected into a mould cavity which is heated, and this step carried out under high pressure. Then the injected parts are cooled to under the Tg of the polymeric material and removed from the mould. The degree of contact is influenced by operational parameters such as pressure, temperature and residence time, which must be optimised. This method required just a few second to mould each piece of a microfluidic device with high throughput, this method is used widely in the plastic industry. A major disadvantage to the utilise of polymer substrates to fabricate the chip are not chemically stabilised with a some of the organic solvents [184].

1.12.2 On-chip fluid manipulation

There are several methods applied for movement of the liquids through the microchip. Hydrodynamic flow is the most common where a microfluidic device connected to a syringe pump through the tubing and connectors to stream liquids through the channel networks [185]. The frictional forces at the walls of the channels cause the parabolic flow of the liquids within the channel as shown in Figure 1-17 (A). The shape and the geometry of the channels and the inclusion of valves pressure affected the liquids flow [186]. The electrokinetic movement has also been used and is due to electroosmotic or electrophoretic forces that present in Figure 1-17 (B). Electroosmotic flow is described

by bulk on the application of an electric field movement based on the charged layer at the channel surface which occurs in glass device. The charge and size of the species affect the movement of species whether ion or non – charges towards cathode at a different rate [178]. Electrophoretic flow can be described by the movement of the solution under the influence of applied voltage potential. The velocity of an ion in unit field strength can be explained the mobility of an ion, where the ion at a various ratio of the charge to size, led to various electrophoretic movement and migrated at different velocities in channels during applied voltage[187]. The drawback of this technique is creating a Joule heating which causes on the band broadening and reduces the resolution of the separation. Also, the type of movement is form gas bubbles in the system because of electrolysis at the electrode, where it leads to breaking in the electric heating and the flow system. For that, the hydrodynamic forces selected to control the flow rate in this project [188].

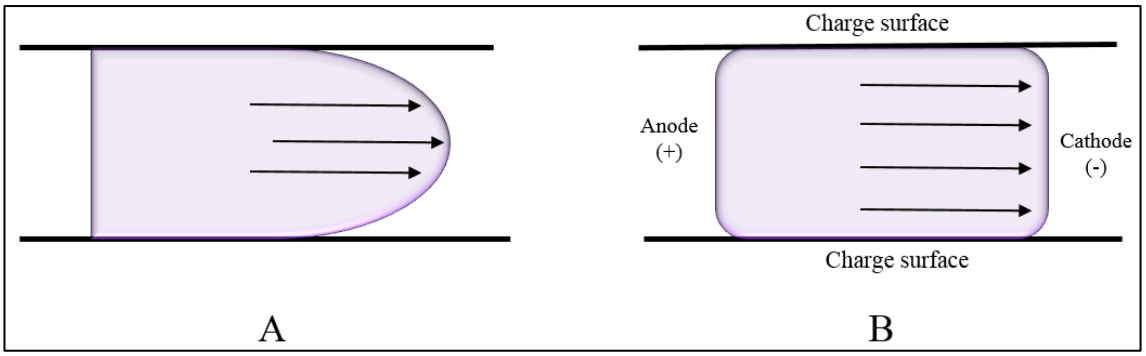

Figure 1-17 movement of the liquid inside the microfluidic channel,(A) a pressure flow of the solution movements in the centre of a channel and (B) the plug flow where the same velocity is exhibited for all molecules except for those very close to the internal surface wall when an electrical field is applied [189].

1.13 Microfluidic device for environmental analysis

Using the microfluidic devices in the environmental analysis has been become a trend that involves different procedures that include extraction, separation, and detection. The detection step is the most challenging and critical step of using the microfluidic for environmental analysis. In general, two major paths are applied for detection techniques

in microfluidic devices. The detection instruments can be integrated with the microfluidic device with or the microfluidic device can be contained to the detector itself [190]. In recent years, the application of the microfluidic device in the environmental analysis field has become attractive, with the low sample and reagents volume required, portability, low waste produce and rapid analysis time, low cost and possibility of carrying out multistep process with pre-treatment or separation of the sample combined with detection [191]. Portability can allow the analysis process to be achieved outside the laboratory which reduces the possibility of contaminating or degradation of the sample and saves the time [192].

The most attractive detection method in the environmental analysis are the advanced optical sensor, electrochemical, and spectroscopic detection methods on-chip to analysis a low concentration of the chemicals pollutants in complex environmental samples [191]. Electrochemical detection provides a sensitive low-cost detection capability [193]. Tanyanyiwa *et al.* described a device with electrophoretic separation and a contactless conductometric detection. PMMA was used to fabricate the device as shown in Figure 1-18 and the electrophoresis separation of a sample containing of sodium, potassium, rubidium and lithium was described. This method achieved LOD around 1.5 µmol L^{-1}. The construction of the device was simple, the detection technique prevented electrode fouling and a high sensitivity was observed. This device was also used to analyse iron (III), cobalt (II) and cadmium (II) with LOD 3.5, 2 and 8 µmol L^{-1} respectively. The technique was also used for the analysis of organic anions, especially the carboxylate: succinate, tartrate, acetate, lactate and oxalate with the LODs determined at 10, 7, 25, 30 and 4.4 µmol L^{-1} [194].

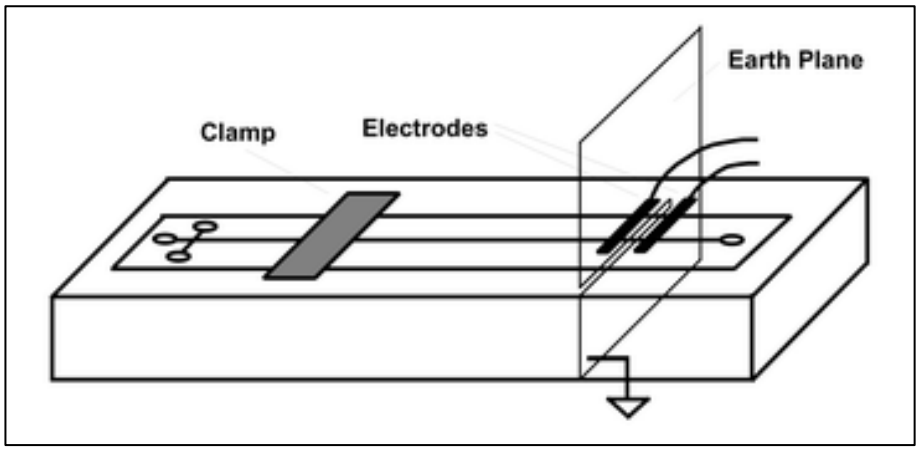

Figure 1-18: Diagram of the chip that use in this work [194]

Spectroscopic detection has also been widely used in microfluidic systems. The first used of the fibre optics coupled to an LED-photodiode depend on molybdenum blue spectrophotometric method with a miniaturised device to analysis orthophosphate in water was carried out by Daykin *et al.* with LOD 0.7 µg L^{-1} of PO_4^{3-} [195]. Beaton *at el*. presented of LOC system for the determination of nitrate (NO_3^-) and nitrite (NO_2^-) for *in suit* analysis of natural water (seawater). This system depends on the spectrophotometric techniques as detection, where the chip was three-absorption cell, one used as reference cell and two used as measurement cell. The chip was integrated a fluidic manifold that allows the selection of one of four standards of analytes and a blank. To control the fluidic, fifteen valves was used that are mounted directly to the chip as shown in Figure 1-19 . Especially designed for syringe pump utilised to pump fluid through three syringes for either sample and standard, where the buffer solution and Griess reagent that used for nitrite analysis. This system is achieved LOD at 1.6 ng mL^{-1} for NO_3^- and 0.92 ng mL^{-1} for NO_2^- [196].

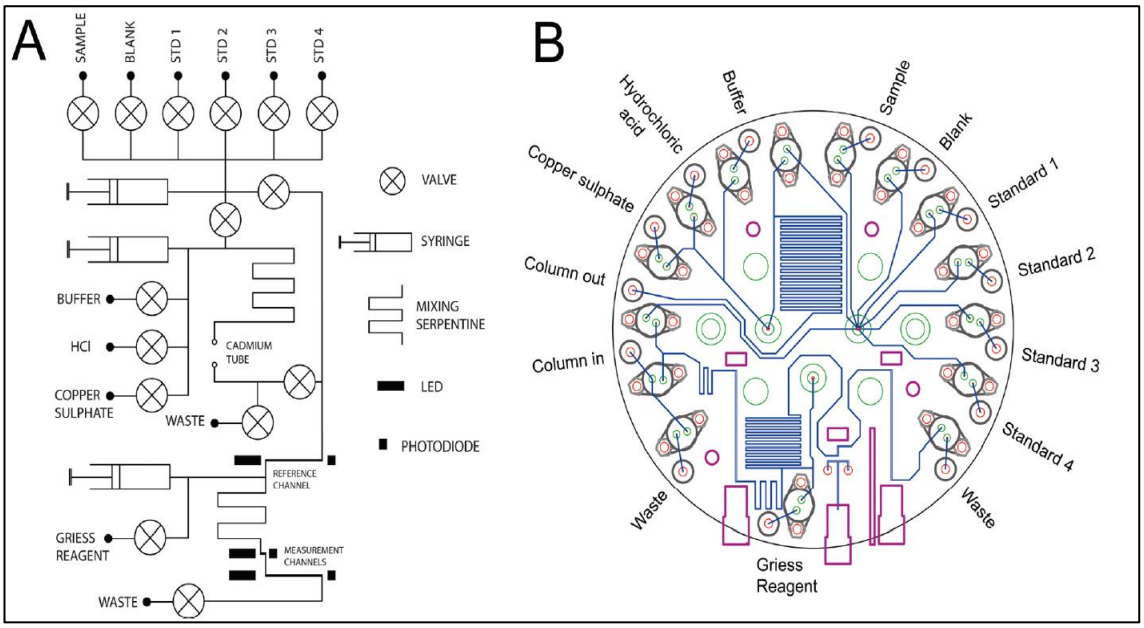

Figure 1-19: Beaton *et al.* LOC system for *in situ* analysis of nitrate and nitrite in natural water where (A) Fluidic path diagram indicating the three syringes, fifteen valves, and three absorption cells. (B) CAD drawing of the microfluidic chip with fluidic connections labelled [196]**.**

Fluorescence is one of the most commonly used detection methods with microfluidic device due to its high sensitive, Broyles *et al.* used this detection method with a quartz chip to determine a mixture of PAHs compounds in aqueous sample include pyrene, benzo (a) pyrene, 1,2-benzofluorene and anthracene, where the LOD were 1, 17, 8.1, 3.1 nmol L^{-1} [197].

1.13.1 Spectroscopic detection

The detection method depending on the spectroscopy is commonly used in the microfluidic systems due to a wide range of applications. The limitation of this detector comes from it is requirement that it needs the light source and reduced the path length of the channel which effect on the sensitivity. For that, the extensive variety of intense light-emitting diodes (LEDs) which can connect with a fibre optics has become strong the miniaturisation of spectrophotometers, and that can be incorporated into microfluidic devices [191].

As explained previously in 1.13, spectroscopic detection technique has been widely applied for quantitative analysis of environmental sample due to the availability of the spectroscopic instrumentation in the majority of laboratory [192]. Both absorbance and luminescence have been used with the microfluidic device [198]. Ultraviolet and Visible (UV-Vis) spectrophotometry is based on the absorbance of light in the frequency ranging of ultraviolet and visible 200 – 800 nm. An organic molecule absorbed the ultraviolet and visible light depend on natural of the functional groups (chromophores) that contain valence electrons of low excitation energy. This technique can be used in quantitative analysis determination via the absorbance of the specific wavelength of light as explained by the Beer – Lambert law [199].

$$A = log \frac{I_0}{I} = b \times C \times \varepsilon \qquad \text{Equation 1-4}^{[199]}$$

Where A is the absorbance, I_0 is the initial intensity of light before absorption, I is the intensity of light after absorption, b is the path length in cm; C is the molar concentration of the analyte and ε is molar absorptivity coefficient (M^{-1} cm^{-1}).

The drawback of combining this technique with microfluidic devices is the detection setup requires a light source to generate radiation at the appropriate wavelength, sample cell and the detector to monitor the intensity of the light. Also, the sensitivity of the analysis process decrease as the optical path length through sample decreases as described by the Beer – Lambert law [200].The UV range is not suitable to use with glass microfluidic as glass absorbs the UV light. All of these reasons contributed to reducing the application of the UV – Vis spectrometer as detection method with microfluidic. Alternatively, chemiluminescence or fluorescence based immunoassays can offer a high sensitive and selective method compared to the absorbance detection method.

1.13.2 Luminescence detection

Luminescence describes the process of re-emission the light as a result of the absorbance of incident light. Also, it can refer to fluorescence and phosphorescence. The Jablonski diagram is used to explained the energy levels of transition within a luminescent molecule as shown in Figure 1-20.

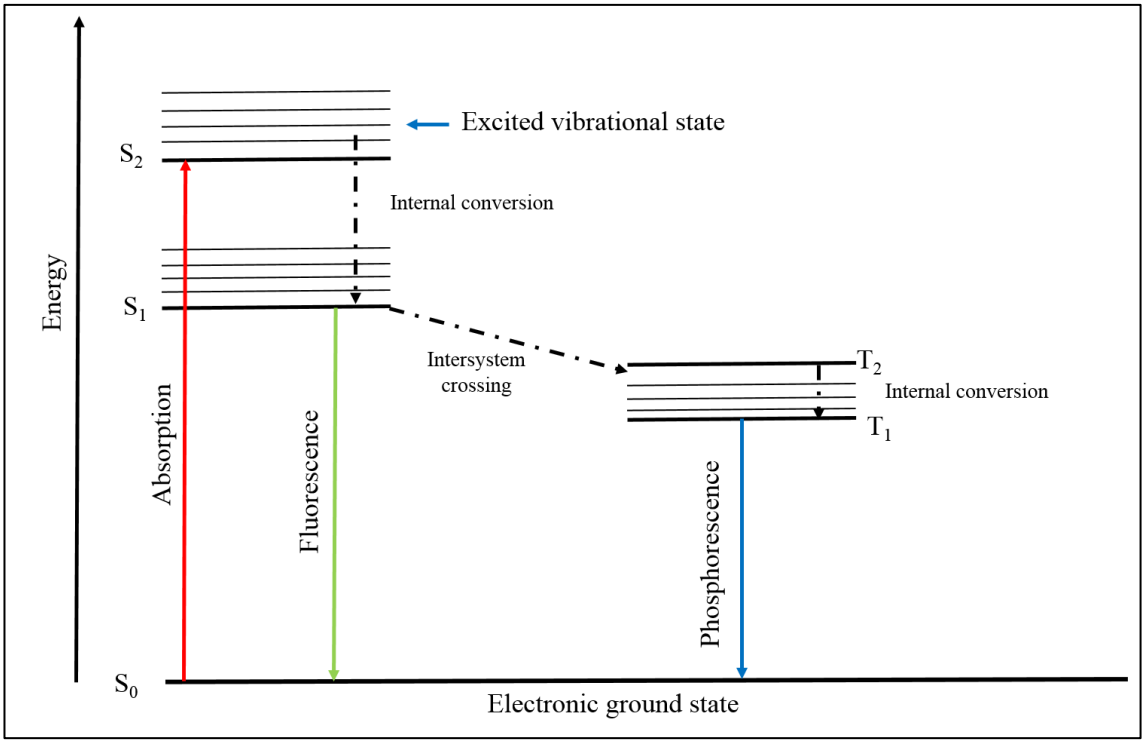

Figure 1-20: Jablonski diagram to explain the luminescence process [199]

The ground state S_0 that is indicated by a bold horizontal line in Figure 1-20 is the electronic states where including the most of the molecules in solution at normal condition, while the thin horizontal lines indicate the vibrational sublevels (S1 or S2). At the appropriate energy the photon interacts with molecules, the photon absorbed which cause to jump the electron to a higher energy level (S_1 or S_2). The electron in the original orbital can remain spin paired with an electron in a high state to form an electron in an 'excited singlet state' or, more unusually, this electron can be realigned parallel to the unpaired electron to form a molecule in a triplet excited state (T1 or T2). There are many ways of an electron in the excited state to dissipate their energy. The first way of release, the

electron energy is through vibrational relaxation results of the electrons lose it kinetic energy rapidly to the lowest level of the first excited state (S_1) through the process known as internal conversion. The kinetic energy might stay within the same molecule or transferred to another molecule around it in internal conversion as indicated by the fine arrow between vibrational levels in the Jablonski diagram. This transition process occurs very fast in range (10^{-14} to 10^{-11} S), for that it can happen immediately following absorbance [199].

In the case of the fluorescence and chemiluminescence, the electron falls from an excited singlet state to one of the sub-levels of the ground state (S_0) and the emitting the photon occur on a nanosecond time scale in range (10^{-9} – 10^{-8} S) [201]. In the case of the chemiluminescence emission, the wavelength based on the species excited in the chemical reaction. When the change in the electron spin to form a triplet excited state, occur cause to form the intersystem crossing. The phosphorescence occurs as the result of the emission process from a triplet state to a ground state. Phosphorescence is slower than the fluorescence with the lifetime of excited state from 10^{-4} to a few second. Chemiluminescent reactions involving triplet states are unusual because the production of a triplet state by a singlet-triplet transition involves a change of in electron spin [202].

In fluorescence, a photon is emitted after absorption light from an external source such as laser or lamp to produce an electronically excited singlet state (S_2). The energy of the emitted photon less than the absorbed photon and is at a longer wavelength and in this case there is no change in spin quantum number and the transition is spin allowed. For that, the emission of the fluorescence wavelength is based on the excitation wavelength [199].

As mentioned previously, the fluorescence is commonly techniques used for the environmental application. Equation 1-5 described the method of calculation the intensity of the fluorescence.

$$I = K\ P_0\ C$$ Equation 1-5[203]

Where c is the concentration of the emitting species (mol dm^{-3}), P_0 is the radiant power of the incident light and k is a constant and I is the intensity of the incident light. According to Equation 1-5, the intensity of light is proportionate to the radiant power, which means it can use to detect the analyte at very low concentrations depending on a powerful light source which led to being very sensitive technique [203]. The disadvantage of this technique is the light sources are expensive.

1.13.2.1 Chemiluminescence

In chemiluminescence (CL), light is emitted as a result of a chemical reaction, similar to fluorescence. Chemiluminescence detection has high sensitivity, as it does not require the light source and measurements made again at dark background reducing background noise. Chemiluminescence is suitable for lab on chip system as it sensitive and simple [204].

The chemiluminescence reaction can be classified into two types, direct and indirect chemiluminescence. In the indirect chemiluminescence, the energy transfers to another molecule (fluorophore) because the intermediate excited species is unable to release the energy by itself, and this re – emits the light. Where indirect chemiluminescence, the initial interaction between an oxidant and a substrate that be usually a chemiluminescence precursor (reductant) in the existence of co – factors to produce an intermediate electronic excited species. Figure 1-21 Shows both types of chemiluminescence reaction [201].

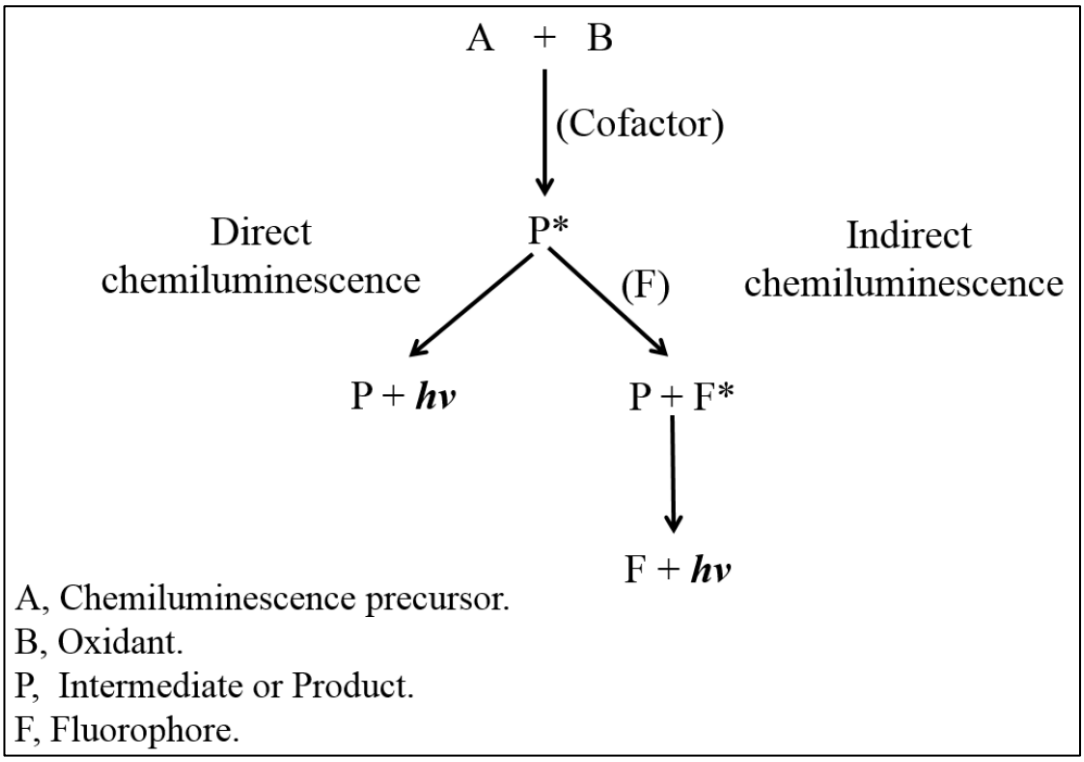

Figure 1-21: The two types of chemiluminescence reaction (direct and indirect reaction) [201].

To emit light from the chemical reaction there are essential requirements, whereas the reaction must be exothermic to generate enough energy, the free energy requirement can be calculated by using Equation 1-6 [202].

$$-\Delta G \geq \frac{hc}{\lambda_{ex}} = \frac{28600}{\lambda_{ex}} \qquad \text{Equation 1-6}^{[202]}$$

Where G: Gibbs energy, h: planck constant (m^2 kg s^{-1}, C: light speed m s^{-1} and λ_{ex} : wavelength m.

Therefore, the blue light emission produces sufficient amount energy of chemical reaction at approximately 300 kJ mol^{-1} while the red light emission around 150 kJ mol^{-1}. This amount of energy should enough to induce the transition of an electron from its ground state to an excited electronic state, and there must be sufficient energy in the reaction pathway. The reagent of chemiluminescence is usually linked with redox reactions using hydrogen peroxide or a similar oxidant. The intensity of light in the chemiluminescence

reaction process is based on the efficiency of the molecules to produce the excited state, that can be described by quantum efficiency or quantum yield and the Equation 1-6 expressed it [205].

$$I_{CL} = \phi_{CL} \frac{-dA}{dt}$$ Equation 1-7 [205]

The quantum yield of CL (ΦCL) can be defined as the product of three ratios as expressed in Equation 1-8.

$$\phi_{CL} = \phi_C . \phi_E . \phi_F$$ Equation 1-8 [205]

Where ΦC is the chemical yield for the fraction of reacting molecules giving an excited molecule, ΦE is the excitation yield for the fraction of such molecules in an electronically excited state and related to the efficiency of the energy transfer, and ΦF is the quantum yield of florescence for emitting a photon. For quantitative analysis, the intensity of emission in a CL process is a function of the concentrations involved in the CL reaction. The rate of the reaction is explained in Equation 1-6.

Chemiluminescence detection is significantly based on experimental parameters that influence on the quantum yield and the rate of reaction, such as the concentration and nature of the CL precursor, pH, the catalyst, ionic strength, temperature, and the solution composition. In addition, The CL detection can be applied to the measurement of a wide range of species that can participate in CL reactions.

Many types of the molecules have been used to give a rise of the chemiluminescence reaction, such as luminol, peroxylates, lophine, and oxalyl chloride. Luminol was chosen for the most chemiluminescence application due to it is commercially available with suitable cost and can be utilised in the aqueous condition. However, another type of molecules required an organic solvent which can be making interference with the analyte or generate a water insoluble product which caused blockages in the microfluidic device

channel [202]. Luminol is discussed further here as it used in this working due to for all its advantages and the iron compounds and HRP can catalyse the luminol reaction which applied in this project.

Luminol one of the most common molecule use to exhibit chemiluminescence reaction; the reaction was first published by Albrecht in 1928.[206], after that it has been studied extensively. Luminol must be in the alkaline solution, and it is oxidised by hydrogen peroxide or hypochlorite to exhibit chemiluminescence (CL) at 425 nm. The catalyst can be used to enhanced the reaction, and this catalyst can be enzymes or metals, where a several of the 3d metals can use as a catalyst such as manganese, cobalt, copper, and iron [202]. The luminol solution must be stored at the dark and cold place due to it sensitivity to light and thermally unstable[207]. Luminol is usually used with hydrogen peroxide, where the hydrogen peroxide works as an oxidising reagent. Figure 1-22 shown the mechanism of luminol and hydrogen peroxide reaction.

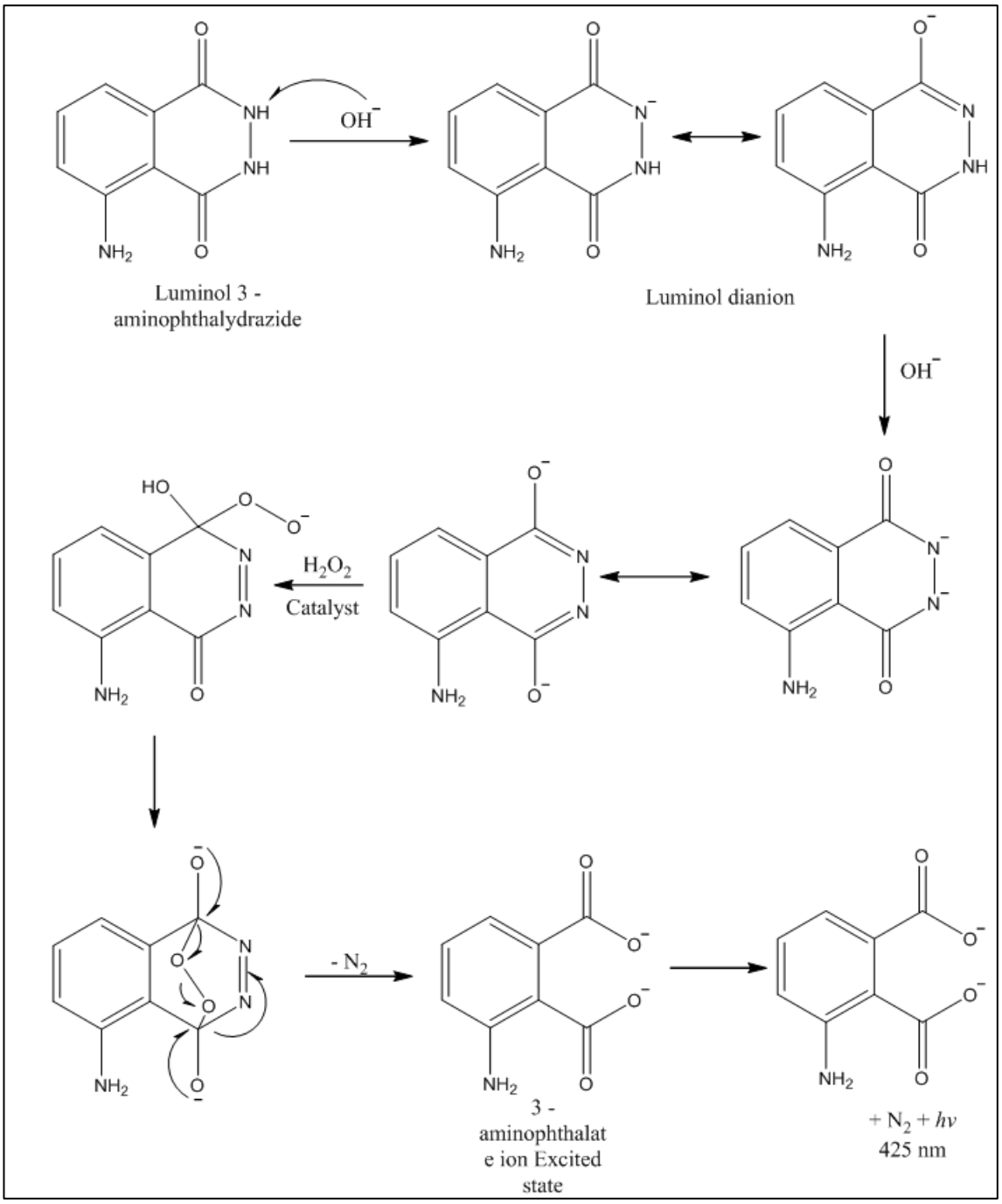

Figure 1-22: Mechanism for the chemiluminescent reaction of luminol with hydrogen peroxide [202].

As shown in Figure 1-22 the mechanism of the reaction luminol depends on the oxidation of it in an alkaline condition to produce the 3–aminophthalate ion at the excited state. To form the negative charge, the nitrogen photon removes due to the alkaline condition therefore the negative charge moves to the carbonyl oxygen and as the result of this the resonance-stabilised luminol dianion form. The hydrogen peroxide is oxidised with the luminol dianion in the present of the cooxidant agent such as ferrocene or HRP. in the

excited state, the 3-aminophthalate ion formed with accompanied by the loss of the nitrogen (N_2) and as result of this process the extra energy is emitted as a photon of light, after this process the molecule back to ground state [208]. The kinetics reaction of the luminol and hydrogen peroxide reaction is rapid as Lind explained the luminol and hydrogen peroxide reaction in aqueous solution can have a rate constant of 2 $x10^5$ s^{-1} [209].

This mechanism explained is one of the most reported in various references as well as within the literature. However, other mechanisms of the luminol reaction have been presented in the literature that deviates slightly from the one explained above [210].

1.13.2.2 Chemiluminescence detection

The chemiluminescence emission always carried out in the dark environment; it required a detector to collect this emission. Usually, there are two types of detector that used to achieve the analysis of chemiluminescence emission, or a charge coupled device (CCD) or the photomultiplier tube which often used in connected with a camera. The entire detector should be working in the range between 400 to 500 nm; due to the light range, luminol emits around 425 nm in aqueous media.

1.13.2.3 Photomultiplier tube

The photomultiplier tube is a type of luminometer detector that has very high sensitivity where is this a vacuum tube involving of an input window, focusing electrodes, an electron multiplier, a photocathode and an anode frequently sealed into an evacuated glass tube. The photocathode excites the electrons based on the light passes through the input so that photoelectrons are emitted into the vacuum. The secondary electron emission as the result of the photoelectrons is accelerated and focused by the focused electrode onto the first dynode where they are multiplied using. The last dynode emitted the multiplied secondary electrons and finally collected by the anode.

Appling the photomultiplier tube for detection mixture of compounds is more challenging because it required being coupled with a monochromator alongside where analytes would have to emit light at various wavelengths and then detected individually. These would make the detection system more complicated, for that, this detection systems are not applied in this work [202].

1.13.2.4 Charged – coupled device (CCD)

A CCD, which is a rectangular array of individual light – sensitive elements called pixels, which is built into a camera. Contrary to a photomultiplier where the signal is obtained from a constant flow of photons, CCD cameras obtain their image in two discrete steps. In the first step, photons interact with the pixels to create photoelectrons that show in step at Figure 1-23, then are stored and integrated into the pixels as shown in step 2 and 3. In the second step, the pixels are integrated and read giving an image, after which the pixels are reset for the next image as demonstrated in step 4, 5, 6 and 7 at Figure 1-23.

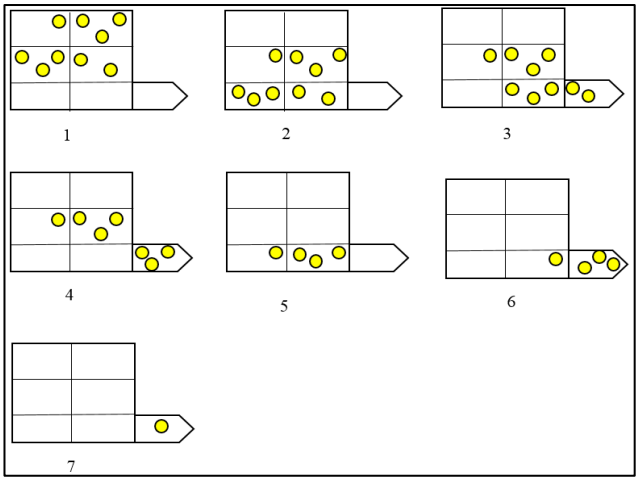

Figure 1-23: Operation of a CCD based on a 2 x 2 pixel chip, where the yellow circles represent photoelectrons that are stored within the pixels [202].

A huge advantage of using a CCD camera over a photomultiplier is that the CCD allows for multiplexing. Therefore, any such device could potential involve multiple antibodies for different applications which would not possible if using a photomultiplier alone [211].

1.13.3 Electrochemistry

In general, the electrochemistry method includes a solution that includes electrolyte and redox species, which is under determination. Depending on the potential applied to the electrochemical cell, redox species in solution undergo either reduction or oxidation. When the process of oxidisation occurs for a species, a positive current appears, and the opposite occurs when the species are reduced. The current is known as Faradaic current, and the Faraday's low of electrolysis is shown in the Equation 1-7

$$m = \left(\frac{Q}{F}\right)\left(\frac{M}{z}\right) \qquad \text{Equation 1-9}^{[212]}$$

Where m is the mass of the species released from the electrode surface (g), F is Faraday's constant (96485.4 C mol^{-1}), z is the number of electron transfer per ion, M is the molecular mass of the species (g mol^{-1}), and Q is the electrical charge passed through the substance (coulomb).

In the electrochemistry process, it is imperative to allow continuous charging of the electrode surface to allow it to produce the current. The current is commensurate to the redox species concentration in the solution and the constant flux of material happen through mass transfer [212].

Electrochemistry measurements accord a high possibility of control. Additionally, electrochemistry offers a high sensitivity with immunoassay as Liu *et al.* achieved LOD at fmol to analysis the proteins by used a sandwich immunoassay [213].

With microfluidic devices, electrochemistry can offer a low cost, simple, and very high sensitivity route to detect analytes, which the sensitivity is close to those seen with CL[214].

1.13.3.1 Electrochemistry detection

Three different electrodes are usually used for measuring the electrochemical redox. These involve a working electrode where the chemistry occurs, reference electrode where the potential is known to relate the measured potential against and gives the stability and a counter electrode which referred to as the auxiliary electrode where is the electrical circuit complete as the current flows between the counter and working electrode [215].

The reference electrode plays an essential role to include the working electrode produced the desired potential, and this is dependent on two factors, the electrical double layer at the working electrode which presents a large voltage to overcome and secondly, the solution resistance which results in Ohmic loss. The reference electrode must give the information back to the potentiostat to ensure the correct potential is applied to the detector. The reduction in the effect of Ohmic loss can be achieved by decreasing the concentration of the solution, using a smaller electrode radii and a slower scan rate applied [216].

1.13.3.2 Cyclic voltammetry

Cyclic voltammetry (CV) is an electrochemistry technique for determination of the electrochemistry behaviour of a system, where the voltage is swept to higher voltage and then returned to the original potential [217]. Figure 1-24 shows the cyclic voltammetry waveform when a scan occurs from V_1 to V_2 and then return to V_1 is representing one cycle.

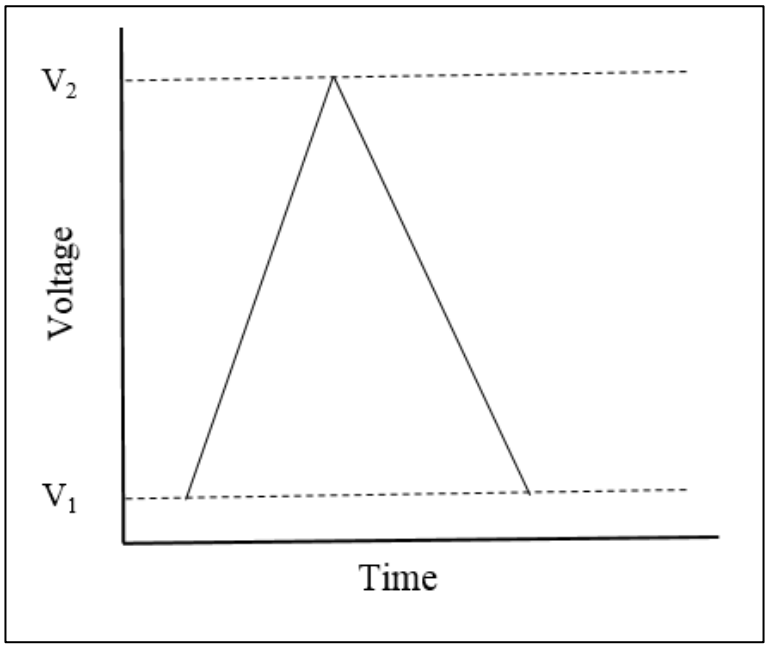

Figure 1-24: cyclic voltammetry waveform[217].

Experiments using cyclic voltammetry are carried out by setting the scan rate that measured in V s^{-1}. The scan rate can be rapid or slow base on the natural of the experiment; the scan rate determination allows characterization of an electrochemical system providing information about the diffusion coefficient and kinetic. Usually, an oxidation step is the first sweep which followed by a reduction, and this process occurs only with reversible reaction; however, only a single peak appeared if the system is irreversible for either reduction or oxidation. During the process, the current measurement usually is normal at the electrode surface area and referred to as the current density. The applied potential is plotted against the current density to make the cyclic voltammogram. The height and width of a peak in a particular process might base on the electrode material, the electrolyte concentration and the sweep rate [218]. Figure 1-25 show the example of a revisable cyclic voltammogram, where the voltammogram shows the and peak potentials and peak current for both the reduction and oxidation peaks at the surface of working electrodes where electrons are transferred between the sample (electrolyte) in solution and the electrodes, which are used to carry out the analysis [219].

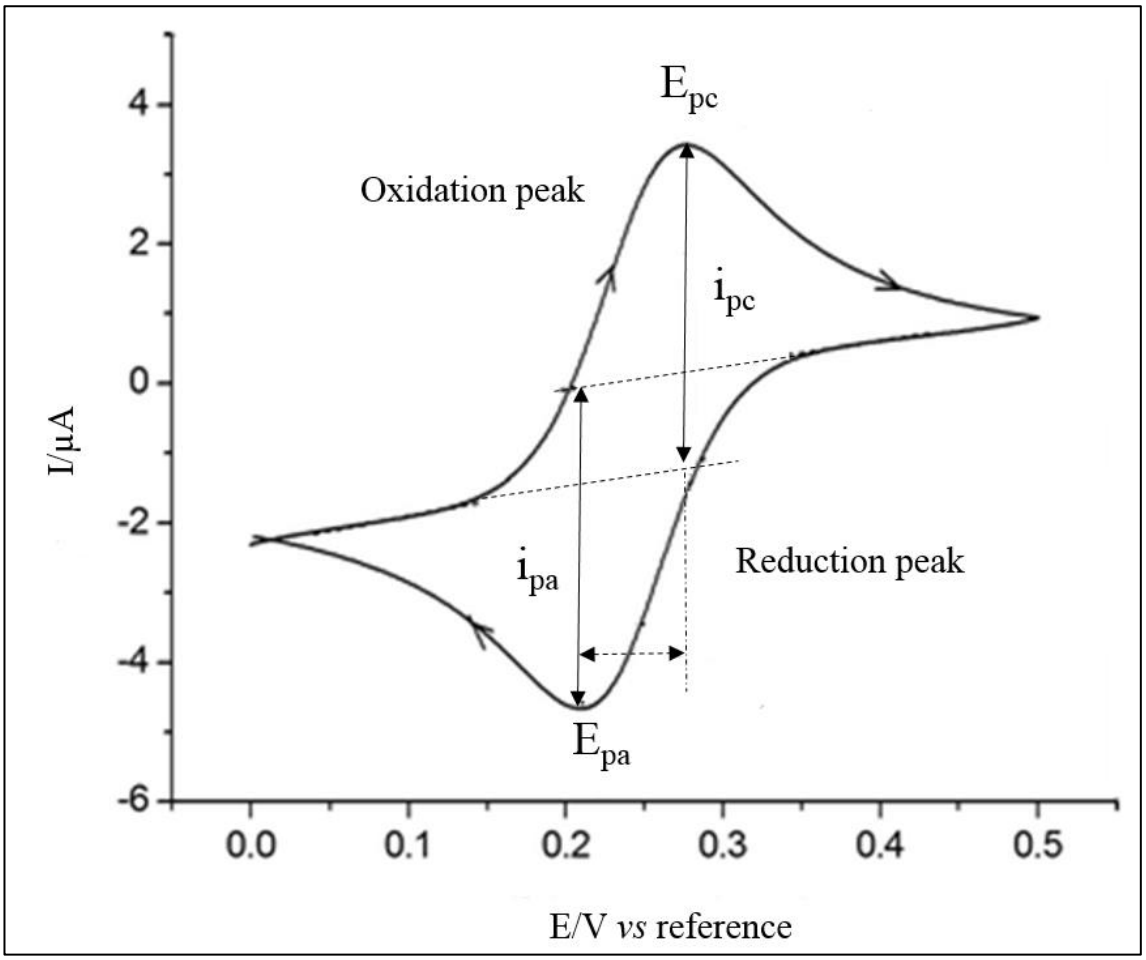

Figure 1-25: Example of reversible cyclic voltammotogrm, Where E_{pc} = peak cathodic potential; i_{pc} = peak cathodic current; E_{pa}= peak anodic potential, and i_{pa}=peak anodic current [218].

From the cyclic voltammogram, can be read the peak potential of the anodic (Epa) and peak potential for the cathodic peak (Epc) directly. The separation between peaks potentials for the reversible reaction is given by the Equation 1-10.

$$\Delta E = E_{pc} - E_{pa} = \frac{0.058}{n} V \qquad \text{Equation 1-10}^{[219]}$$

In the Equation 1-10 the n represent the number of a mole in the reversible reaction. The number of electron transfer in reversible reaction only can be measurement from the peaks separation. However, the ΔE it is difficult to calculate from completely irreversible processes, which are, provide only one potential peak. Therefore, a fast one electron transfer exhibits a ΔE at about 0.058 V. In addition, this value is difficult to achieve when the redox reaction is slow.

From the cyclic voltammogram and by using the Randles-Sevcik equation (Equation 1-11) can apply for quantitative analysis for analyte concentration. Equation 1-11 can be used for individual peaks current, *i*p (cathodic or anodic peak) in reversible and irreversible system.

$$i_p = \frac{n^2\ F^2\ V\ A\ D}{R\ T}$$ Equation 1-11[219]

Where D is analyte diffusion coefficient (cm2 sec^{-1}), v is scan rate, F is Faraday constant (96485 C mol^{-1}), n is number of electrons in the half-reaction for the redox couple, T is absolute temperature (K), R is universal gas constant (8.314 J mol-1 K^{-1}), C is concentration (mol cm^{-3}) and A is electrode area (cm^2). The Equation 1-11can be rewritten as following.

$$i_p = (2.687)n^{3/2}AD^{1/2}\ CV^{1/2}$$ Equation 1-12[219]

1.13.3.3 Square wave voltammetry

The first concept of Square wave voltammetry (SWV) appeared in 1952 by Barker and Jenkins[220]. However, the technology available at the time limited it is applicability. Recently, due to the significant development that has occurred for potentiostats which reflected SWA technique to become more available and it is widely used in an analytical field [221]. This technique provides high sensitivities that can be achieved, compared to cyclic voltammetry that makes it becoming popular in analytical chemists and the development of different fields systems.

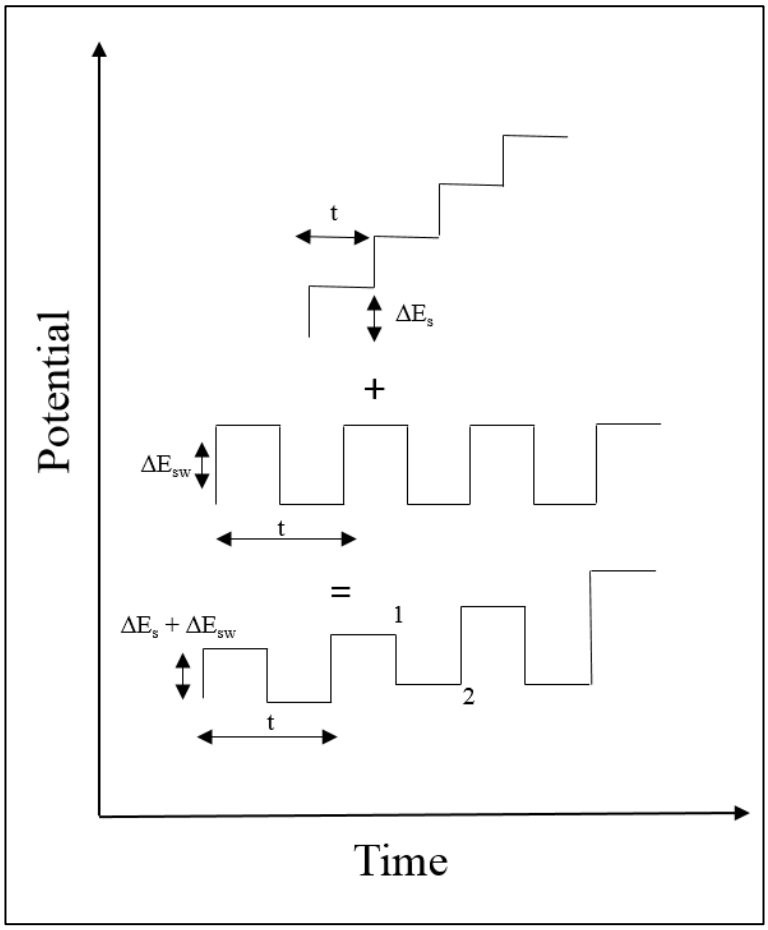

Figure 1-26: Diagram of the square wave waveform where a staircase waveform and square wave waveform are combined to show the overall square wave voltammetric waveform [222].

As shown in Figure 1-26 the square wave voltammetric waveform as a result of staircase waveform superimposed onto a square wave. The square wave signal generated is taken at two points within the waveform, where the current at point 1 and point 2 are then subtracted as described in Equation 1-13.

$$\Delta I = I_2 - I_1 \qquad \text{Equation 1-13}$$

Square wave voltammetry has become very common technique as detection method due to it sensitivity that can differentiate between charging (capacitance) and faradic current. The result of subtracted off the capacitance from the overall current measured is used to present the current in a square wave, and this includes the faradic current from the redox reaction of the analyte, all of this led to increasing the sensitivity.

1.14 Aim of PhD

This literature review has shown that of the analysis of environmental water sample is a complicated process due to the sample matrix, which required applying extra steps, therefore led to increase the cost of analysis. In addition, to get result with acceptable accurate and precision using high cost and completed equipment is required. In addition, the analysis process required many steps, from sample collection to analysis, which start from collecting the sample then storage it under special condition to avoid any contamination. Finally, that transport it to laboratory to start the analysis procedure. This entire reasons make the process of analysis of the environmental water sample by conventional methods is time-consuming and costly. Recently, microfluidic devices have been used widely for detection of environmental chemicals pollutants with the aim of developing portable system device to reduce analysis time, amount of reagent, and increase the accuracy of the results.

The aim of this project is developing a portable system device capable to monitoring the mixture of organic chemical pollutant in environmental water sample depend on the integration of solid phase extraction (SPE) with immunoassay technique and use the chemiluminescence (CCD) and electrochemistry (SWV) as detection. Benzo (a) pyrene was selected as a priority pollutant due to it is influence on the human health and widespread presence in the environment. Progesterone and β-estradiol were also selected emerging pollutants in the environment.

- The first objective was to develop a method to extract and pre – concentrate the mixture of environmental pollutants from a river water sample. The river water was selected as example of environmental water sources as river water is abundance in UK. From the literature review, it was decided to use a monolithic silica modified through in situ covalent attachment of phases by C_{18} to extract and

pre – concentrate the progesterone, β-estradiol and benzo(a) pyrene from river water sample at one step by pumping 100 mL of water sample through the silica monolith sorbent and elute the analytes with less than 1 mL by suitable organic solvent.

- The second objective was to develop a simple but sensitive and selective detection method suitable for incorporation within an in situ device. The immunoassays technique was selected to improve the selectivity of the analysis. The new method was created to immobilise the three different types of antibody on the same solid support surface, where the indium tin oxide (ITO) electrode was used as solid support surface while the electrochemical technique (CV) used to modify the electrode surface. Both chemiluminescence with (CCD) system and electrochemistry (SWV) were evaluated for detection the organic pollutants at the same time, where they both provide high sensitivity.
- The third objective was to miniaturise the detection by incorporating the CL immunoassay within a microfluidic device. Where two different materials (polymer and glass) were use with two different chip designs where created to build up microfluidic device. The target of this step was to makes the system more portable and minimises the use of reagents.

Chapter 2. Experimental

This chapter describes all of the reagents, materials, instrumentation and procedures used in this work to achieve the aim of the thesis. The purified water that was utilised in this project was purified using the Elgastat Prima 3 reverse osmosis water system [Elga Ltd., High Wycombe, UK]. Sample preparation of the triple mixture of organic pollutants was carried out using the silica monolith that is described including; fabrication and modification of the monolithic silica column, characterisation of the monolithic materials, and the pre - concentration evaluation methodology.

Chemiluminescence immunoassay and square wave voltammetry (SWV) detections were used to determination the organic pollutants. There were four main experiments applied to complete this process including; chemical modification of the solid support surfaces, immobilisation of antibodies onto the surfaces, antibodies and antigens reaction, and the final steps with chemiluminescence or electrochemistry detection.

2.1 Reagents

All the reagents were purchased from the suppliers as shown in the following Table 2-1. The chemicals will be listed based on the experiments sequence.

Table 2-1: Reagents

Chemical	Supplier	Purity/Grade
Polyethylene oxide	Sigma-Aldrich, Poole, UK	-
Acetic acid	Sigma-Aldrich, Poole, UK	≥99%
Nitric acid	Fisher Scientific, Loughborough, UK	70%
Tetraethyl orthosilicate	Sigma-Aldrich, Poole, UK	98%

Tetramethyl orthosilicate	Sigma-Aldrich, Poole, UK	98%
Ammonia solution	Fisher Scientific, Loughborough	Analytical grade
Chloro (dimethyl) octadecylsilane	Sigma-Aldrich, Poole, UK	95%
Anhydrous toluene	Sigma-Aldrich, Poole, UK	99.8%
2,6-lutidine	Sigma-Aldrich, Poole, UK	≥ 99 %
Tetrahydrofuran anhydrous	Sigma-Aldrich, Poole, UK	≥ 99.9 %
Methanol	Fisher Scientific, Loughborough, UK	HPLC grade
Acetonitrile	Fisher Scientific, Loughborough, UK	HPLC grade
Progesterone	Sigma-Aldrich, Poole, UK	99%
β-Estradiol	Sigma-Aldrich, Poole, UK	98%
Benzo (a) pyrene	Sigma-Aldrich, Poole, UK	96% HPLC
Anti-Progesterone antibody	AbCam, Cambridge, UK	-
Anti-Estradiol antibody	AbCam, Cambridge, UK	-
Anti – benzo (a) pyrene	Thermo Fisher Scientific, Paisley, UK	-
Progesterone – HRP	AbCam, Cambridge, UK	-
phosphate buffer saline tablet	Sigma-Aldrich, Poole, UK	-
Acetone	Fisher Scientific, UK Ltd	≥99.9%
3-aminopropyl-trimethoxysilane (APTMS)	Sigma-Aldrich, Poole, UK	99%
(3-glycidyloxypropyl)-trimethoxysilane (GPTMS)	Sigma Aldrich	≥98%

Luminol	Sigma-Aldrich, Poole, UK	≥97%
Hydrogen peroxide	Fisher Chemical, Loughborough, UK	Analytical grade
N-(3-Dimethylaminopropyl)-N'-ethylcarbodiimide hydrochloride (EDC)	Sigma-Aldrich, Poole, UK	≥99.0%
N-hydroxysulfosuccinimide sodum (salt sulfo-NHS)	Sigma-Aldrich, Poole, UK	98%
Tween® 20	Sigma-Aldrich, Poole, UK	-
Bovine serum albumin (BSA)	Fisher Scientific, UK Ltd	98%
Ferrocenecarboxaldehyde	Sigma-Aldrich, Poole, UK	98%
N,N-Dimethylformamide	Sigma-Aldrich, Poole, UK	≥99%
Tetrabutylammonium perchlorate	Sigma-Aldrich, Poole, UK	≥99.0%
Sodium borohydride	Sigma-Aldrich, Poole, UK	98%
4-nitrobenzenediazonium tetrafluoroborate	Sigma-Aldrich, Poole, UK	97%
Potassium chloride	Sigma-Aldrich, Poole, UK	≥99.0%
Potassium carbonate	Sigma-Aldrich, Poole, UK	≥99.0%
Ethanol	Fisher Scientific, Loughborough, UK	HPLC grade

2.2 Equipment

Throughout this work, there were a variety of different equipment and materials used as listed in the Table 2-2.

Table 2-2: materials used

Materials	Supplier
Hot plate-stirrer	VWR International, USA
Omnifit straight connecters , 2 ways (11 × 52 mm)	Kinesis, Cambridge, UK
Two-piece tight fitting	Kinesis, Cambridge, UK
Polytetrafluoroethylene (PTFE) tubing	Adtech Polymer Engineering Ltd., Stroud, UK
Fusion 100 Classic Syringe Pump	Chemyx, Stafford, USA
SEMPREP 2 Sputter Coater	Nanotechnology Ltd., Sandy, UK
Prodigy™ C_{18} column 5 µm (150 x 4.6 mm)	Phenomenex Inc,Torrance, CA, USA
Ag/AgCl reference electrodes	Alvatek, Tetbury, UK
Tin doped indium oxide (ITO) electrode (7 × 50 × 0.7 mm)	ITO coated glass, Delta Technologies limited, USA
Vive spin 500, 30,000 MCWO	Sartorius Mechatronics, UK Ltd.

2.3 Instruments

All the instrumentation used for the experiments are listed in Table 2-3.

Table 2-3: Instruments

Instruments	Supplier
Brunauer-Emmett-Teller (BET)	Micromeritics Ltd., Dunstable, UK
Scanning electron microscope (SEM)	Cambridge S360Instruments, Cambridge, UK
Energy-dispersive X-ray spectroscopy system (EDX)	INCA 350, Oxford Instruments, Abingdon, UK
UV – Vis spectrophotometer lambda Bio 10	PerkinElmer, California, USA
HPLC-UV system, module 785 A	PerkinElmer, California, USA
Biochip array holder	RANDOX, Crumlin, UK
Palm Sens potentiostat	Palm Instruments, Netherland
Charge-coupled device (CCD) camera fitted with an 8 mm high resolution pixel lens	QHXCCD, US
K1 contact angle goniometer	Kruss, Hamburg, Germany
Datron M7 CNC milling machine	Datron Dynamic, Mühltal, Germany

2.4 Fabrication of silica monolithic rod

The silica monolith rod was prepared by using the procedure reported by Nakanishi [73b] with some modification. The required weight of polyethylene oxide 0.305 g with an average relative molecular mass MW = 200,000 was mixed with 4 mL of (0.02 M) acetic acid for TMOS fabrication and 0.28g of polyethylene oxide with an average relative molecular mass MW = 200,000 mixed with 2.53 mL of 1 M nitric acid for TEOS fabrication. All the chemicals were placed inside a 50 mL polyethylene centrifuge tube that was placed in an ice bath. After that, the reagents were mixed using a magnetic stirrer

for 30 min until the polymer was completely dissolved. Then, 2 mL of tetramethyl orthosilicate (TMOS) or 2.26 ml of tetraethyl orthosilicate (TEOS) was added to the solution and mixed for another 30 min until the solution became homogenous. The mixture was left for 10 min to remove any air bubbles that might have formed during the mixing process. A 1 mL (4.78 mm) plastic syringe was used as the mould to give the rod-shaped of the monolith. To prepare the syringe, firstly the outlet was closed using polytetrafluoroethylene (PTFE) tape, then 1 mL of a homogeneous mixture was added gently inside the syringe to avoid the formation of air bubbles. After that, the top of the syringe was covered by a small lid and closed tightly with (PTFE) tape. Finally, the syringe was placed into a glass beaker and put in the oven at 40 ºC for three days. The rods of semi – solid gel formed with a white colour and it was easy to remove the rod from the plastic syringes after the lids were removed. The monolithic rods were placed in a distilled water bath at room temperature to remove any residues, where the water was changed every 2 hours for up to 8 hours until the pH of the water became neutral. After the monolithic was removed from the water bath, it was dried at room temperature and the monolithic rods were treated with 30 mL of 1 M ammonia solution to etch the surface. The alkaline solution was prepared by mixing 6 mL of 5 M of NH_4OH with 24 mL of distilled water in a conical flask, and the monolith was then added. The flask was wrapped with aluminium foil, placed in a silicon oil bath, and refluxed for 24 hours at 80 º C. The purpose of this etching process was to form the mesoporous, which led to an increase in the surface area of the monolithic rods [73b]. After that, the rods were placed in a distilled water bath to remove any residues where the water was changed every two hours until the pH of the water became neutral. The monolithic rods were then placed in the oven for 6 hours at 40 ºC until they were dry. Finally, the monolithic rods were placed in a furnace oven for 3 hours at 550 ºC to decompose the organic residues without affecting the

monolith structure. The silica monoliths were cut to suitable length depend on the type of application and then prepared for the flow system.

2.4.1 Preparation of silica monolithic rods for a flow system

The monolithic silica rod was cut into appropriate lengths (2 cm) to reduce the time of the experiment process, and the system was designed to allow the pre – concentration process occur easily through the system. The monolithic silica rods with an internal diameter 3.7 mm for TMOS and TEOS was connected with borosilicate tubing (2.10 mm, i.d and 3.90 mm) using heat shrinkable PTFE tube (4.8 mm internal dimeter). The monolithic silica rods were placed in the middle of the shrinkable tube, with the borosilicate tube fitted on the ends and then placed in the furnace oven at 380 °C for 30 min to seal the heat shrinkable tube around the monolithic silica rods and borosilicate tube as shown in Figure 2-1.

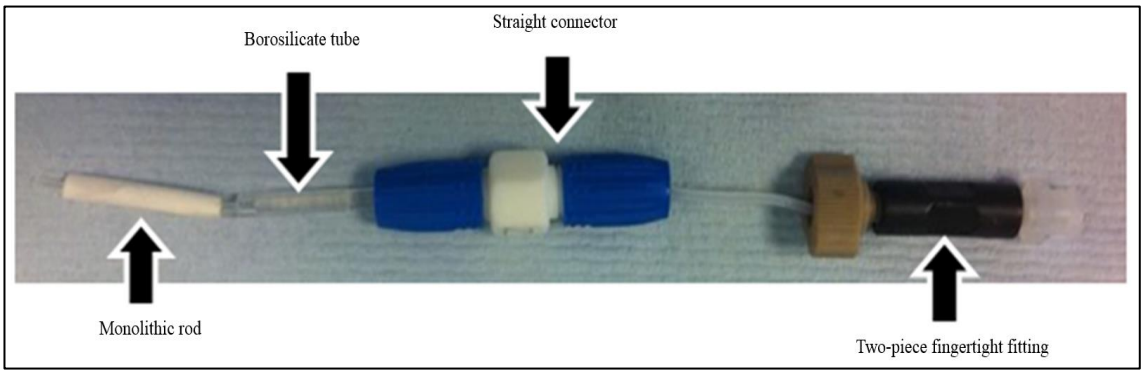

Figure 2-1: Silica monolith rods sealed in heat shrinkable tube with borosilicate tube for connection.

Finally, the encapsulated rod was connected to the flow system by using straight connectors (Ominifit Kinesis). After this step, the system was ready for further processing including surface modification or solid phase pre – concentration. This method was very useful for making the monolithic rods into a column with no leakage during the continuous flow pre – concentration process. The syringe pump was connected to the tubing using a two-piece finger tight fitting.

2.4.2 Surface modification of silica monolithic rod with C_{18}

The silica monolith rod was chemically modified with an octadecyl group to obtain the reverse phase coating on the surface by using a procedure similar to that described by Xie [104]. The monolithic silica column was initially washed with 1 ml of anhydrous toluene at a flow rate of 20 µL min^{-1}. Then followed by continuously flowing a mixture of the derivatisation reagent (1 g chlorodimethyl octadecyl silane (CDMOS) in 10 mL anhydrous toluene with 10 drops of 2, 6-lutidine) at a flow rate of 30 µL min^{-1} at 80 °C for 6 hours. After that, the monolithic silica rod was washed to remove any residues from the rod at a flow rate of 100 µL min^{-1} with 1 mL of anhydrous toluene followed by 1 mL of tetrahydrofuran (THF). The wash process was continued with 1 mL of methanol/water followed by 1 mL of methanol. Finally, the C_{18} silica monolithic rod was placed in the oven at 40 °C for 24 hours before use.

2.5 Monolithic materials characterisation

2.5.1 SEM analysis

As described in section 1.8.2, the morphology of the prepared silica monolith was characterised by scanning electron microscopy (SEM) to determine the through pores by averaging the size of 20 pore diameters. The scanning electron images of the silica monolith were obtained using high vacuum mode by setting an accelerating voltage of 20 kV and a probe current of 100 pA. The samples were coated with a thin layer of gold-platinum (thickness around 2 nm) using the Sputter Coater.

2.5.2 Brunauer-Emmett-Teller (BET) analysis

As described in section 1.8.1, the physical properties of the bulk monolith (average pore diameter, surface area, and the pore volume) were investigated using a Surface Area and Porosity Analyser. For this stage and as mentioned in section 2.4, inside a 1 mL disposable plastic syringe used as a mould to fabricate the silica monolith using the same

polymerisation mixture as previously described. After completing the fabrication procedure of the silica monolith, and removed all unreacted materials were it washed by distilled water. The monolith rod was dried in the oven at 40 ºC for 24 hours. The BET isotherms of nitrogen adsorption and desorption use to determine the porous properties of the monoliths. The isotherms were analysed to find out the surface area based on the BET model. The nitrogen adsorption isotherm using the BJH (Barrett-Joyner-Halenda) model was used to measure the pore size and pore volume distribution of pores within the monoliths.

2.5.3 EDX analysis

The dispersive X-ray (EDX) analysis was used to find out the chemical composition of monolithic materials before and after modification of the surface of the silica-based monolith with C_{18}. EDX analysis was performed using an INCA 350 EDX system.

2.6 Evaluation of extraction of silica monolith modified surface

2.6.1 Preliminary experiment to pre - concentrate the organic pollutants from the C_{18} silica monolith

UV – Vis spectrophotometry was used to evaluate the ability of the TMOS C_{18} modified monolithic column to pre – concentrate the non – polar organic pollutants from the water sample and increase the concentration of the analyte to the required concentration. TMOS was selected in this experiment due to having large surface area compare with TEOS, (see section 3.2.1). Another aim of this experiment was to find the ideal organic solvent to use in the elution step for the analyte, where the comparison was between methanol and acetonitrile that is common to use in case of organic pollutants [111, 223]. The purpose of using UV – Vis spectrophotometer was to determine extraction recovery by comparing the absorbance of the analyte (progesterone) extraction with the absorbance of the non-processed analyte standard solutions. A serial of a different concentration of progesterone

standards (0.5, 2, 4,10,15,20 and 25 µg mL^{-1}) were prepared to make the calibration curve. This concentration consider is high but was selected to studies the ability of silica monolith was high concentration. All the standards prepared by dissolving an accurately weighed amount of progesterone in distilled water. UV – Vis spectrophotometer was chosen as the simple method for evaluation of the process.

As explained in section 1.2.2, solid-phase extraction (SPE) procedures commonly involve four step as follows: activation of the sorbent by a suitable solvent, loading of the sample, removing of impurities and unbinding compounds (washing), and elution of the target analyte. The total volume of the column was measured by pumping the solvent into the column until the first drop was seen at the outlet.

Progesterone was used to evaluate the ability of TMOS silica monolith for pre – concentration process. 20 mL of progesterone (1 µg mL^{-1}) was loaded in C_{18} – TMOS monolith followed by 5 mL of distilled water to washing the column, which was repeated three times. Finally, 5 mL of acetonitrile was passed through the monolith column to elute the progesterone; the procedure followed is shown in Table 2-4. The absorbance of the scan of progesterone standard (1 µg mL^{-1}) in the range 900 – 200 nm was obtained to find out the optimum λ_{max} (254 nm) of the analyte. After each pre – concentrate step the elution was collected in a separate beaker, and 3 mL of each fraction were used to fill the UV – Vis spectrophotometer quartz cuvette. Absorbance measurements were made with a blank either of acetonitrile or methanol at each experiments stage and all of these experiments were repeated three times.

Table 2-4: The process to evaluate the ability of TMOS to pre – concentrate the analyte

Step	Solvent	Flow rate ($\mu L\ min^{-1}$)	Volume (mL^{-1})	Time (min)
Wash	Distilled water	100	5	5
Loading	Progesterone standard (1 µg/mL)	100	20	20
First Wash	Distilled water	100	5	5
Second wash	Distilled water	100	5	5
Third wash	Distilled water	100	5	5
Elution	Methanol & Acetonitrile	100	5	5

2.6.2 HPLC method for characterisation of silica monolith

To fully evaluate the ability of the two types of C_{18} silica monolith (TMOS and TEOS) to pre – concentrate the organic pollutants progesterone, HPLC was used. The HPLC measurement technique is widely used in environmental organic pollutants applications. For progesterone analysis, a column was C_{18} and the mobile phase used was acetonitrile/water (75:25) under gradient conditions at room temperature (around 25°C). 20 µL of sample was injected into the system that was a flow rate at 1 mL min^{-1}, the UV –Vis detection wavelength was adjusted to 254 nm. A calibration curve was prepared based on the peak area of different serial dilutions of progesterone standards (0.1, 0.07, 0.04, 0.01 and 0.005 mg mL^{-1}).

2.6.3 Evaluation of the ability of both types of silica monolith rods to pre – concentrate.

In order to choose the preferred of silica monolith and the optimum condition of flow rate for the pre – concentration process of organic pollutants. 100 mL of a stock sample of progesterone (10 µg mL^{-1}) prepared in acetonitrile was pumped through both types of monoliths (TMOS and TEOS) at a range of different flow rates (100, 300, 500, 700, 900 and 1000 mL min^{-1}) at loading step. A washing step was then repeated three times to remove all the residues from the silica monoliths by pumping 1 mL of distilled water into the monolith each time at 100 mL min^{-1}. Finally, 1 mL of acetonitrile was injected to elute the analyte from the silica monoliths. Each step was collected in a separate beaker, and then injected into the HPLC system to calculate the extraction recovery using the Equation 1-3.

2.6.4 Progesterone pre – concentration

In order to investigate the ability of the C_{18} modified silica monolith (TMOS) to pre-concentrate a large volume of the sample, the process started with cleaning and conditioning of the column; this was carried out using acetonitrile 1 mL, followed by 1 mL of distilled water. 100 mL of progesterone standard sample prepared in distilled water at concentration (1 µg mL^{-1}) because the LOD of the HPLC system, this volume was then loaded into the silica monolith column at a flow rate 900 mL min^{-1} and then washed three times with 1 mL of distilled water at a flow rate 100 mL min^{-1}. Finally, 1 mL of acetonitrile was pumped through the monolith column to elute the analyte. At elution step, 1 mL of organic solvent was elected to increase the concentration of the analyte and to collect the enough volume of sample which will use in more experiments. All fractions were collected for additional analysis by HPLC. The same process was repeated with a river water sample spiked with 1 µg mL^{-1} of progesterone.

2.6.5 Organic pollutants extraction and pre – concentration

2.6.5.1 Preparation of standards solutions

A stock solution of the pollutants progesterone and estradiol were prepared separately by dissolving an accurately weight amount of 1 mg in 10 mL of acetonitrile for each pollutant to achieve a concentration of 0.1 mg mL^{-1}. All stock solution were divided into 1 mL aliquots and stored at – 20 ºC until required. The priority pollutants benzo (a) pyrene was prepared by dissolving 100 mg in 100 mL of acetonitrile, then divided into 1 mL aliquots and stored at – 20 ºC until required. Working standards of the analyte was then freshly prepared in the range (100, 75, 50, 25, 10 and 1 µg mL^{-1}) by diluting the stock solution in the distilled water and stored at 4 ºC. Mixed standards of the analytes (1 µg mL^{-1}) were prepared by diluting the accurate volume of stock solution for each analyte in 100 mL of distilled water. 100 mL of a river water sample was spiked with the accurate volume of stock solution for each analyte to make concentration at (1 µg mL^{-1}). The chemical structure of all the analytes are shown in Table 2-5.

Table 2-5 : Chemical structure of the organic pollutants analytes targets in this study

Analyte	Structure
Progesterone	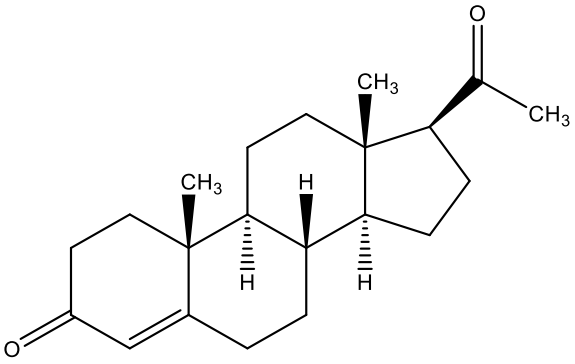
Estradiol	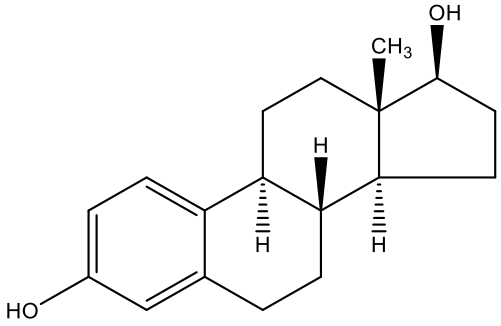
Benzo(a)pyrene	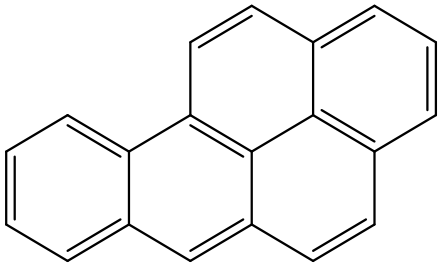

2.6.6 Optimisation of the HPLC

For HPLC analysis, the optimum UV detection wavelength and mobile phase composition were investigated using a mixture of three analytes (progesterone, estradiol and benzo (a) pyrene). Two ratios of mobile phase composition acetonitrile/water (75: 25) and (80: 20) were studied, the second step was to optimise the UV detector wavelength (250, 240, 230 and 220 nm). All values of peak area for each analyte were compare to the peak area for the analytes at different run to find out the large value of peak area.

2.6.7 Organic pollutants pre – concentration

The procedure for pre – concentrating the sample started with cleaning and condition of the column by passing the acetonitrile, followed by water. 100 mL of the sample of progesterone, estradiol and benzo (a) pyrene was then loaded into the TMOS - C_{18} monolith column at a flow rate of 900 µL min^{-1}, the column was then washed three times using 1 mL of distilled water at a flow rate of 100 µL min^{-1}. Finally, the elution step was carried out by pumping 1 mL of acetonitrile at a flow rate of 100 µL min^{-1}. All fractions were collected for analysis by HPLC. The same procedure was applied to the spiked river water sample.

2.6.8 Analytical figures of merit

Parameters of the Method validation, involving limit of detection (LOD), the lower limit of quantification (LLOQ) and linearity, were evaluated to confirm that the results of the method were appropriate and reliable for the analysis desired.

2.6.8.1 Linearity

In chemical analysis, the concentration of the sample is normally directly proportional to the concentration of an analyte in the sample within a given range. The average of three runs of each standard solutions, progesterone, estradiol and benzo (a) pyrene at a concentration of 100, 75, 50, 25, 10 and 1 µg mL^{-1} were obtained, and the calibration curves were plotted for each analyte. Linearity was evaluated statistically by the least squares regression method.

$$y = b + mx \qquad \text{Equation 2-1}$$

Where x: the concentration of the analyte (µg mL^{-1}), m: the slope, b: the intercept on the y-axis and y: the signal response (peak area, absorbance or light intensity). A good linearity is obtained when the correlation coefficient (R^2) is close to 1[224].

2.6.8.2 Limit of detection (LOD) and lower limit of quantification (LLOQ)

The limit of detection can be defined in an instrumental analysis process as "the minimum concentration of the analyte that can be determination by the detector" [225]. The value of LOD is often defined as the blank single plus three standard deviations of the blank. The definition of the lower limit of quantification (LLOQ) is "the lowest concentration of the analyte that can be quantified with acceptable accuracy and precision" [225]. To accept the value of LLOQ must be bigger than the blank value plus ten standard deviations of the blank. The calculation of the LOD and LLOQ depends on the value of the blank that is not applicable for chromatographic technique because any interferences s is separated from the analyte. However, the calibration curve can be uses to estimate the LOD by depending on the value at the intercept from the calibration curve, which is used instead of the blank, and the standard deviations of the intercept used in place of the standard deviation of the blank. The LOD and LLOQ were calculating using following equations.[226], [225]

$$y_{LOD} = y_B + 3\,S_{y/x} \qquad \text{Equation 2-2}$$

$$LOD = (y_{LOD} - y_B / m) \qquad \text{Equation 2-3}$$

$$y_{LLOQ} = y_B + 10\,S_B \qquad \text{Equation 2-4}$$

$$LLOQ = (y_{LLOQ} - y_B / m) \qquad \text{Equation 2-5}$$

Where $S_{y/x}$ is the standard deviation of a predicted y-value for each x concentration in a regression, m is the slope of the calibration curve, and y_B is the y-intercept.

2.7 Detection of organic pollutants

Chemiluminescence immunoassay and electrochemistry (square wave voltammetry) techniques were selected as detection methods to analysis the mixture of progesterone, estradiol and benzo (a) pyrene in this project. There were both based on a competitive immunoassay technique where the experiment required the immobilisation of antibodies onto a solid support surface followed by the chemiluminescence or electrochemistry (square wave voltammetry) immunoassay. Four main steps were applied in this experiment: chemical silanisation of the solid support surface, antibodies immobilisation on the surface, antibody and antigen reaction and detection. The major challenge in this experiment was reproducibility of the immobilisation of the antibodies onto the solid support surface, which could form the main part of a microfluidic device. Different methods were investigated for immobilising the antibody onto the solid support surface, microscope slides (0.8 × 0.8 cm) were initially used in this investigation.

2.7.1 Optimisation of chemiluminescence reagent

As described in section 1.14.2.1 the chemiluminescence immunoassay reaction depends on reagents concentration, the horseradish peroxidase (HRP), luminol, hydrogen peroxide (H_2O_2) and pH. The luminol is depend on the pH value to work where the pH must be above 9 [202], for that this factor would not study as will describe in section 4.1.3. In order to find out the optimum condition of the horseradish peroxidase (HRP)-luminol chemiluminescence reaction the concentration of luminol, H_2O_2 and progesterone – HRP were investigated. 0.5 mL Eppendorf tubes were used, where the blank tube was filled with phosphate buffer saline (PBS) with the mixture of 20 mM of luminol and H_2O_2. The sample tube was filled with progesterone – HRP and the mixture of 20 mM of luminol and H_2O_2. The tubes were placed under CCD camera to detected the light emitted and where the CL emission intensity was measured by ImageJ software, where this software

measure the intensity of light in placed select manually. The blank tube was used to obtain background values, also to detect any contamination of the reagents as shown in Figure 2-2.

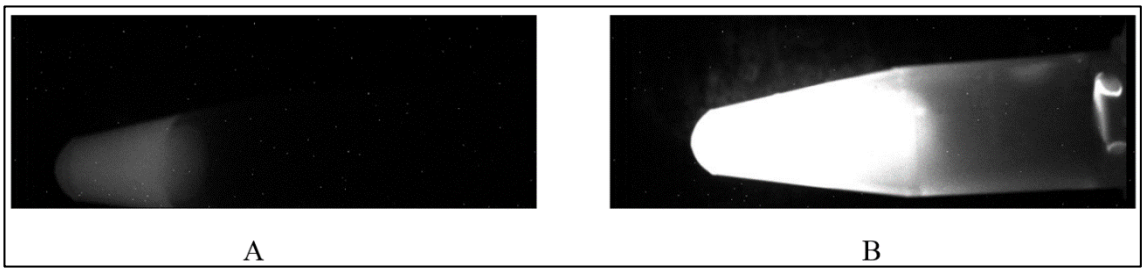

Figure 2-2: CCD image of two Eppendorf tubes with chemiluminescence reagents where the (A) is the blank (PBS + 20 mM of mixture luminol + H_2O_2, (B) is a sample well included HRP + 20 mM (luminol + H_2O_2).

2.7.1.1 Optimisation of the HRP concentration

The concentration of the progesterone – HRP was investigated to study the effect on the chemiluminescence signal. 10 mM of PBS was used to dilute the progesterone – HRP (the original concentration of HRP was 1 mg mL^{-1}) to give 0.5, 1, 5, 10, 15 and 20 µg mL^{-1} respectively. The luminol and H_2O_2 concentration were fixed at 20 mM. For the blank, a 40 µL mixture of luminol and H_2O_2 was added to 10 µL of PBS in Eppendorf tube, and for standard 40 µL of the mixture luminol and H_2O_2 was added to 10 µL of progesterone – HRP in the tube.

2.7.1.2 Optimisation of H_2O_2 concentration

The effect of the concentration of the H_2O_2 was investigated on the chemiluminescence signal with the progesterone – HRP and luminol. The concentration of H_2O_2 standards were 10, 20, 30 and 40 mM where a 40 mM of H_2O_2 was prepared by adding 0.4 ml solution of 10 M H_2O_2 to 100 ml of purified water. In addition, this concentration was used to prepare all another concentration.

2.7.1.3 Optimisation of luminol concentration.

The influence of the concentration of the luminol on the chemiluminescence signals were investigated with the progesterone -HRP and H_2O_2. Different concentration of the luminol in the range 10, 20, 30 and 40 mM were prepared by dissolving 0.7 g of luminol in 100 ml of 10 mM NaOH to obtain a 40 mM luminol solution and then diluted to different concentrations.

2.7.2 Chemical silanisation of solid support surface

Glass microscope slides were used as the solid support surface; these were cut into squares shape (0.8 × 0.8 cm). Before any chemical silanisation process, the slides were cleaned using anhydrous acetone for 15 min under sonication; then the slides were placed in an oven for 1 hour at 90 °C to dry. After that, the dried slides were placed in the solution containing 2 mL of (3aminopropyl) triethoxysilane (APTMS) silanise reagent with 20 mL anhydrous acetone for 1 hour at room temperature.

For silanisation of the glass surface with (3-glycidyloxypropyl)-trimethoxysilane (GPTMS), 1 M sodium hydroxide, ethanol and purified water were used to clean the glass slides for 10 minutes under sonication so, then placed in the oven for 1 hour at 90 °C to dry. After that, the slides were placed in a solution containing the range of concentration 1 to 10 % of GPTMS in 50 mM glacial acetic acid in ethanol: water (95:5) for 1 hour at room temperature.

After each silanisation treatment, an anhydrous acetone and purified water were used sequentially to wash the slides after APTMS-treatment, and the ethanol and purified water were used to wash slides after GPTMS-treatment to remove any unreacted products. All slides were then dried in the oven at 90 °C for overnight. The properties of the glass surface change after silanisation from hydrophilic to hydrophobic so that the contact angle

of a droplet measurement used to determine the success of the process by determining the water with the glass surfaces.

2.7.3 Antibody immobilisation on the silanised glass surface.

2.7.3.1 Antibody immobilised onto APTMS modified glass surfaces.

To immobilise the progesterone monoclonal antibody onto the APTMS silansation glass surface. 10 µL aliquot of anti – progesterone antibody was mixed with equal volumes of an activation buffer at pH 7 for 15 min. The activation buffer consisted of 2.2 mg of N-Hydroxysulfosuccinimide sodium (sulfo – NHS) salt and 0.8 mg of N-(3-dimethylaminopropyl)-N-ethyl-carbodiimide hydrochloride (EDC) dissolved in 2 ml of PBS to activate the carboxyl group on the antibody. A 5 µL of this solution was pipetted onto the -NH_2 functionalised glass surface and left covered in the fridge at 4 °C overnight. All the slides were then washed with 0.1 vol. % Tween® 20 in 10mM PBS and stored in PBS before use.

2.7.3.2 Antibody immobilise onto GPTMS modified glass surface.

The procedure used to immobilise the anti - progesterone on the modified glass surface was the similar manner to the procedure described for the APTMS slides in section 1.7.3.1, with the exception that there was no linker in the activation buffer. A 15 µL of 10 mM PBS was mixed with 5 µL of anti – progesterone solution, this was spotted onto the glass surface and left covered in the fridge at 4 °C overnight.

2.7.4 Characterisation of antibody immobilisation

2.7.4.1 Contact angle measurement

To evaluate the silanisation quality and reproducibility of the modified glass surface and to confirm the glass surface was chemically modifying, the Water Contact angle measurements were used. The Kruss DSA – 10 MK2 drop shape analysis system (drop size 5 µL) was used for measurement. The contact angle of two modified surface were

measured by averaging the contact angle of water droplets from five separate measurements for each surface (n=5) and comparing the measurements with the blank glass (not modified).

2.7.4.2 The HRP – luminol – hydrogen peroxide chemiluminescence detection

After the antibody had been immobilised onto the surface, the antibody (anti – progesterone) and antigen (progesterone – HRP) reaction was carried out. Then the stock solution of progesterone – HRP was diluted with 10 mM PBS and a 10 µL aliquot of it was pipetted onto antibody spots on the glass surface and incubated for 1 hour at room temperature. The glass slides were washed again with PBS buffer, to remove all the unbounded analyte or progesterone – HRP from the surface. After that, 40 µL of the mixture of luminol and H_2O_2 20 mM was added to each slide. All of these experiments were carried out using a biochip array holder (RANDOX, UK) as shown in Figure 2-3, which allowed measuring 9-glass slide in the same time where the glass slides were located in all cell.

Figure 2-3: An array biochip array holder (RANDOX), which is capable of multiple detections on glass slides and plastic slides, cell holder was aligned under the CCD camera inside the box for CL detection.

The array biochip holder was placed inside a light – proof box to measure the chemiluminescence signal with CCD camera as shown in Figure 2-4. The box was closed after the biochip array was located under the camera and the images were recorded using EZCAP (QHY6) software that was set up on the laptop connected to the camera.

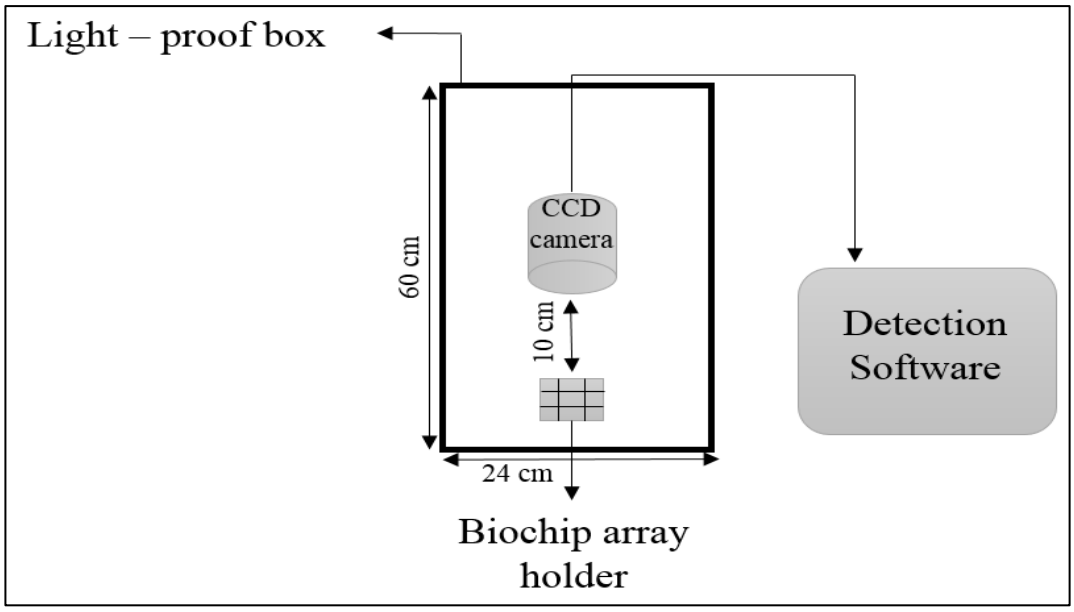

Figure 2-4: Schematic showing the general experimental set up for the chemiluminescence detection.

The set up consists of a black box where the CCD camera was located, with a stage under the camera to hold the solid support surface that holds the sample. The camera was connected to the laptop for an image is processing.

2.7.5 Electrochemistry detection.

2.7.6 Modification of the solid support surface by electrochemistry.

A tin-doped indium oxide (ITO) electrode which was made from a layer of a film of ITO on a glass surface was used as a solid support surface while it dimensions (7 × 50 × 0.7 mm). This electrode was divided into three area by used circular stickers of 6 mm diameter as shown in Figure 2-5.

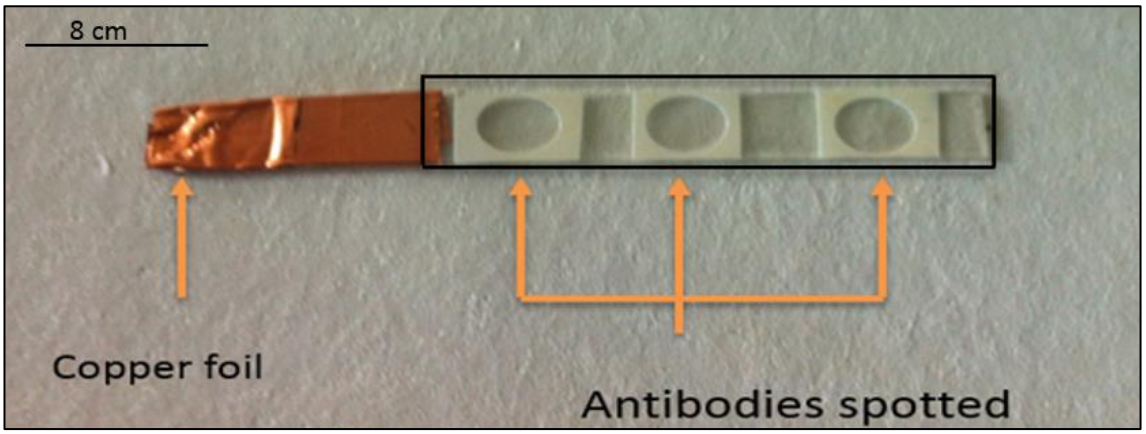

Figure 2-5: The ITO electrode used in electrochemistry modification.

The ITO electrode surface needed to be modified to enable the antibodies immobilisation onto the surface. The modification process was achieved by covering the surface with a functional group using an electrochemical technique. The ITO surface was modified in two main step, first to attach nitrobenzene to them to form phenylamine as reported by Don *et al.*[138]

The first solution used in the modification procedure was made up of 2 mM 4-nitrobenzenediazonium tetrafluoroborate and 0.1 M tetrabutylammonium perchlorate (TBAP) in acetonitrile. The ITO electrode was dipped into the solution and then connected to cyclic voltammetry system via electrode as shown in Figure 2-6. Three electrodes were used in this system a nickel wire as the counter electrode and Ag/AgCl as the reference electrode with the ITO electrode forming the working electrode. All the solutions were degassed by nitrogen gas before using. All scans were conducted at a scan rate of 100 mV s^{-1}.

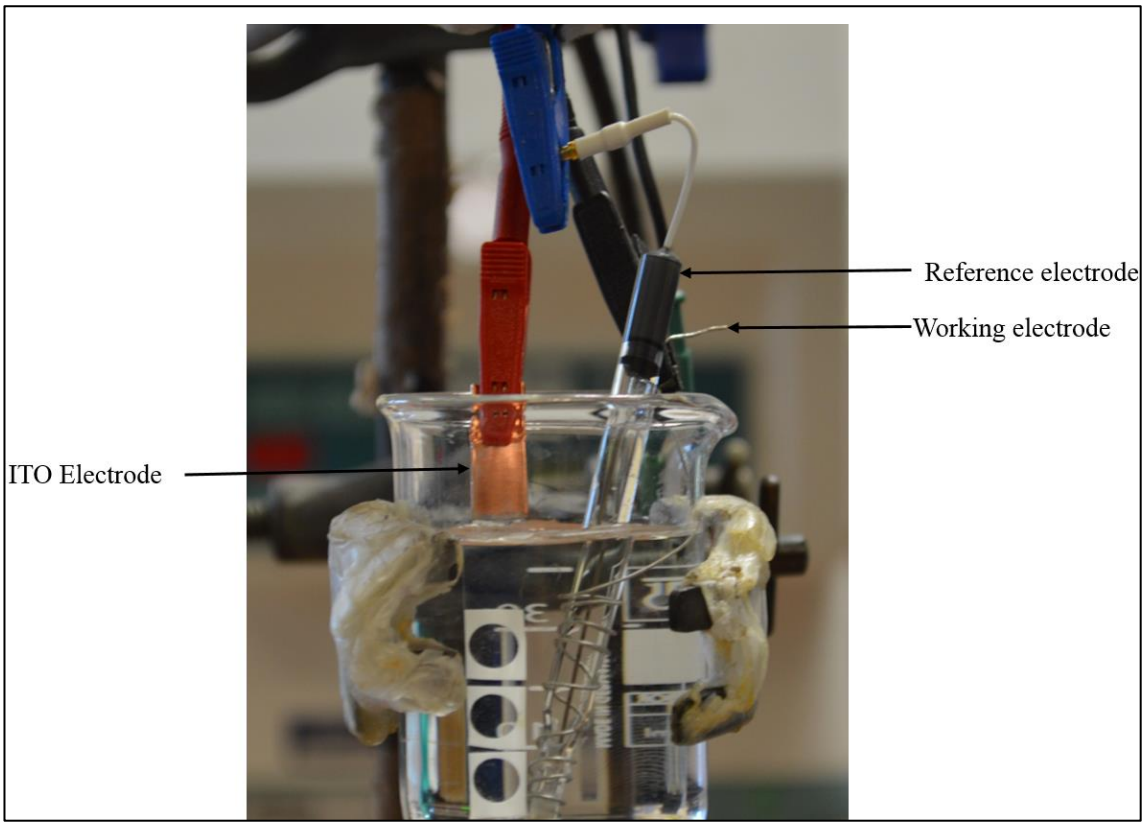

Figure 2-6: Set up of the electrochemical cell with, three electrodes dipping into an aqueous ethanol solution

A modified electrode surface with nitrobenzene was carried through electrochemical reduction of the first solution during the four reduction-oxidation cycles. Voltage was applied starting at +0.7 V and scanning down to -0.4 V, with a return sweep to +0.7 V, this was repeated for 4 scans. It was assumed that after the first scan, a monolayer was formed on the electrode surface, and subsequent scans formed a multilayer. The electrodes were then washed with PBS buffer.

In the second step to form the phenylamine group, the electrodes were dipped in aqueous ethanol: 0.1 M of KCl (10:90, v/v) solution. The scans started at +0.4 V with a sweep to -1.0 was returned to + 0.4 V over four scans. After this step, the amine group should have been formed on the electrode surface for the antibodies immobilisation.

2.7.7 Labelling and immobilisation of the antibodies with ferrocene carboxaldehyde.

All the antibodies (anti – progesterone, anti - estradiol and anti – benzo (a) pyrene were chemically modified by labelling with a ferrocenecarboxaldehyde (Fc – CHO) redox tag before being immobilised onto the ITO electrode surface, following method the developed by Okochi *et al.* [227]. This procedure was achieved by mixing 10 µL of a stock solution of antibodies with 190 µL of 10 mM PBS. Separately, another solution was prepared by dissolved 20 mg of ferrocenecarboxaldehyde in 200 µL of N,N-dimethylformamide (DMF) and the solution of the antibodies was added to it. The pH of the final solution was adjusted to a value of 9 by added 5 µL of aqueous potassium carbonate (1 M), then the mixture was left for 30 min to incubate at room temperature. A 2 mg of sodium borohydride was then added to the mixture as a reducing agent, and then the mixture was left for another 10 min. After that, the pH of the mixture was adjusted to 7 by adding hydrochloric acid HCl (0.1 M); then the mixture was left for another 10 min. The Whatman® universal indicator paper (pH 1-11) was used to confirm all pH changes were by spotting a small amount of the mixture onto the paper. The solution was then placed into a centrifuge at 12,000 rpm for 20 mins to purify the antibodies and remove the excess ferrocenecarboxaldehyde. The supernatant was then transferred into a Vivaspin® 500 centrifuge tube and re-centrifuged (12,000 rpm for 10 mins), so the liquid was transferred into the collection part of the Vivaspin® tube, *via* the membrane. Then 100 µL of PBS was added to the tube and was centrifuged for a third time (12,000 rpm for 10 min). The final solution was stored in a fridge at 4°C until use.

The antibodies were then immobilised onto the ITO electrode surface by mixing 100 µL of antibodies solution with the same volume of an activation buffer described in Section 2.7.3. After that, 10 µL of the antibody solution was pipetted onto the ITO electrode surface within the circular adhesive tape and left covered for 18 hours in the fridge at 4°C.

The electrode was then washed with a PBS-Tween 20 solution, (10 mM PBS, 0.1% v/v). Finally, the electrodes were washed again with a PBS – Tween 20 solution, and then the electrodes were saved in PBS at 4°C until use.

2.7.8 Evaluation of the electrochemical method for antibody immobilisation.

In order to examine the success of the electrochemical method to immobilise the antibody onto the modified ITO electrode, cyclic voltammetry was used. The modified ITO electrode in the PBS buffer was measured as blank, while the second electrode; a 15 µL of 1 pg mL^{-1} of progesterone was added to the immobilised antibody and left for 30 min at 4 °C to complete the incubation process. Finally, the ITO electrode was washed with PBS to remove unbound progesterone before connected with the electrochemical system. The result for the modified electrode was compared between the blank and the immobilised antibody. Cyclic voltammetry was run at scan rate 100 mV s^{-1}, and all measurements were in a present of PBS solution.

To evaluate the influence of the concentration of the analytes on the peak current; further, the experiment was carried out. Three different of ITO electrodes were measured using the cyclic voltammetry (CV) and square wave voltammetry (SWV) after completed immobilisation of antibody onto the electrode surface. In the first electrode was 10 µL of 1µg mL^{-1} of progesterone standard was added to each spot, where 10 µL of progesterone standard at the concentration of 1 ng mL^{-1} and 1pg mL^{-1} were added to the second and third electrode respectively. After completed the incubation process (30 min) each electrode was washed with PBS buffer before measuring step.

2.7.9 Oxidisation of antibody ferrocene tag (Ab – Fc) onto the surface.

In order to obtain the chemiluminescence signal and detect the analytes, the ferrocene labelled antibodies was oxidised using cyclic voltammetry. The ITO electrode was dipped

into the PBS and connected to the voltammeter. The voltammetry scan started at – 0.05 V with a sweep to 0.8 V (without returning) for one a scan at scan rate 0.01 V s^{-1}. All the Fc group should have been oxidised on the ITO electrode surface after this step. The Fc oxidised should then act as a catalyst for the luminol and hydrogen peroxide reaction to give the chemiluminescence signal as described in section 1.14.2.1.

2.7.10 Optimisation of incubation time for antibody - antigen reaction

Time is a crucial factor for any analysis process, the incubation time of antibody - antigen reaction was therefore investigated. The labelled anti – progesterone was immobilised onto ITO electrode surface, and after completion of the immobilisation process, 10 µL of the progesterone standard (100 ng mL^{-1}) were pipetted onto the anti – progesterone and numbered for different time (15, 30 and 60 min). A 10 µL of progesterone standard was added to the first antibody spot on the electrode, and then the electrodes were left covered at room temperature, after 30 min the second volume of antigen was pipetted onto the second spot. After 15 min the final 20 µL of the standard was pipetted onto the third spot and after 1 hour the electrode was washed with PBS buffer to remove all unbound antigen. Finally, two methods were applied to measure the electrode where first detection method based on square wave voltammetry (SWV) to measure the peak current, and the second detector was the CCD camera to measure the chemiluminescence signal.

2.7.11 Evaluation of interference effects on organic pollutant detection

The immunoassay analysis technique is a highly selective method, but interferences may occur with a mixture of organic pollutants.[228] The interference studied was carried out on three types of antibody (anti – benzo (a) pyrene, anti - estradiol and anti – progesterone) that had been sequentially immobilised within the circular adhesive tape on the same electrode. Three ITO electrodes were prepared with antibodies in that order, and the standards of each analyte were prepared in acetonitrile at 100 ng mL^{-1} concentration. A 10 µL aliquot of progesterone standard was added to the first electrode, and the same

volume of estradiol standard was pipetted to the second. Finally, the same volume of benzo (a) pyrene standard was pipetted on the third electrode. All the electrodes were left covered for 30 min for incubation; then the electrodes were washed with PBS buffer to remove unbounded analytes. The effect of interferences on the antibodies were determined by two different techniques CL and SWV.

In the case of using the square wave voltammetry (SWV) to determine the interference the same procedure for prepared the ITO electrode was done. However, during determined the interference of anti – progesterone the standard sample was consisting of the mixture of estradiol and benzo (a) pyrene, while with anti – estradiol the standard sample a mixture of progesterone and benzo (a) pyrene. Finally, in case of anti – benzo (a) pyrene, the standard sample was a mixture of progesterone and estradiol.

2.7.12 Evaluation of the stability of ferrocene tags

After completion of immobilisation of the labelled antibody onto the ITO electrode, the stability of the labelled antibody and the activity of the ferrocene tag after the oxidised need to be investigated. For that, the ITO electrode was placed under CCD camera to determine the CL emission after added the luminol and H_2O_2 before the oxidation the ferrocene tag. The same electrode, after completion the oxidation step of ferrocene tag was directly measured under CCD camera. The same electrode was stored in PBS buffer at 4 °C for 1 day and measured again, then stored for 3 days at 4 °C in the same buffer and measured again under CCD camera to find out if any changing in the CL emission signal.

2.7.13 Effect of the analyte concentration on the CL emission signal

In order to study the effect, the concentration of the analyte on the CL emission signal of the labelled antibody. 10 µL of the standard progestogen (100 ng mL^{-1}) was added to immobilised antibody on the electrode surface. The electrode was left at 4 °C for 30 min

to complete the incubation process. The electrode was washed with PBS buffer to remove unbounded analyte, then placed under CCD camera to measure changing in the CL emission signal buffer and after added the analyte.

2.7.14 Preparation of calibration curve for analytes

To determine the mixture of organic compounds in the environmental water sample, preparing calibration curves for each analyte is required. In this work two different types of detection used, so the first calibration curves were made using the SWV. In order to make these calibration curves, six different ITO electrodes were prepared for each analyte. After completion of immobilised the labelled antibody onto the electrode surface, a serial of different concentrations were prepared for each analyte at 100, 50, 25, 10 and 1 pg mL^{-1}. Following completion of incubation process, each electrode washed with PBS buffer to remove unbounded analyte and measured by SWV. The calibration curve was plotted between the concentration of the analyte and the difference between the highest value of the peak current of blank (labelled antibody without analyte) and the highest value of peak current of analyte (interaction between labelled antibody and analyte).

Three different ITO electrode were prepared for each analyte to make the calibration curve for analytes for chemiluminescence immunoassay method. Used circular stickers divided each electrode into three areas, where the first area in each electrode used as blank (labelled antibody). The analyte was added to the second and third areas, and each electrode left at 4 ºC for 30 min to completion the incubation process. After washed each electrode with PBS buffer, each electrode was placed under CCD camera to measure the CL emission light for each spot. The total of CL emission light for the second and third spot was substrate from the value of CL emission signal of a blank. The calibration curve was plotted between the concentration of the analyte (50, 10, 1 and 0.5 pg mL^{-1}) and the change of CL emission signal.

2.8 Microfluidic chip fabrication

2.8.1 Polymer chip fabrication

The polymer microfluidic devices used in this project were fabricated at the University of Hull by Dr Nathan Brown's group using an injection moulding process as explained in section 1.13.1 and Figure 2-7 show general steps of the fabricate a polymer microfluidic.[181]

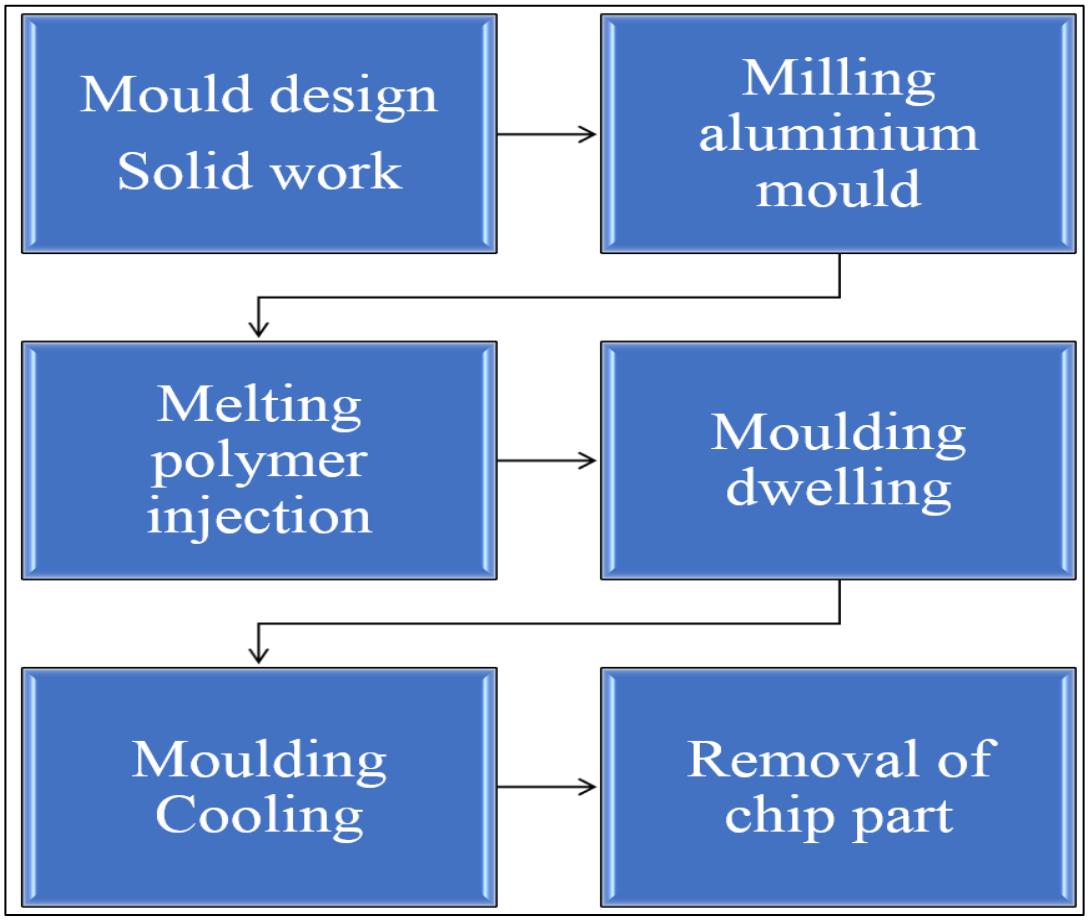

Figure 2-7: A scheme of the fabrication process of polymer microfluidic device.

At first, the SolidWorks software was used to design the mould of the chip. An aluminium mould was prepared by milling with a CNC machine. In an injection-moulding machine, the milled mould was inserted to produce parts of the microfluidic chip. Based on the gravity, the granular polymer (COC) was fed from a hopper into a heated chamber where it was melted. The melted polymer was then mixed and injected into the aluminium mould

cavity, a process known as ‘dwelling’. The polymer device was then cooled and ejected from the mould.

2.8.1.1 Microfluidic chip design

The two layers were moulded to form the chip as shown in Figure 2-8. The dimension of the device was 40mm × 40 mm (length and width) and 1 mm thick. The top layer consisted of a detection chamber and two holes, where the shape of the chamber was 0.1 mm deep, 7 mm wide and more than 15.5 mm long. The first hole was drilled at the end of the chamber (inlet), and another hole was drilled at the end of small channel coming from another side of the chamber. The bottom layer contained rectangular shape 0.7 mm deep and 7 mm wide, which was precisely aligned with the chamber of the top layer. The diameter of the access holes were 1.5 mm in order to connect the polymer chip with the syringe pump.

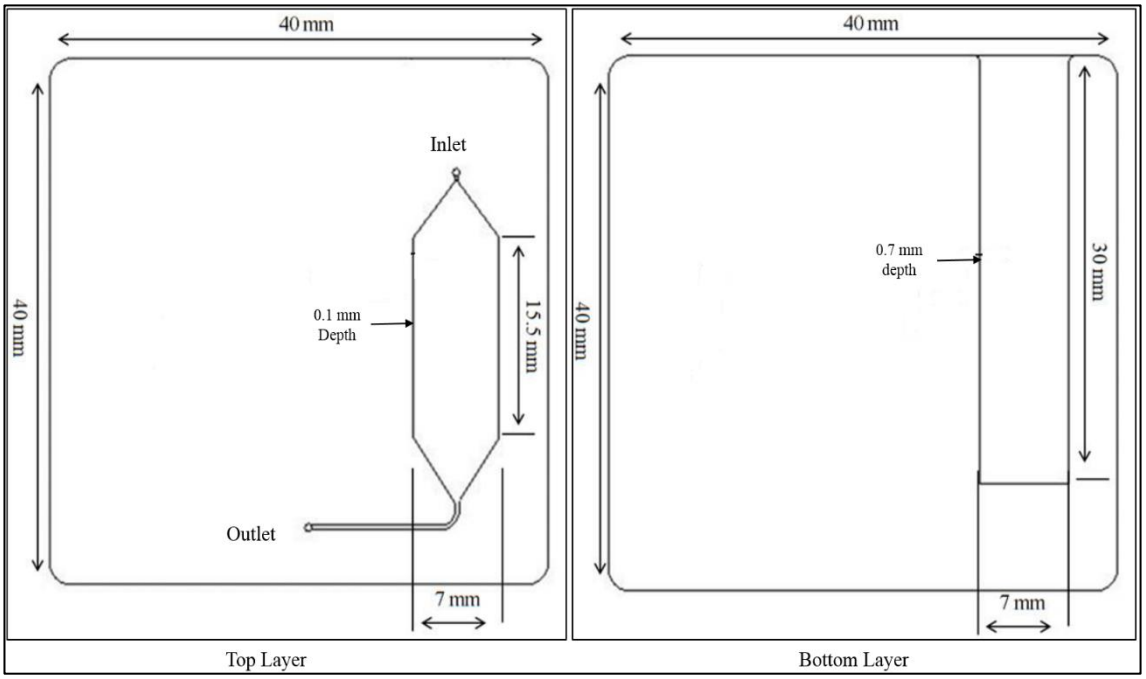

Figure 2-8: Dimensions of the top and bottom layers of the polymer chip

Initially, the top and bottom layers were bound together using double-sided adhesive tape and a roller to ensure the two layers were sufficiently bound to minimise the risk of

leakage. The assembly of the chip is shown in Figure 2-9, the chamber in the top layer was placed directly above the bottom layer where the ITO electrode could be then inserted.

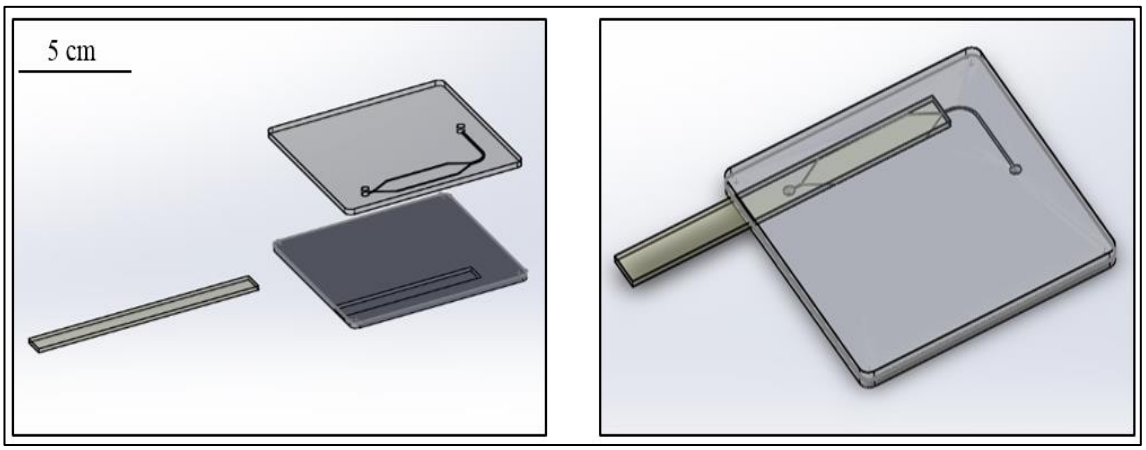

Figure 2-9: Assembly of the polymer microfluidic parts

2.8.1.2 Detection organic pollutant in polymer chip

A completely assembled device is shown in Figure 2-10, which demonstrated all three parts of the device. The ITO electrode with the electrochemically immobilised antibodies was slotted into the polymer microfluidic device.

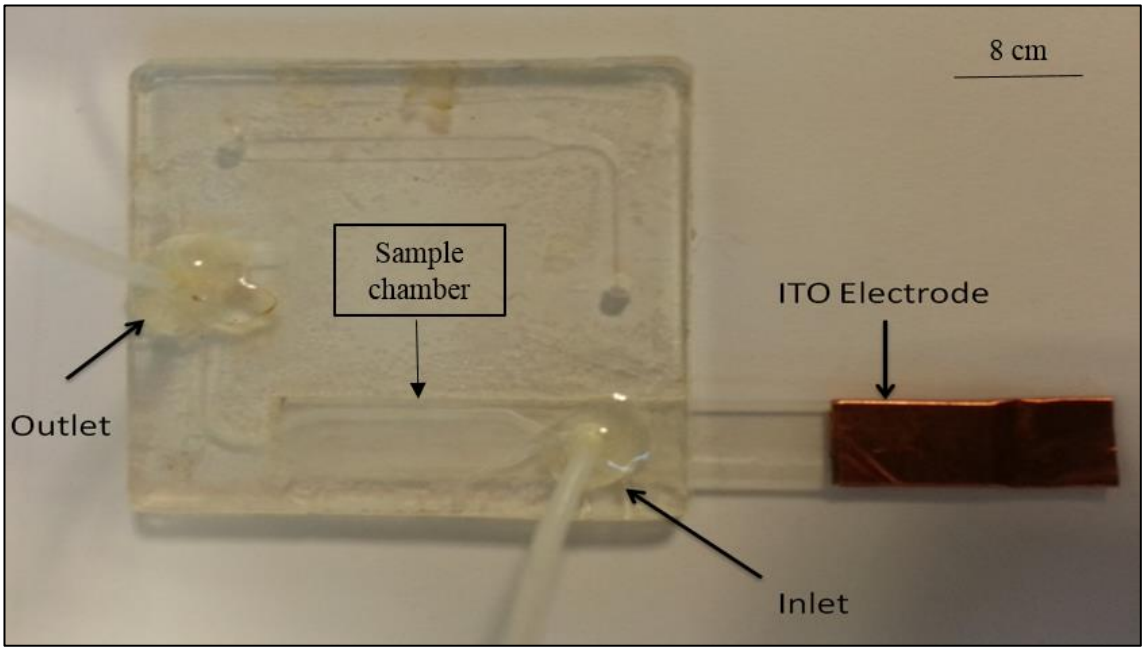

Figure 2-10: COC polymer microfluidic device with the ITO electrode and tubing

The COC polymer chip was connected with PTFE tube at the inlet and outlet holes with epoxy glue as shown in Figure 2-10. The inlet tubing was above the ITO electrode, so the

sample and chemiluminescence reagents could flow over the immobilised antibodies, then exit from the outlet tubing. The chip was placed inside the light – proof box and the syringe pump was connected to plastic chip through the PTFE tubing, and the flow of the reagents was controlled at 10 µL min^{-1}, to measure the chemiluminescence signal with CCD camera as shown in Figure 2-11.

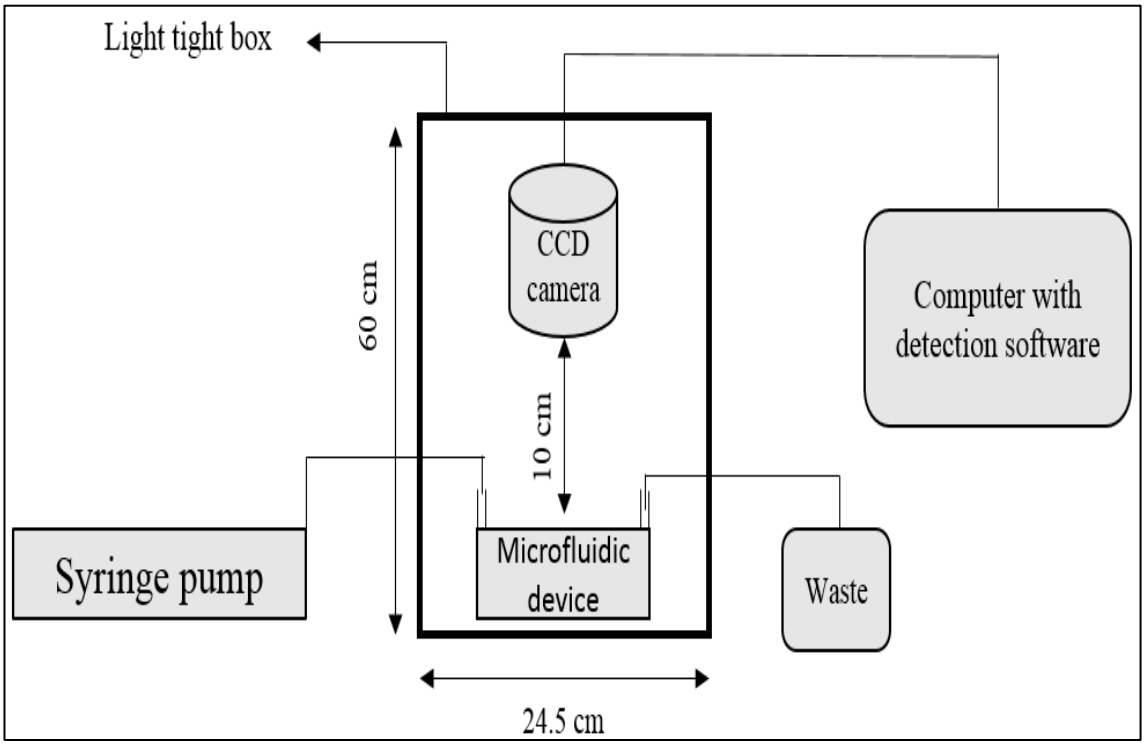

Figure 2-11: Schematic showing the experimental set up for the microfluidic device with the chemiluminescence detection.

2.8.2 Glass microfluidic fabrication

Dr Alex Iles using a Datron 7 CNC milling machine also designed a glass microfluidic device fabricated at the University of Hull. The designs were initially drawn using AutoCAD as shown in Figure 2-12.

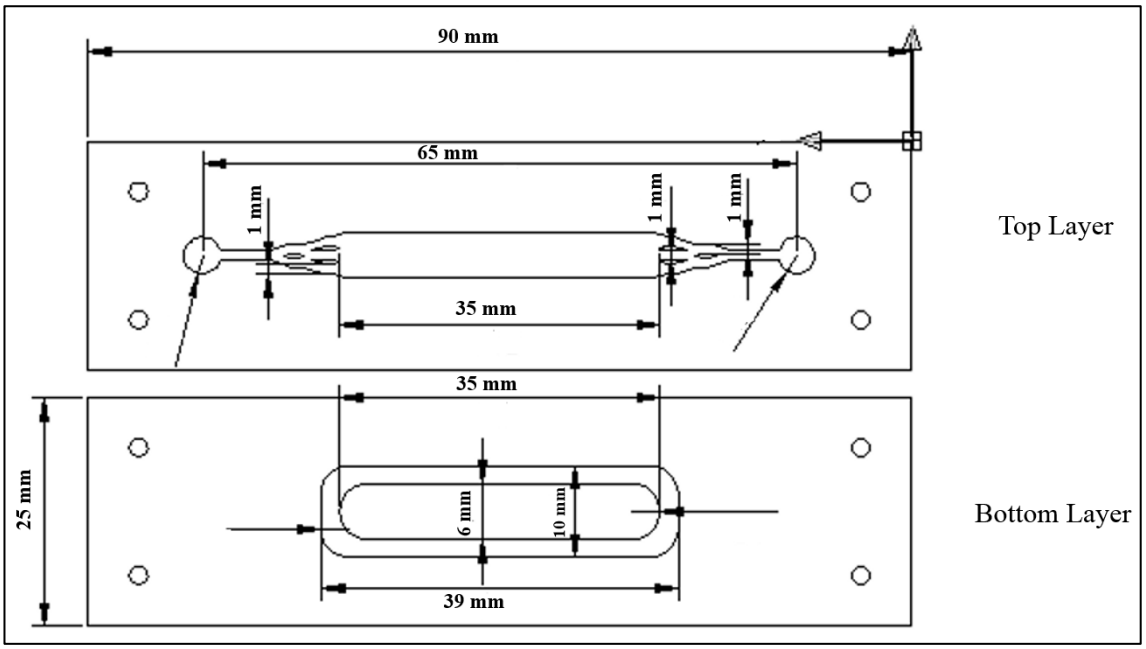

Figure 2-12: Dimensions of the top and bottom layers of the glass chip

The dimension of the device was 90 mm × 25 mm (length and width), where the lower chamber layer was 1.15 mm thick Schott B270 glass. An inner cavity was cut all the way through, and an outer pocket milled to a depth of 0.45 mm. The upper chamber layer was 3 mm thick Schott B270 glass. The flow chamber was milled to a depth of 150 µm. All channels to the flow chamber were 1 mm in width. The volume of the flow chamber and channels (excluding inlets) was approximately 34 µL. The design was transferred to Solidworks and then SolidCAM to make the tool paths for the CNC machine as shown in Figure 2-13.

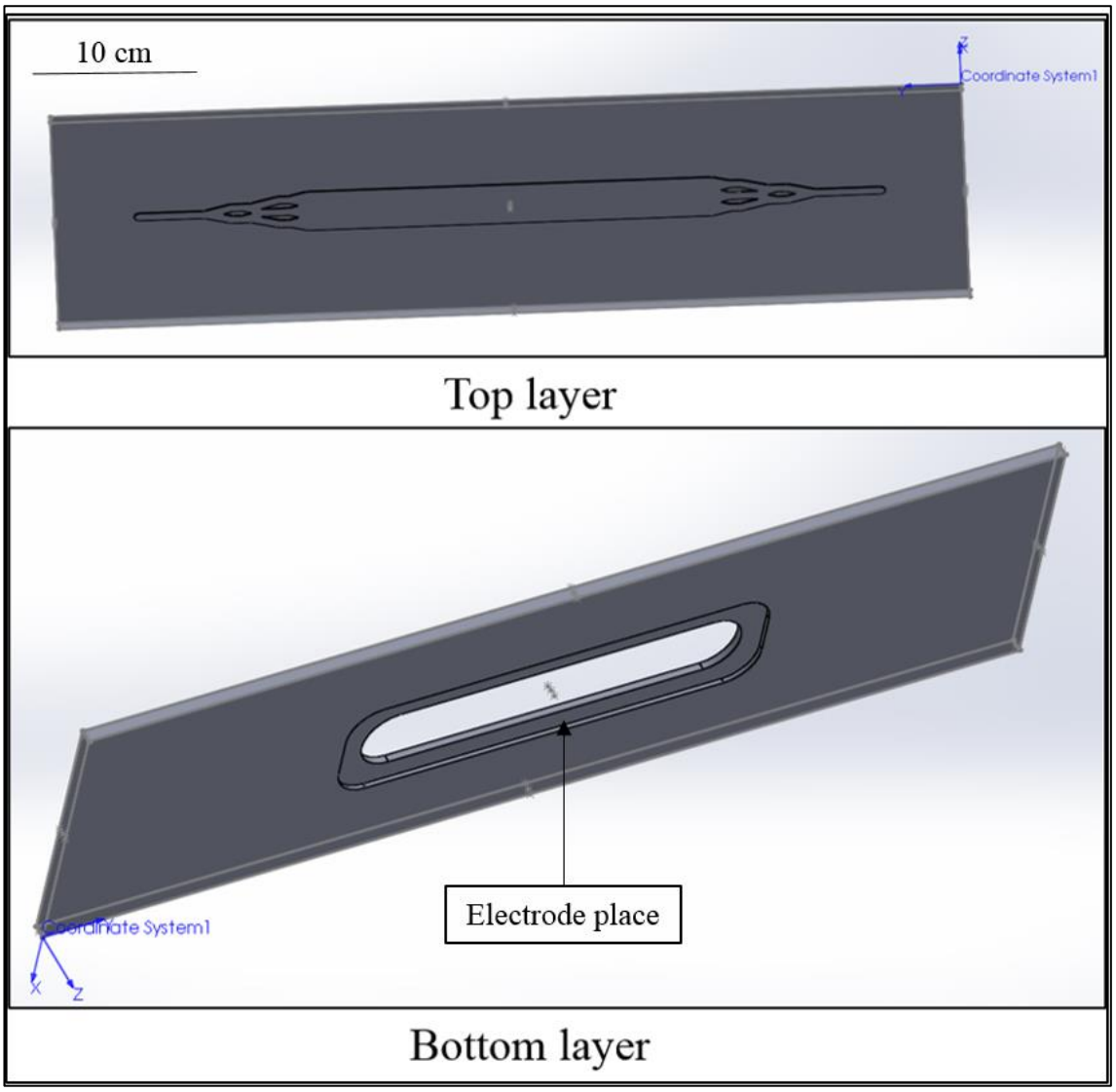

Figure 2-13: The top and bottom layer of the glass chip

The Datron M7 CNC machine, operated at speeds of 5,000 – 50,000RPM, and the x, y and z - movements moved at a maximum speed of 16m/min. The machine was pre-installed with an automated tool length measure. A coolant system that uses ethanol was installed into the machine, which sprays the coolant, plus air, around the spindle of the machine during use. The coolant and air pressure were variable.

The top layer channels and flow chamber were milled with 1 mm diamond end mill tool into the 3mm thick Schott B270 glass, and for access holes, a similar tool was used but 1.5 mm diameter. The bottom layer chamber and pocket were milled with a 1.5 mm diamond end mill tool into the 1.15 mm thick Schott B270 glass. After that the top and

bottom layer were cleaned thoroughly and thermally bond them together with approximately 300 g of weights at approximately 590 °C overnight, to give a chip as shown in Figure 2-14.

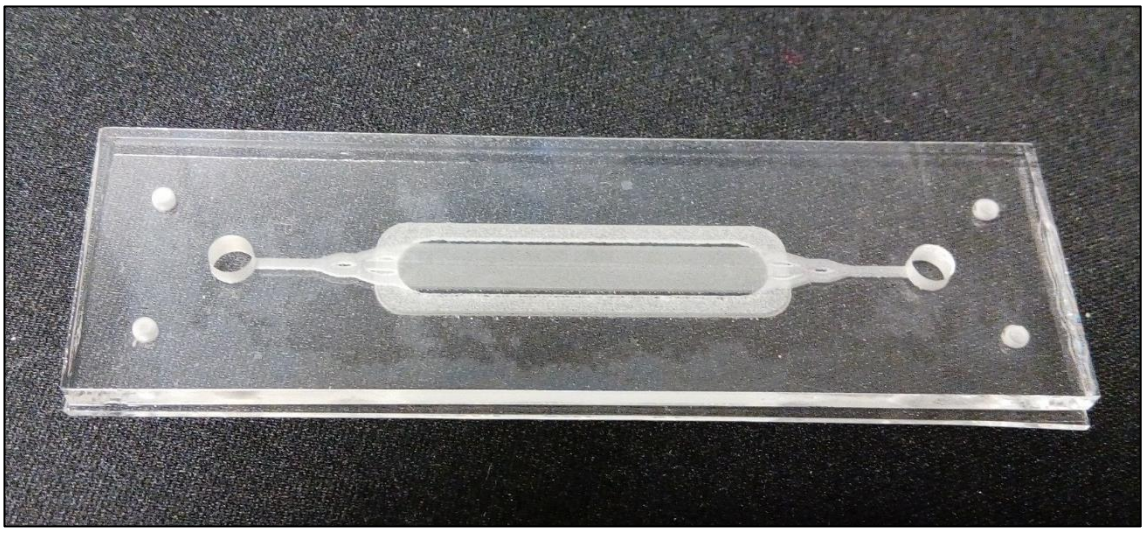

Figure 2-14: Assembly of the top and bottom layers of glass chip

2.8.2.1 Design and fabricated of ITO electrode and clamps

The ITO glass electrode was cut with a Datron 7M CNC machine to fit tightly inside the glass chip. The ITO electrode was redesigned as illustrate in Figure 2-15, where the dimension of the electrode became 34.8 × 5.8 mm (length, width) with 2.9 mm thick.

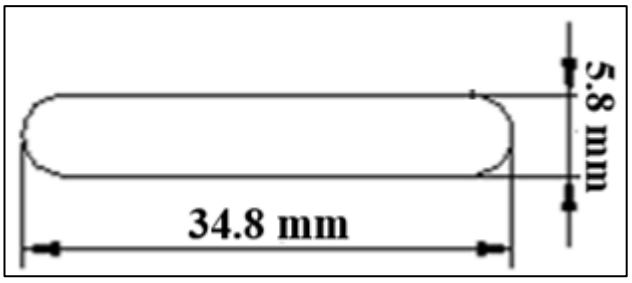

Figure 2-15: Redesign of the ITO glass electrode

The clamps were produced to seal the new glass chip design; Figure 2-16 shows the design of the top and bottom layer of the clamp. The dimension of the two parts of the clamp was 50 × 50 mm (length and width) with 10 mm thick for each layer; six bolt holes with dimension (5 × 8 mm). Both layers of the clamps were closed sealed the chip with screws.

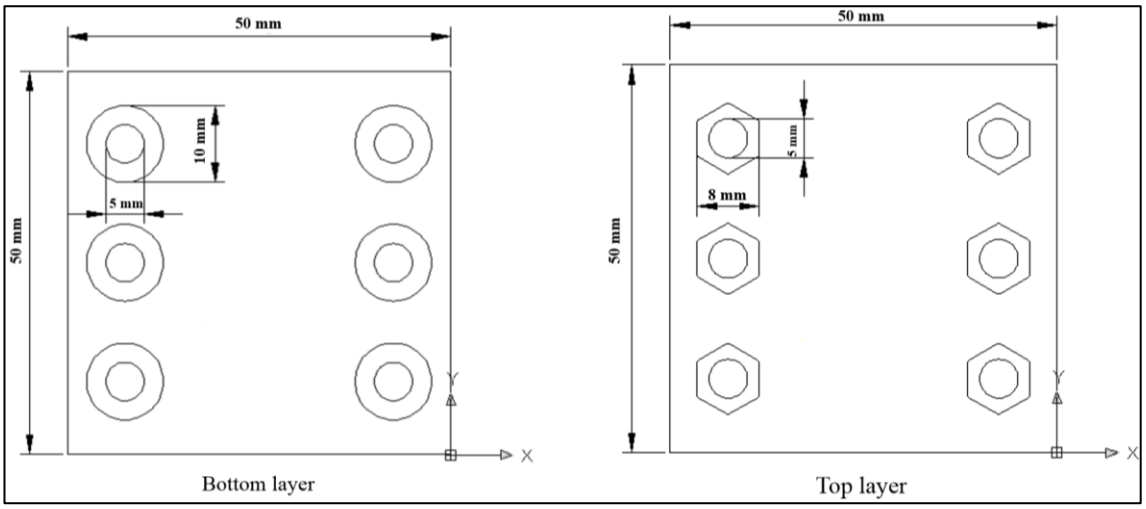

Figure 2-16: The design of top and bottom layer of clamps

2.8.2.2 Detection of the organic pollutant in the glass chip

The complete assembly of all parts of the chip is shown in Figure 2-17. To connect the chip with the flow system two Luer tips were cut from plastic syringes (size 5 mL), and pushed into the inlet and outlet holes, to fit tightly. Araldite 2014 glue was placed outsides of the Luer tips to make sure they were fixed, and that gave a convenient "plug and play" interface. The clamp with bolts loosely assemble. The chip was placed upside down, the ITO electrode inserted when the layer face was down for fit within the recess of the bottom layer. A rubber seal was (1.5 mm thick) placed over the ITO layer, making sure it within the outer recess of the bottom layer. Then the chip was fit in the clamp, and the bolts were gently tightened into the clamps. The bolts were then tightened until the rubber sealed could see be pressing up against the bottom glass layer. This can be noted a change of the appearance of the seal when the air gap between the seal and glass was eliminated; the rubber will appear dark black. The chip was connected to the syringe pump (at 10 µL min^{-1}) to introduce the sample and chemiluminescence reagents through PTFE tube was needed to the sealed. Finally, the chip was ready to use. The chip was then placed inside the light – proof box to measure the chemiluminescence signal with CCD camera as shown in Figure 2-11.

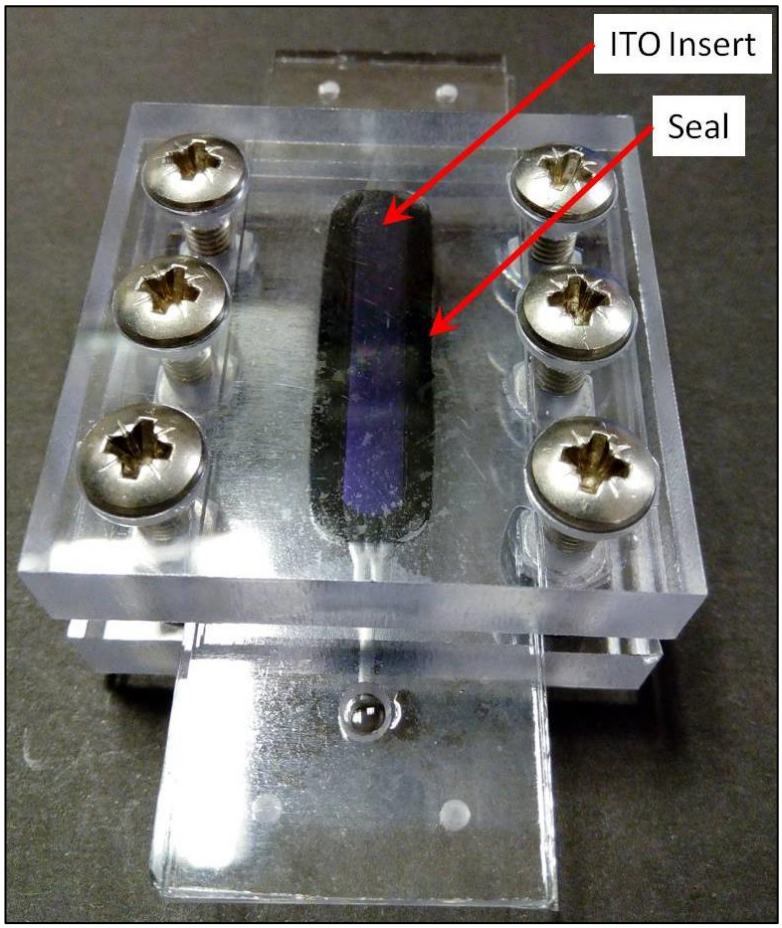

Figure 2-17: Glass chip with ITO electrode

Results and Discussion

Chapter 3. Development of silica monolith for sample preparation

One of the main steps in any sample analysis process is sample preparation that can include filtration, extraction, digestion, separation, and pre - concentration. Efficient sample preparation involves removal of interfering materials such as salts and buffer and this is necessary, as most instruments cannot handle such contaminated sample matrixes directly. Also, analysis of hormones and PAHs compounds in river water sample at low concentrations (ng L^{-1}) in complex matrices requires a step such as using SPE to pre - concentrate the sample, which reflects on improving the sensitivity of detection [49]. As mentioned in the literature review in Section 1.3, new materials, which can be utilised as a sorbent for SPE, are the recently developed monolithic materials.

In this chapter, evaluation of SPE using two type of silica monoliths will be discussed based on TMOS and TEOS. In addition, a comparison between methanol and acetonitrile to elute the analytes from silica monolith is made to find out that is the best to use to pre - concentrate the river water sample.

3.1 Fabrication of silica monolith

The fabrication procedures for the silica monoliths were described in Section 2.4, where the silica monolith rod was prepared inside a disposable plastic syringe (1 mL) that was used as a mould. The starting mixture consisted of an alkoxy silicon derivative (TMOS or TEOS) in the presence of water – soluble organic polymer, polyethylene oxide (PEO). Acetic acid was used as catalysts for TMOS, whereas the nitric acid was used for TEOS, as described in the first chapter, to start the hydrolysis and condensation reaction[77-78].

After completion of the gelation process, the monolith structure shrank, so it became easy to release the silica monolith rod from the mould. Then the silica monolith rod was treatment with 1 M of an aqueous ammonia solution at 80 °C for 24 hours. After that, washed the rod in the distilled water to remove all the residues, put the rod in the oven for 3 hours at 550 °C to remove all the organic residues as mentioned in section 1.5, the final shape of the silica monolith rods shown in Figure 3-1.

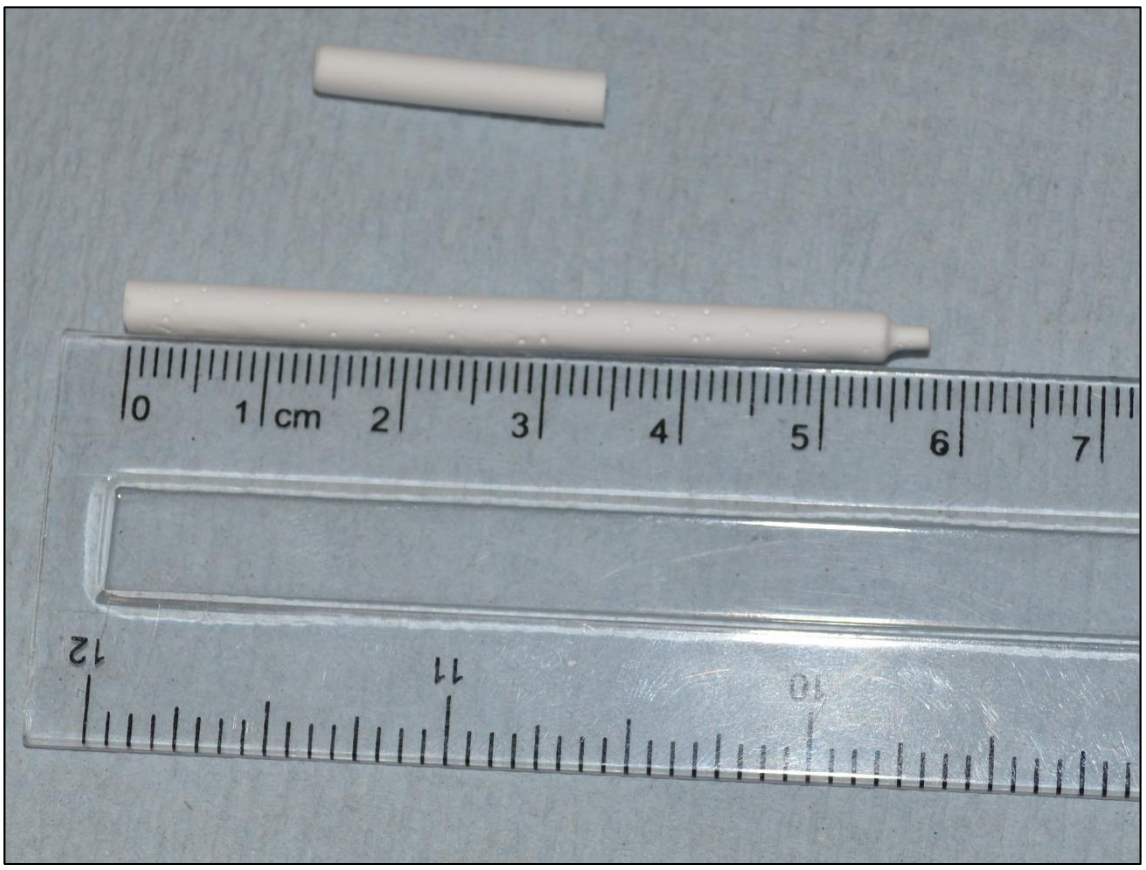

Figure 3-1: Image of monolithic silica rods prepared by using the sol-gel method.

SEM was used to present the influence of each step of the sol-gel process on the internal structure of the silica monolith rod. The steps as explained in section 2.4 were applied. Figure 3-2 shows the internal structure of the TMOS silica monolith after each step in the fabrication process. Image (A) shows the SEM of the internal structure of TMOS after the gelation process and before treatment with aqueous ammonia solution. The through pores that form the macroporous structure can be clearly seen and the surfaces are smooth.

Image (B) shows the internal structure image of the TMOS after treatment with ammonia solution and the calcination process. The surface of the silica monolith rods changed after hydrothermal treatment, becoming roughened. This roughened surface is an indication that mesopores have been created on the surface skeleton by a dissolution – precipitation process as an explanation in section 1.5.3 [90-91].

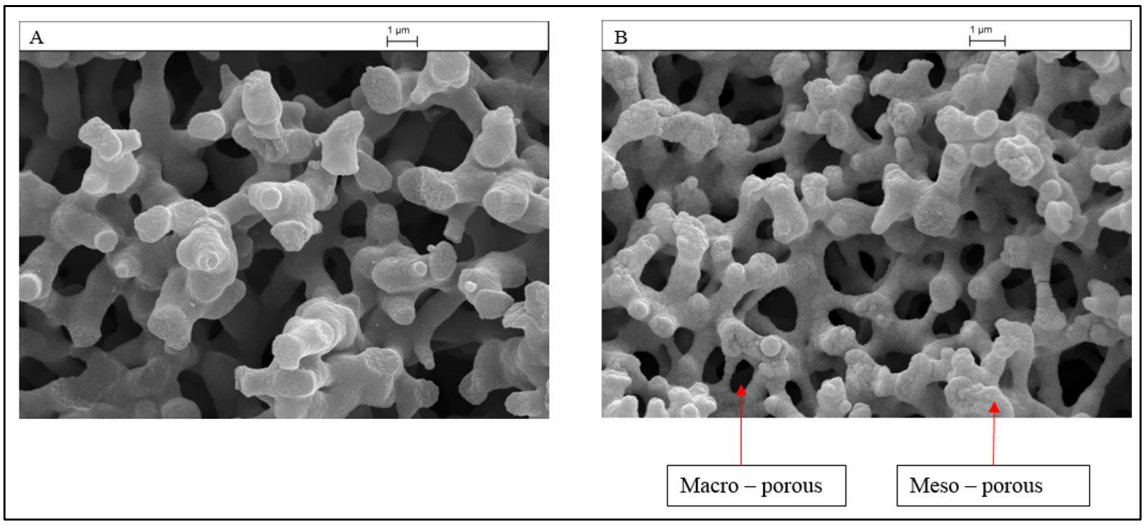

Figure 3-2: SEM images of the internal structure of silica monolith rods consisting of TMOS + PEO (200K) + 1 M Acetic acid(A) before 1 M NH_4OH treatment, (B) after 1 M NH_4OH treatment.

3.1.1 Hydrothermal treatment of the silica monolith by ammonia

The surface area of the sorbent is one of the most important factors that influence on the extraction efficiency. Therefore, the formation of the mesopores on the silica monolith surface needs to be substantial to obtain a high surface area. Based on this point, the hydrothermal treatment of the silica monolith with ammonia becomes a vital step in order to improve the extraction efficiency as explained in Section 1.5.1.3. The surface area of the silica monolith was measured, and isotherms obtained before the ammonia treatment and after by using BET method. The calculation of the particular surface area of the TMOS (prepared with PEO 200 K) monolith rod before ammonia treatment was found about 30 ± 12 $m^2 g^{-1}$ while after ammonia treatment the surface area jumped to 404 ± 1.8

$m^2 g^{-1}$. The increasing the surface area is an indicator to form the mesopores on the silica monolith surface.

The isotherm curves obtained for the TMOS monolith rod before and after hydrothermal treatment is shown in Figure 3-3. Figure 3-3 (A) shows the isotherm for TMOS monolith rod before hydrothermal analysis, where the isotherm curve obtained is similar to the type II isotherms that explained in section 1.8.1, Figure 1-11. The type II isotherm obtained is for a macroporous absorbent where the pore size is more than 50 nm. Figure 3-3 (B) shows the isotherm curve of the TMOS monolith rod after the hydrothermal treatment, where the isotherm curve is similar to type IV. As discussed previously in section 1.8.1, type IV is obtained for mesoporous materials where the pore size in the range between 2 to 50 nm [107-108].

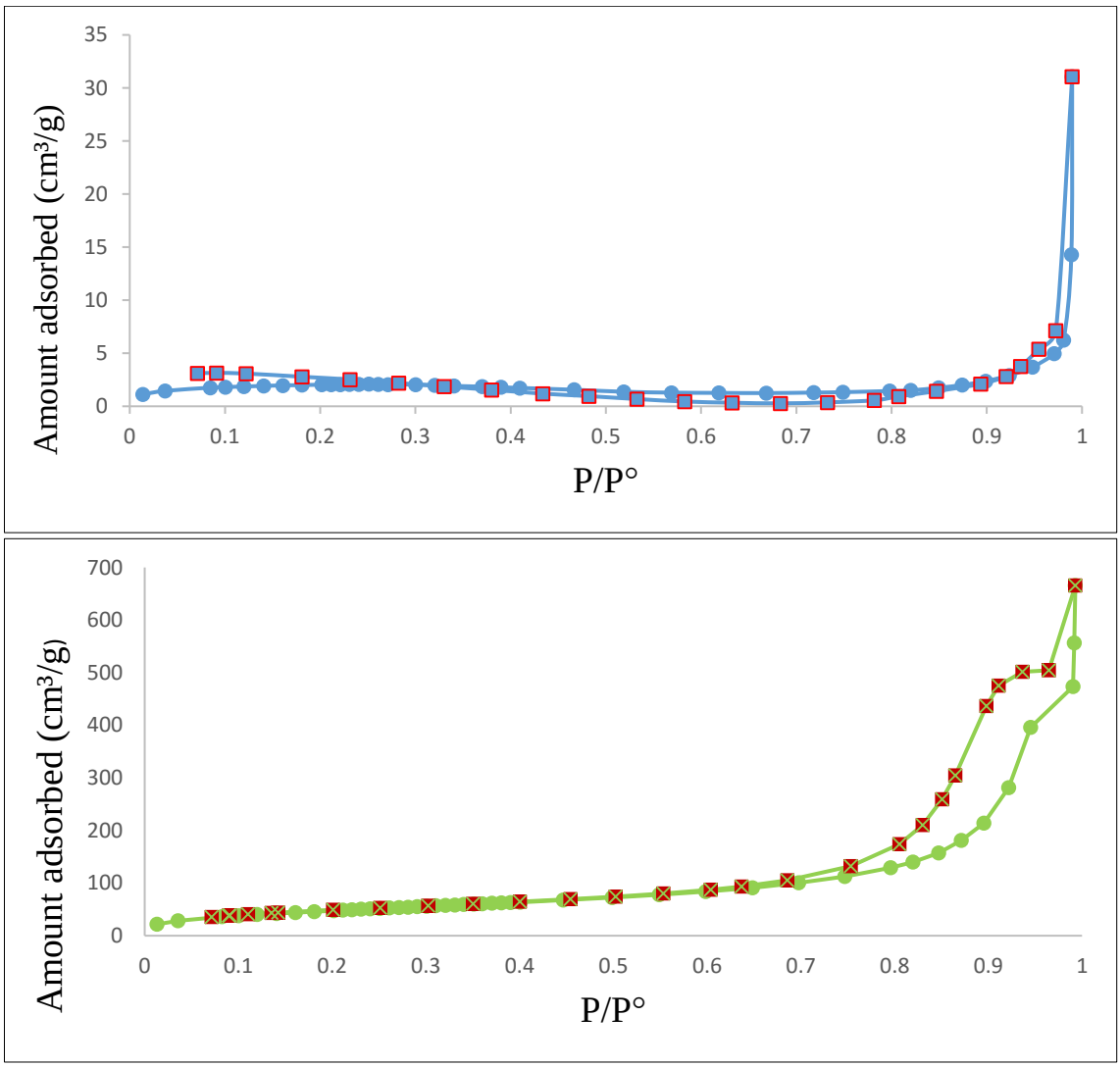

Figure 3-3: BET isotherm curves for TMOS monolithic silica. Isotherm (A) is for TMOS monolithic silica before hydrothermal treatment, and isotherm (B) is for TMOS monolithic silica after hydrothermal treatment.

This result supports the assumption that the internal structure of the silica monolith rod and the surface area based on the form of the mesopores using the hydrothermal treatment with ammonia solution. Therefore, this result shows the importance of the hydrothermal treatment steps in order to form the mesopores in the surface of silica monolith that led to increasing the surface area significantly [90-91].

3.1.2 Comparison between TMOS and TEOS

SEM was used to compare the morphology of the TMOS and TEOS monoliths. Figure 3-4 shows the internal structure of the TMOS and TEOS at different magnifications, high

and low. Both types of structure are similar, but the pore size of TEOS is relatively larger than TMOS, and the structure of TMOS appears to be denser. The approximate pore size of both types were measured by averaging 20 pore diameters from the SEM images. The average of pore size for TMOS was 1.4 ± 1.2 µm while the TEOS had an average of pore size 2.3 ± .08 µm.

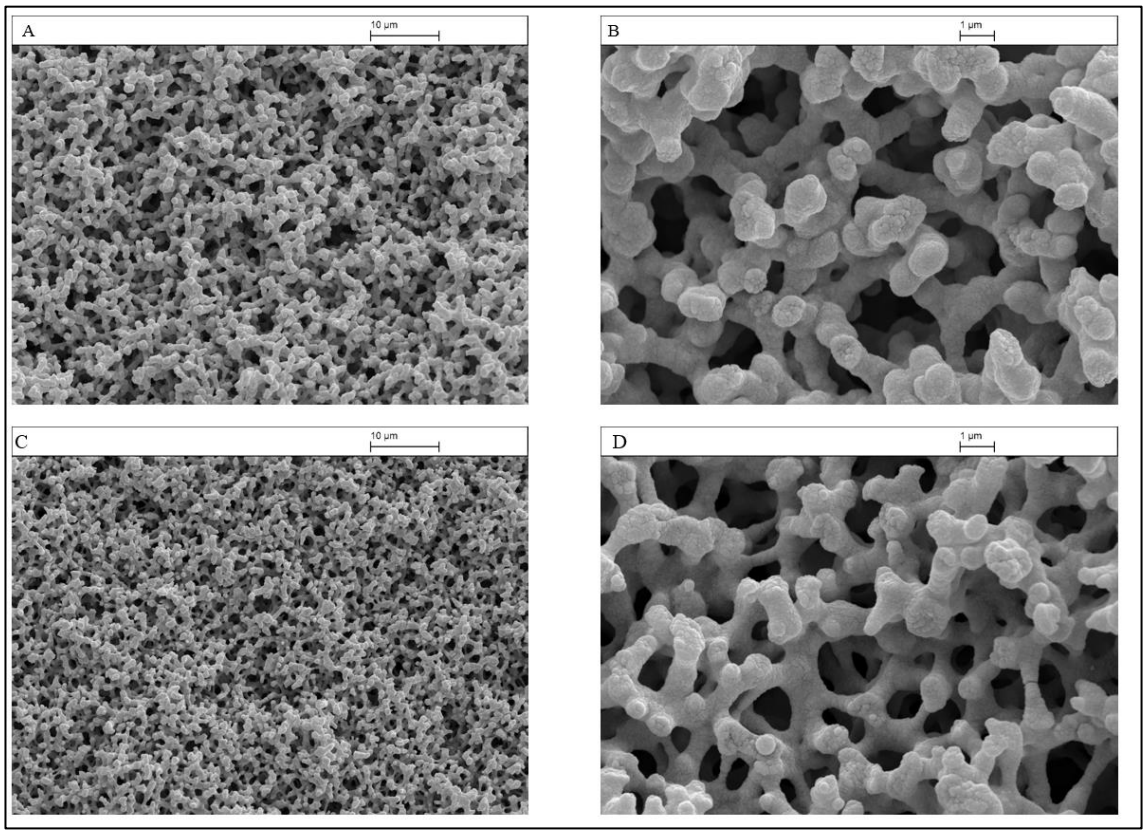

Figure 3-4: SEM image of (A & B) TEOS, (C & D) TMOS the scale bar for (A & C) are 10 µm with low magnification and the scale bar for (B & D) are 1 µm with high magnification.

These results showed the TMOS provide a dense structure with a small pore size, which improved the chance of interaction between the analyte and the silica monolith surface, therefore, increase the extraction or pre – concentrate efficiency. TEOS provide a good permeability compare with TMOS, which means low backpressure during the flow experiments. Further comparison between the two types will discuss later when comparing the extraction efficiency.

3.1.3 Impact of the porogen size on the synthesis of the silica monolith

Two different molecular weight of porogen (100 K and 200 K) of polyethylene oxide (PEO) were used for the preparation of both types of silica monolith TMOS and TEOS. The BET method was applied to calculate the surface area and porosity of both types as explained in section 2.5.2. Table 3-1 summarised all the result obtained for both types.

Table 3-1: The physical properties of the internal structure of TMOS and TEOS monoliths

Type of monolith	BET Surface Area ($m^2 g^{-1}$) ± RSD % n=3	Average Pore Diameter (nm) ± RSD % n=3	Pore Volume ($cm^3 g^{-1}$) ± RSD % n = 3	Pore Size Diameter (µm) ± RSD % n = 3
TMOS (PEO 100 K)	357.52 ± 2.4	8.76 ± 11.21	0.92 ± 4.9	1.1 ± 9.1
TMOS (PEO 200 K)	404.66 ± 1.46	7.82 ± 4.83	0.94 ± 3.72	0.96 ± 3.4
TEOS (PEO 100 K)	295.26 ± 2.32	12.42 ± 5.3	1.5 ± 6.7	2.8 ± 3.6
TEOS (PEO 200 K)	314.1 ± 3.78	10.63 ± 3.82	1.2 ± 8.3	2.2 ± 4.6

The specific surface area of the TMOS monolith used PEO 100 K was found to be approximately 357.52 $m^2 g^{-1}$, whereas the TMOS monolith prepared with 200 k PEO provided a higher surface area about 404.6 $m^2 g^{-1}$. The difference in the diameters of the mesopore for both types were not great. Using TEOS, a higher surface area was obtained with PEO 200 K, which offered a surface area around 314.1 $m^2 g^{-1}$ as compared to 295.26 $m^2 g^{-1}$ for PEO 100 K. As a result of this experiment, the higher molecular mass porogen (PEO 200 K), was selected for the proceeding experiments.

The results in Table 3-1 show there is a decrease in the through pore size for 200 K PEO. The reason for this decrease could be the quicker growth of the silica network before the structure of the silica monolith is frozen pending the phase separation as mentioned in section 1.5.3 [87, 89]. The surface area increases with an increase in the concentration the molar mass of the porogen (PEO) in the starting mixture, conversely through a reduction in the through pore size lead to an increase in the backpressure with the flow through experiment as discussed later.

The long procedure required to fabricate the silica monolith rods could have an effect on the reproducibility. To investigate the reproducibility of the fabrication process, three different batches of the silica monolith were fabricated in different time, and investigated by measuring the relative standard deviation (RSD) of their physical properties, the pore size, the pore volume and the surface area. Table 3-1 shows the % RSDs obtained were less than 10 %, indicating the reproducibility of the preparation process of the silica monolith rods was passable. The results of the through pores obtained from measuring the SEM images showed % RSD values of between 15 to 20 %, the measurements of the pore size distributions in the SEM images always presents variation.

3.2 Modification of the silica monolith with C_{18}

After the silica monolith had been fabricated, C_{18} was used to modify the surface of the silica monolith as explained in section 2.4.2. The reagent that was used to modify the silica monolith surface was chlorodimethyl octadecyl silane (CDMOS) that produced an octadecyl – silica surface, where this step was carried out by the continuous flow of the reagents through the pores of silica monolith rod. The reaction of the reagent (CDMOS) with the silanol group on the silica monolith surface is shown in Figure 3-5.

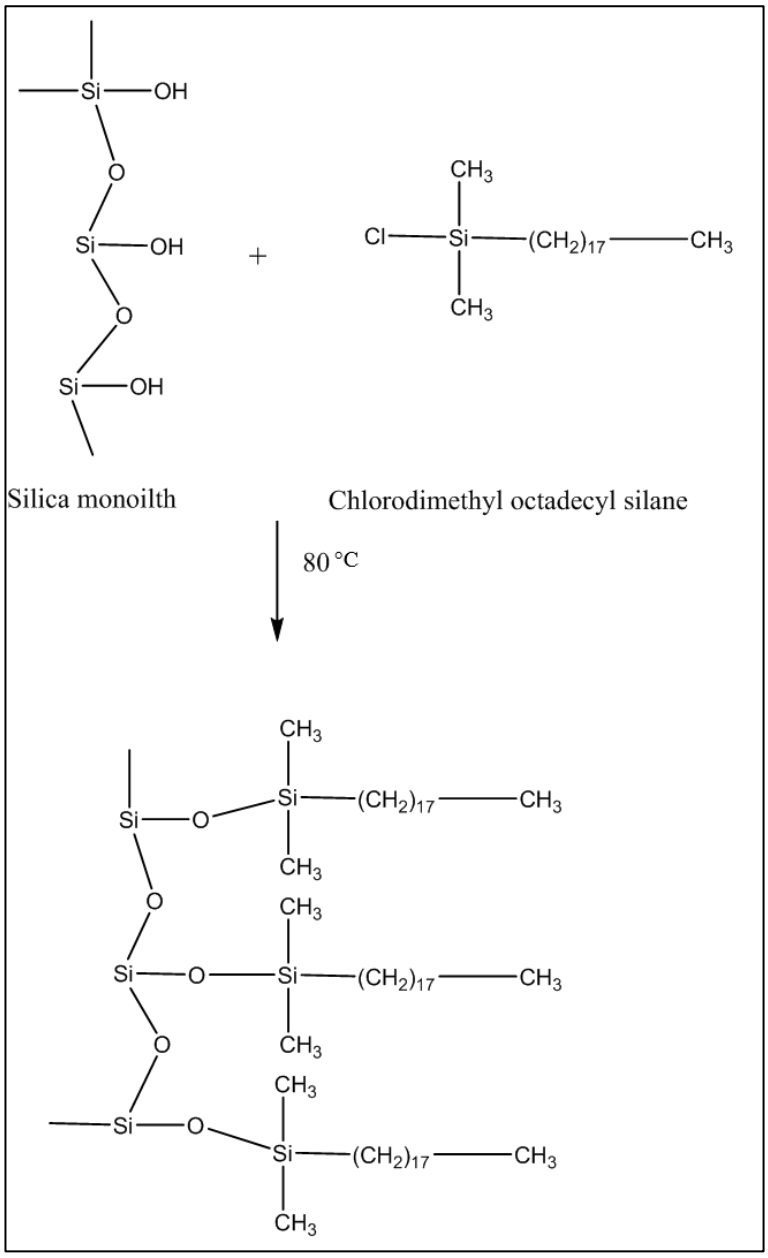

Figure 3-5: Formation of octadecyl – silica (C_{18} – silica) on the silica monolith surface.

To evaluate the method for modification the surface of the silica monolith, SEM was applied to compare the morphology of the silica monolith before and after modification the surface with C_{18}. The N_2 adsorption *via* the BET method was used to investigating the influence of modification the surface with the C_{18} process on the surface area and pore size.

The TMOS silica monolith was chosen to modify by C_{18}, and the SEM analysis was used to investigate the effect of modification process on the structure morphology and compare the variation occurred in the internal structure of silica monolith before and after

modification with the octadecyl group. Figure 3-6 shows the SEM image of the internal structure of TMOS monolith where image (A) before modified the monolith surface and image (B) after the C_{18} modified the surface.

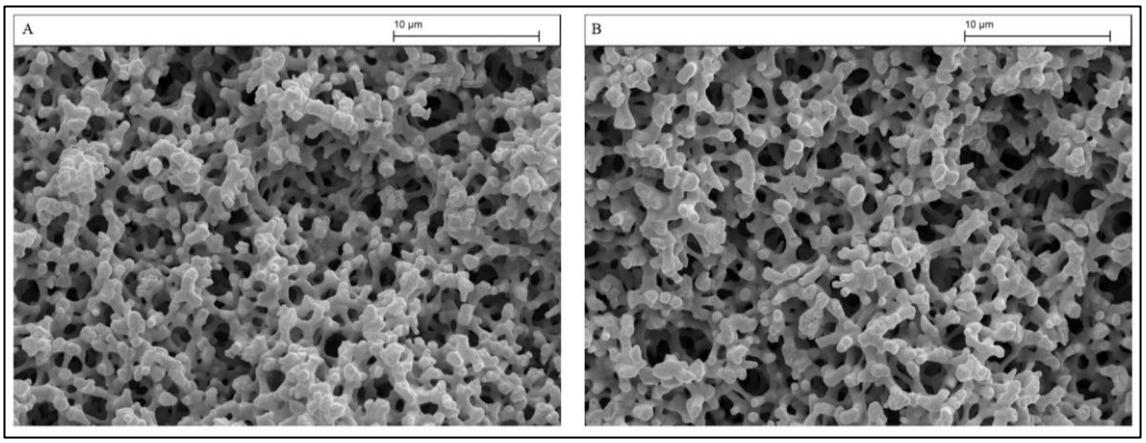

Figure 3-6: SEM image for TMOS, (A) shows the internal structure before modified monolith surface and (B) shows the internal structure after modified the monolith surface by C_{18}.

Figure 3-6 shows there is no great difference in the internal structure of TMOS silica monolith when comparing between before and after modification. Therefore, the SEM image not appropriate method to confirm the process of C_{18} modification of the surface.

To confirm the process of modification of the silica monolith surface was complete successfully. Further experiments were carried out using BET method to measurement the change in surface area and the average pore size diameter of mesoporous of the TMOS silica monolith after modification with C_{18}.

Table 3-2: The physical properties of TMOS silica monolith before and after modification by C18

Type of monolith	BET Surface Area (m^2g^{-1}) ± RSD % n=3	Average Pore Diameter (nm) ± RSD % n=3	Pore Volume (cm^2g^{-1}) ± RSD % n = 3	Pore Size Diameter (µm) ± RSD % n = 3
TMOS	405.24 ± 1.15	7.57 ± 2.75	0.92 ± 1.1	0.96 ± 4.9
TMOS after modification	373.46 ± 1.76	7.12 ± 1.78	0.89 ± 1.12	0.73 ± 2.8

Table 3-2 shows the physical properties of TMOS before and after C_{18} modification, where it can be seen the surface area decreased after the modification process to around 373 m^2g^{-1} compare to 405 m^2g^{-1} before modification. While in the volume or size diameter of the mesoporous and the through pore, the changing was slightly. The decrease in the surface area after modification could be because of blocking of the micropore access (pore size < 2 nm) in the internal silica monolith structure by the bonded phase, as explained in section 1.7 [49]. Decreasing in the surface area of TMOS silica monolith indicator to successful modification procedure.

The reproducibility of the procedure to modify the silica monolith surface by C_{18} was investigated three different monoliths. The surface area, the through pore, pore volume and the mesoporous gave % RSD values of less than 5 %, therefore this procedure to modify the silica surface showed good reproducibility.

3.2.1 EDX analysis

EDX analysis was another method applied to evaluate the procedure of a modification of the TMOS silica monolith surface by octadecyl group. The silica monolith mainly consists of silicon (Si), oxygen (O) and carbon (C), and as would therefore be expected the EDX spectra of the silica monolith before modification in Figure 3-7 was found to have 52% for Si, 40% for O and 5% for C. Figure 3-8 shows the EDX spectra for the modified TMOS silica monolith. The percentage of carbon has increased to nearly 24%, indicating the presence of the octadecyl group on the TMOS silica monolith surface.

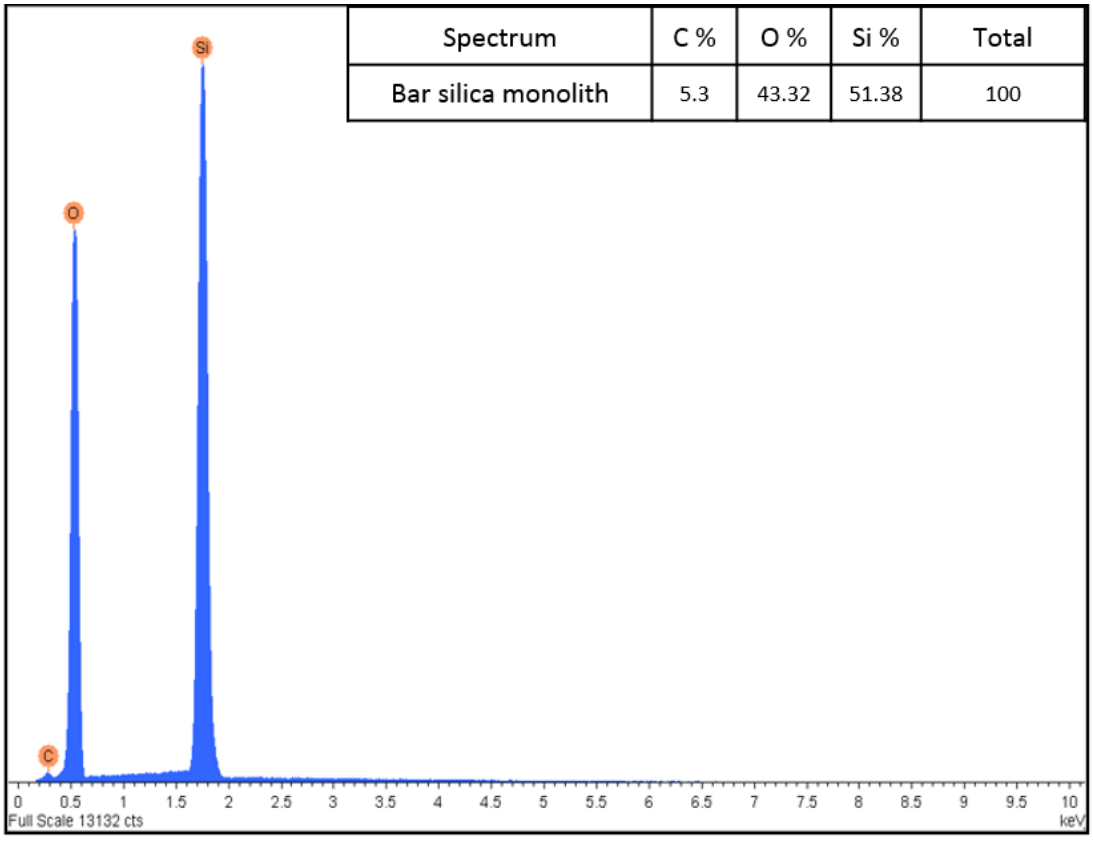

Figure 3-7: EDX spectra for non – modified TMOS silica monolith

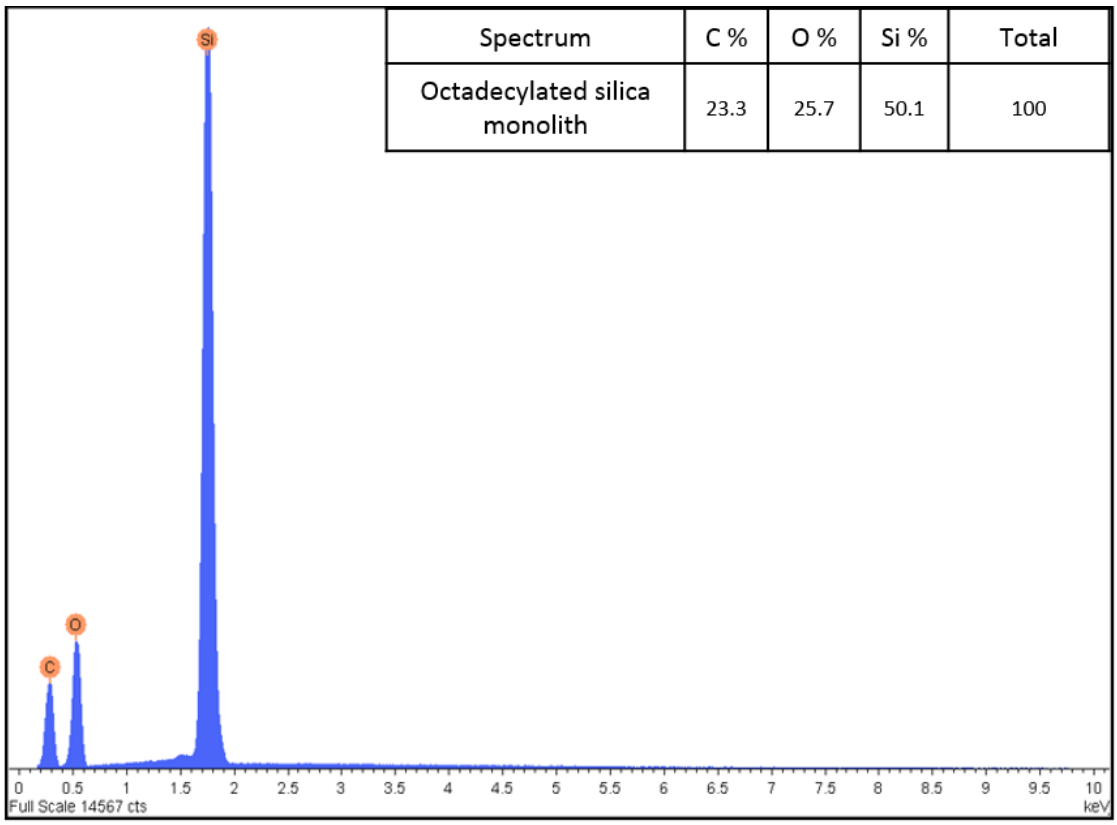

Spectrum	C %	O %	Si %	Total
Octadecylated silica monolith	23.3	25.7	50.1	100

Figure 3-8: EDX spectra for modified TMOS silica monolith

3.3 Solid phase extraction

After physical characterisation of the silica monolith, the ability of the C_{18} silica monolith to extract and pre – concentrate, the analytes from river water sample were investigated. The C_{18} modification was chosen to carry out the extraction and pre – concentrate experiment due to the long alkyl chain being hydrophobic, which increases the interaction between the sorbent and selected hydrophobic compounds.

3.3.1 Preliminary experiment to pre – concentrate the organic pollutants

The most effective method for characterising the SPE sorbent is the evaluation of the extraction efficiency, of selected analytes. However, before going deeply into this investigation, a preliminary simply experiment was carried out to study the ability of C_{18} modified silica monolith to pre – concentrate the non – polar organic pollutants and find out the best organic solvent to elute the analytes. All the details of this experiment including the materials sample preparation and set up of UV – Vis spectrophotometer was

explained in section 2.6.1. The first step was to optimise the UV – Vis spectrophotometer detecting by finding the λ_{max} as shown in Figure 3-9.

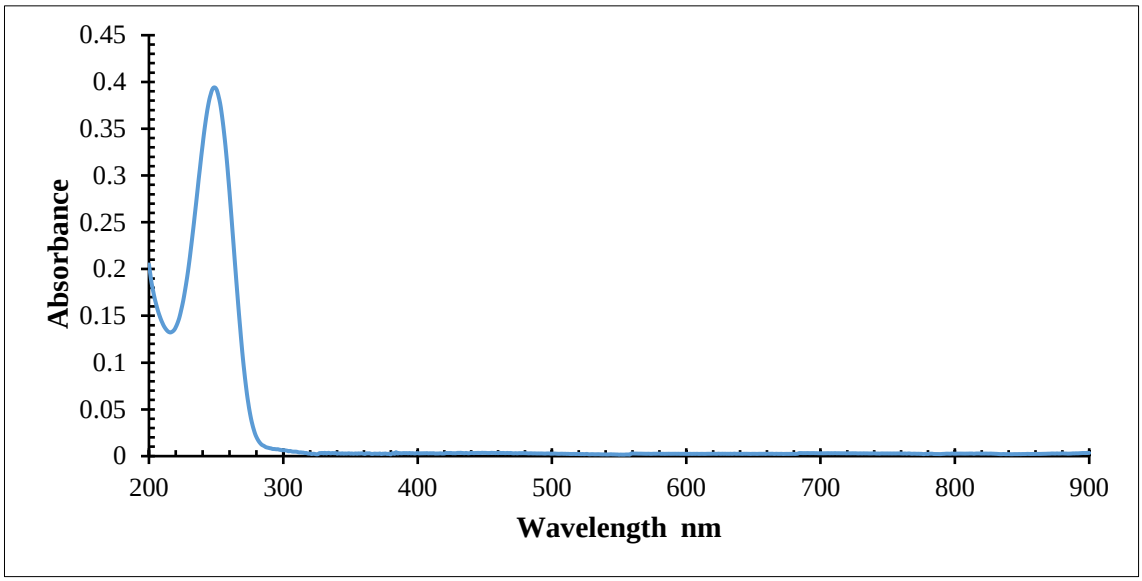

Figure 3-9: UV – Vis spectra scan of 10 µg ml^{-1} of progesterone.

Figure 3-8 shows the UV – Vis spectra for a progesterone standard, where the λ_{max} was at 254 nm. This wavelength was then used to prepare the calibration curve as shown in Figure 3-10.

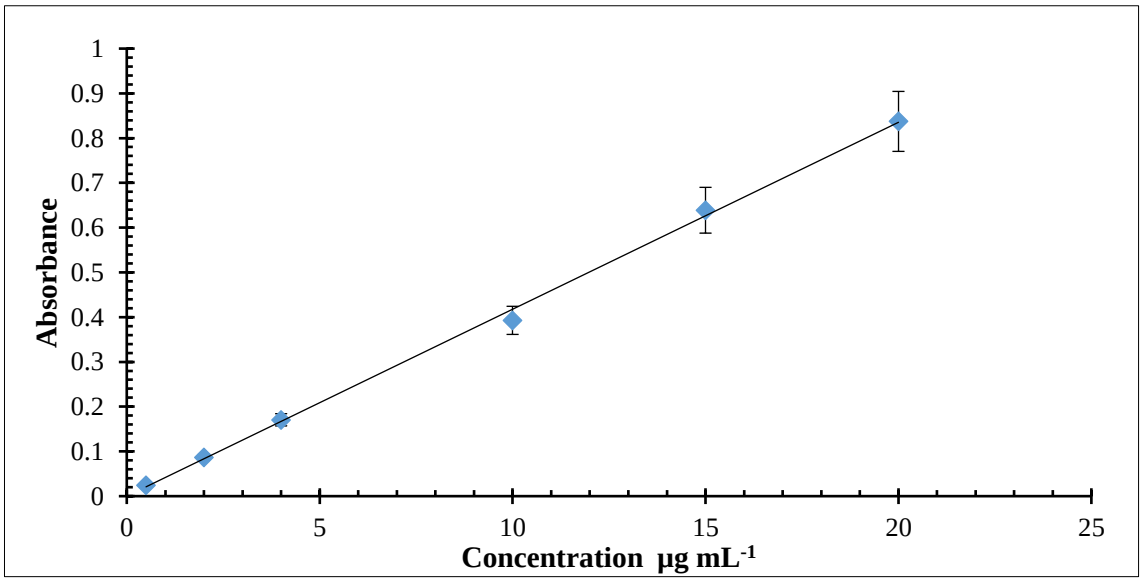

Figure 3-10: Calibration curve for progesterone with use UV – Vis spectrophotometer at 250 nm, (n = 3). The error bar indicates one standard deviation.

The absorbance of progesterone standards in the concentration range of 0.5 to 25 µg mL^{-1} at 250 nm wavelength gave excellent linearity, with an R^2 value of 0.9985 and a line equation of y = 0.0418x. The limit of detection of was calculated by using Equation 2-3, which was 1.01 µg mL^{-1}.

To measure the extraction efficiency a 20 mL aliquot of 1 µg mL^{-1} progesterone was initially loaded on the monolith column with a flow rate 100 µL $min^{-1,}$ followed by 5 mL of distilled water for washing step which was repeated three times. The complete experiment was carried out twice once where 5 mL of acetonitrile was used to elute the progesterone, secondly where 5 mL of methanol was used. 3 mL of each fraction was transferred to a quartz cuvette for absorbance measurements.

To elucidate the percentage recovery during the pre – concentration of progesterone from C_{18} modified TMOS, the results were plotted as a bar chart for each step during the pre – concentration process, where the grey bar present the absorbance of the progesterone standard as shown in Figure 3-11.

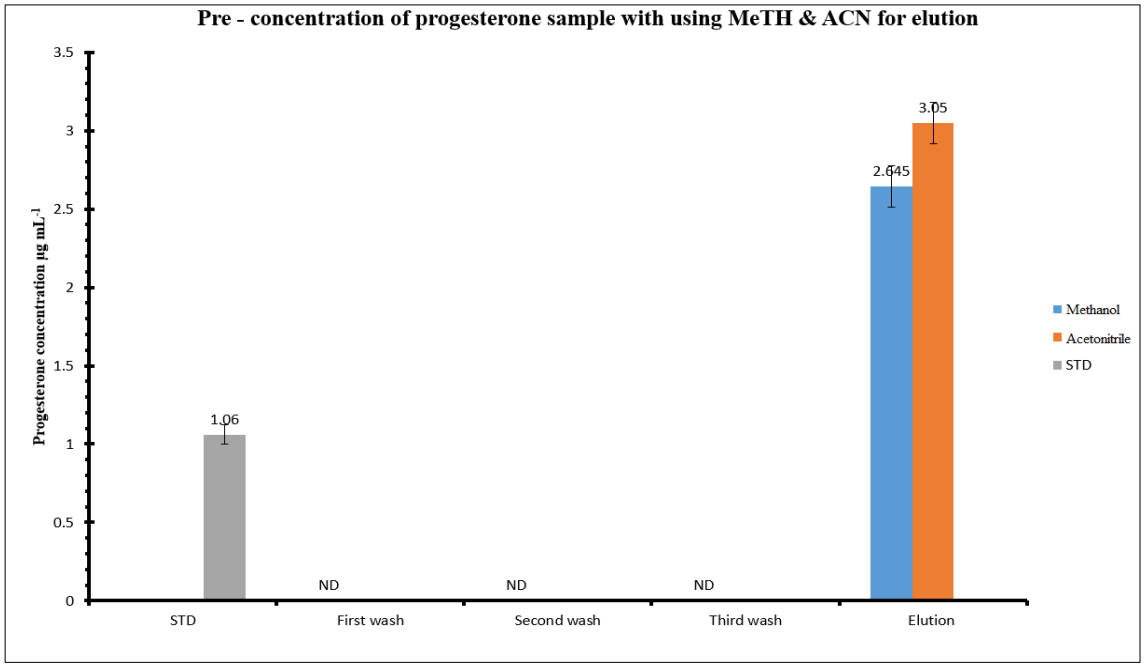

Figure 3-11: pre -concentration of the progesterone sample (1 µg ml^{-1}) using methanol and acetonitrile for elution step, (n = 3). The error bar indicates one standard deviation.

As would be expected no analyte was eluted in the loading and washing steps as a result of the hydrophobic surface of the silica monolith. The percentage of pre – concentration of the target analyte was calculated from the concentration in the eluted solvent using the calibration curve, where each analysis was carried out in triplicate. Figure 3-11 shows the ability of C 18 modified TMOS monolith to pre - concentrate progesterone from a water sample. When the elution step was carried out with methanol, the progesterone concentration was 2.65 µg mL^{-1} (66.13 %), while with acetonitrile the concentration increased to 3.05 µg mL^{-1} (76.3%).

To conclude this experiment, the C_{18} modified silica monolith showed a high ability to pre – concentrate and extract the non – polar organic compounds from a water sample. Moreover, the acetonitrile shows high efficiency compare with methanol. The acetonitrile capable to dissolve the analyte more than methanol because of the acetonitrile dipole moment higher the methanol. As a result of that, the acetonitrile was chosen to use in following experiments in the elution step.

3.3.2 Compare the extraction efficiency between TMOS and TEOS

The first step with using silica monolith was test the effect of it with blank sample, where 1 mL of distilled water was pass through the TMOS column and injected into the HPLC system as shown in Figure 3-12.

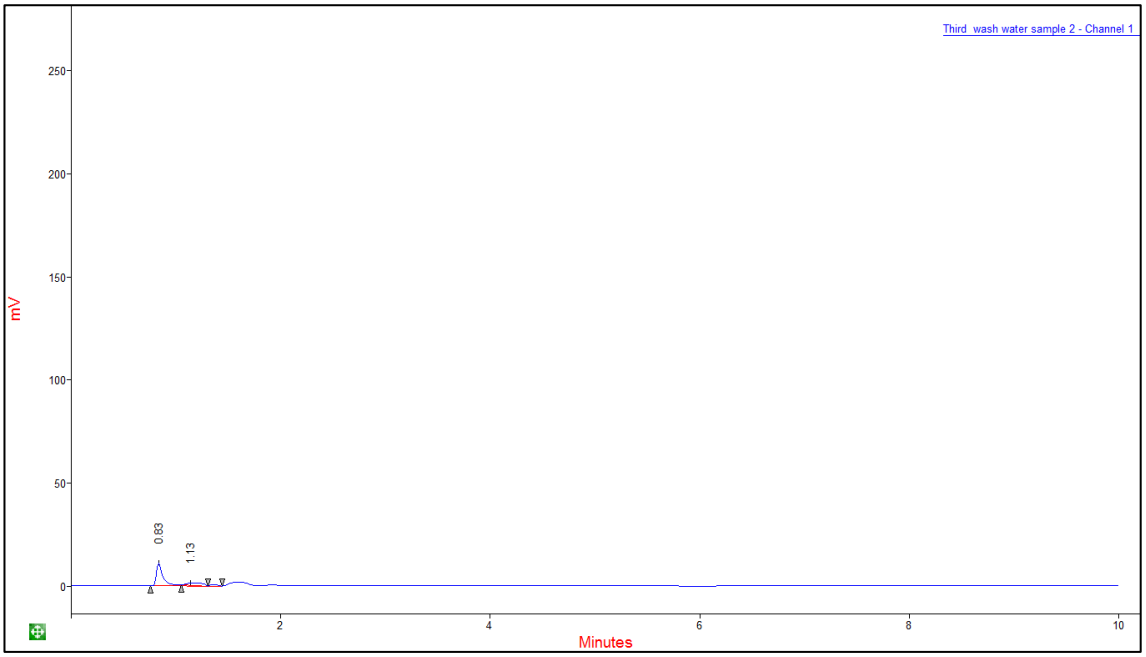

Figure 3-12: The chromatogram of the blank

Figure 3-12 shows there is no effect of the TMOS column on the blank, where this step is necessary to confirm that.

In order to select, the suitable C_{18} modified silica monolith column to extract and pre – concentrate the non- polar organic pollutants, the extraction efficiency were calculated for both TMOS and TEOS monolithic column as described in section 2.6.3. 1 µg mL^{-1} of progesterone was passed through both types of silica monolith column at a different flow rate (100, 300, 500, 700, 900, 1000 µL min^{-1}) to find out the optimum flow rate to apply in the following experiment. 1 mL of progesterone standard (10 µg mL) was pumped though the silica column, following by 1 mL of distilled water to remove unbonded analyte thrice, finally 1 mL of acetonitrile used for elution step where the flow rate fixed at 100 µL min^{-1}. Each fraction was collected, and 20 µL was injected into HPLC system.

Figure 3-13 show the HPLC chromatogram of extraction process for progesterone using the C_{18} TMOS modified column (A) shows the chromatogram of the progesterone standard (10 µg mL^{-1}), where the retention time of the directly injected progesterone standard was at 7.63 min (B) shows the chromatogram of the loading fraction, (C) shows the chromatogram of the washing step and (D) represent the chromatogram of the elution fraction.

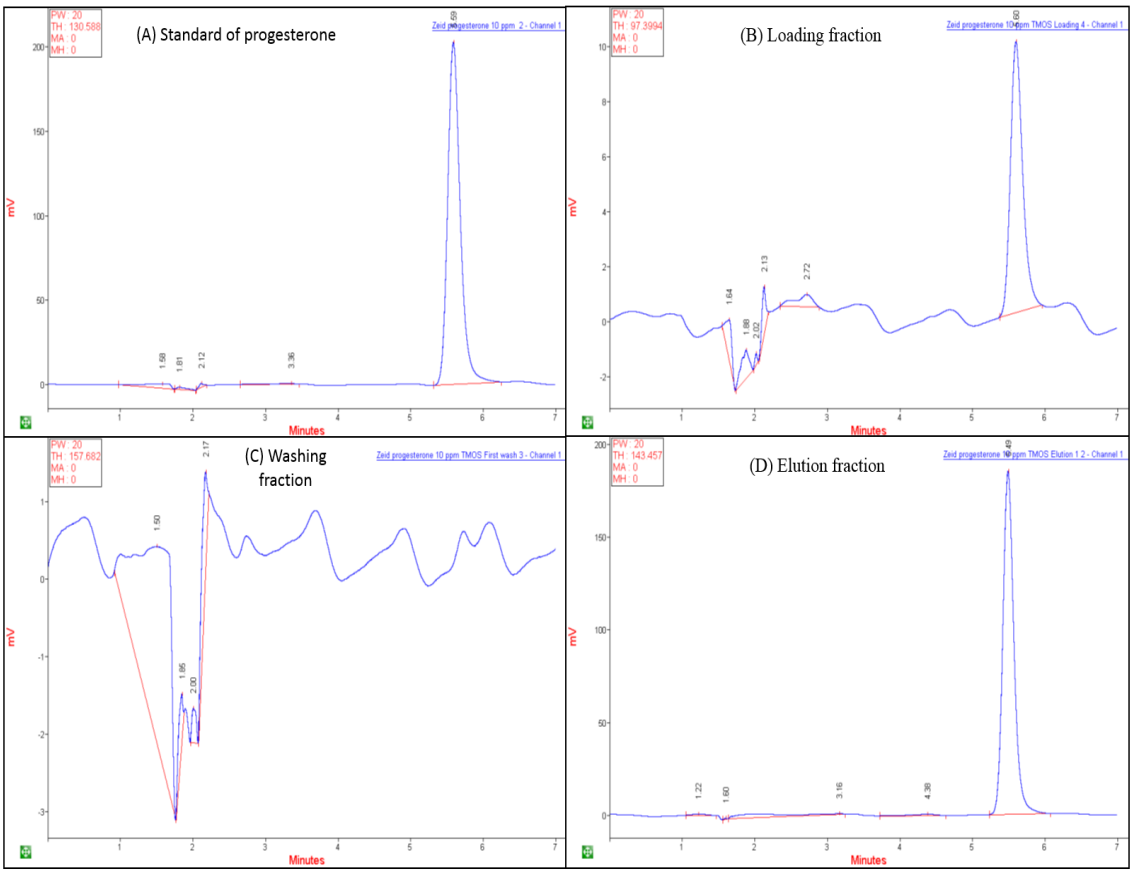

Figure 3-13: HPLC chromatogram of extraction of the target analyte by the C_{18} TMOS modified column, where (A) standard solution of progesterone (10 µg mL^{-1}) was directly injected into the HPLC system, (B) Loading fraction, (C) washing fraction and (D) elution fraction.

Figure 3-13 shows the chromatograms of each extraction process, where the analyte is detected at very low level in the loading step and in washing step is not detected at all because it retained in the C_{18} modified column. The progesterone was then eluted with acetonitrile, which is used with water in the mobile phase to decrease the noise of the baseline.

To evaluate the percentage recovery for the extraction of the progesterone by both types of C_{18} modified column TMOS and TEOS as explained in 2.6.3, the Equation 2-1 was used to calculate the percentage. The chromatographic peak areas for the direct injection of the standard sample were compared with the peak area obtained for each fraction in the extraction process while each analysis was carried out in triplicate. The percentage extraction recovery of 10 µg mL^{-1} progesterone through TMOS and TEOS monolithic columns are presented in Figure 3-14.

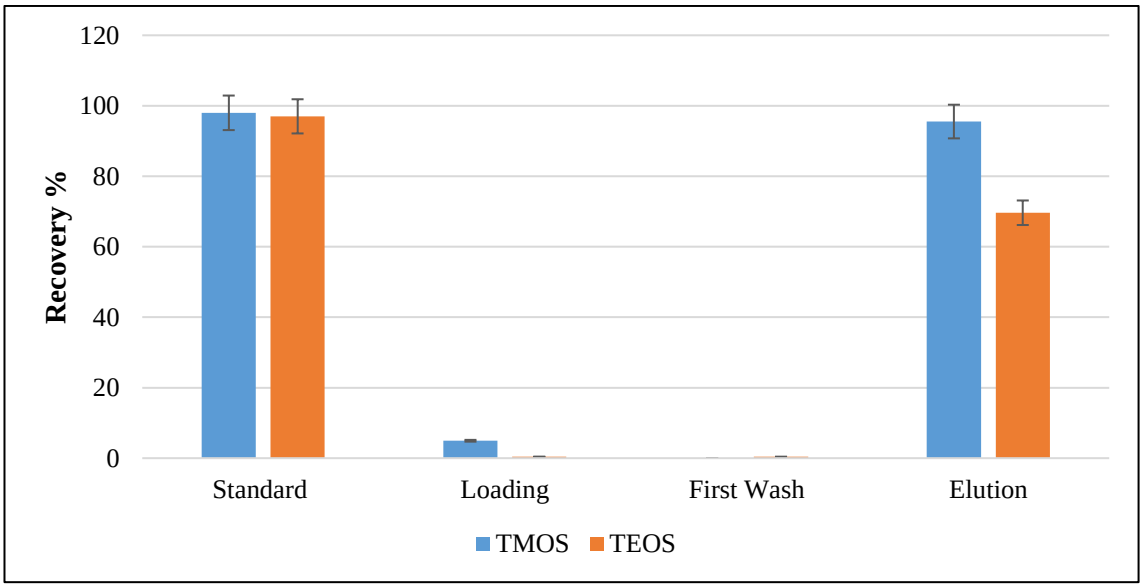

Figure 3-14: The extraction efficiency of progesterone using C_{18} modified column (TMOS & TEOS), (n = 3). The error bar indicates one standard deviation.

Using the TMOS C_{18} modified monolith column, the extraction efficiency achieved was around 93%, and the loading fraction was detected around 5%. In the washing step, no analyte was detected at all. The remaining 2% was retained in the column. While using the TEOS C_{18} modified column, the extraction efficiency was nearly 70%, with no analyte detected during the loading and washing step. However, 30% of the analyte was still linked with the C_{18} surface. As the result of this experiment, the C_{18} TMOS monolith column achieved high extraction efficiency compare with the C_{18} TEOS monolith column.

3.3.3 Optimising the flow rate

Optimising the flow rate of the solvent used for each step in the extraction or pre – concentrate process is important. The effect of the sample flow rate for progesterone was investigated using both types of C_{18} silica monolith (TMOS and TEOS) with different flow rate 100, 300, 500, 700, 900 and 1000 µL min^{-1} as explained in section 2.6.3. The impact of the different flow rate on the extraction efficiency of 10 µg mL^{-1} progesterone by passing 1 mL through both types of the C_{18} modified monolith (TMOS and TEOS) is shown in Figure 3-15.

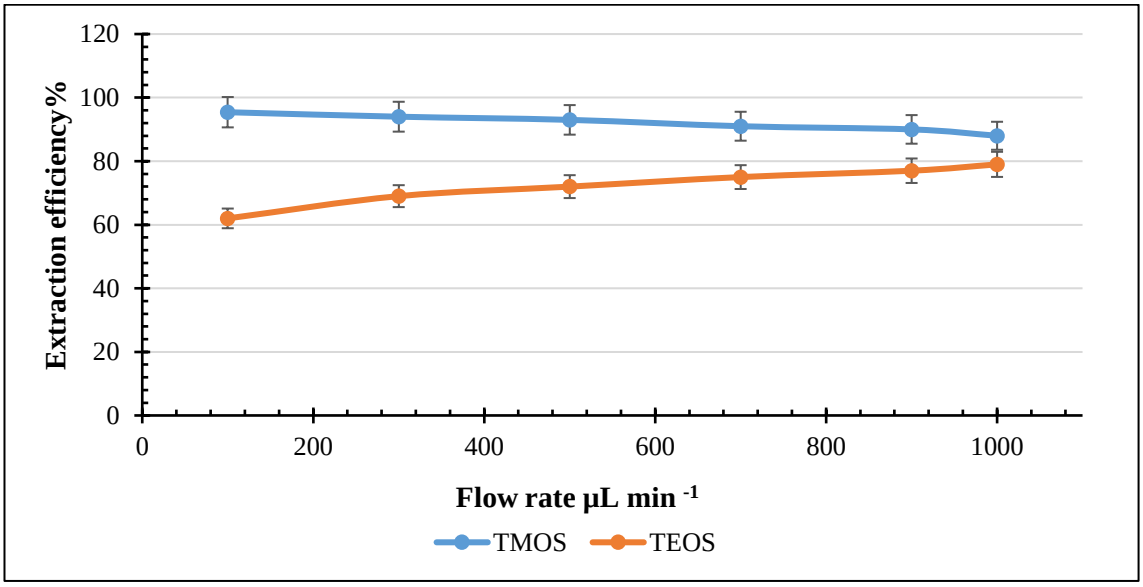

Figure 3-15: Effect of the flow rate on the extraction efficiency of 10 µg mL^{-1} of progesterone by TMOS and TEOS C18 modified monolith (n=3). The error bar indicates one standard deviation.

The effect of changing the flow rate on the extraction efficiency percentage it clearly to see in Figure 3-15, where the efficiency of the extraction percentage for TMOS decreased as the flow rate increased (blue line). A flow rate for 100 µL min^{-1} gave the highest extraction efficiency (nearly 95 %), as decreasing the flow rate led to an increased opportunity for interaction between the analyte and modified surface of the sorbent, and this resulted in higher adsorption of the target analyte to the surface of the C_{18} modified silica monolith. After a flow rate of 500 µL $min^{-1,}$ the extraction efficiency of the analyte

decreased to under 90% until it approached 83 % at 1000 µL min^{-1}. That indicated there was a quantity of progesterone that did not interact with the silica monolith surface but instead emerged in the loading or washing steps.

In Figure 3-15 the orange line represents the effect of changing the flow rate on the extraction efficiency by using TEOS modified monolith. The extraction efficiency of TEOS was lower than TMOS but in this case, it increased with increasing flow rate, where the percentage recovery at a flow rate 100 µL min^{-1} was 62% and raised to the highest percentage at flow rate 1000 µL min^{-1}. The reason behind this result is that the through pores of the TEOS are bigger than TMOS and with reduced flow rate the solution of sample flow the easiest way to pass through a column, which reduces the possibility of interaction between the analyte and the surface of the silica monolith. While with increasing the flow rate the pumping power forces the solution to flow all the ways, therefore the possibility of interaction between the analyte and the silica surface are increased as shown in the extraction efficiency with high flow rate [77].

To conclude this experiment, the TMOS shows great ability to extract the analyte compare with TEOS as explained in section 3.3.2 even with changing the flow rate, where the maximum extraction efficiency with TEOS was around 80% at 1000 µL min^{-1} while in this flow rate the TMOS achieved extraction efficiency around 83%. As a result of that, the TMOS C_{18} modified monolith was used in all the extraction and pre – concentration experiments for non –polar organic pollutants. In addition, the flow rate at 900 µL min^{-1} achieved a recovery percentage nearly 90%, which is little less that recovery percentage at 100 µL min^{-1}. A flow rate at 900 µL min^{-1} was therefore selected for the experiment in order to reduce the time required for the pre – concentration of the large volume of the

sample, where the river water sample use in the experiment was 100 mL pre – concentrate the analytes to level within the detection limits.

3.4 Pre – concentration of the analytes

3.4.1 Figure of merit for the progesterone calibration curve

The calibration curve that was obtained to calculate the concentration of progesterone after each step of the pre – concentration process was evaluated in term of linearity, LOD and LLOQ to verify the reliability and applicability when analysed using HPLC – UV system that was set up as described in section 2.6.2. Standard solutions of progesterone at concentration 0.1, 0.07, 0.04, 0.01 and 0.005 mg mL^{-1} were analysed by HPLC where each concentration was analysed three times, and the peak areas were plotted against concentration, where Figure 3-16 shows the calibration curve.

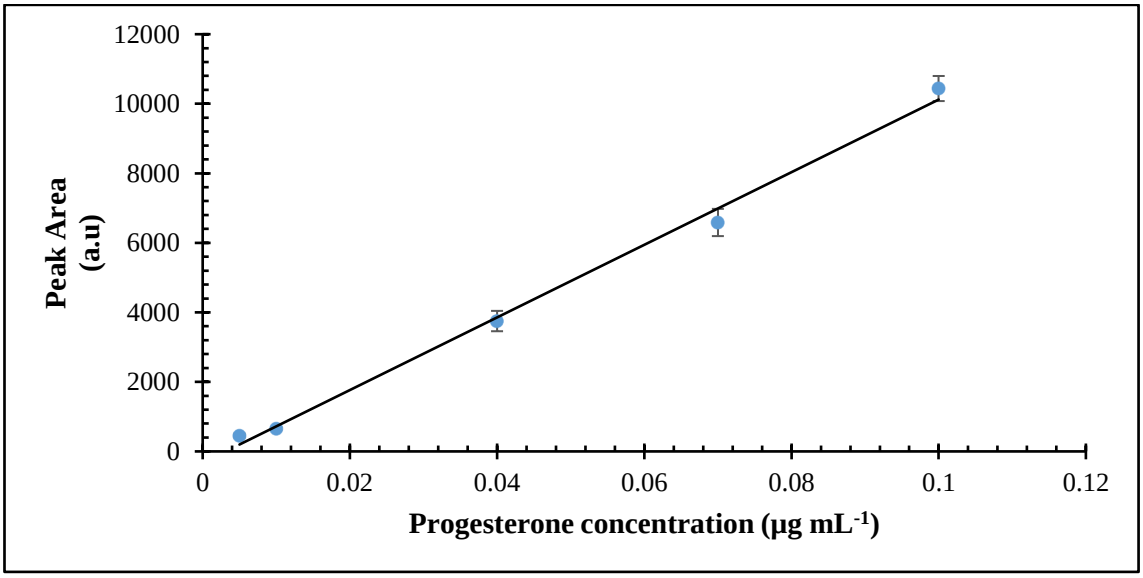

Figure 3-16: Calibration curve of progesterone standard solutions with peak area plotted against concentration (µg mL^{-1}), (n = 3). The error bar indicates one standard deviation.

The HPLC – UV calibration curve for the progesterone that analysed with system showed a good linearity over the range used and gave a correlation coefficient (R^2) ≥ 0.9952 where the linear equation obtained is shown in Equation 3-1.

$$y = 104448\,x - 324.23$$ Equation 3-1

The LOD was 9 µg mL^{-1} and the LLOQ was 30 µg mL^{-1} as calculated using Equation 2-3, Equation 2-4, Equation 2-5 and Equation 2-6 respectively.

3.4.2 Pre – contraction of the progesterone

In order to study the ability of the TMOS C_{18} modified monolith to pre – concentrate a high volume of the water sample, 100 mL of standard progesterone water sample at concentration (1 µg mL^{-1}) was pumped through the TMOS C_{18} modified monolith as described in section 2.6.4. The concentration of sexual sex hormones (progesterone and β-estradiol) in river water sample is at the 1 ng L^{-1} [229] and even using a more sensitive detection method such as CL as planned later, pre – concentration was necessary. The flow rate of the syringe pump was set up at 900 µl min^{-1}. After that, the TMOS monolith was washed three times with 1 mL of distilled water at the same flow rate. For the elution step, 1 mL of acetonitrile was pump into TMOS monolith at 100 µg mL^{-1} of flow rate. All the fractions were collected and injected into HPLC system, which set up as explained in section 2.6.2. Figure 3-17 show the HPLC chromatogram of pre – concentration of progesterone by using C_{18} TMOS modified column where, (A) shows the chromatogram of the progesterone standard (1 µg mL^{-1}), which is injected directly to the HPLC system, (B) shows the chromatogram of the loading fraction of 100 mL of progesterone standard, (C) represent the chromatogram of the elution fraction.

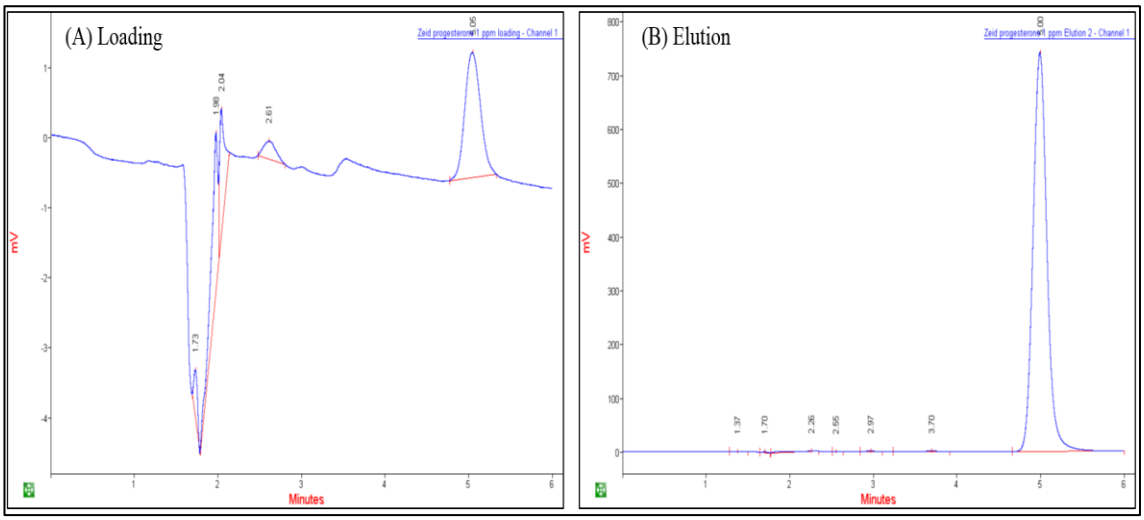

Figure 3-17: HPLC chromatogram of pre - concentrate the target analyte by C18 - TMOS modified column, where (A) Loading fraction, (B) elution fraction.

As shown in Figure 3-17, (A) for the elution step the peak is very small and close to the noise peaks and this concentration is lower the LOD (as explained in section 3.4.1). After completion of the pre – concentrate process of the progesterone peak area was significantly increased and achieved concentration which calculated by using Equation 3-1 at 85.24 µg mL^{-1}.

According to the result achieved during this experiment the C_{18} - TMOS modified monolith showed a high ability to pre – concentrate the target analyte even with a huge volume of the sample where the concentration increased from 1 to 85.24 µg mL^{-1}, which means the recovery percentage, was 85.24%. Figure 3-18 illustrate the pre – concentration profile for a low concentration standard, 1 µg mL^{-1} progesterone using the C_{18} – TMOS modified monolith column at flow rate 900 µL min^{-1}.

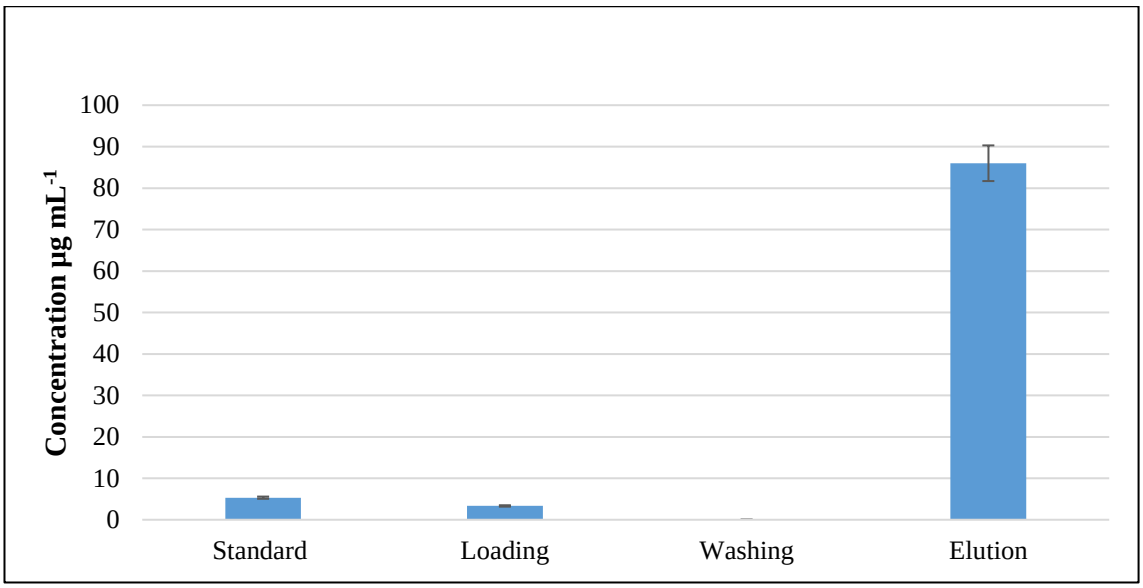

Figure 3-18: The pre-concentrated profile for progesterone, (n=3). The error bar indicates one standard deviation.

3.4.3 Pre – concentration of the progesterone from river water sample

As explained previously in section 2.6.7 the same procedure that followed in pre – concentration standard sample of progesterone by using TMOS C_{18} modified monolith was repeated with river water sample spiked with progesterone (1 µg mL-1). Figure 3-19 shows the chromatograms for the pre – concentration process of river water sample.

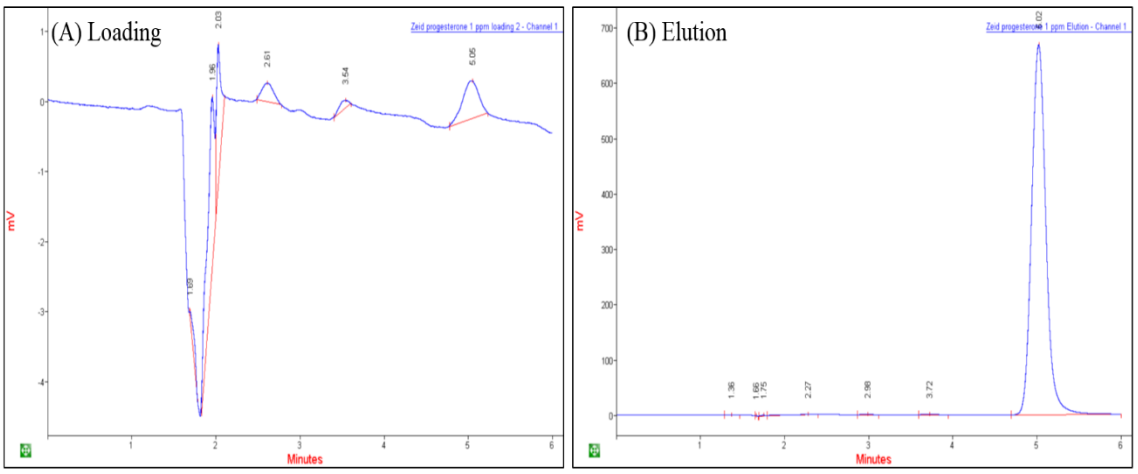

Figure 3-19: HPLC chromatogram of pre - concentrate the target analyte in river water sample by C18 TMOS modified column, where (A) Loading fraction, (B) elution fraction.

According to Figure 3-18, the TMOS C_{18} modified monolith showed a good result to pre – concentrate the analyte from river water sample as well. Where the concentration of progesterone increased from 1 to 78.72 µg mL^{-1} (78.72 %) recovery, which calculated using Equation 3-1. The extraction recovery was decreased slightly when compare the result between standard sample and river water sample and the reason of that is related to the matrix in the river water sample that can interact in the stationary phase, which led to decrease the opportunity of interaction of the analyte.

In addition, in this experiment, the backpressure increased due to the presence of the river water matrix. However, the TMOS C_{18} modified monolith shows high ability to select the target analytes. Figure 3-20 demonstrated the result of the pre – concentration process of the low concentration of progesterone in river water sample (1 µg mL^{-1}), which increased after passed through TMOS – C_{18} monolith column and eluted with 1 mL of acetonitrile to 78.72 µg mL^{-1}.

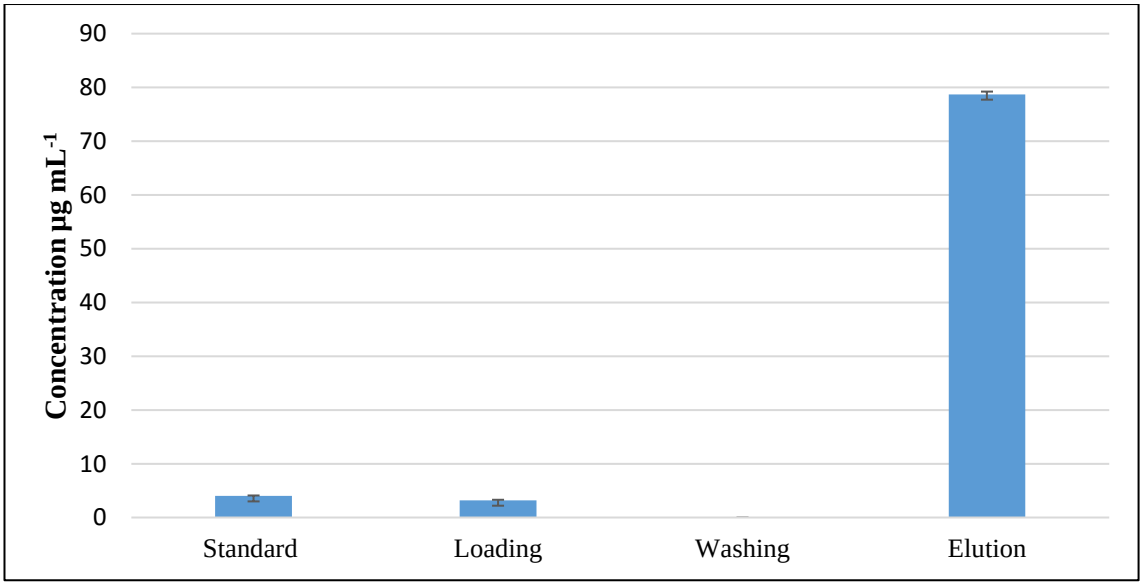

Figure 3-20: The pre-concentrated profile for progesterone from river water sample. (n=3). The error bar indicates one standard deviation.

3.5 Multi - analyte extraction and pre – concentration

3.5.1 Optimisation of HPLC

In order to analyse the mixture of organic pollutants consisting of (benzo (a) pyrene, progesterone and β-estradiol) the HPLC – UV separation method needed to be investigated to achieve the best condition to separation. As described in section 2.6.5.1 the standards for each analyte were prepared separately in acetonitrile in the concentration range of 100, 75, 50, 25, 10 and 1 µg mL^{-1} and were then injected directly into the HPLC system after optimising it to obtain the calibration curve for each analyte.

Two main factors were investigated to optimise the HPLC system for a good separation result, of the mixture organic pollutants compounds (benzo (a) pyrene, progesterone and β-estradiol). Firstly, the composition of the mobile phase (acetonitrile: water), and secondly, the wavelength of the UV detector. The first step was to optimise each compound separately. Dubois *et al.* [230] analysed the benzo (a) pyrene by using UV – Vis spectrophotometer and found out the λ_{max} at 250 nm with acetonitrile and water as the mobile phase. Also as mentioned previously in section 3.3.1 the λ_{max} of the progesterone was 250 nm as well. Therefore, as explained in section 2.6.6 the standard mixture of (benzo (a) pyrene, progesterone and β-estradiol) at concentration 1 µg mL^{-1} was injected directly to HPLC – UV system, where the ratio of the mobile phase composition tested were (75:25 and 80:20) acetonitrile, water respectively. While the range of wavelengths studied were (220,230,240 and 250 nm). Chromatograms for the separation of the organic mixture with a mobile phase composition of acetonitrile: water, 75:25 at a various range of wavelengths (250, 240, 230 and 220) are presented in Figure 3-21, where the Table 3-3 summarises all the results obtained.

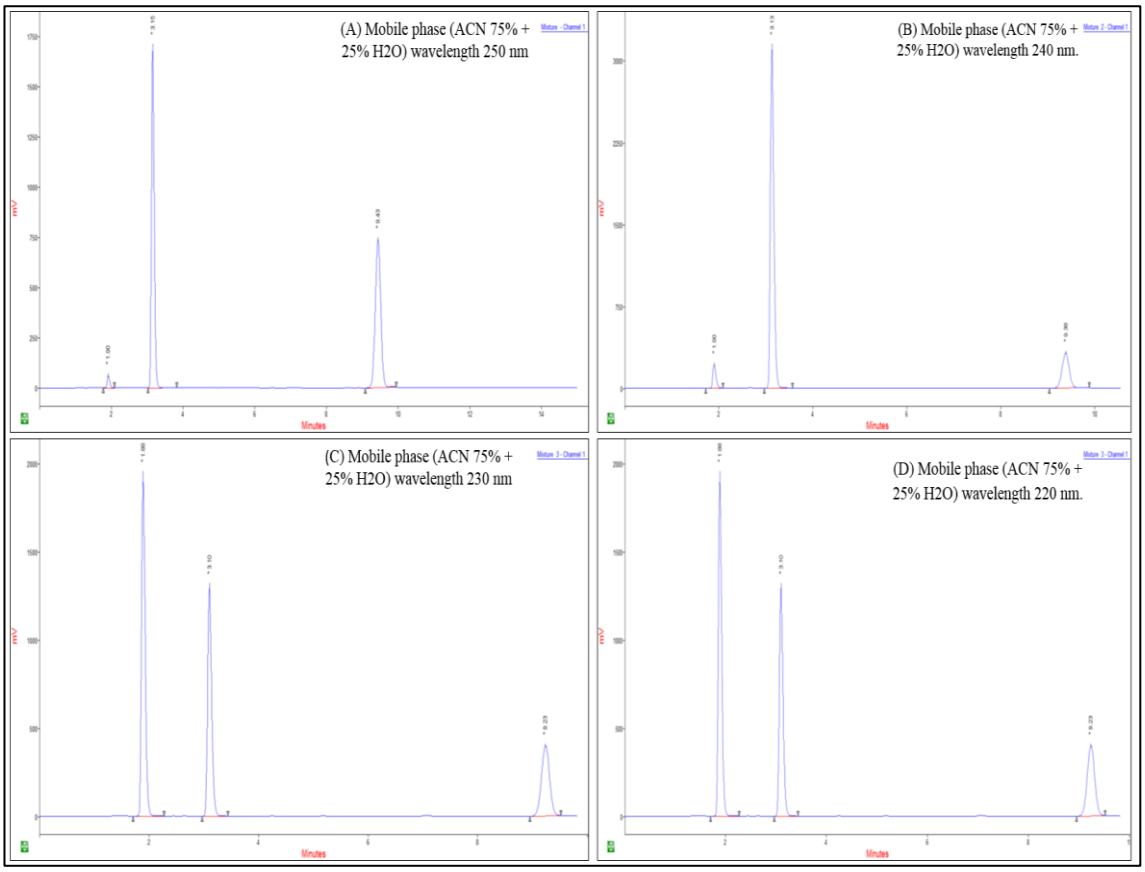

Figure 3-21: HPLC chromatogram for mixture of (benzo (a) pyrene, progesterone, β-estradiol with mobile phase composition (acetonitrile: water, 75, 25) to optimise the absorbance wavelength where, (A) shows the chromatogram of the organic compounds mixture at 250 nm, (B) shows the HPLC chromatogram of mixture at 240 nm, (C) present the HPLC chromatogram of mixture at 230 nm and (D) shows the HPLC chromatogram of mixture at 230 nm.

Table 3-3: The retention time and peak area of the triple organic pollutants mixture (estradiol, progesterone and benzo (a) pyrene) 100 µg mL^{-1} that injected directly into the HPLC, (n = 3).

	Wavelength 250 nm	
Compound	**Retention time (min), ± RSD %**	**Peak area (a.u), ± RSD %**
β-estradiol	1.82 ± 4.2	335.1 ± 1.5
Progesterone	3.13 ± 1.8	9311.36 ± 1.4
Benzo (a) pyrene	9.45 ± 1.04	7734.1 ± 1.1
	Wavelength 240 nm	
β-estradiol	1.87 ± 3.1	1123.1 ± 6.5
Progesterone	3.13 ± 4.8	14704.98 ± 1.95
Benzo (a) pyrene	9.3 ± 0.28	3673.64 ± 7.8
	Wavelength 230 nm	
β-estradiol	1.85 ± 3.9	8962 ± 0.5
Progesterone	3.17 ± 1.8	7131.33 ± 4.6
Benzo (a) pyrene	9.46 ± 3.4	4590 .67 ± 9.8
	Wavelength 220 nm	
β-estradiol	1.9 ± 1.9	8690 ± 5.82
Progesterone	3.14 ± 1.7	6646.1 ± 6
Benzo (a) pyrene	9.3 ± 0.8	4027.67 ± 1.5

According to Figure 3-21 and Table 3-3, it is clear to see the retention time was stable at different wavelength while the values of the peak area of estradiol were significantly increased when the wavelength was changed from 250 to 240 nm because the absorbance for the analytes specially the benzene ranges increase with decrease the wavelength. The progesterone achieved the highest peak area (14704.98) at a wavelength 240 nm, after that with a decrease in the wavelength the peak area decreased as well. The highest peak area for benzo (a) pyrene was at wavelength 250 nm while the peak area was reduced by decreasing the wavelength as well.

The separation was then repeated with a mobile phase composition ratio of acetonitrile: water, 80:20 at 230 nm wavelength because this wavelength was obtained the highest peak area for the organic pollutants mixture. Figure 3-22 present of the chromatogram of the mixture separation.

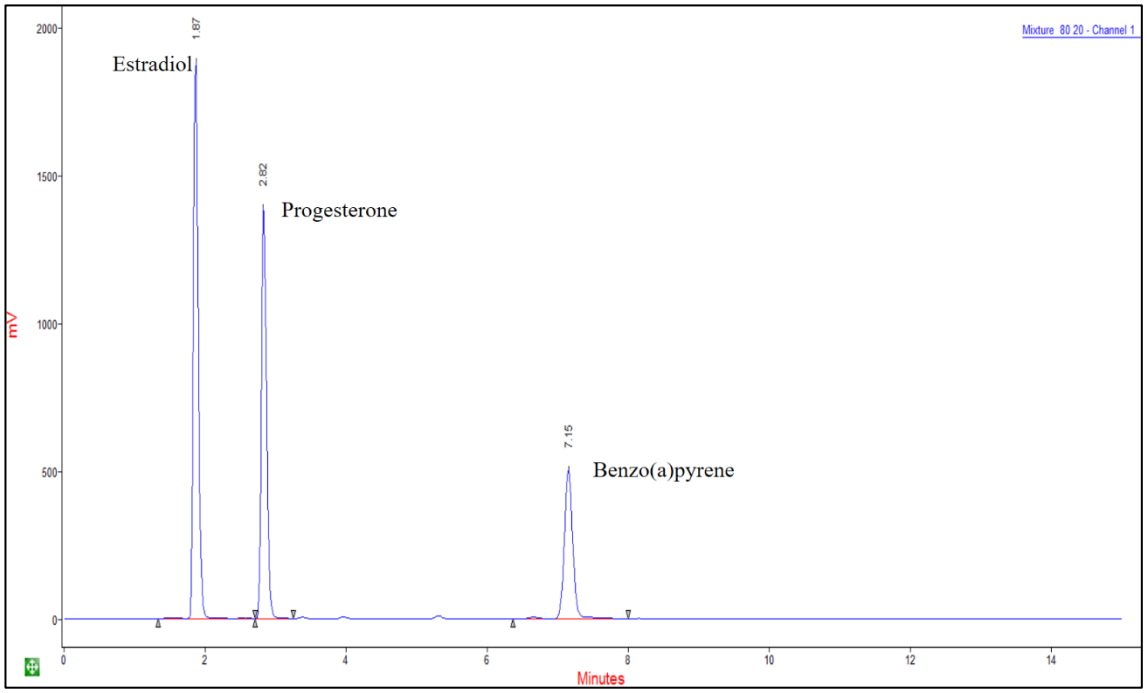

Figure 3-22: HPLC chromatogram for the mixture (benzo (a) pyrene, progesterone and β-estradiol with mobile phase composition (acetonitrile: water, 80, 20) at 230 nm.

The result of the separation of the organic compounds mixture is shown in Figure 3-22, where the estradiol achieved a high peak area at 8962 and the retention time was slightly

decreased. The progesterone provided a peak area around 7131.33 and the retention time was decreased to 2.82 min. The peak area of the benzo (a) pyrene was nearly 4590 .67, but the retention time was significantly reduced to 7.15 min.

According to the results obtained in the optimisation of HPLC – UV system to analysis the organic pollutants mixture, the acceptable peak area for each compound obtained with mobile phase ratio of acetonitrile: water at (80:20) while the wavelength was at 230 nm. For this reason, the HPLC – UV system will set up at 230 nm of wavelength and the mobile phase composition of acetonitrile: water will be at ratio 80:20 for all the following experiments.

3.5.2 Figure of merit for calibration curves of estradiol, progesterone and benzo (a) pyrene.

The linearity, LOD and LLOQ were assessed from the calibration curves for each pollutant compounds. These calibration curves were also used to calculate the concentration of estradiol, progesterone and benzo (a) pyrene fractions after each of pre – concentration stage. Standard solutions of each analyte at a concentration (100, 75, 50, 25, 10 and 1 µg mL^{-1}) were directly injected separately into HPLC - UV system that was set up at 230 nm wavelength, where the ratio pf mobile phase composition was (acetonitrile: water, 80: 20). Each concentration was analysed three times, and the peak area was plotted against concentration, Figure 3-23 shows the calibration curve for each analyte.

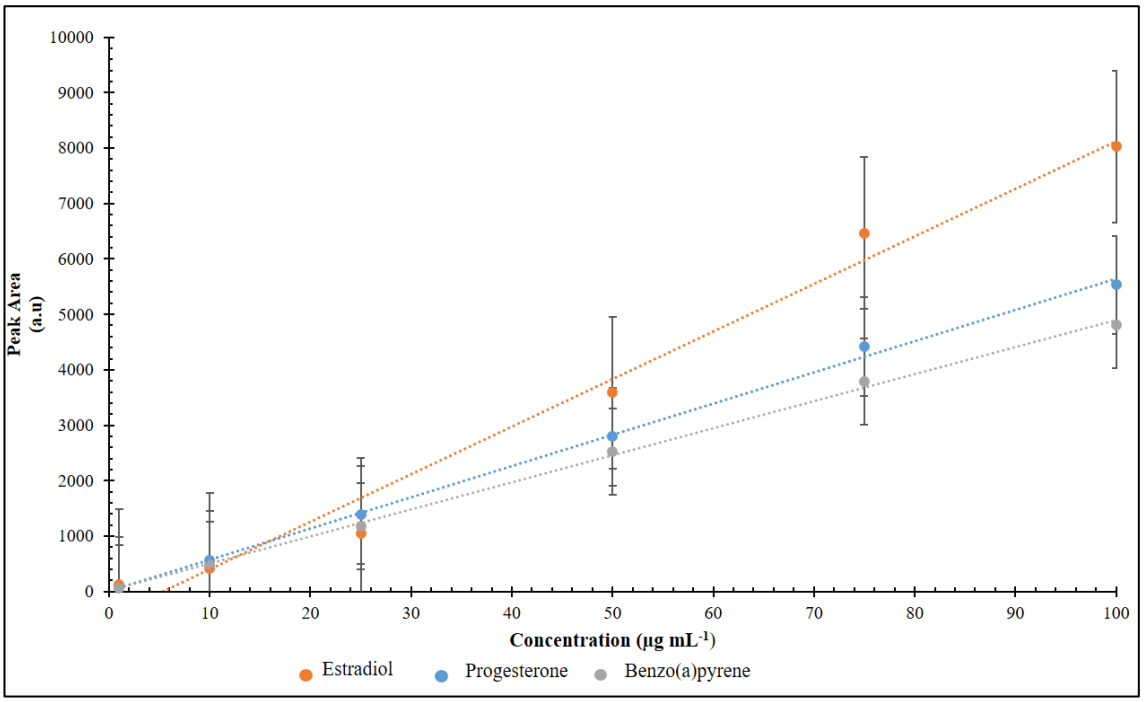

Figure 3-23: Calibration curve of the estradiol (orange line), progesterone (blue line) and benzo (a) pyrene (grey line) standard solution with peak area plotted against their concentration, (n = 3). The error bar indicates one standard deviation.

The calibration curves of the targets analytes show good linearity over the range used and offered good values of correlation coefficient (R^2). All the results of LOD and LLOQ were calculated using the equations Equation 2-2, Equation 2-3, Equation 2-4 and Equation 2-5 respectively. Table 3-4 summarised all the results obtained from calibration curves in Figure 3-23.

Table 3-4: Analytical figure of merit of estradiol, progesterone and benzo (a) pyrene

Analyte	LOD (µg mL^{-1})	LLOQ (µg mL^{-1})	Linearity	Correlation coefficient (R^2)
Estradiol	17.8	59.38	Y= 53.801 x – 65.504	0.981
Progesterone	0.165	0.552	Y= 56.196 x + 17.464	0.998
Benzo (a) pyrene	0.278	0.928	Y= 48.89 x + 12.079	0.994

3.5.3 Pre – concentrate the mixture of organic pollutants

In order to decrease the LOD value and increase the sensitivity of the detection method for the organic pollutants compounds, the pre – concentrate procedure was applied as explained in section 2.6.7. The standard mixture consisted of estradiol, progesterone and benzo (a) pyrene were prepared in 100 mL of distilled water at concentrations of 1 µg mL^{-1}. 100 mL of the mixed standard was loaded onto the TMOS – C_{18} modified monolith at a flow rate 900 µL min^{-1}. After that, 1 mL of water was pumped through the modified monolith at the same flow rate for the washing step that was repeated three times. Finally, 1 mL of acetonitrile was passed through the monolith to elute the analytes, where the flow rate set up at 100 µL min^{-1}. All the fractions were collected separately and injected into the HPLC - UV system. The wavelength of the HPLC – UV system was set up at 230 nm, and the ratio of mobile phase composition was (acetonitrile: water, 80:20). Figure 3-24 shows all the chromatograms obtained for each pre – concentrate step for the pollutant mixture.

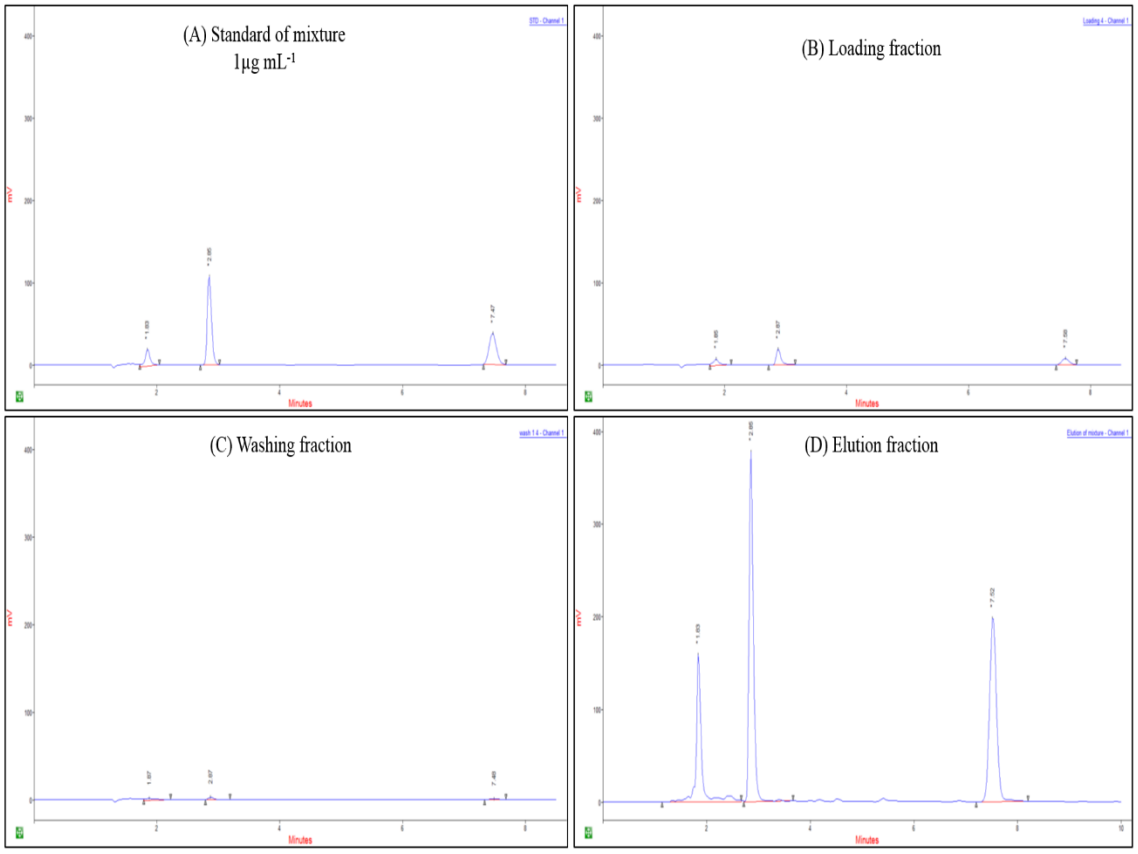

Figure 3-24: HPLC chromatogram of pre – concentrate standard mixture of organic pollutant through TMOS – C18 modified column where, (A) shows the standard of mixture (1 µg mL^{-1}, (B) shows the chromatogram of loading fraction, (C) shows the chromatogram of the washing fraction and (D) represent the chromatogram of the elution fraction.

In Figure 3-24, (A) shows the chromatogram of the mixture standard, the progesterone peak area is great than that for both estradiol and benzo (a) pyrene. (B) shows the chromatogram of the fraction obtained during the pre – concentration step, very small peaks can be seen for all analytes which indicator to the TMOS – C_{18} modified monolith provide a good ability to interact with more than one analyte in the same time. The total fractions of triplicate washing steps are shown in (C) where no peaks can be recognised due to the strong interaction between the analytes and C_{18} modified surface. Finally, (D) present clearly peaks for all analytes of the elution fraction, which was carried out with 1 mL of acetonitrile. All the concentration of each fraction were calculated using the

linearity equations of each analytes given in Table 3-4. All the result of the concentration are presented in Figure 3-25.

Table 3-5: The concentration of each analyte after pre – concentration process of the standard mixture of (estradiol, progesterone and benzo (a) pyrene), (n = 3).

	Concentration at each step (µg mL^{-1})		
Analyte	**Loading (100 mL), ± RSD %**	**Washing (3 mL), ± RSD %**	**Elution (1 mL), ± RSD %**
Estradiol	2.29 ± 8	1.7 ± 8.7	59.61 ± 4.37
Progesterone	1.52 ± 4.5	0	84.79 ± 1.57
Benz (a) pyrene	1.3 ± 8.5	0	80.93 ± 2.21

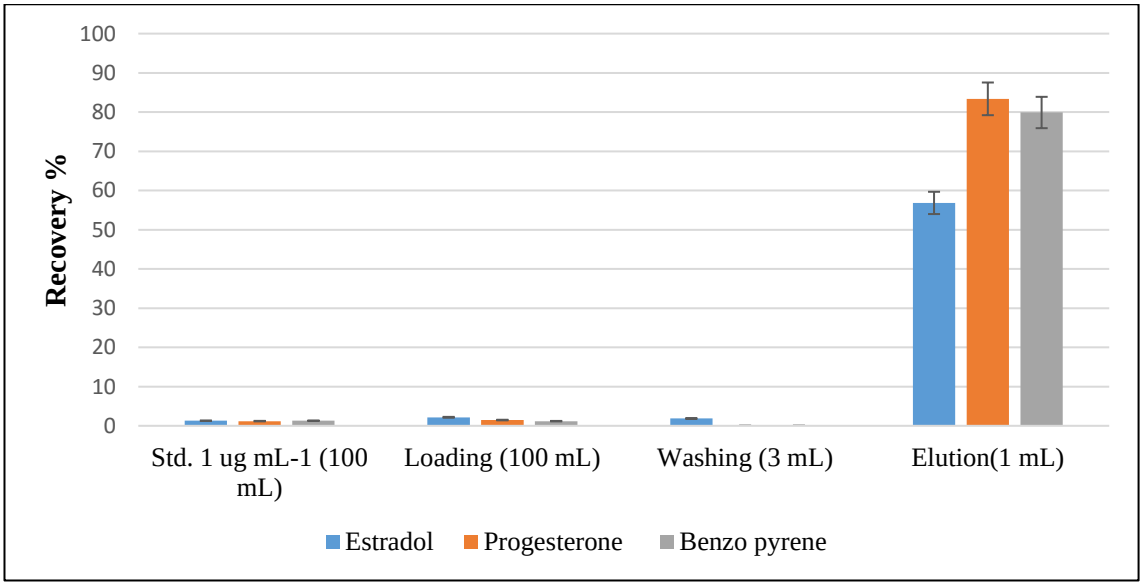

Figure 3-25: The pre – concentration efficiency of 1 µg mL^{-1} of estradiol, progesterone and benzo (a) pyrene using TMOS C18 modified column. The average recovery was obtained from three consecutive experiment, (n = 3). The error bar indicates one standard deviation.

According to Table 3-5 and Figure 3-25, it clearly can be seen the concentration for all the analytes were increased after the pre – concentrate procedure was. Recoveries of the estradiol, progesterone and benzo (a) pyrene with the TMOS – C_{18} modified column were found to be 57%, 84% and 80% respectively. Progesterone and benzo (a) pyrene achieved a good recovery percentage. While the estradiol offered poor recovery in this might be because of the strong interaction occurred between the estradiol and C_{18} modified the surface, which required slow flow rate at elution step or strong organic solvent rather than acetonitrile. However, the all recovery percentage obtained in this procedure it covered the LOD of the detection techniques applied in this project as will be discussed later.

3.5.4 Pre – concentrate mixture of non – polar organic pollutants from river water

In order to investigate the ability of TMOS – C_{18} modified column to pre – concentrate the targets analytes from river water sample. 100 mL of river water was spiked with estradiol, progesterone and benzo (a) pyrene at (1 µg mL^{-1}) and loaded through the TMOS – C_{18} modified column. This was followed by 1 mL of distilled water for washing step, then 1 mL of acetonitrile for the elution step. Figure 3-26, represent the chromatograms of each fraction step of pre – concentrate procedure.

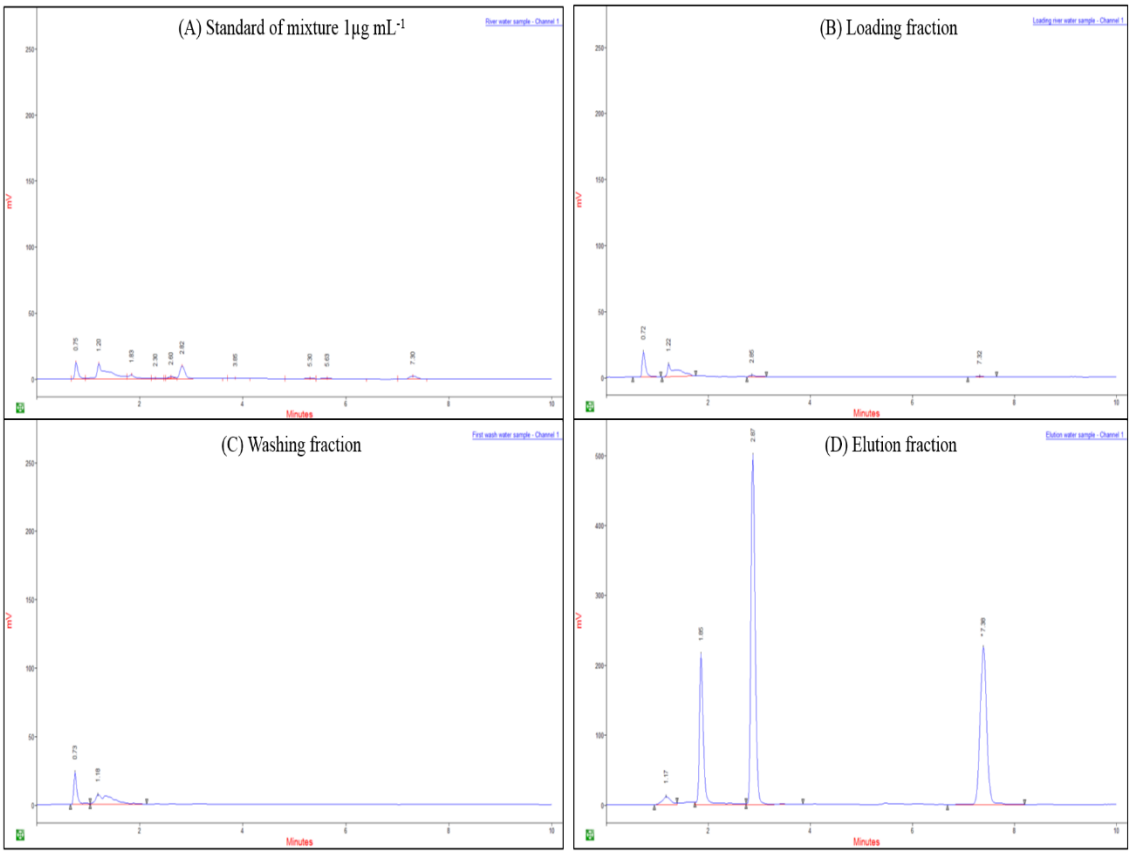

Figure 3-26: HPLC chromatogram of pre – concentrate river water sample spiked with estradiol, progesterone and benzo (a) pyrene at (1 µg mL^{-1}) by using TMOS – C18 modified column where, (A) shows the river water sample before pre – concentration process, (B) shows the chromatogram of loading fraction, (C) shows the chromatogram of the washing fraction and (D) represent the chromatogram of the elution fraction.

Figure 3-26, (A) shows the chromatogram of a standard river water sample showing a very small peak close to the nose of baseline. While the (B) and (C) represent the chromatogram of the loading and washing fractions, which also shows a very small peak. After completion of the pre – concentration step of the peak for all of the analytes became clearly to see, which means the pre – concentration procedure of the river water sample spiked with analyte was successful. The concentration of each fraction was calculated using the line equations of each analyte presented in Table 3-4. All the concentration of each fraction are summarised in Table 3-6. While Figure 3-27 demonstrated the efficiency recovery of pre – concentrate of the river water sample standard spiked with estradiol,

progesterone and benzo (a) pyrene (1 µg mL^{-1}) using the TMOS – C_{18} modified monolith column.

Table 3-6: Concentration of each fraction of pre – concentration of river water sample spiked with non – polar organic compounds procedure, (n = 3).

Analyte	Concentration of each fraction (µg mL^{-1})			
	Standard of river water sample, ± RSD %	Loading (100 mL), ± RSD %	Washing (3 mL), ± RSD %	Elution (1 mL), ± RSD %
Estradiol	1.7 ± 1.2	0	4.22 ± 0.74	50.13 ± 5.27
Progesterone	0	0	0	62.54 ± 5.8
Benz (a) pyrene	0.16 ± 0.09	0	0	59.51 ± 4.3

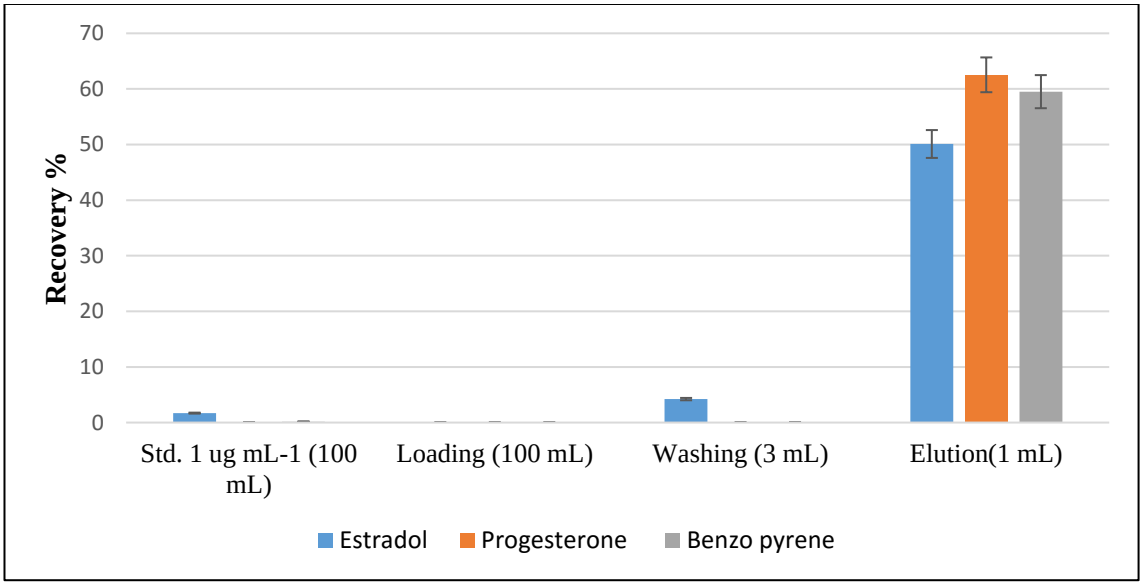

Figure 3-27: The pre – concentration efficiency of river water sample spiked with 1 µg mL^{-1} of estradiol, progesterone and benzo (a) pyrene using TMOS C18 modified column. The average recovery was obtained from three consecutive experiment, and the error bar indicates one standard deviation.

The result presented in Figure 3-26 and Table 3-6 demonstrated the ability of TMOS – C_{18} to pre – concentrate the targets analytes from river water sample. In the loading step, none of the analytes were detected due to all the concentration were below the LODs. While in the washing step, a small amount of estradiol was present with concentration 4.17 µg mL^{-1}, while progesterone or benzo (a) pyrene was not seen. Pre – concentration was seen in the elution step where the concentrations of estradiol, progesterone and benzo (a) pyrene were 50.13 %, 62.54 % and 59.51 % respectively. All of these concentrations were suitable for LODs for detection methods discussed later in the thesis.

When compare the percentage of analytes recovery between the standard sample (distilled water) and the really sample (river water), it clearly to see the percentage foe each analytes is significantly decreased as shown in Table 3-7.

Table 3-7 : Comparing for recovery percentages for analytes

	Recovery percentage %	
Analyte	Standard sample (Distilled water	Really sample (River water)
Progesteone	84.79	62.54
Estradiol	59.61	51.13
Benzo (a) pyrene	80.93	59.51

As shown in Table 3-7 the recovery percentage for progesterone and benzo (a) pyrene were dramatically decrease from 84.79 , 80.93 % in distilled water to 62.54 , 59.51 % in river water respectively. Where the recovery percentage of estradiol slightly decrease from 59.61 to 51.13 %. The reason of this because the river water is reach in different elements and compounds which can interact with the analyte which make it hard to remove from the column. In addition, the compounds can interact directly with the surface, therefore the opportunity of the interaction between the analytes and the surface decrease. As result of this experiment, the silica monolith column will not reuse, because the

residues of compounds will need extra procedure to remove it, which required extra cost and more work.

The time is vital factor in any analysis procedure, and in this method was carried out in around 2 hours that make it suitable for portable system device. However, according to this result with river water sample this method achieved more than 50 % recovery for all analytes, and this the target of use this method for pre – concentration. For that, the TMOS monolith will connect with the microfluidic system for filed application.

3.6 Conclusion

SPE is the most powerfully technique that use for sample preparation in any analysis process. Silica monolith which is use as sorbent in SPE was applied in this project according to it properties, as provide a high surface area, bimodal of pore and high satiability with variety of organic solvent.

The method of fabrication of silica monolith is long procedure (5 days), but the amount of products can be enough to apply in 20 different experiment. Also the process of modified the surface with C_{18} is easy.

Two type of silica monolith were used TMOS and TEOS, where the TMOS provide higher surface area (404 m^2g^{-1}) than TEOS (301.1 m^2g^{-1}) which increase the opportunity to intract the analyte with surface. While the TEOS offer high pore size (2.2 µm) rather than TMOS (0.96 µm), which effect on the permeability of the sample movement through the sorbent. Also the process of modified the TMOS surface with C_{18} was successful done, because the surface area and pore size were decrease of TMOS from (404 to 373.46 m^2g^{-1}) and (0.96 to 0.73 µm) respectively, after completed the modification process. In addition, the EDX result confirm that where the percentage of C was increased from 5.3 to 23.3.

When compared the extraction recovery between TMOS and TEOS, the TMOS show high ability to extract the analyte. Also acetonitrile has showed more performance to elute the analyte rather than methanol. The pre-concentration of the analytes mixture of from standard (distilled water) using C_{18} TMOS, the percentage recovery for progesterone, estradiol and benzo (a) pyrene were at 84.79, 59.61 and80.93 % respectively. While with really sample (river water) the percentage recovery were 62.54, 50.13 and 59.51 respectively.

To conclude that, the target of using the silica monolith for sample preparation was successfully achieved, which make this method suitable to apply to achieve the main target of this project.

Chapter 4. Antibody immobilisation

As discussed in the introduction section, several methods can be used as more portable options for environmental pollutants detection. These include spectroscopic and fluorescence detection, but these required an optical system for light excitation or illumination. Moreover, are not suitable for all types of substrate materials, as they may absorb UV light. Electrochemistry techniques can provide a low-cost portable option using cyclic voltammetry (CV) and highly sensitive square wave voltammetry (SWV). Chemiluminescence is also an extremely sensitive detection system where the light is emitted from chemical reactions, which means a light source or special optical system is not required. Although both these methods can be used to detect directly pollutants they can lack selectivity, and this can be improved by combination with immunoassay, where the immunoassay system offer high selectivity and both type of detections featuring with high sensitivity.

In this project immunoassay with electrochemistry and chemiluminescence detection were selected to mounter the organic pollutants in environmental water samples.

For detection of the organic pollutants with portable system device, successful immobilisation of the antibody onto the solid support surface is vital. Two different methods were investigated for antibody immobilisation onto the solid support surface (chemical modification and electrochemical modification).

A glass surface was chosen as the solid support surface for the immobilisation chemical process, and this was modified with different silanisation reagents (APTMS and GPTMS). To confirm the silanisation step was carried out correctly, the contact angle measurement of a water drop on the surface, before and after silansiation was measured.

For the electrochemistry immobilisation process, an ITO electrode was used as the solid support surface. This method was selected to gain more control of the immobilization, where (CV) could be used to confirm this step.

4.1 Chemiluminescence immunoassay detection

4.1.1 Optimisation the reagent of chemiluminescence reaction

The intensity of chemiluminescence signal depends on four main factors, pH value, and concentration of luminol, hydrogen peroxide and catalyst, which in this project was HRP, which had been added as the label to the antibody. The luminol concentration and the value of pH associate together, because of the intensity of luminol is decreased at lower pH value, while luminol intensity significant increased at high pH value. At pH value less than 8, there was no different between the CL light intensity of sample and the blank, while at pH more than 9, the CL intensity of the analytes was significantly increased, and even the blank intensity simply increased. The optimum pH for the luminol reaction was prepared at pH 11[231].The effect of all these reagents were investigated, where the HRP was selected as it successively converted into intermediary complex during the chemiluminescence reaction before regenerated to free peroxidase. This step with HRP produce luminol radicals that generate the light emitter [207].

The experiments being carried out in an Eppendorf tube as explained in section 2.7.1. The CCD camera was used to detect the light emitted from the sample, where ImageJ software used to measure the CL emission intensity. The results of the optimisation experiments for each reagent are discussed below.

4.1.2 Optimisation of HRP concentration

Firstly, to optimise the chmiluminescence reagents, the progesterone – HRP was selected as example because the all catalysts enzyme comes from the same supplier and has the properties. The concentration of progesterone - HRP label, which uses as a catalyst for

chmiluminescence reaction, was the first reagent optimised. The experiment of optimised the progesterone – HRP was carried out at fixed concentration of luminol and hydrogen peroxide at 20 mM. The range of concentrations investigated was between 1 to 15 mM as the method explained in section 2.7.1. The blank was a mixture of luminol and hydrogen peroxide at 20 mM concentration with 10 µL of PBS and this was used to obtain the background. The results obtained for different concentration of progesterone – HRP were plotted against CL emission intensity as shown in Figure 4-1.

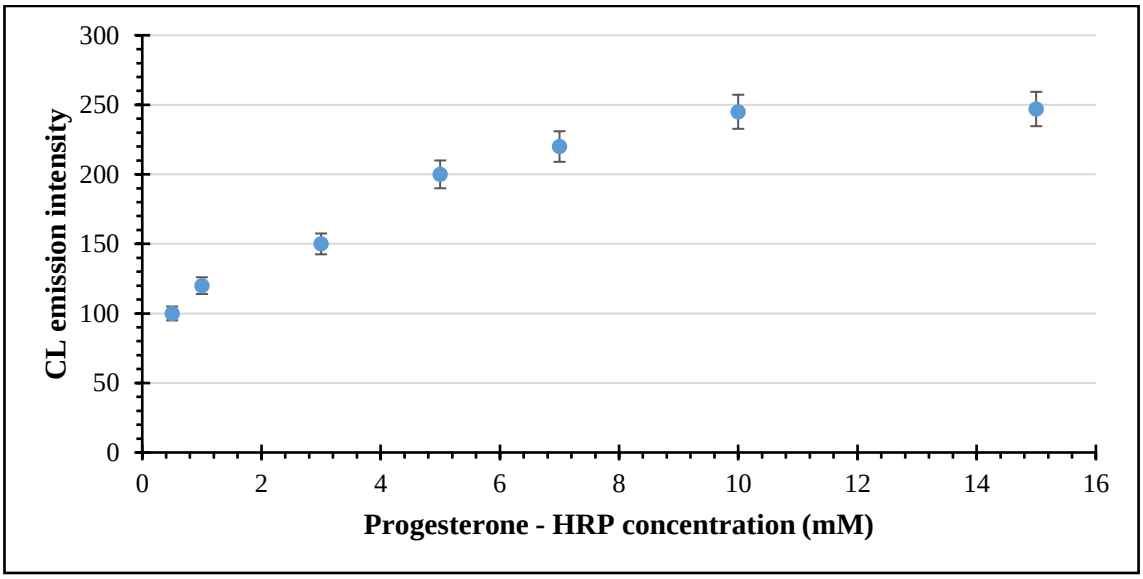

Figure 4-1: Effects of the changing progesterone - HRP concentration on the CL emission intensity, (n = 3). The error bar indicates one standard deviation

Figure 4-1 shows the CL emission increased with increased progesterone – HRP concentration until reaching a maximum of 250 CL emission intensity at 10 mM. The CL emission intensity then remained stable up to 15 mM. As result of this experiment, the following experiment of CLIM the concentration of the HRP catalyst will set up at 10 mM.

4.1.3 Optimisation of luminol concentration

In order to optimise the luminol concentration, the experiment was carried out at fixed concentration of hydrogen peroxide at 20 mM and the concentration of progesterone – HRP at 10 mM. The CL emission intensity, which obtained in a range between 0.5 to 30 mM are shown in Figure 4-2 .

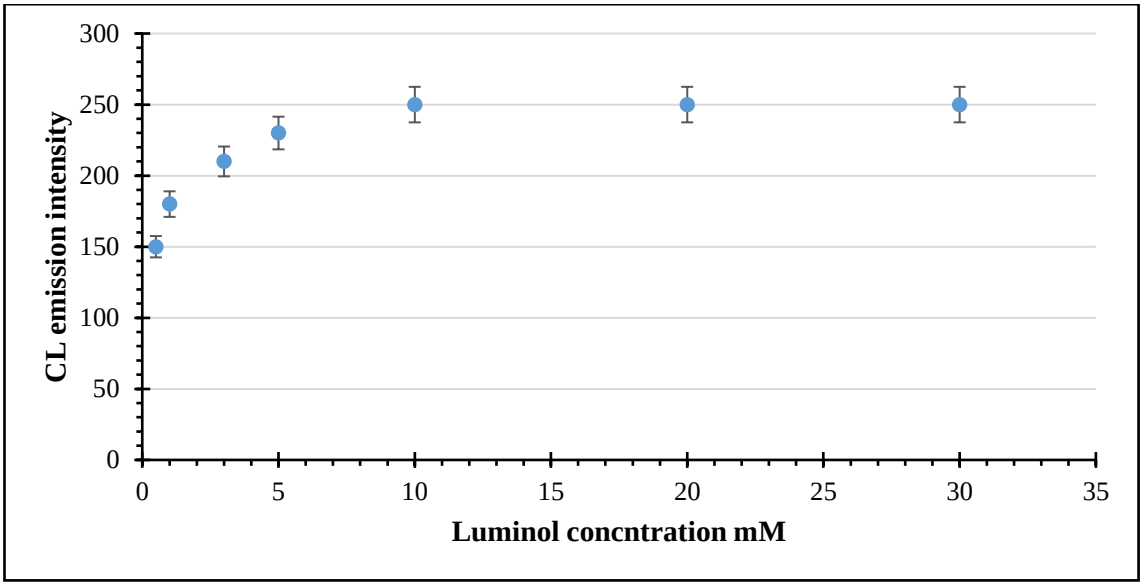

Figure 4-2 Effect of the luminol concentration on the signal intensity of CL detection, (n = 3). The error bar indicates one standard deviation

As can see in Figure 4-2, where the CL emission intensity increased slowly with luminol concentration between 0.5 to 5 mM. The RLU value approached to the maximum of luminol concentration at 10 mM, and remained stable up to 30 mM. The luminol concentration used in this project was 10 mM.

4.1.4 Optimisation of hydrogen peroxide concentration

The effect of the hydrogen peroxide (H_2O_2) concentration on the intensity of CL signal was also investigated. The concentration of luminol was fixed at 20 mM and the concentration of progesterone – HRP at 10 mM. The results for the concentration of H_2O_2 in the range 0.5 to 30 mM are shown in Figure 4-3 .

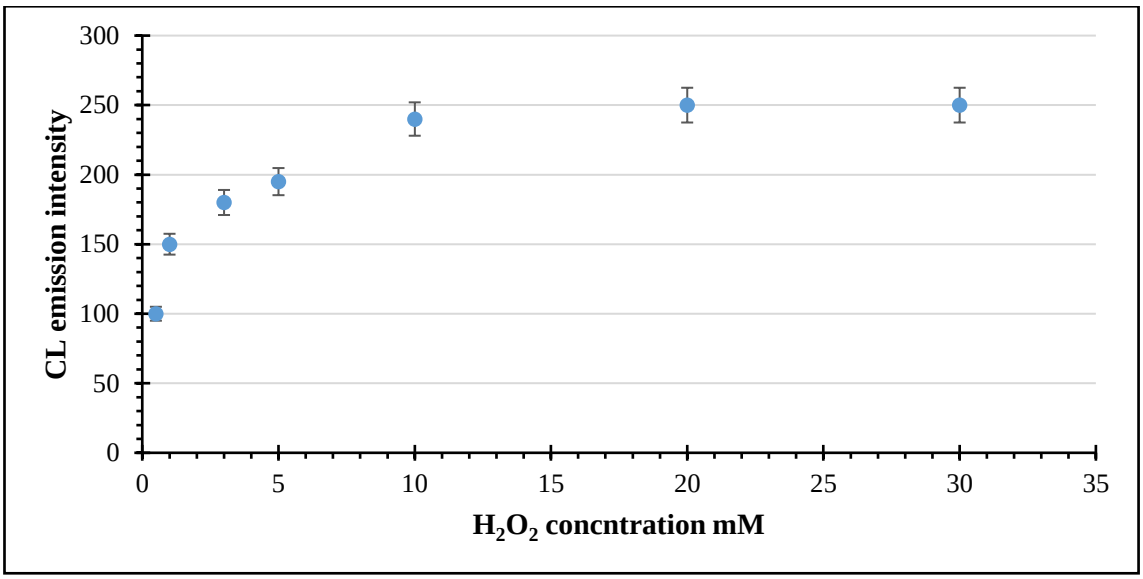

Figure 4-3: Effects of the H_2O_2 concentration on the signal intensity of CL detection, (n = 3). The error bar indicates one standard deviation

As shown in Figure 4-3, the CL emission intensity increased as the H2O2 concentration increase up to 20 mM and then stabilised up to 30 mM.

As the result of the optimisation experiments of all CL reagent. The progesterone – HRP was fixed at 10 mM while the concentration of luminol and H_2O_2 were set up at 20 mM.

4.2 Chemical silanisation of glass surface

As described in Section 2.7.2 the glass microscope slides were used as the solid support surface for antibody immobilisation, where APTMS and GPTMS used as silane reagents. With use, APTMS silane reagents resulted formed the amine group on the glass surface, which changed the nature of the surface from hydrophilic to hydrophobic. The process of silanised the glass support surface by using APTMS is shown in Figure 4-4. Where the GPTMS silane reagent, the surface covered by an epoxy group which make the surface hydrophobic as well.

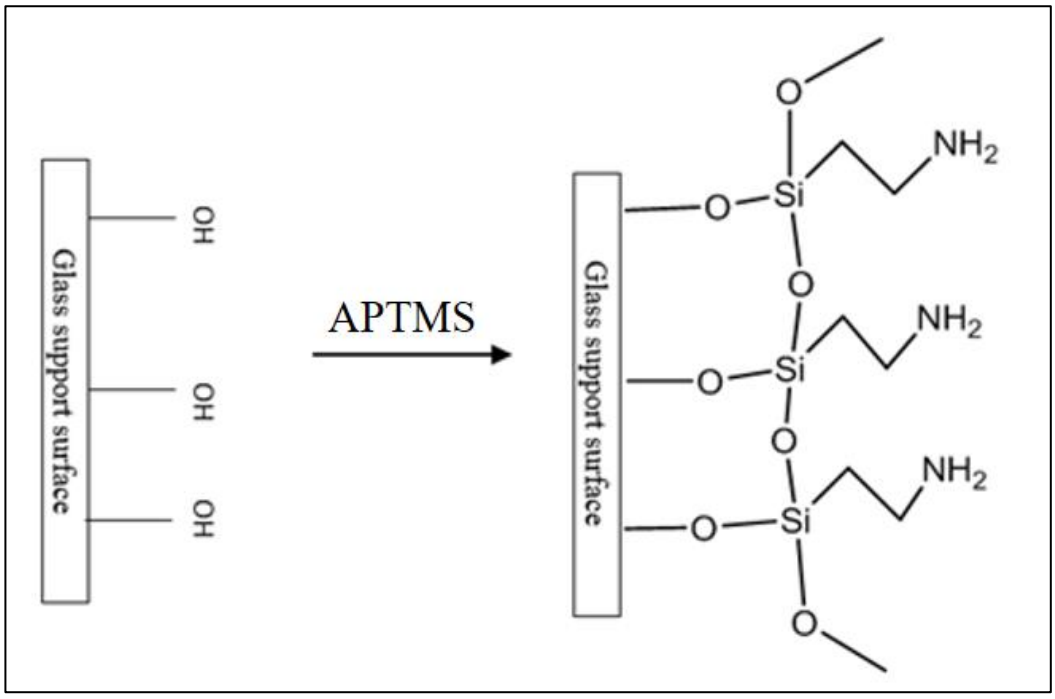

Figure 4-4: Process of silanisation of glass support surface [156].

4.2.1 Assessment of surface modification using contact angle measurements

To evaluate effectiveness and reproducibility of the silanisation chemical modified process for both types of silanisation reagents (APTES and GPTMS), the water contact angle measurement was applied as explained in section 2.7.4.1. Several silanisation reagent concentrations evaluated in order to find out which concentration achieved the highest contact angle value to use in following experiments. Four different concentration in the range 1 to 10 % v/v were used to treat glass slide. An average of these measurements were used to obtain the bar chart in Figure 4-5 that presents the results of contact angle for different concentration of APTES and GPTMS.

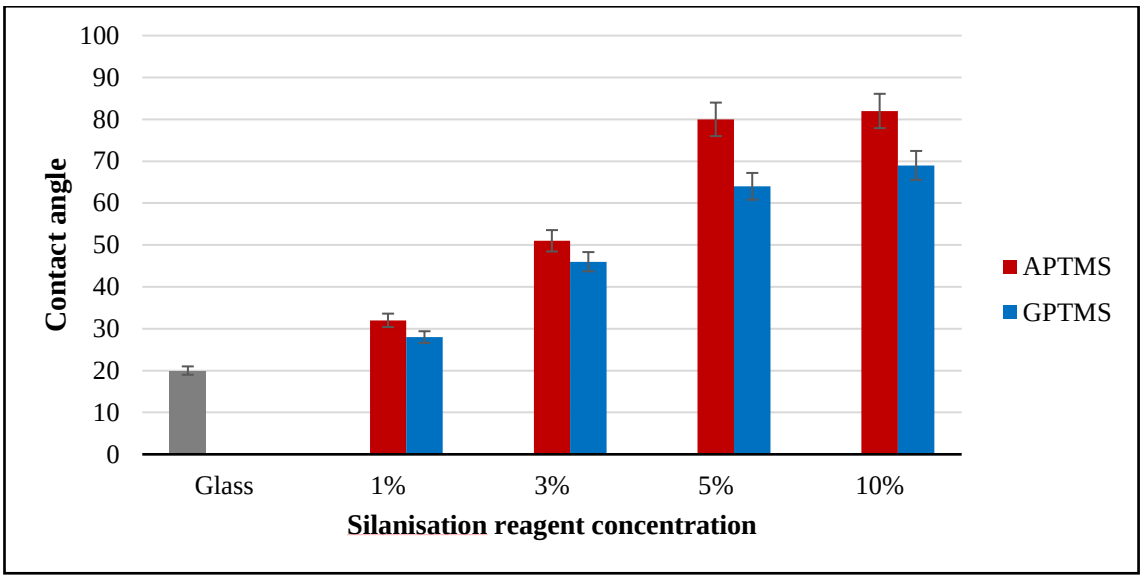

Figure 4-5: Contact angle measurement for various concentration of APTMS and GPTMS, (n = 3). The error bar indicates one standard deviation

Figure 4-5 shows the results of the contact angle with the glass surface increased after completion of the silanisation process with either APTMS or GPTMS. This increase in the contact angle measurement gave an indication of successful silanisation.

The highest contact angle measurements were achieved at concentration 10 % v/v for either APTMS or GPTMS, which were 82° ± 5.7°, 69° ± 4.3 respectively. While, with concentration 5% v/v the contact angle measurements were slightly decreased to 80° ± 7.1° and 64° ± 2.7° for APTMS and GPTMS respectively. The glass chip treated in the 10 % of silansitaion reagents was found during the experiment formed the white staining on the surface which required more cleaning with acetone. For that, the 5 % v/v concentration of APTMS and GPTMS were chosen to carry out the immobilisation of antibody on the glass surface.

The contact angle increase due to presence of the amine group on the glass surface with use of APTMS and the epoxy group with use of GPTMS *via* covalent binding, which make the surface more hydrophobic. However, the silanisation process is very sensitive to moisture, and the experiment must be carried out in a dry place [232].

In the next experiment, the effect of the time allowed for interaction between the silansing agent and the surface on the success of the surface modification was modified via contact angle measurements. Figure 4-6 shows the photographs of the drops on the initial glass slide after the silanisation process with 5 % v/v APTMS at different interaction times.

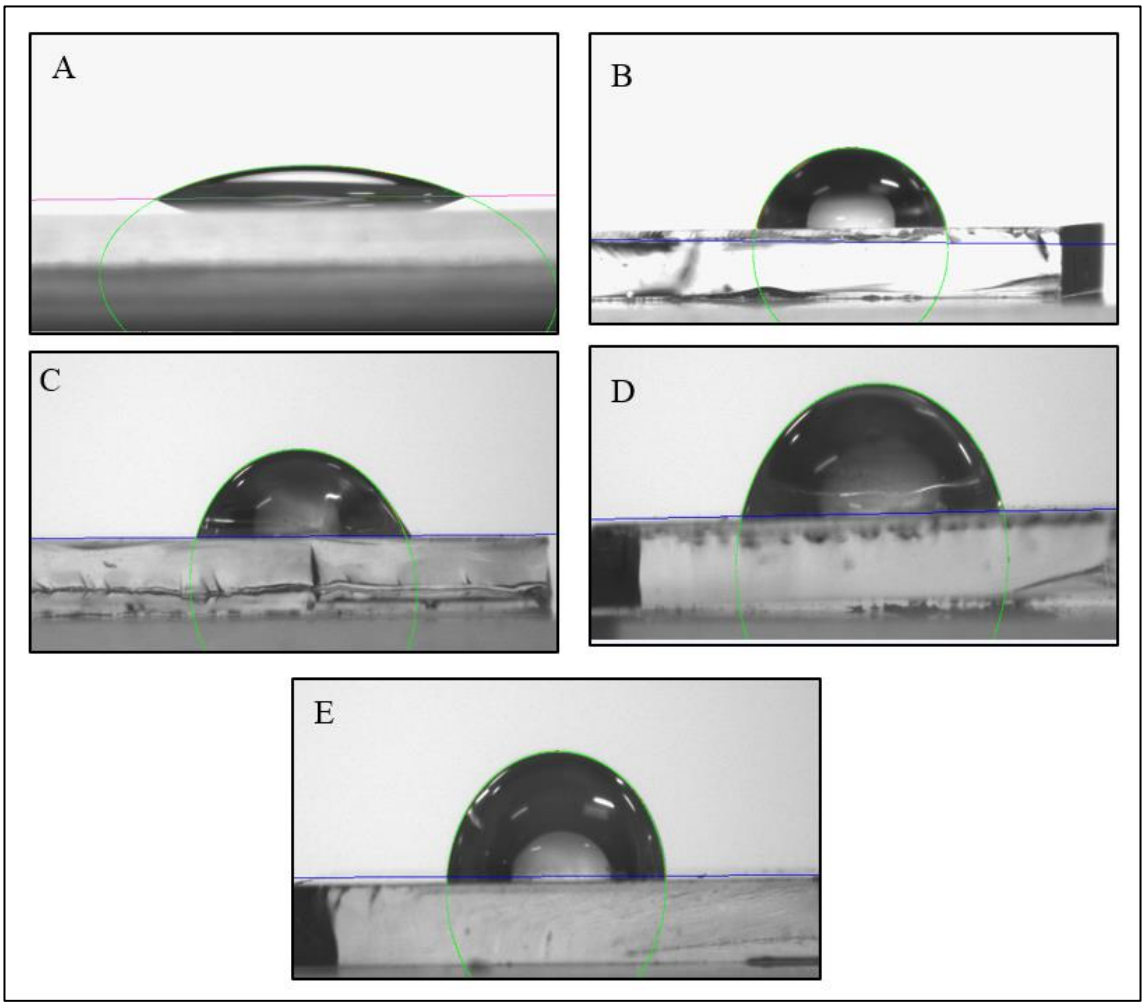

Figure 4-6: Photographs of water droplet at various interaction times for silanisation process where, (A) shows the contact angle of pure glass, (B) 30 min of silanisation process, (C) 60 min of silanisation process, (D) 90 min silanisation process and (E) 120 min silanisation process.

The result of contact angle measurements that showed the effect of interaction time ranging from 30 to 120 min by using 5 % v/v of APTMS presents in Figure 4-7.

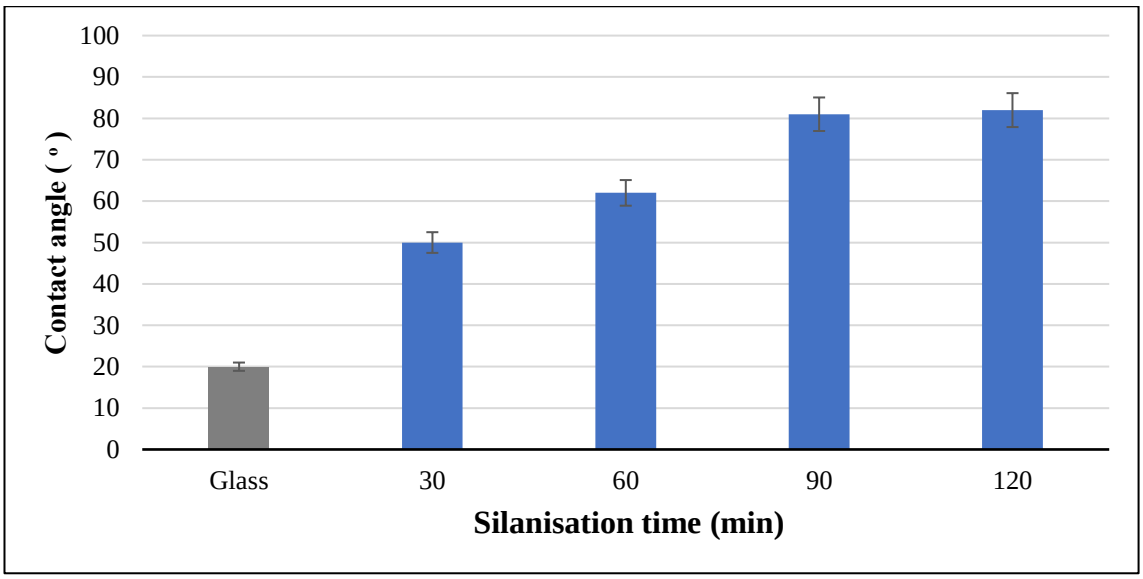

Figure 4-7: Effect of the time of the treatment process of the glass slide with APTES on the contact angle measurement, (n = 3). The error bars indicate one standard deviation

The contact angle increased with increasing time up until 81° ± 4.1° and 82° ± 2.1° for reaction times 90 and 120 min respectively. The increase between the 90 and 120 mins within the error bars and therefore the interaction time for the silansition process of glass surface was chosen to be 90 min for further experiments.

4.2.2 Evaluation of success of the chemical immobilisation of antibody by chemiluminescence

CL detection was used to verify of immobilisation of the antibodies on the glass surface. For the APTMS modified glass slide the EDC and sulfo – NHS were used as cross-linker as described in section 2.7.3. The mechanism of immobilisation the antibody onto the APTMS modified surface is demonstrated in Figure 4-8. The interaction between the glass surface and antibody was achieved through coupling of the primary amino group on the sailanised surface to the carboxylic acid group of the antibody via an amide linkage formed using sulfo – NHS and EDC as explained in section 1.11.7.3. The EDC start the reaction with the carboxyl group on the antibody to form unstable amino reactive (O –

acylisourea ester). Then, the sulfo – NHS stabilises the intermediate amino – reactive by converting it to amino reaction NHS – ester. In the final stage, the amide bond was formed between the amino group on the surface and the antibody. This mechanism is similar to method uses for the coupling of amino acids for peptide synthesis. After complete the step, the surface of glass should cover with antibodies.

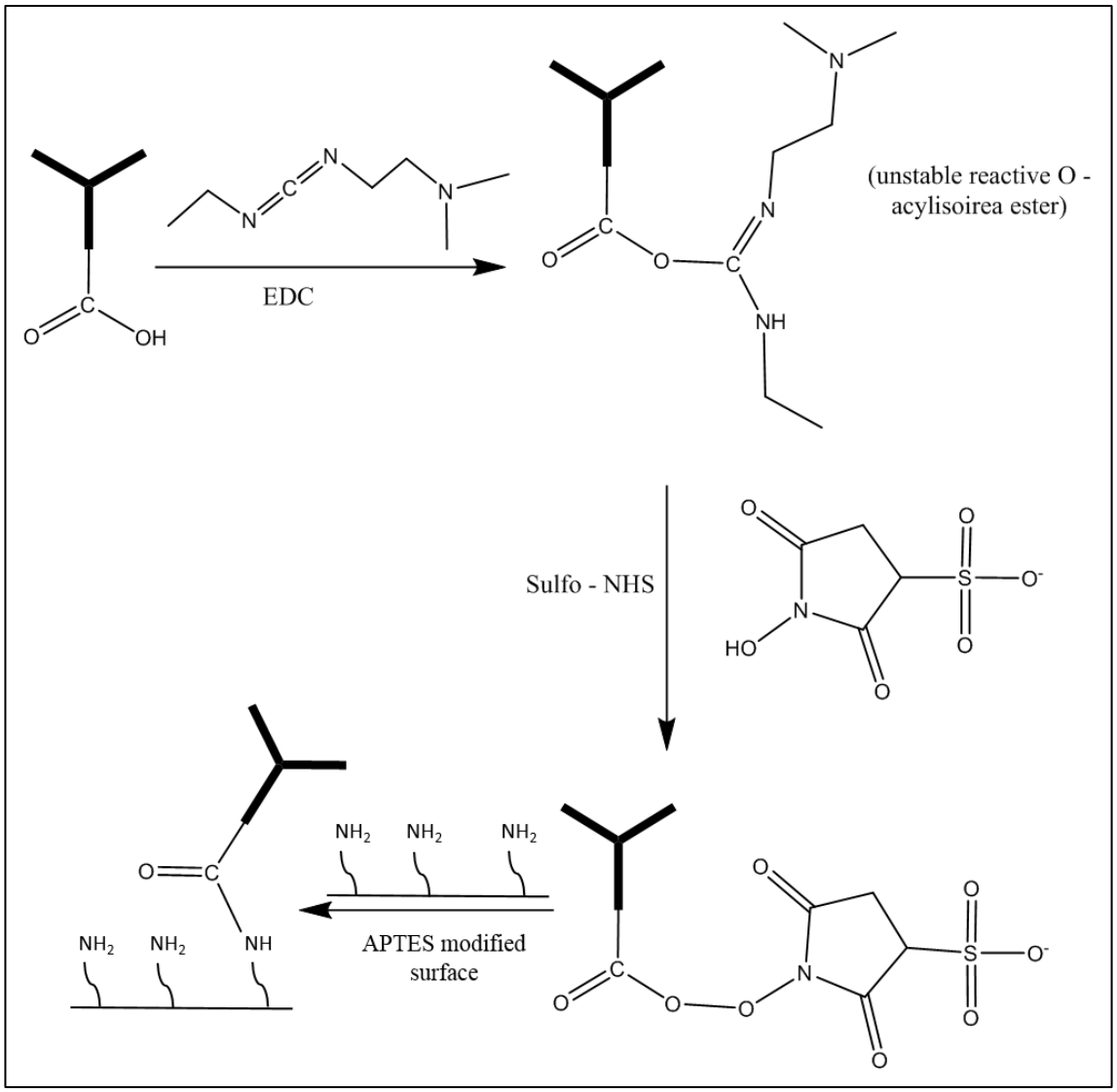

Figure 4-8: Mechanism of the immobilisation process for the antibody onto the APTMS modified glass surface by using activation buffer of EDC and sulfo – NHS [233].

For the glass surface modified with GPTMS, the antibodies were mixed with PBS buffer and spotted directly to the glass modified surface as described in section 2.7.3.2. This step was carried out without a crosslinker because the polarity of the carbonyl functional group

(C = O) make the carbon atom more electrophilic and reactive with nucleophiles primary amine in the antibody [142].

After completion of the immobilisation of the antibodies onto the glass surface, and adding the antigen – HRP as explained in section 2.7.4.2, all the glass slides were measured by chemiluminescence detection. Figure 4-9 shows examples of the CCD images of the interaction of the antibody immobilised on the glass slide in the biochip array holder with antigen – HRP in the present of CL reagents.

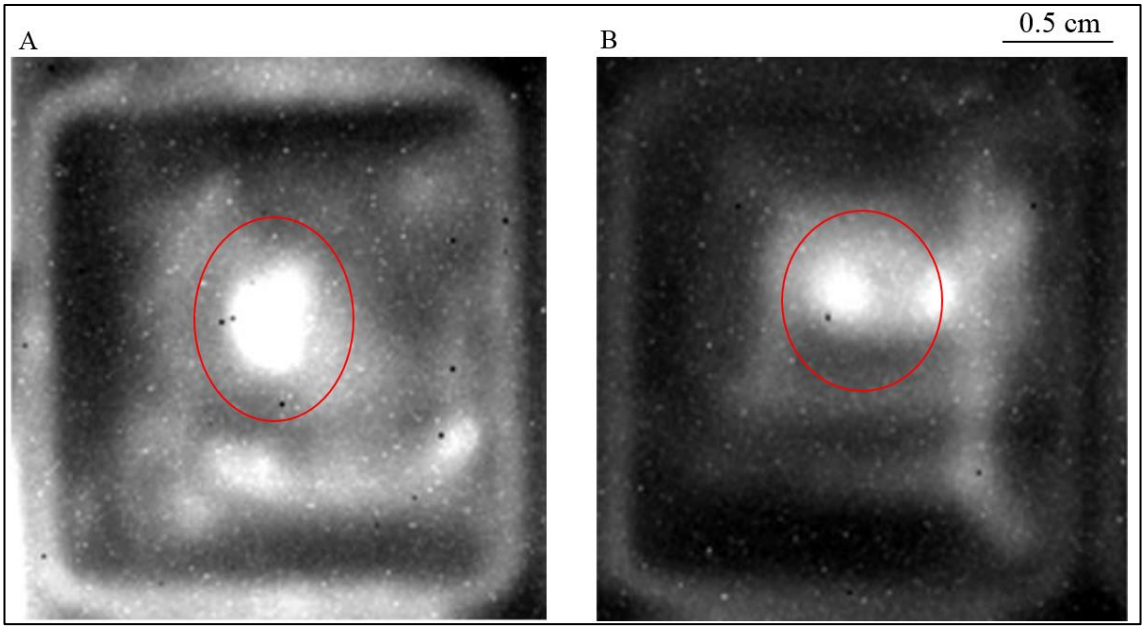

Figure 4-9: Two examples of a CCD image of the CL emission signal emitting from progesterone - HRP attached to an immobilised antibody on the surface of microscope slides. The glass surface was chemically modified using APTMS, the scale bar 0.5 cm.

For examples are given in Figure 4-9 emitted light can be seen. The images are however different in A there is more general emission with a bright spot in the centre. The appearance of one spot would be expected from the experimental procedure. In B, there is less general background. These results confirm that the antibodies were immobilised and that the reaction between the antibodies and the antigens had occurred. The images in Figure 4-9 are however only two examples of many replicates for both APTMS and

GPTMS, and it was found in the fact that it was very difficult to obtain consistent results and with the most example, no CL signal was observed. In other cases, the antibodies appeared too dispersed all over the surface as clearly shows for APTMS modification in Figure 4-10. Figure 4-11 shows similar results for the glass modified with GPTMS.

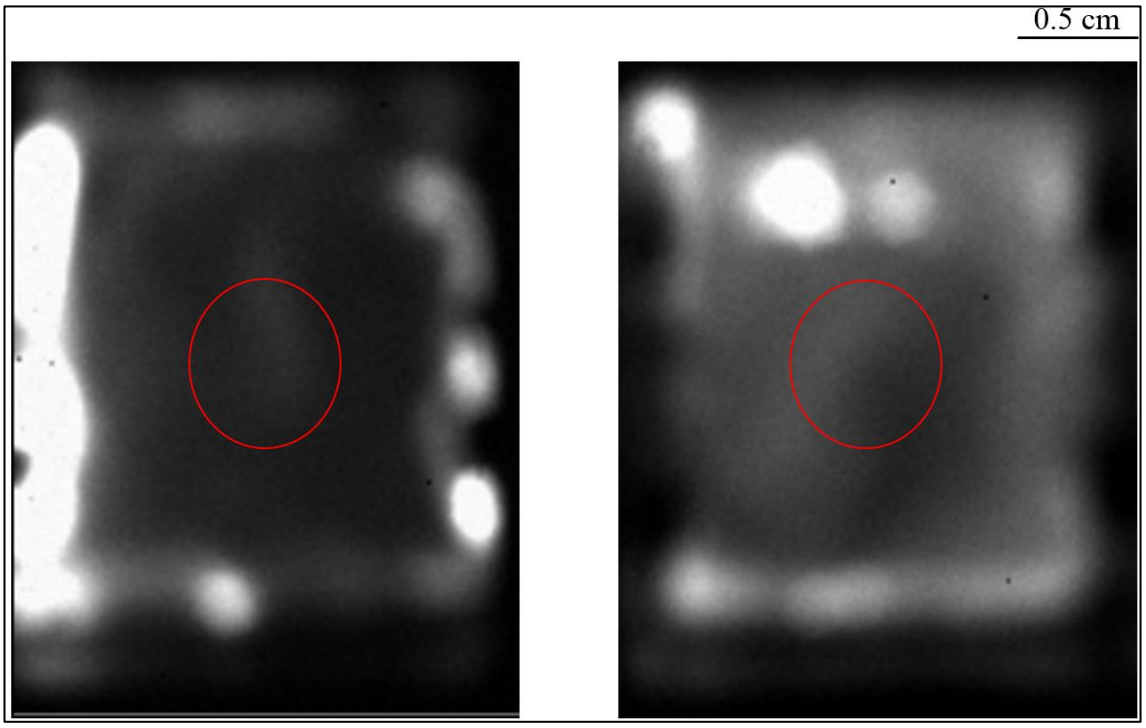

Figure 4-10: Two examples of a CCD image of CL signal emitting from progesterone - HRP attached to an immobilised antibody on the surface of microscope slides (0.8 × 0.8 cm). The glass surface was chemically modified using APTMS, where the red circle line showed place of the antibodies were spotted and they found to be spread over the surface, the scale bar 0.5 cm.

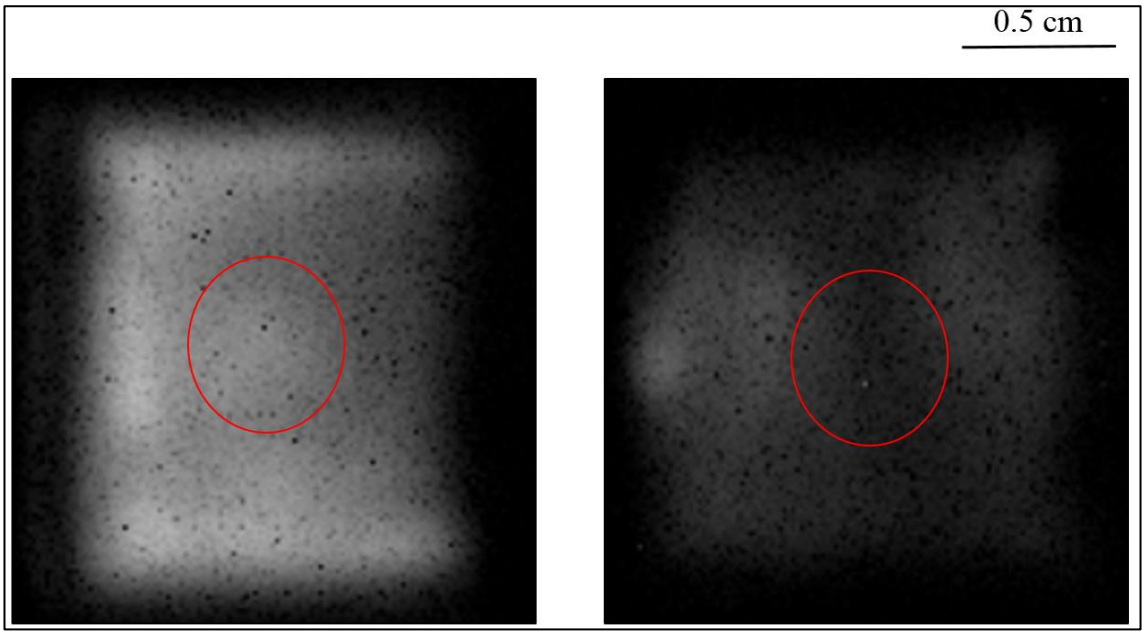

Figure 4-11: Two examples of a CCD image of CL signal emitting from progesterone - HRP attached to an immobilised antibody on the surface of microscope slides (0.8 × 0.8 cm). The glass surface was chemically modified using GPTMS, where the red circle line showed place of the antibodies were spotted and the antibodies were found to be spread over the surface, the scale bar 0.5 cm.

The silanisation and immobilisation process is quite long with several steps and many possible variables that could be influencing the results. As mentioned previously, the silanisation process is very sensitive, and several factors could influence it including preparation of the slide, temperature, humidity and the additional step using HRP for competitive immunoassay. If the silanisation process were not reproducible, immobilisation of the antibody onto the surface would be effected as well.

Another important factor with this type of immobilisation is antibody orientation as discussed in section 1.11.9 and shown in Figure 1-15. In a case of using the GPTMS for modification of glass surface, the interaction occurs between the epoxy group in the surface and the primary amine that placed in Fab region of the antibody. Resulting in bond in this way could lead to an undesirable antibody orientation, so reduced the opportunity for interaction between the antibody and antigen – HRP.

To overcome the reproducibility of immobilisation the electrochemistry technique reported by Dou *et al.* [138] was used as an alternative method to modify the solid support surface.

4.3 Electro method for modification the ITO electrode

Electrochemistry method was used to introduce the amino group onto a conductive surface, such as a tin-doped indium oxide (ITO) electrode. This method was fast, a reproducible and the procedure could be monitored through cyclic voltammetry (CV), which led to increasing the reproducibility of immobilisation process. The method also avoided the problem of antibody orientation as described by Dou *et al*.[138]. Furthermore, there was no need to use an HRP label. Instead, the idea was to label the antibody with a metal catalyst ferrocenecarboxaldehyde (Fc – CHO) before spotting onto the ITO electrode for fast electron transfer [138]. The antibody was labelled with FC – CHO on the amino acids present in the Fab region, therefore improving sensitivity, as these would be freely available in interact. The principle of modifying the antibody is shown in Figure 4-12 .

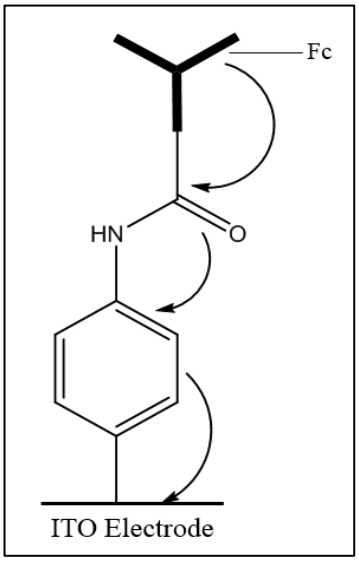

Figure 4-12: The theoretical concept for the electrochemical protocol for antibody immobilisation the arrows are representative of the transfer of an electron through a molecular wire [234].

As the result of forming the amino group onto the ITO electrode surface as will explain in section 4.3.2, it allows the carboxyl group in the antibody to react and form an amide bond. These create a molecular wire which conducts electric current between the electrode and the antibody [234]. This is due to the presence of the amide bond between the antibody and ITO electrode that, allows resonance between the nitrogen and oxygen atoms.

The arrows in Figure 4-12 shown an oxidation process where the ferrocene (Fc) loses an electron to the electrode surface. Figure 4-12 also shows how the immobilisation process for the antibody creates a rigid structure, which facilitates correct antibody orientation. If the antibody was to orientate upside down the bulky ferrocene groups would be crowded by the benzene ring onto electrode surface that would not be favourable.

4.3.1 Labelling the antibody with ferrocenecarboxaldehyde (Fc – CHO)

As explained previously the antibody was chemically labelled with Fc – CHO redox tags before spotting onto the ITO electrode, as described in section 2.7.7. In this step the Fc – CHO was linked to the antibody through the formation of a Schiff – base by increasing the pH to 9 using potassium carbonate (K_2CO_3) to allows the formation of the product [Ab – N = CH – Fc]. After that, adding the sodium borohydride ($NaBH_4$) was added to reduce the imine into amine to form the final product [Ab – NH_2 – CH_2 – Fc]. Figure 4-13 illustrated the process of labelling the antibody with Fc – CHO.

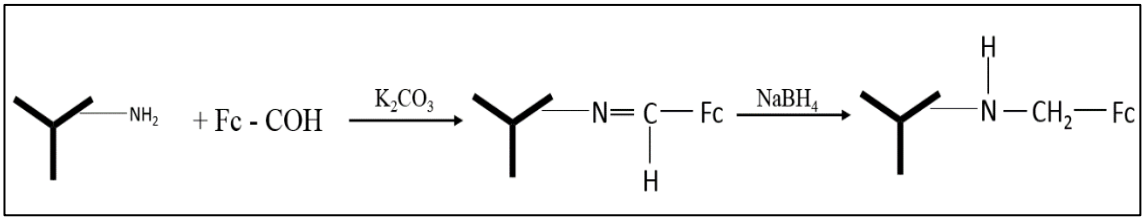

Figure 4-13: Reaction schemes for labelling of antibody with Fc-CHO [235]

4.3.2 Modification of the ITO electrode

To immobilise the antibody onto the ITO electrode surface, a modification step was carried out onto the ITO electrode to form the functional group that binds to the antibody. These were achieved through electrochemical reduction (CV) as described in Section 2.7.8.

The modification process reaction for the ITO electrode surface is provided in Figure 4-14. The ITO electrode was dipped in a solution made up of 4-nitrobenzenediazonium and tetrabutylammonium perchlorate (TBAP) dissolved in acetonitrile. Through the electrochemical reduction, a nitrobenzene-modified surface was formed for the first step. Subsequently, in the second step, the cyclic voltammetry was used to reduce the nitrobenzene surface to phenylamine.

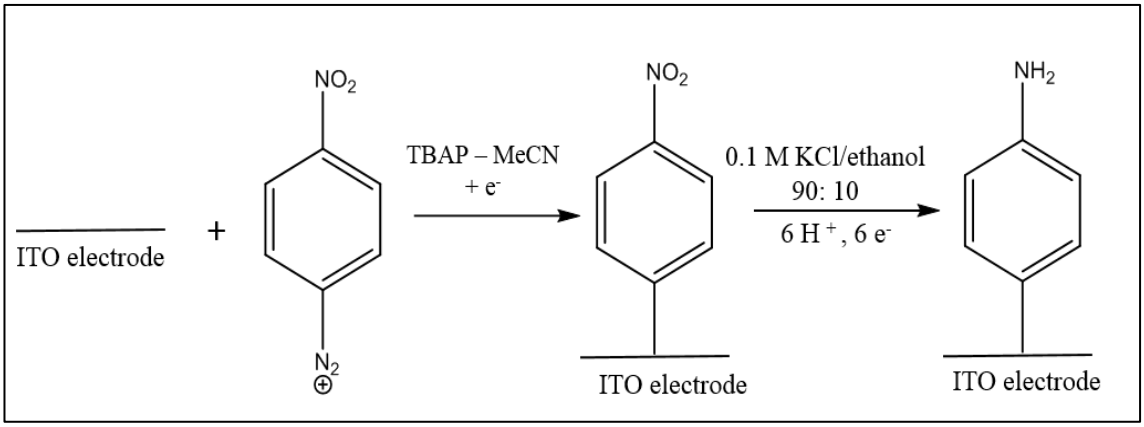

Figure 4-14: Schematic of the modification process of the ITO electrode.

In the first step, the diazonium ion is capture an electron that had produced from the ITO electrode and the N^{2+} is cleaved from the benzene rings as N_2 molecule [236]. The phenyl radical left over the binds to the ITO surface to form a stable covalent bond. Therefore, the nitrobenzene was formed into the ITO electrode surface. After that, the nitrobenzene surface is converted to phenylamine through electrochemical reduction (CV).

The cyclic voltammograms for the first reaction onto the ITO electrode surface carried out in the solution of 4 – nitrobenzenediazonium are shown in Figure 4-15. During the

first potential scan, an irreversible reduction peak was observed at about 0.07 mV that was attributed to the reduction of the diazonium group. While in the second, third and fourth potential scan, the potential current peaks were strongly decreased. This behaviour gave an indication that the ITO surface electrode was almost covered by nitrobenzene and the electron transfer from the ITO electrode to the solution was blocked.

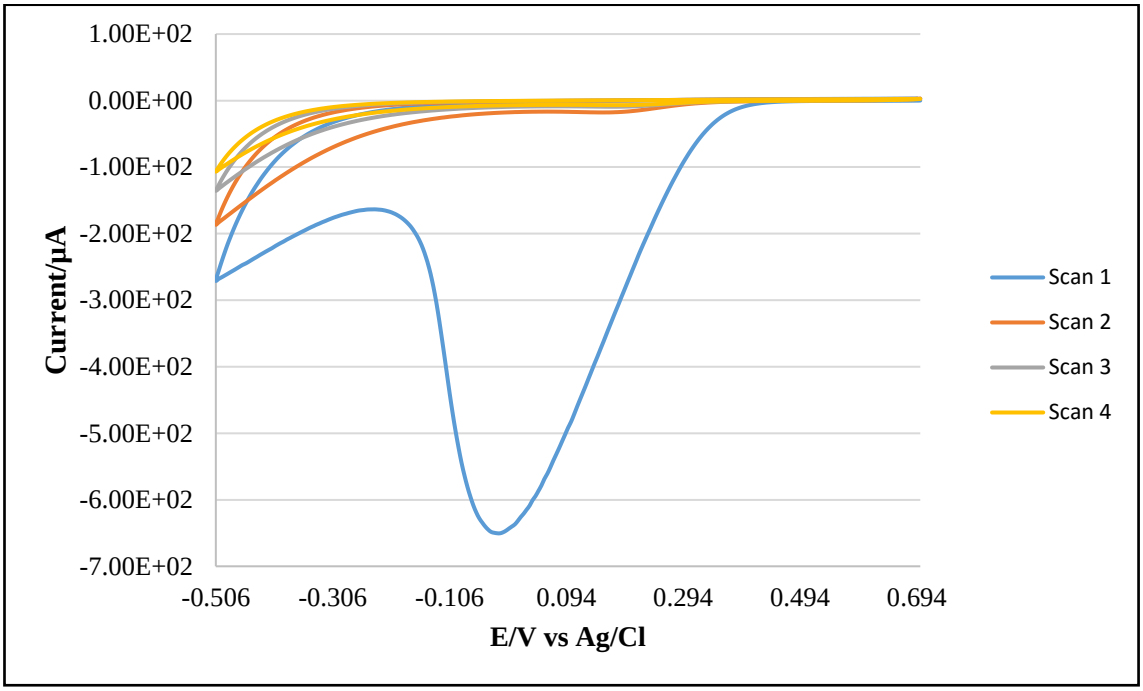

Figure 4-15: Cyclic voltogram of the reduction process of the nitrobenzene diazonium onto the ITO electrode surface in the degassed solution of 4-nitrobenzenediazonium and TBAP in acetonitrile. The cyclic voltammetry started at +0.7 V scanning down to -0.4 V and with a return sweep to +0.7 V performed over four scans with a scan rate of 10 mV s^{-1} at room temperature.

The cyclic voltammograms of the second step which was carried out in the aqueous solution (ethanol: KCl) for four continuous cycles are shown in Figure 4-16. In the first cycle, an irreversible peak (A) appeared at -1.004 V on the cathode sweep, while on the reverse scan, an oxidation peak (B1) appeared at – 0.247 V and there no oxidation peak was observed corresponding to peak A. New reduction peak was observed (B2) that was reversible with (B1) at – 0.391 V, while the second cathodic sweep.

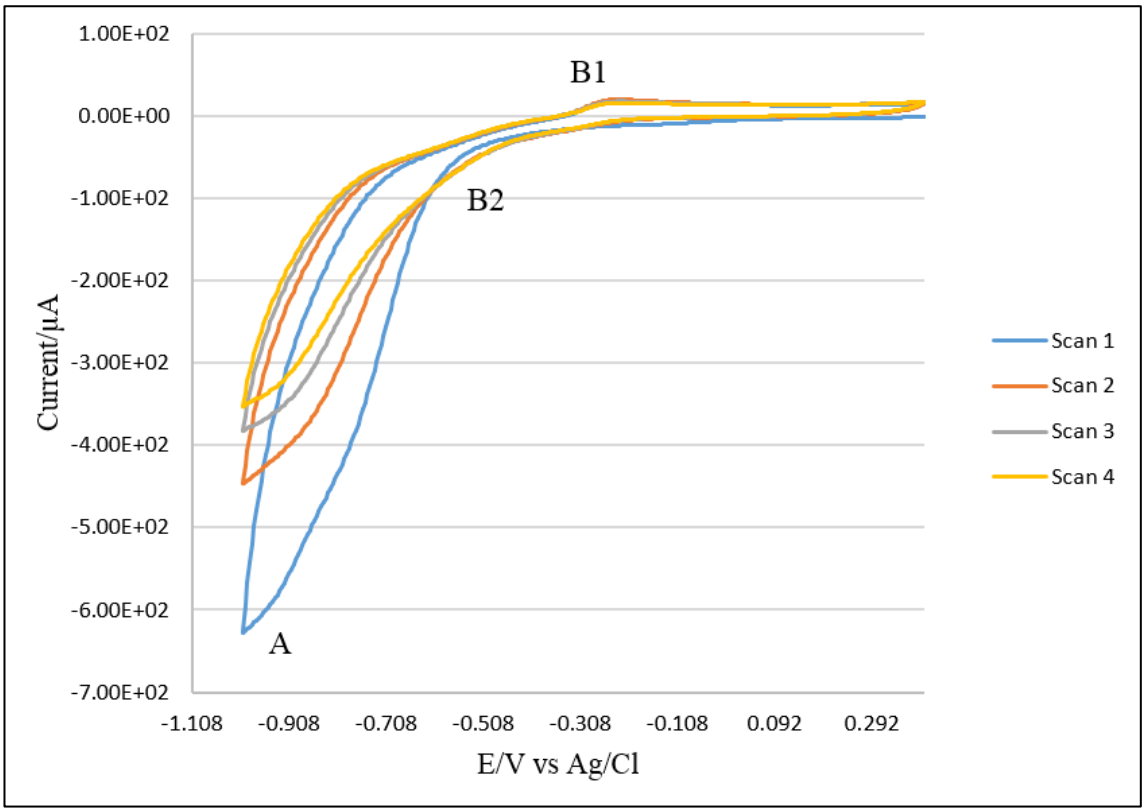

Figure 4-16: Reduction of nitrobenzene on the ITO electrode in degassed 0.1 M KCl-ethanol (90:10, v: v) by cyclic voltammetry. The peak potential is at -1.0 V and scan rate 0.1 V s^{-1} at room temperature.

These phenomena demonstrate that the electrochemistry created products due to the irreversible reduction of nitrobenzene of (A) and these give rise the peaks at B1 and B2. The nitrobenzene underwent an irreversible four electron reduction to form hydroxylamine and another reduction of two electrons to form phenylamine, as described in the literature[237] [238]. In the literature it is mentioned that hydroxylamine could be easily converted into nitrosobenzene reversibly through a two electrons oxidation/reduction mechanism [236]. Consequently, it is supposed that the same electron transfer mechanism of nitrobenzene can be enforced onto the ITO electrode using an electrochemical oxidation and reduction as illustrated in Figure 4-17.

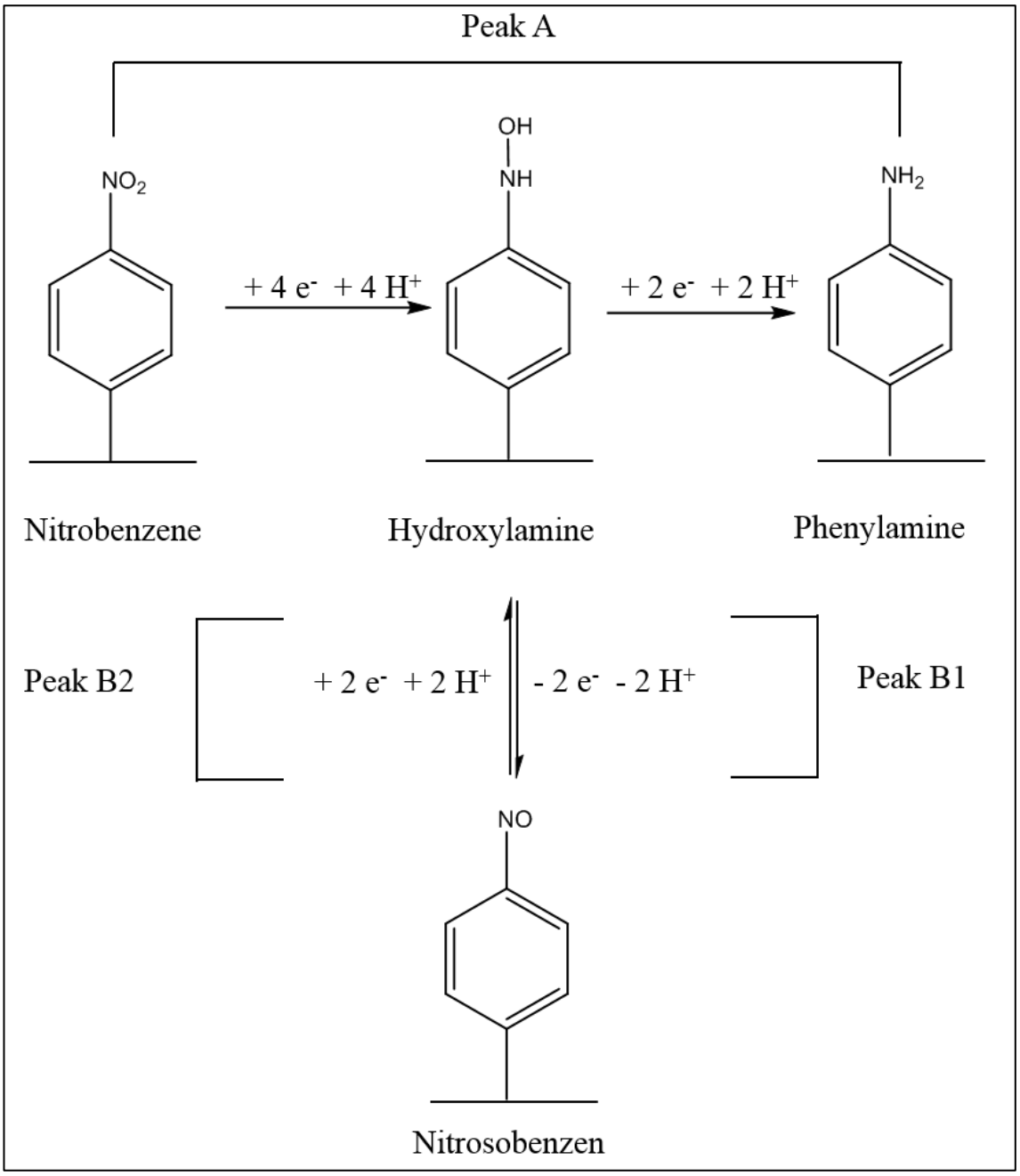

Figure 4-17: Electrochemical oxidation and reduction mechanism of nitrobenzene at the modified ITO electrode [238].

4.3.3 Immobilisation of antibody labelled with ferrocene onto ITO electrode

After completing the process of labelled the antibody with ferrocene, the antibody was immobilised onto the ITO electrode surface. The immobilisation of the labelled antibody was achieved through the coupling of the primary amine group of the phenylamine modified electrode surface and the carboxylic acid group on the Fc region *via* an amide

bond. The activation reagent (EDC and sulfo – NHS) were used as with the APTMS modified surface as explained in section 4.3. The scheme of the procedure for immobilisation of Ab – Fc onto the ITO electrode is illustrated in Figure 4-18.

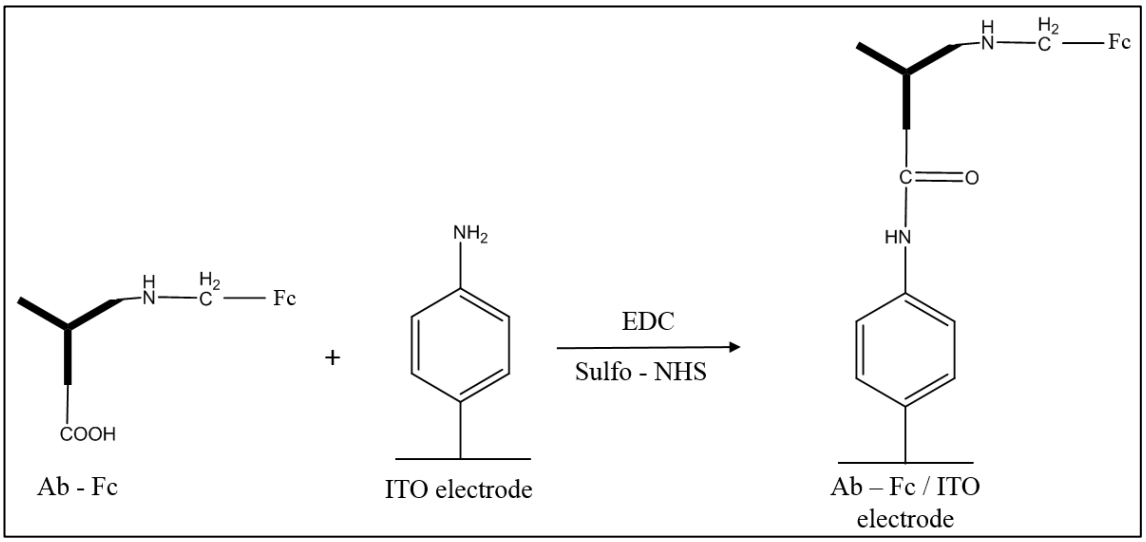

Figure 4-18: The reaction of immobilisation of labelled antibody (Ab – Fc) onto ITO electrode surface.

4.4 Characterisation of the antibody immobilised onto the ITO electrode surface

After completion of the immobilisation process of the labelled antibody onto modified ITO electrode surface, cyclic voltammetry measurement was obtained of the surface for the modified ITO electrode without antibody (blank) and the modified ITO electrode in the presence of the labelled antibody. Figure 4-19 represent the cyclic voltammogram comparing of the blank ITO surface and ITO surface with the labelled antibody.

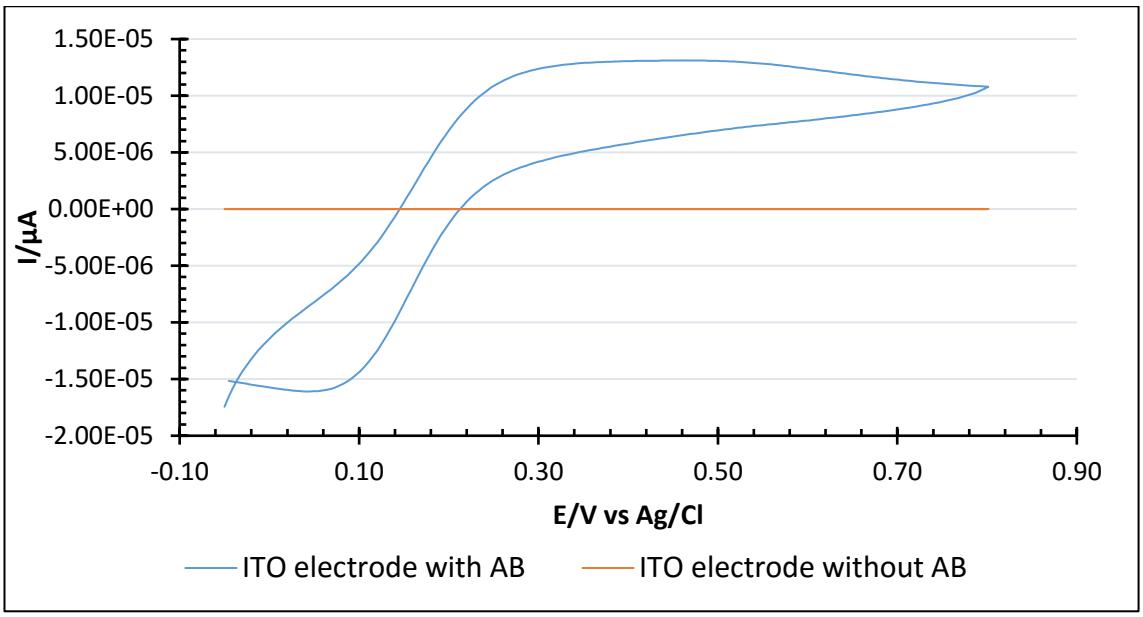

Figure 4-19: Cyclic voltammograms of blank ITO electrode surface and ITO electrode surface in percent of labelled antibody. The san rate was 100 mV s^{-1}, and the entire scan carried out in 10 mM of PBS at pH 7.5.

The cyclic voltammograms shown in Figure 4-19, show that the ITO electrode with the labelled antibody exhibits a reversible redox peaks at 0.38 and 0.05 V. This peak related to the ferrocene/ferrocenium redox process since the blank surface of ITO electrode did not exhibit these peaks and give an initial indication of the efficient immobilisation of the labelled antibody onto the ITO electrode.

Further measurements were then carried out to find out the stability of the labelled antibody onto the surface before preparing a calibration curve. Figure 4-20 shows the cyclic voltammograms for the labelled antibodies on the ITO electrode at a range of scan rates between 10 to 1000 mV s^{-1}.

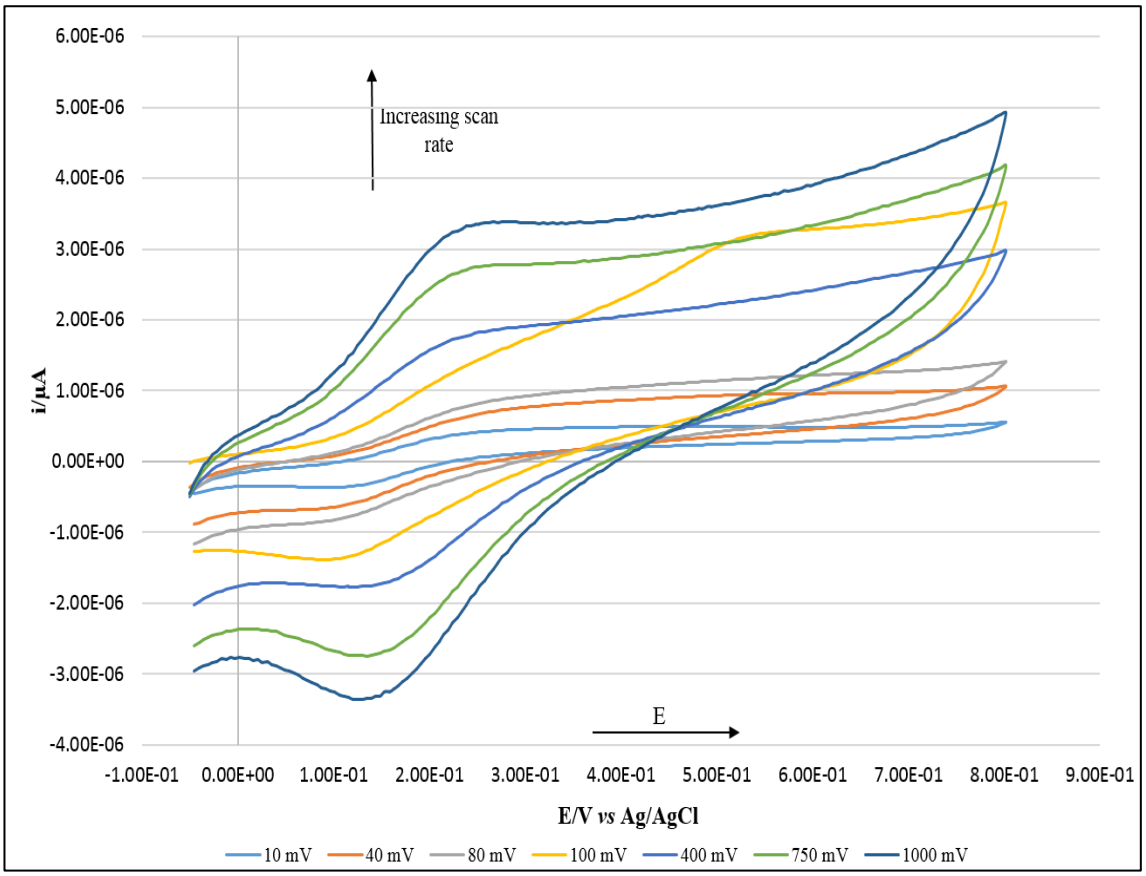

Figure 4-20: Cyclic voltammograms of labelled antibody on the ITO electrode surface with scan rates from 10 mV s^{-1} rising to 1000 mV s^{-1}.

In Figure, 4-20 can be seen the peak current is increasing with an increase in the scan rate. The oxidation peak occurs at + 0.28 V, which is clearer at the higher scan rates, represents the oxidation of ferrocene to the ferrocenium cation; with the corresponding reduction was seen at +0.25 V confirming the immobilisation process has been successful. In addition, this experiment shows the stability of the labelled antibody immobilised onto ITO electrode at various scan rate.

4.4.1 Effect of the different concentration of the analyte on the labelled antibody

The change in current with the concentration of the analyte was then investigated using cyclic voltammetry measurement as described in section 2.7.8. An initial cyclic voltammogram was obtained for the ITO electrode surface that contains labelled anti –

progesterone with no analyte (blank). The cyclic voltammogram for labelled anti – progesterone without progesterone, and after adding 15 µL progesterone 1 pg mL^{-1} is shown in Figure 4-21.

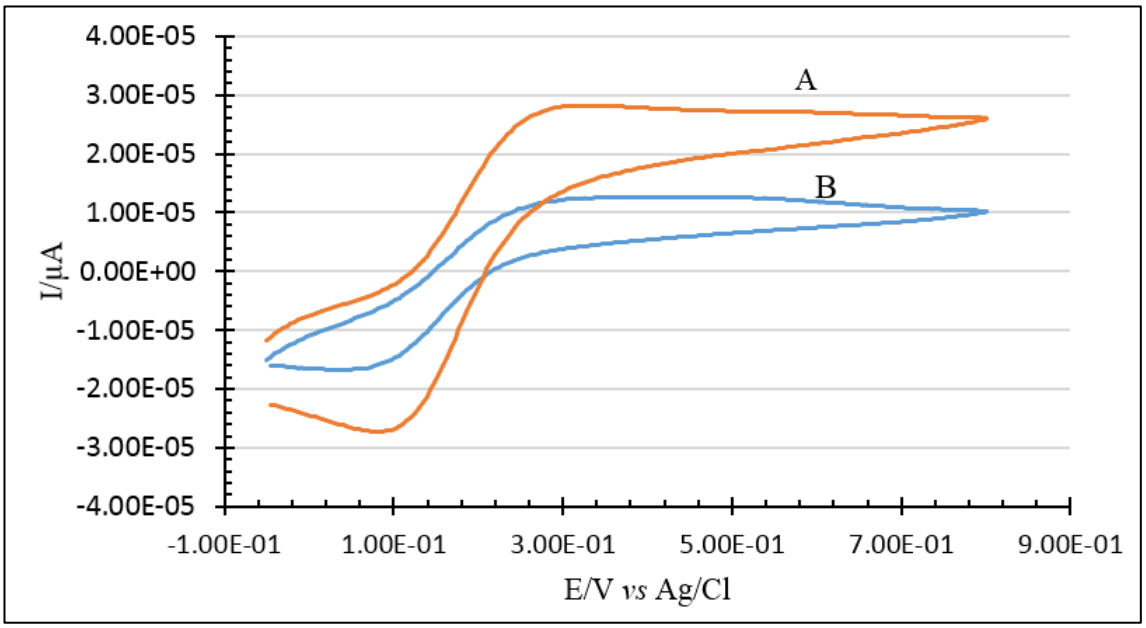

Figure 4-21: Cyclic voltammogram of (A) ITO electrode with labelled anti – progesterone used as blank, (B) ITO electrode with labelled anti – progesterone after adding progesterone (1 pg mL^{-1}). The scan rate was 100 mV s^{-1} and all scan carried out in PBS buffer at pH 7.5.

It can be seen that the current had reduced when the analyte was added (B) compared to the blank (A). The current intensity in voltammogram (B) had decreased because of the antibody-antigen binding. Also to investigated the influence of different concentration on the peak current, three different concentration of progesterone (1 µg mL^{-1}, 1 ng mL^{-1} and 1 pg mL^{-1}) were added onto labelled anti – progesterone. These different concentrations were selected as low, medium and high concentration to study the influence at big range of concentration. Figure 4-22 shows the effect of different concentration on the peak current.

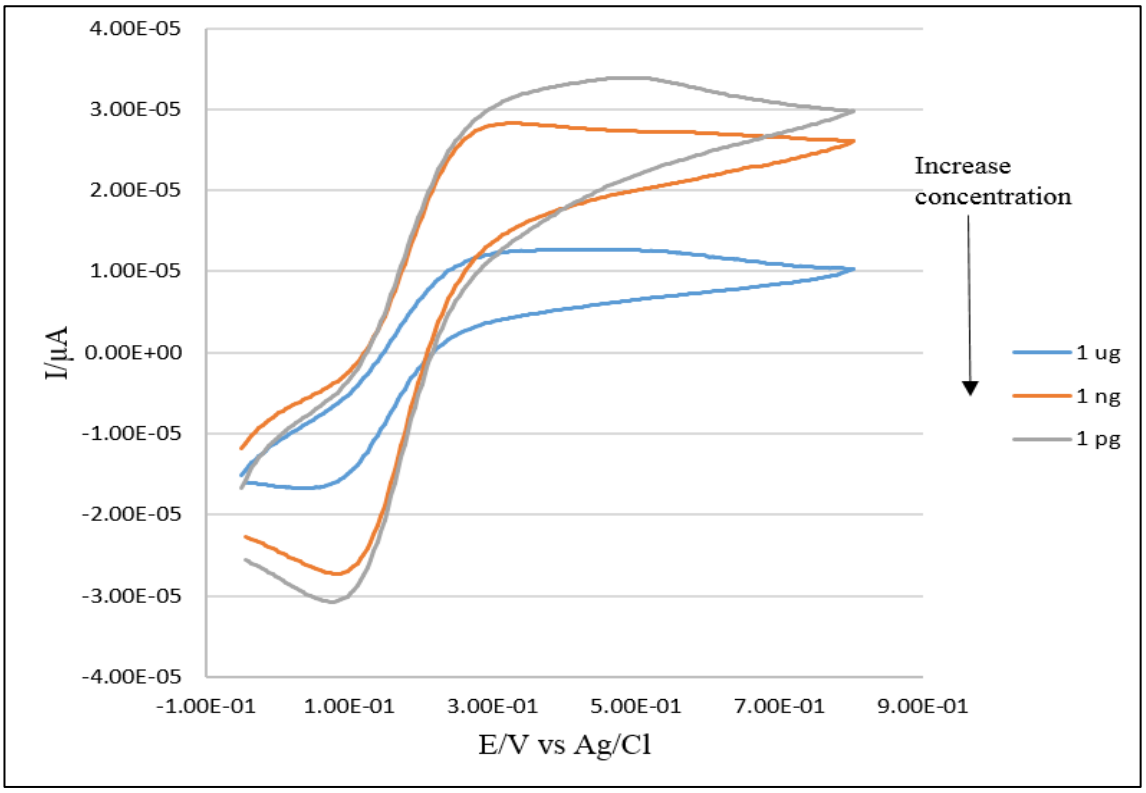

Figure 4-22: Cyclic voltammograms for different concentration of progesterone. The scan rate was 100 mV s^{-1} and all scan carried out in the PBS buffer at pH 7.5.

Looking at Figure 4-22, it clearly shows, the concentration of progesterone increased the peak current decreased (for cyclic voltammetry for both the oxidation and reduction peaks). These would be expected as the ferrocene labels are firstly located on the paratope region of the antibody these are being blocked out by the antigen.

The correlation between the paratope region on the antibody and antigen epitope is first because of electrostatic and hydrophobic interaction, and secondly by Van der Waals interaction and hydrogen bonding [120]. Hence, all of this causes a radical change in the local environment of the ferrocene species would be enough to change the formal oxidation performance.

4.4.2 Optimisation of the incubation time

The incubation time is the time required to complete the interaction between the antibody and the antigen and optimisation of the incubation time is required. These were carried

out on three separate ITO electrode contain the labelled anti – progesterone at 15, 30 and 60 min following the procedure described in section 2.7.10. Figure 4-23 shows the average results of three electrodes obtained from each spot.

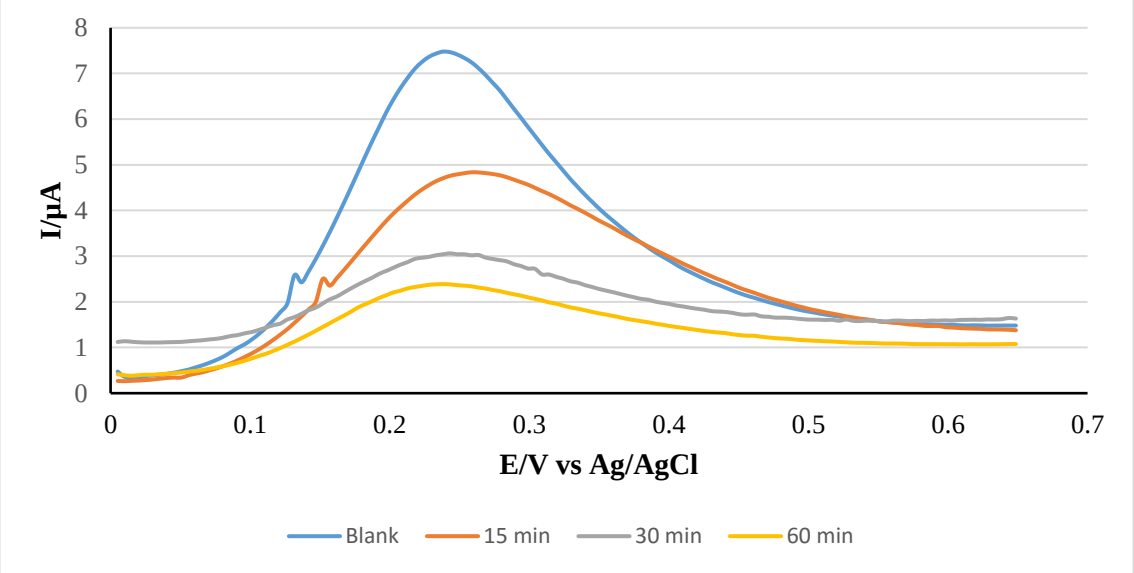

Figure 4-23: Square wave voltammograms of labelled anti – progesterone of blank and after added progesterone 1 pg mL^{-1}at various incubation time. Frequency 25 Hz, amplitude 1 mV, all scan carried out in the PBS buffer at pH 7.5.

In Figure 4-24 it can be seen that the peak current was reduced with increased incubation time. These results show that increasing the incubation time provides more opportunity to complete the interaction between the antibody and antigen, which means the antigen "blocking" the ferrocene moieties and reducing the voltammetric response primarily to those found in the paratope region. The incubation time for 60 min gave the minimum peak current. However, the difference with the 30 min of incubation was small while the difference was greater for 15 min. It was decided that in order to get a suitable short incubation time, but at the same time have high sensitivity, 30 min of incubation time should be used for future measurements.

4.4.3 Figure of merit for calibration curves of estradiol, progesterone and benzo (a) pyrene by SWV.

Calibration curves were obtained by square wave voltammetry at different concentration of progesterone, estradiol and benzo (A) pyrene (100, 50, 25, 10 and 1 pg mL^{-1}). Three separate ITO electrode were used, 15 µL of each concentration was added to labelled antibody and left for 30 min at 4 °C for incubation process as described in section 2.7.8, the example of the result obtained are presented in Figure 4-24.

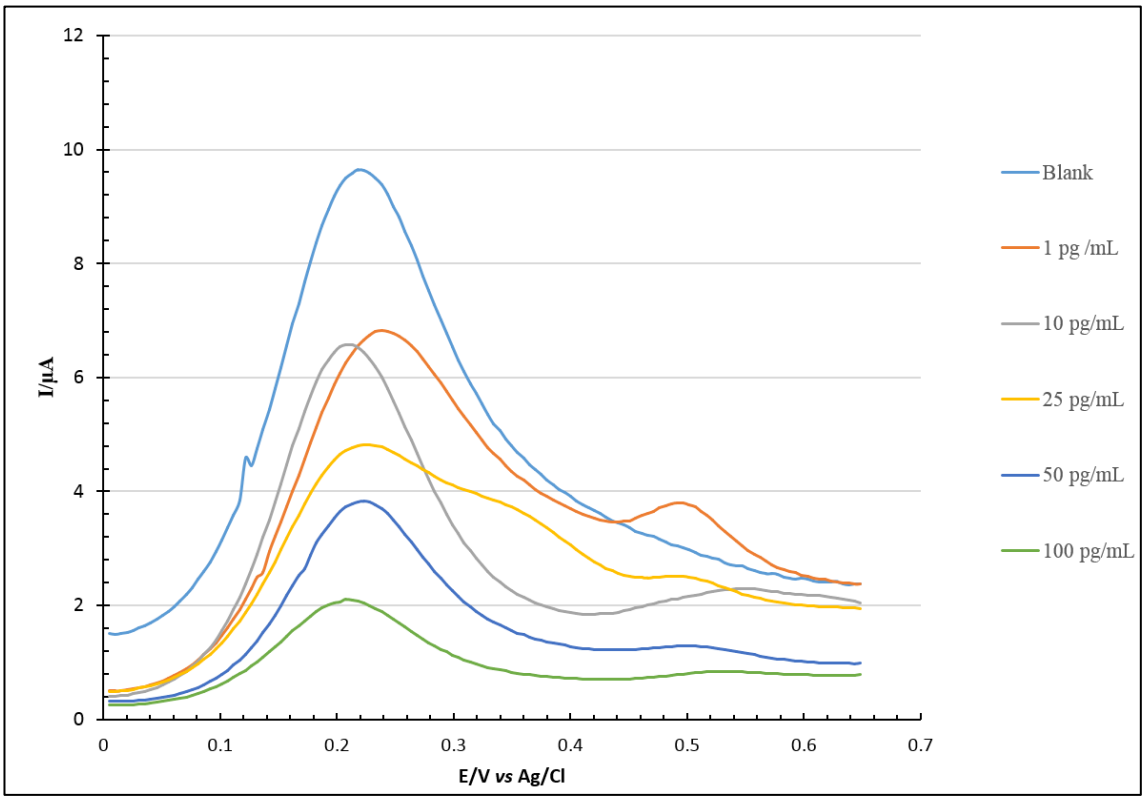

Figure 4-24: Square wave voltammograms for different concentration of progesterone, frequency 25 Hz, amplitude 1 mV all scan carried out in the PBS buffer at pH 7.5.

The linearity, LOD and LLOQ were assessed from the calibration curves for each pollutant compounds. Standard solutions of each analyte at the concentration (100, 50, 25, 10 and 1 pg mL^{-1}) were added to labelled antibody immobilised onto the ITO electrode and completed the incubation process for 30 min. Each electrode was washed with PBS buffer to remove unbounded analyte before the measurement step. Each concentration

was analysed three times, and the peak current was plotted against concentration. Figure 4-25 shows the calibration curve for each analyte.

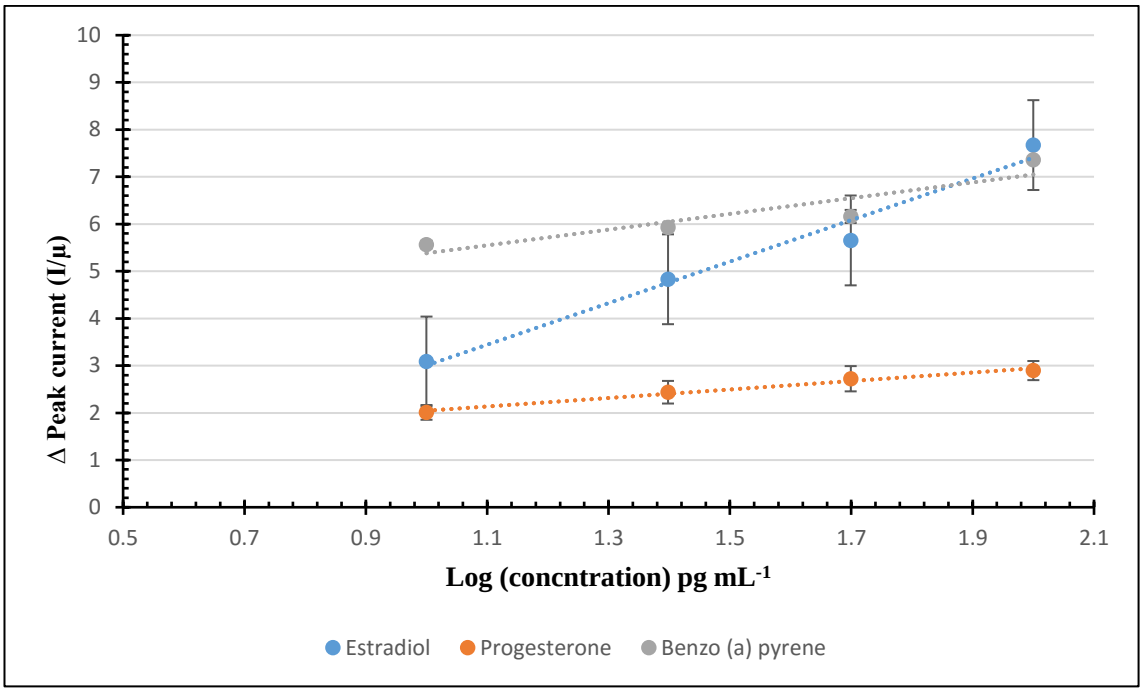

Figure 4-25: Calibration curve of the estradiol (blue line), progesterone (orange line) and benzo (a) pyrene (grey line) standard solution with Δ peak current plotted against their concentration, (n = 3). The error bar indicates one standard deviation.

The calibration curves of the targets analytes shows a good linearity over the range used and offered good values of correlation coefficient (R^2) for progesterone and estradiol, where with progesterone the R^2 value were excellent for both as its near 1. Where the R^2 for benzo (a) pyrene was quiet low, in spite of this analyte shows acceptable linearity. All the results of LOD and LLOQ were calculated using the equations Equation 2-2, Equation 2-3, Equation 2-4 and Equation 2-5 respectively. Table 4-1 summarised all the results obtained from calibration curves in Figure 4-25

Table 4-1: Analytical figure of merit of estradiol, progesterone and benzo (a) pyrene

Analyte	LOD (pg mL^{-1})	LLOQ (pg mL^{-1})	Linearity	Correlation coefficient (R^2)
Estradiol	7.69	25.64	y= 4.3995 x – 1.3956	0.975
Progesterone	0.71	2.3	y= 0.8987 x + 1.1461	0.984
Benzo (a) pyrene	0.26	0.85	y= 1.666 x + 3.7155	0.84

Table 4-1 shows the LOD value for all analytes, where the benzo (a) pyrene achieved the lowest LOD value at 0.26 pg mL^{-1} by using this technique, also the LOD value for progesteone was very low (0.71 pg mL^{-1}) which gives indcuation this technique was very sensitive. The highest value of LOD was for estradiol (7.69 pg mL-1) but as well shows the power of this technique. The values of LLOQ for progetrone and benzo(a)pyrene are very low for the concentration can be quantified with acceptable accuracy and precision are (0.85 and 2.3 pg mL^{-1}) respectively, where in case of estradiol was quite high (7.69 pg mL^{-1} but still acceptable if compare with expensive and complicated insturments.

4.4.4 Determination of interference of analytes by square wave voltammetry

The aim of this project is multi-analysis of organic pollutants at river water sample, so the plan was to immobilise three different types of antibodies on the same ITO electrode. At the same time, it will be important that when the sample is analysed the antibodies will be selective for the analytes of interest.

Anti – benzo (a) pyrene, anti – estradiol and anti – progesterone were labelled with ferrocene and immobilised onto ITO electrode respectively as described in section 2.7.11

and shown in Figure 4-26, Figure 4-27 and Figure 4-28. A standard mixture with benzo (a) pyrene, estradiol and progesterone at 100 pg mL^{-1} was added to each antibody.

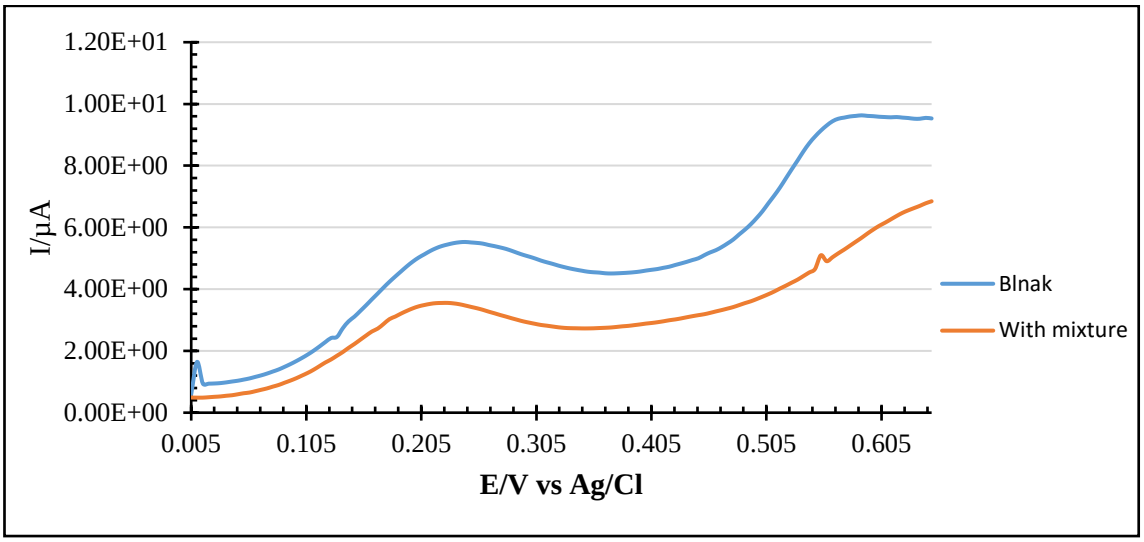

Figure 4-26: Square wave voltammogram of labelled anti – benzo (a) pyrene, where the blue line present is the blank and the orange line present with mixture Frequency 25 Hz, amplitude 1 mV, all scan carried out in the PBS buffer at pH 7.5.

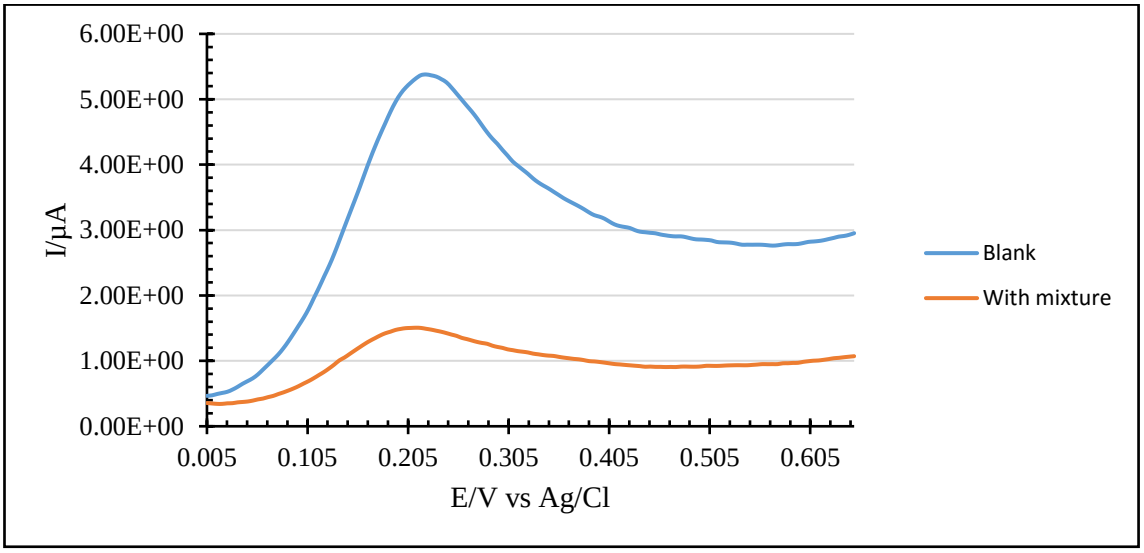

Figure 4-27: Square wave voltammogram of labelled anti – estradiol, where the blue line present is the blank and the orange line present with mixture Frequency 25 Hz, amplitude 1 mV, all scan carried out in the PBS buffer at pH 7.5.

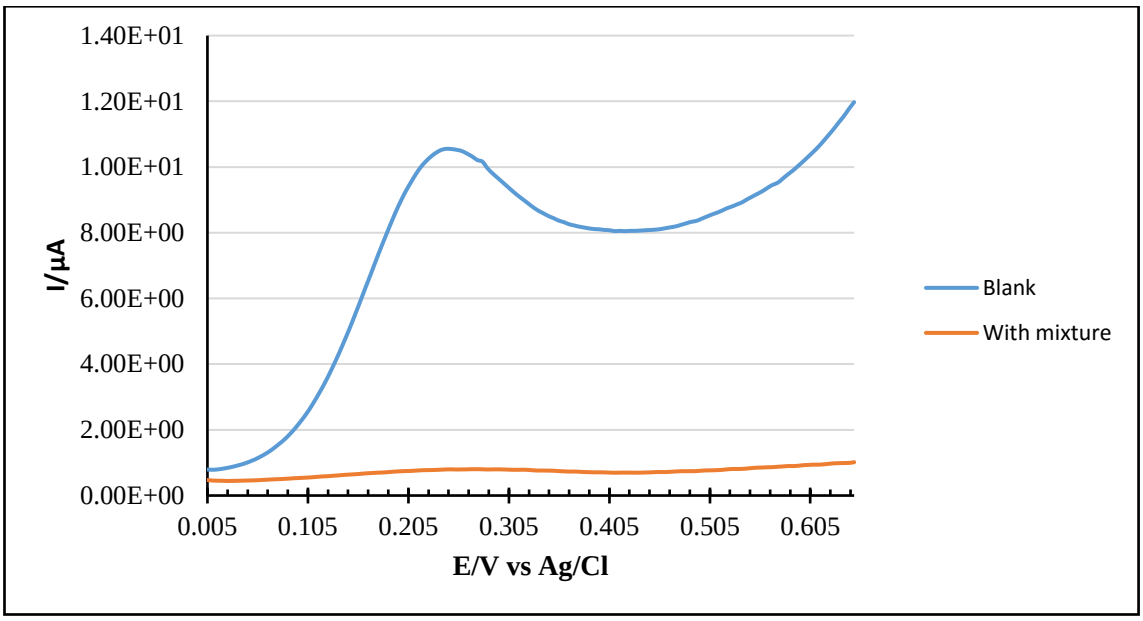

Figure 4-28: Square wave voltammogram of labelled anti – progesterone, where the blue line present is the blank and the orange line present with mixture Frequency 25 Hz, amplitude 1 mV, all scan carried out in the PBS buffer at pH 7.5.

Figure 4-26 shows the effect the adding the mixture sample of organic pollutants on the anti – benzo (a) pyrene. Other compounds (progesterone and estradiol) and the different in peak current of the blank did not affect the peak current and the sample related to the amount of benzo (a) pyrene that linked with the antibody. These showed high selectivity for anti – benzo (a) pyrene. However, in Figure 4-27 and Figure 4-29, the square wave voltammogram showed a massive gap between the square wave voltammogram of the blank and square wave voltammogram of the labelled antibodies. This different in the square wave voltammogram related to reaction occurred between the analytes with the labelled antibodies as the similarity in the structure of the estradiol and progesterone as shown in Table 2-5, which can be affected. In addition, this technique depends on the movement of the electron between the antibody and the surface, for that the progesterone and estradiol are semi polar, which means they can interact with ferrocen particles that can be speared in over the antibody. As result of the interaction the movement of electron would effected which cases the massive variation between the voltammgram of the blank and the voltammgram of the sample, while this not happened with benzo (a) pyrene that

is completely non – polar. According to these results, this technique would not suitable to apply in this project. In addition, the real sample water (river water) will not apply to this system.

4.5 Conclusion

In this chapter, the methods of immobilising the antibody onto solid support surface were discussed. Firstly, the optimisation of the chemiluminescence reagent was investigated in order to find out the optimum concentration which were 20 mM for H_2O_2 and 10 mM for luminol while 10 µg mL^{-1} for HRP.

The chemical silanisation were carried out for glass surface by using APTMS and GPTMS, where the measurement of the contact angle of the surface was the method used to confirm the changing in the surface of the glass. The immobilisation of the antibody on the two different modified glass surface was evaluated by chemiluminescence detection. The result obtained in this experiment showed the poor reproducibility of immobilisation the antibody on two types of silanised glass. Many factors effected on the silansation procedure for example temperature, pH, humidity and additional step using enzyme as catalyst for competitive immunoassay that make the control of it very hard. Also the antibody orientation play many role in this step, because in this procedure it not depend on control of the antibody orientation which make the antibody could immobilise from any part as explain in Figure 1-15.

An alternative method was used to overcome the drawbacks of chemical silanisation based on modified the ITO electrode by electrochemistry technique and modified the antibody with ferrocene; this method showed high reproducibility which makes it for useful to combine with the microfluidic device.

The square wave voltammetry technique which based on the same method of immobilised the antibody was used as detection method for the organic pollutants. This technique (SWV) was achieved LOD at 7.69, 0.69 and 0.255 pg mL^{-1} for estradiol, progesterone and benzo (a) pyrene respectively, which it showed high sensitive with labelled antibody. However, this detection faced difficulties with the interference experiments, especially in case of progesterone and estradiol, for that this technique would not be used to measuring river water sample. In addition, this detection technique required special desgine of microfluidic system to insert the electrodes inside the chip which make the designe of chip very complicated and required extra steps. All of this will make the SWV as detection commensurate with the objective of this project.

Chapter 5. Organic pollutants detection

In the previous chapter, the successfully and reproduction method of immobilising the labelled antibody with ferrocen onto modified ITO electrode was demonstrated. Also, the square wave voltammetry detection showed high sensitivity to determination of organic pollutants by measuring the change in current, where it achieved very low LOD concentration for the analytes (0.2 – 7 pg mL^{-1}). However, this detection has disadvantage with analysis the mixture in the same times as described in Section 4.4.4. For that, another detection technique would use to achieve the target of this project.

The chemiluminescence immunoassay method was selected as an alternative detection method for motoring the mixture of organic compounds and combine it with microfluidic device system as shown in this chapter. Following work in this chapter, the antibodies tagged with ferrocene, where the ferrocen would oxidise to use as catalyst for chemiluminescence reaction instant of use enzyme HRP, which led to reduce the cost.

Results obtained from two different design of the microfluidic devices that used in this work will discuss and show the ability to combine it with TMOS – C_{18} silica monolith and ITO electrode.

5.1 Oxidation of labelled ferrocene on the antibody

The ferrocene was acted as a catalyst for chemiluminescence reaction with luminol and H_2O_2 by Wilson *et al.* through oxidised the ferrocene tags on the antibody by cyclic voltammetry [239]. The ferrocene tagged was chosen to carry out with chemiluminescence detection instead of expensive HRP reagent. In this case, the oxidised ferrocene that labelled the antibody van be producing a huge CL emission signal due to the oxidised ferrocene react with luminol with H_2O_2 that generation the light without add any enzyme.

While adding the analyte to the antibody binding would occur with an antibody that blocking the ferrocene moieties.

Before analysis, the ferrocene tags had to be oxidised as described in section 2.7.9. The linear sweep voltammogram of oxidation the ferrocene tag is shown in Figure 5-1 with the cyclic voltammetry scans starting at 0.05 V with a sweep to 0.8 V without return at 0.01 V s^{-1}. After completion of this process, the entire ferrocene group should be oxidised on the ITO electrode surface as shown in Figure 5-2.

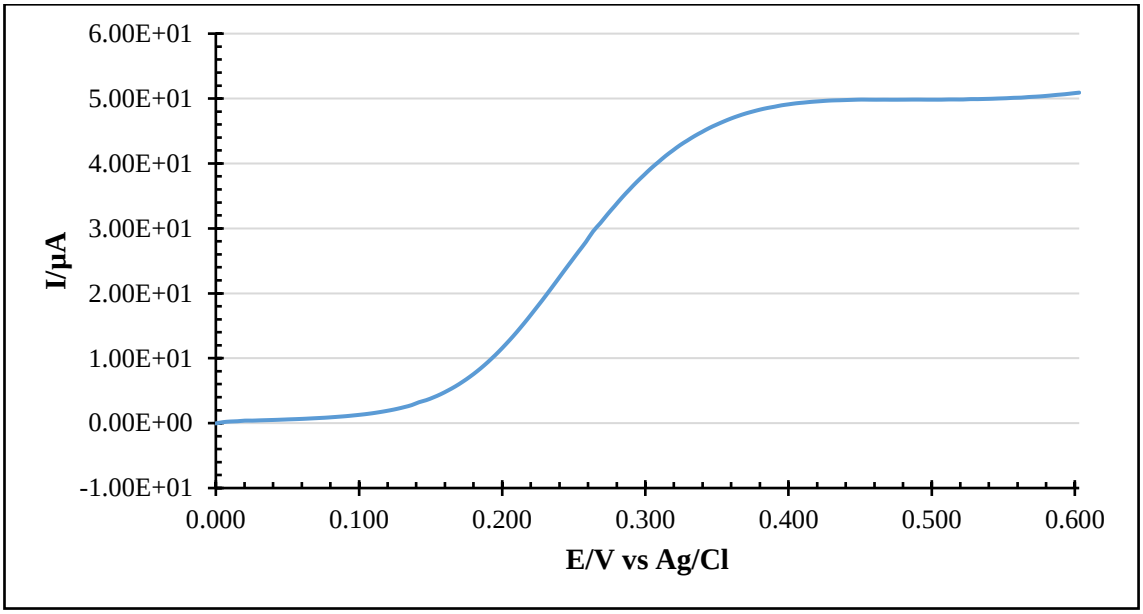

Figure 5-1: cyclic voltammogram of ferrocene labelled of antibody oxidisation at the scan rate of 10 mV s^{-1}.

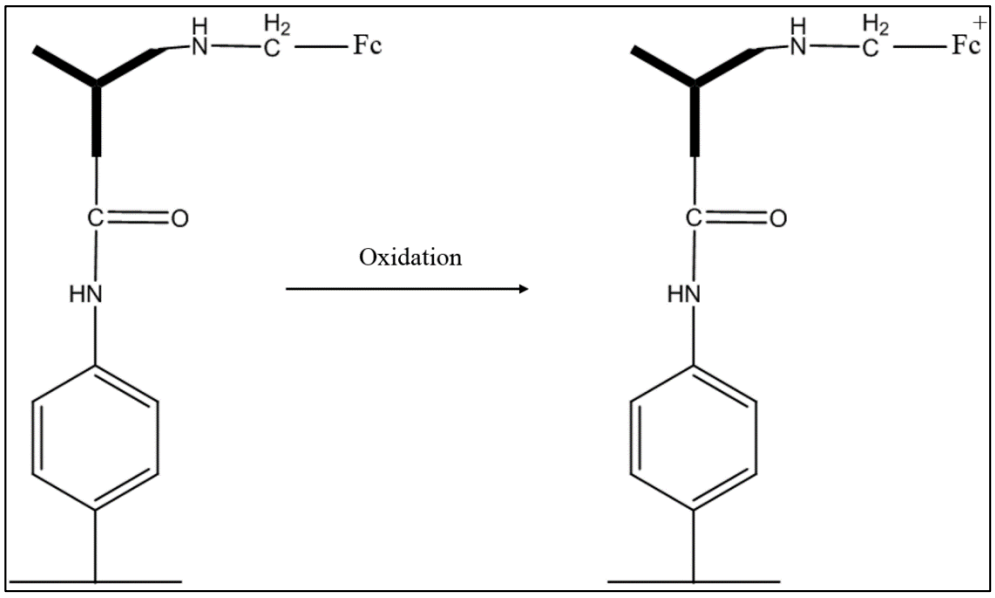

Figure 5-2: Oxidation process of the ferrocene labelled of antibody.

After completed the oxidised step, the ITO electrode washed with PBS buffer and took place for the chemiluminescence reaction with luminol and H_2O_2. The chemiluminescence signal was determined using a Charge – Coupled Device camera (CCD) and ImageJ software to analysis the image, where the exposure time was set at 100 s. The example of an image that observed for the reaction of the luminol and H_2O_2 with labelled anti – progesterone immobilised onto ITO surface is shown in Figure 5-3.

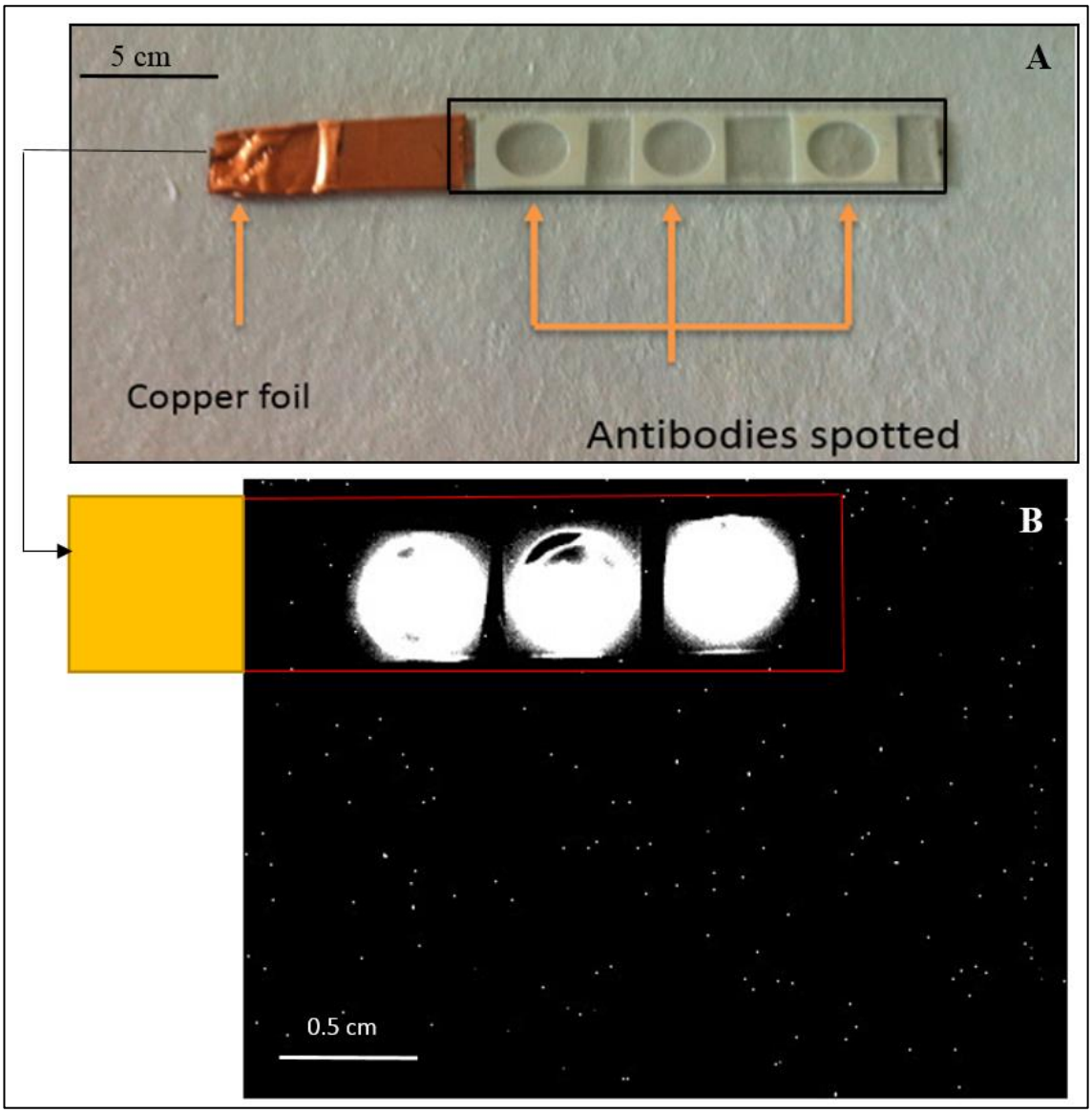

Figure 5-3: (A) ITO electrode prepared with copper foil and separate for three places by circle adhesive tape for immobilisation the labelled antibody, (B) image of chemiluminescence emission light from the places of immobilised anti – progesterone upon addition of luminol and H_2O_2.

Figure 5-3 shows three spots of labelled antibody on the ITO electrode at the same concentration. The intensity of light generated by labelled antibody reaction was comparable for each spot, with the average of CL emission signal being 245 ± 4.7 RLU Relative Light Unit). This experiment gave a strong indication that the labelled antibodies were effectively immobilised on the ITO surface and even after washing with PBS, there was not any spreading occurring from the spot area. In order to investigate the reproducibility and effectiveness of immobilisation the labelled antibody on the ITO

electrode surface, this experiment was repeated many time (n=4). The reproducibility within and between individual electrodes were investigated with four electrodes, where the results are present in Table 5-1.

Table 5-1: Precision of immobilisation of labelled antibody on the ITO electrode surface.

Within electrode	Spot 1 RLU	Spot 2 RLU	Spot 3 RLU	Average ± STD	RSD %
Electrode1	248.24	247.9	230.41	242.18 ± 10.19	4.21
Electrode 2	235.27	230.5	228.7	231.49 ± 3.41	1.47
Electrode 3	213.21	215.74	214.98	214.64 ± 1.31	4.82
Electrode 4	210.27	211.84	219.3	225.53 ± 4.82	2.26
Total of electrode				225.53 ± 4.93	2.14

Table 5-1 shows the data obtained for the RSD % measurements on the same electrode were between 1.47 and 4.82. These results proved the immobilisation protocol showed high reproducibility for the same electrode. When comparing between electrodes, the RSD % was 4.38 for the same immobilisation procedure for antibodies. Consequently, this method was effective and reproducible both for the same electrode, also between electrodes.

5.1.1 Evaluated the stability of ferrocene tags

If developing a portable system, the immobilisation process and the oxidation of the ferrocene would be carried out and then the electrode would be store ready for use. Therefore, it was important to know the stability of the antibody after completion of the oxidation of ferrocene cation. Chemiluminescence emission measurements were carried

out on the same ITO electrode over a few days as described in section 2.7.12. The initial measurement was made before oxidation of the ferrocene tags, and immediately after completion of the oxidation step. The third measurement was then carried out 1 day after the oxidation process and finally a measurement was made of the same electrode 3 days after the ferrocene tag was oxidised. After of every measurement the ITO electrode was washed with PBS buffer and stored in PBS at 4 °C. All the chemiluminescence images are presented in Figure 5-4.

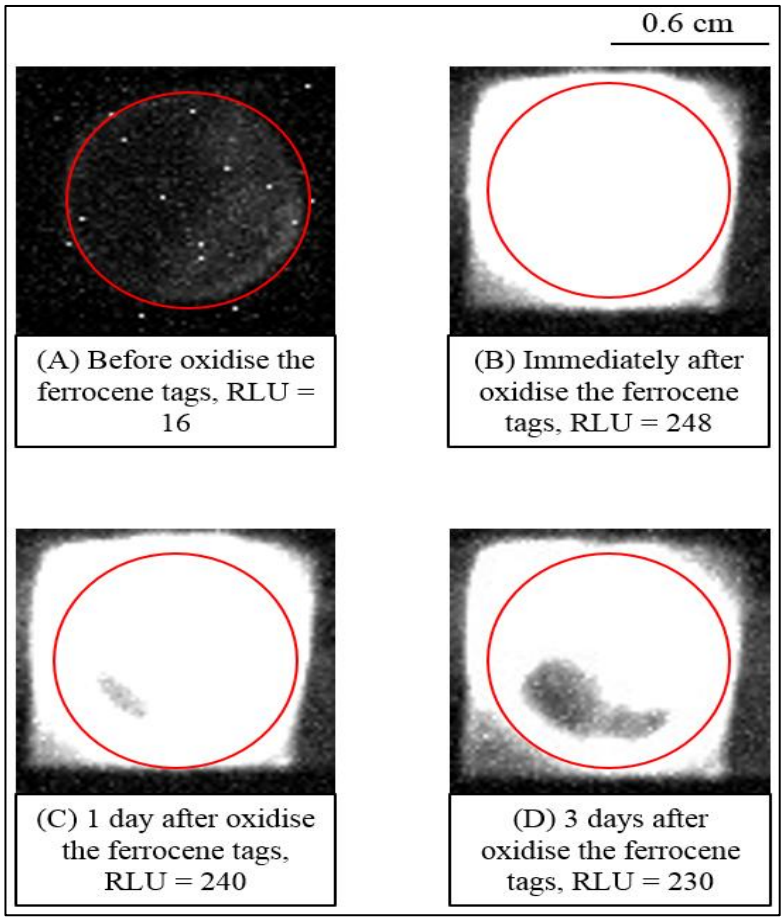

Figure 5-4: chemiluminescence image for anti – progesterone, where (A) represent the ferrocene labelled antibody, (B) immediate after oxidised the ferrocene, (C) after 1 day of oxidised the ferrocene and (D) after 3 days of oxidised the ferrocene.

In Figure 5-4 (A) before oxidation shows no CL emission signal would be expected, (B) showed the emission after oxidation of ferrocene tags, while (C) shows the CL image after one-day storage in PBS, and image (D) after three days. These results show an excellent stability for the ferrocene oxidation with the CL emission signal just decreasing

slightly. In addition, the system would always need to calibrate the method would be suitable for use with the microfluidic system, which requires the simplest process with minimum steps of reaction at the time of measurement.

5.1.2 Chemiluminescence detection of analytes

The next step was to investigate the effect of the antigen concentration on CL emission signal. Following the process explained in section 2.7.13 and the result shown in Figure 5-5 were obtained.

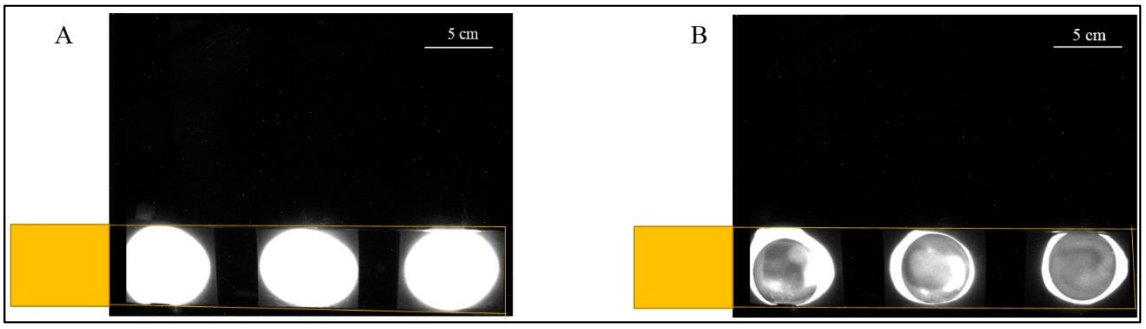

Figure 5-5: chemiluminescence image for immobilised anti - progesterone onto ITO electrode upon addition of luminol and H_2O_2 (A) blank, (B) 100 ng mL^{-1} of progesterone.

Figure 5-5 (A) is blank without progesterone were three clear intense CL images are seen. In Figure 5-5 (B) the progesterone has been added, and the intensity of the emitted light is clearly seen to be reduced (B). The CL emission signal for the blank electrodes was 245 ± 1.85 RLU, while the average of RLU for the electrode with progesterone was decreased to 90 ± 7.4. These decreased in the intensity of light was compatible with the decrease in current in the previous chapter. In a similar manner increasing the concentration of analyte led to a reduction signal as the environment, surrounding the ferrocene tags has been blocked due to the antibody and antigen reaction.

5.1.3 Optimise the incubation time of antibody antigen interaction

The time of analysis is a vital factor in all the analysis process particularly at the point of care testing where there needs to be a balance between a short time and good sensitivity. For that, the incubation time needed to complete the antibody antigen reaction was studied. The experiment of influence the incubation time on immunoassay were carried out at room temperature in the range 15 to 60 min, where the concentration of the progesterone was 1 µg mL^{-1}.

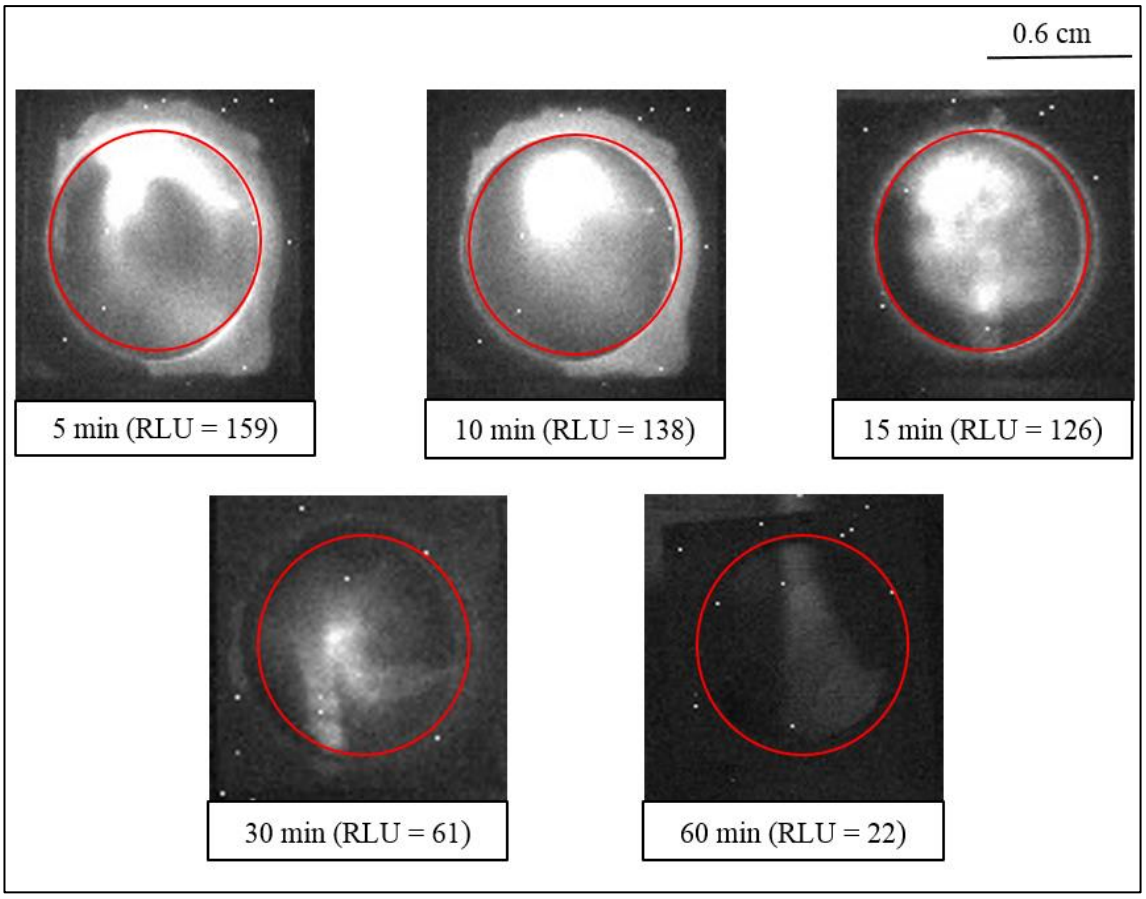

Figure 5-6: Example of chemiluminescence image for anti - progesterone and 1 µg mL^{-1} of progesterone reaction at different incubation times at room temperature.

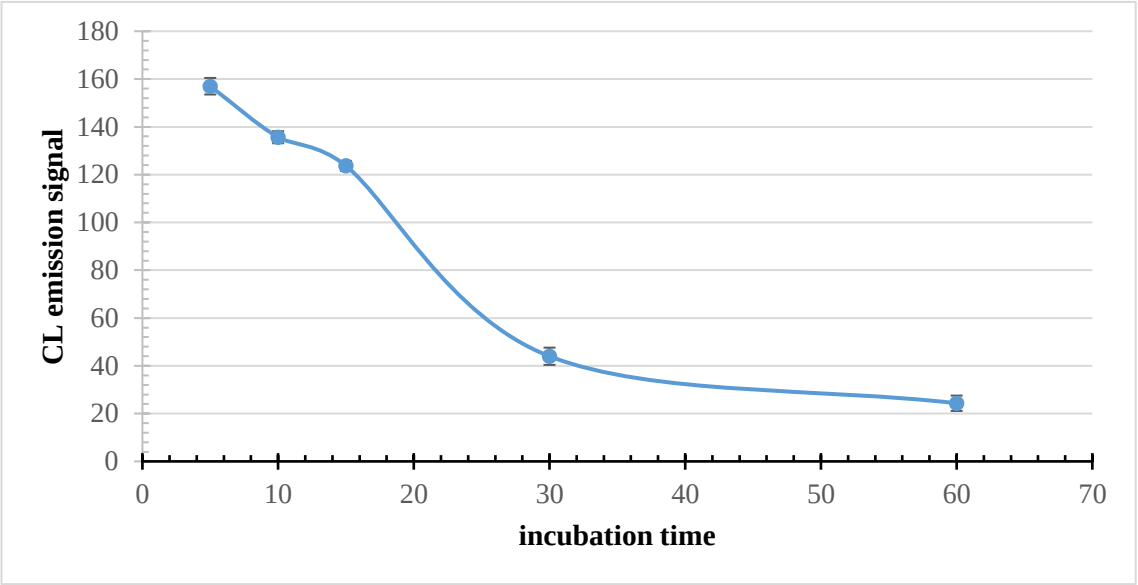

Figure 5-7: The graph shows the influence of the incubation time for anti – progesterone and 1 µg mL $^{-1}$ progesterone interaction on the chemiluminescence intensity (RLU), (n = 3). The error bar indicates one standard deviation.

Figure 5-6 shows the image for the CL spots, and it can clearly be seen that the intensity decrease as the time increase. The CL emission intensity is plotted versus incubation time in Figure 5-7. The lowest CL emission was seen at 60 and 30 min as before the electrochemical measurement. Again, the difference between 30 and 60 min was not great so an incubation time of 30 min was sufficient for antibody-antigen interaction and was chosen for the subsequent experiments.

5.1.4 Optimisation the exposure time

The exposure time was investigated to find out the optimum condition for the analysis process with the chemiluminescence immunoassay technique. Exposure time is the required time of an image is taken to obtain the highest chemiluminesence signal. Consequently the chemiluminescence was investigated over different exposure times ranging between 100 s and 850 s. Figure 5-8 represents the variance in the chemiluminescence signal observed as the exposure time changes.

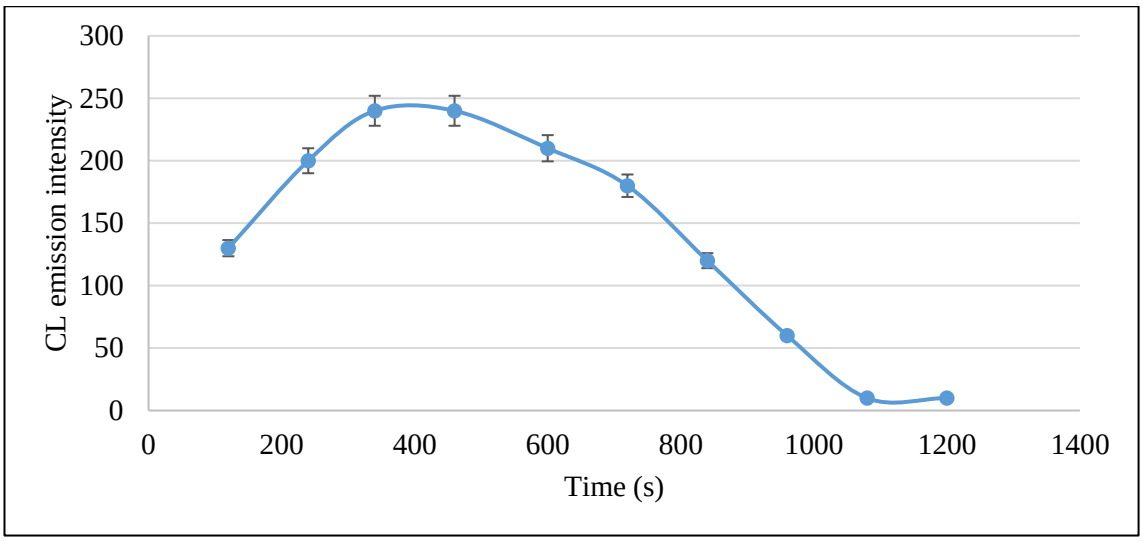

Figure 5-8: Graph of the influence of exposure time of the image taken to get the CL emission intensity, (n = 3). The error bar indicates one standard deviation.

Figure 5-8 shows that an exposure time of 200 S provided the highest value of RLU which is a short time and thus appropriate for the development of the microfluidic analysis system and steady at the same intensity until 400 S. The light signal stated to decrease after 400 S, and this is because of the chemical reaction having completed and concluded while an image is still being taken.

5.1.5 Interference studies for the analyte

As for the electrochemical measurements an interference considered was carried where three different of labelled antibody (anti- benzo (a) pyrene, anti – estradiol and anti – progesterone) were immobilised sequentially on the same ITO electrode as described in section 2.7.11.

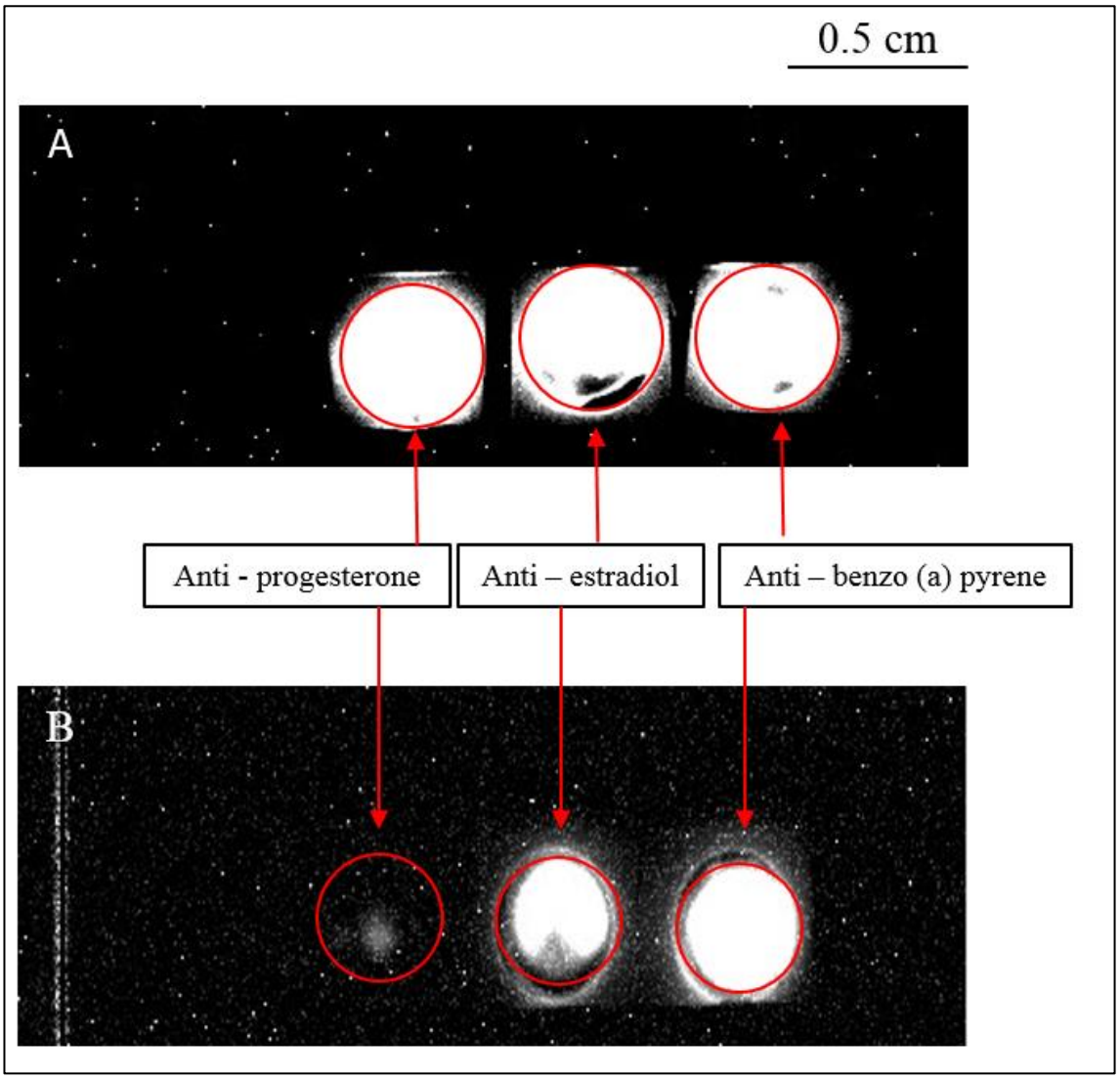

Figure 5-9: Example of interference study of the effect of 100 ng mL $^{-1}$ progesterone on chemiluminescence signal of three different antibodies, (A) is showed the blank of the ITO electrode where the each spot present different type of antibody, and (B) showed the effected of added the analyte (progesterone 100 ng mL^{-1}) onto three spots.

The results for the addition of progesterone (100 ng mL^{-1}) shown in Figure 5-9. With (A) being the image before addition of the 100 ng mL^{-1} standard and (B) the image afterwards. The effect of the progesterone standard on the anti – progesterone is clear to see where the chemiluminescence emission signal was significantly decreased which means the progesterone was completely joined with anti - progesterone. The spot for anti – benzo (a) pyrene was not effect at all, while the anti – estradiol spots was slightly affected.

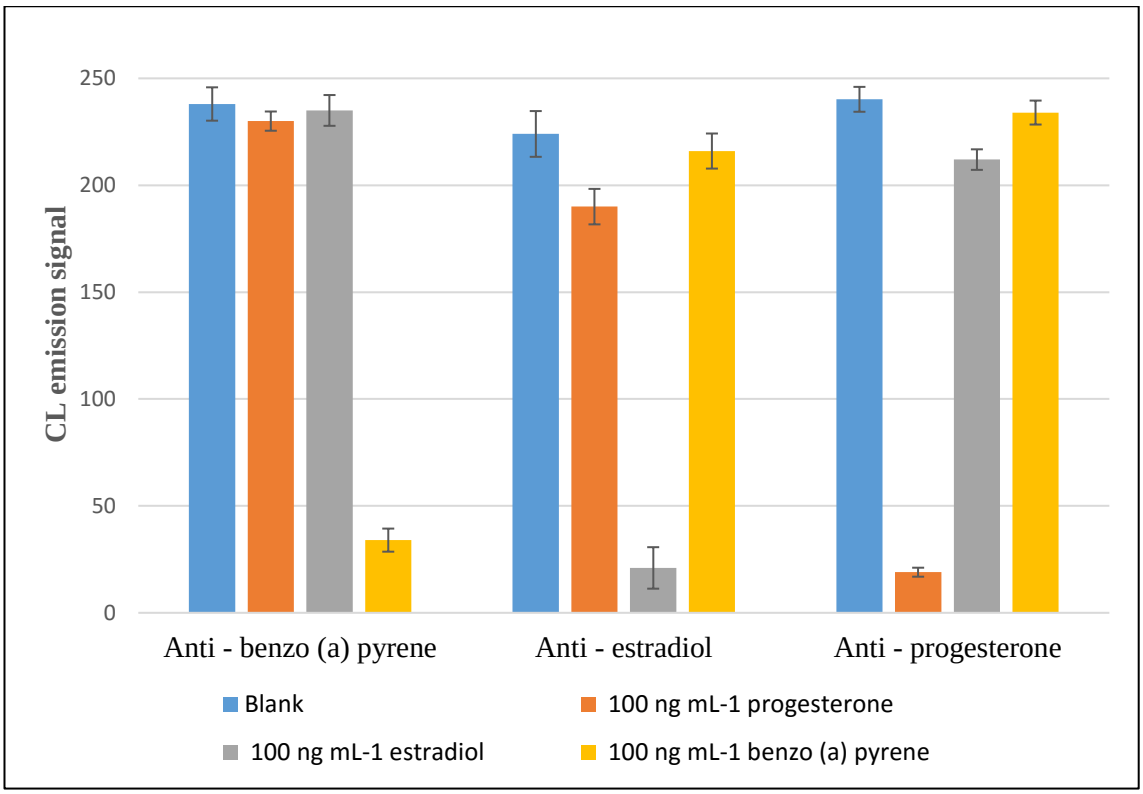

Figure 5-10: Results of CL emission signal for cross – reactivity investigated for each antibody, where the blue bar present the blank, the orange bar present the effect of progesterone standard, the grey bar show the effect of estradiol standard and the yellow bar present the influence of the benzo (a) pyrene standard. The error bar indicates one standard deviation.

According to the results shown in Figure 5-10, the CL emission for anti – benzo (a) pyrene was not effect at all with progesterone and estradiol standards. The CL emission for anti – progesterone was not affected by benzo (a) pyrene standard, but it was slightly effected by estradiol. For anti – estradiol the RLU was slightly effect with progesterone, while with benzo (a) pyrene was no affect. To conclude this experiments, the results obtained gives an indication the interference effected for analytes with three types of antibody can be acceptable if compared with the results of interference with using the electrochemical technique (SWV) that discussed in section 4.5.3 which showed in Figure 4-26, Figure 4-27 and Figure 4-28. The interference study shows high ability of chemluminescence to determine the mixture of organic compound rather than (SWV), and this refer to the principle of CL and SWV working. In case of SWV it depend of movement the electron

from antibody to the electrode surface to complete the electrochemical circle, so when the analyte add to the antibody the possibility of the interaction occur between the analyte and the labelled ferrocene particles is high especially with polar or semi polar compounds which are in this study progesterone and estrdiol. While in case of the CL, the principle of it depend on the interaction between the CL reagent and the catalyst (ferrocene) so the linking between the antibody and the analyte will not effect on this reaction.

5.2 Calibration curve for each analyte by chemiluminescence immunoassay technique.

As described in chapter 3 the analytes from the river water sample would be pre – concentrated on C_{18} modified silica monolith column and to achieve the target of this project the SPE would couple with the chemiluminescence immunoassay. The coupling between two tecqniue would be on – line through the microfluidic device. The target of this system is enhance the sensitivity and selectivity of the analysis process due to the concentration of the estradiol and progesterone in environmental water sample very low (1 ng L^{-1})[229].

Calibration curves were obtained to determine benzo (a) pyrene, estradiol and progesterone fractions after completion of analysis process with chemiluminescence immunoassay. A set of benzo (a) pyrene, estradiol and progesterone standards solution were prepared at concentrations of 100, 10, 1, 0.1, 0.05 pg. mL^{-1} and analysed using the chemiluminescence immunoassay described in section 2.7.14.

The standard solutions of each analyte were spotted onto second and third spots while the first spot was used as a blank reference to improve the precision of the measurements. The average CL emission signal for the second and third spots were subtracted from that of the first spot. The variance of CL emission signal in RLU (Δ CL emission signal)

between the sample and the blank spots were plot against the concentration of each analyte as shown in Figure 5-11.

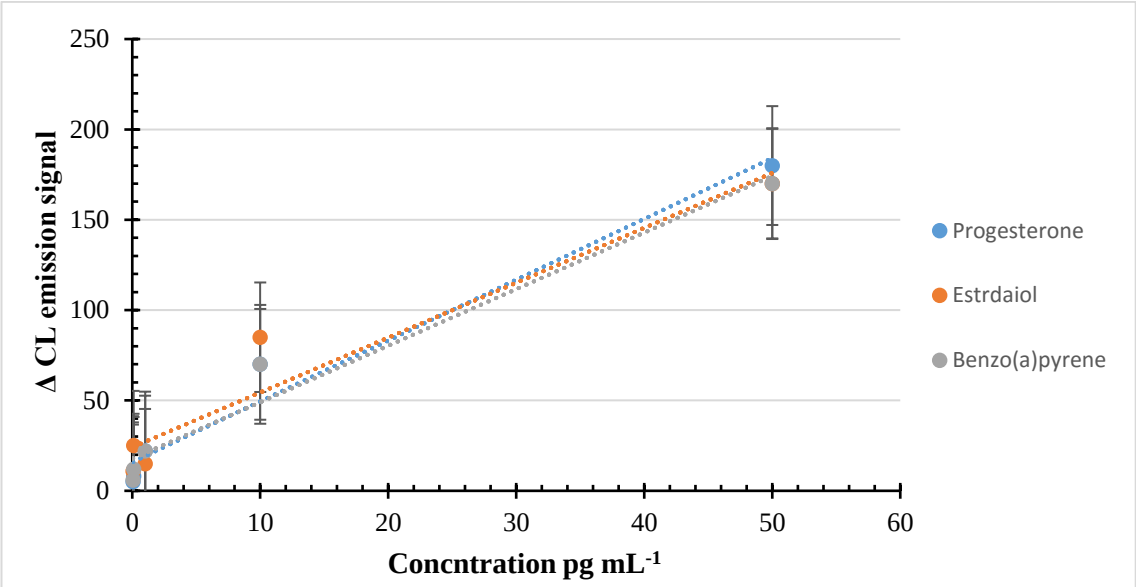

Figure 5-11: CL immunoassay calibration curves for benzo (a) pyrene (yellow line), estradiol (blue line) and progesterone (grey line) for concentration ranges from 100 to 0.05 pg mL^{-1}. The error bar indicates one standard deviation.

The figures of merit obtained from the calibration curve for each analyte are present in Table 5-3 where the Equation 2-3, Equation 2-4, and Equation 2-5 were use in these calculations.

Table 5-2: Analytical figures of merit for estradiol, progesterone and benzo (a) pyrene by using chemiluminescence immunoassay detection.

Analyte	LOD (pg mL^{-1})	LLOQ (pg mL^{-1})	Linearity	Correlation coefficient (R^2)
Estradiol	20.5	68.33	Y= 3.0357 x + 24.073	0.93
Progesterone	12.95	43.16	Y= 3.3659 x + 15.837	0.97
Benzo (a) pyrene	13.97	46.56	Y= 3.31293 x + 17.728	0.96

The LODs for progesterone and benzo (a) pyrene were of similar values at 12.95 and 13.97 pg mL^{-1} respectively, while the LOD for estradiol was a little higher value at 20.5 pg mL^{-1}. This LOD values will be adequate for river water analysis after completion of the pre – concentration step as discussed in section 3.4.3.

5.3 Development of pre – concentrate the analytes from a river water sample followed by CL immunoassay

As explained in section 3.5.4, the SPE is a major step for environmental pollutants analysis to separate of the analytes from the matrix in the sample. The matrix of the environmental sample can lead to an influence of the selectivity of the immunoassay method by causing non – specific hydrophobic interaction with the antibody [42]. To examine the whole process developed; so far before combined with the microfluidic system, this investigation was carried out by pre – concentrate the analytes from river water sample. Initially, the 100 mL of river water sample was spiked with 1 pg mL^{-1} of each analyte (benzo (a) pyrene, progesterone and estradiol) then it loaded into the C_{18} TMOS monolith column at a flow rate 900 µL min^{-1}. The washing step was carry out with 1 mL of distilled water, and 1 mL of acetonitrile injected for elution and the fraction was collected and added to the ITO electrode that contains three spots each one with a different type of labelled antibody. After 30 min, the electrode was wash to remove unbound analytes and finally, analysed by chemiluminescence. This step was repeat four times and the Δ CL emission signal was calculate as previously described. Figure 5-12 shows the CL emission image for ITO electrode, where (A) was blank (antibody + CL reagent) and (B) after addition of the elution fraction from the SPE.

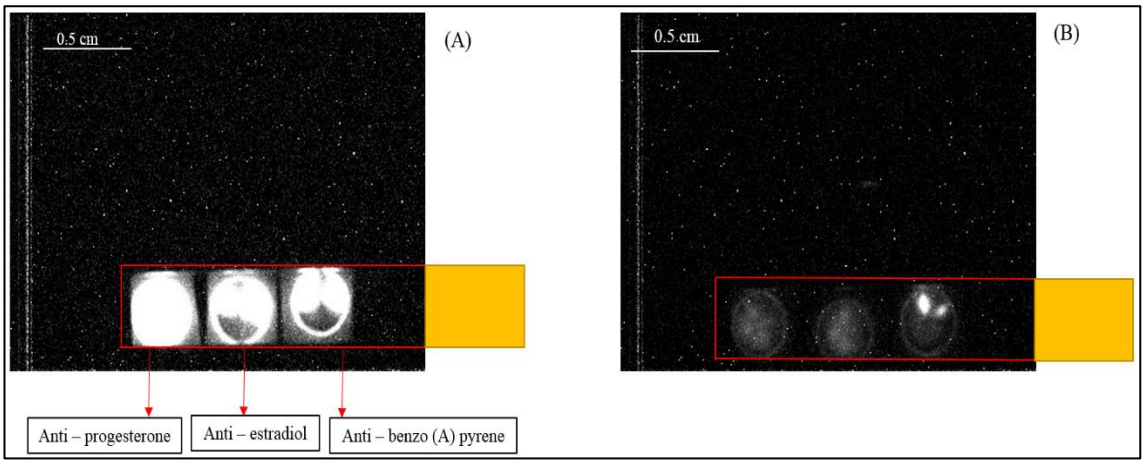

Figure 5-12: chemiluminescence image of (A) blank ITO electrode and (B) the same ITO electrode after addition of the SPE elution fraction.

Figure 5-12 shows the CL emission intensity for the blank in (A). (B) Shows that the signal has decreased significantly after addition of the elute fraction from the SPE pre – concentration step onto the spots of antibodies. The change in CL emission intensity obtained shown in Table 5-4. The calibration curves in Table 5-3 were used to calculate the concentration of each analyte.

Table 5-3: The Δ CL emission intensity value and the concentration of three analytes that spiked with river water at concentration 1 pg mL^{-1} and pre – concentrated by using C18 TMOS monolith column

Analyte	Δ CL emission intensity value after substrate from the blank, ± RSD % (n = 4)	Concentration pg mL^{-1}
Progesterone	59.23 ± 14.5	49
Estradiol	60.43 ± 11.4	42
Benzo (a) pyrene	81 ± 7.9	32

Table 5-4 shows that the concentration of progesterone and estradiol were increased from 1 pg mL^{-1} to 49 and 42 pg mL^{-1} respectively, after pre – concentrated the river water sample with the C_{18} TMOS. In addition, the concentration of benzo (a) pyrene was increased to 32 pg mL^{-1}. Therefore, this step provides the ability of the C_{18} TMOS monolith column to pre – concentrate the mixture of organic chemical pollutants at a very low concentration as discussed in section 3.5.3. All the concentrations of the analytes were above the LODs presented in Table 5-3; thus, the methods of combining the SPE with chemiluminescence immunoassay off-chip was achieve.

5.4 Environmental pollutants analysis in chip

5.4.1 Polymer chip

Once the analysis of environmental pollutants mixtures was successfully achieved using the ITO electrode for the CL immunoassay off-chip, the electrode with the immobilised antibodies were inserted into the microfluidic chip described in section 2.8.1. During the CL assay, to fill the sample chamber, the reagents of CL has flowed over the electrode at 10 µL min^{-1}. The total capacity of the sample chamber was 22 µL that was fill up at 23 min. Figure 5-13 shows the plastic chip placed under the CCD camera, before the pump the reagents into the detection chamber.

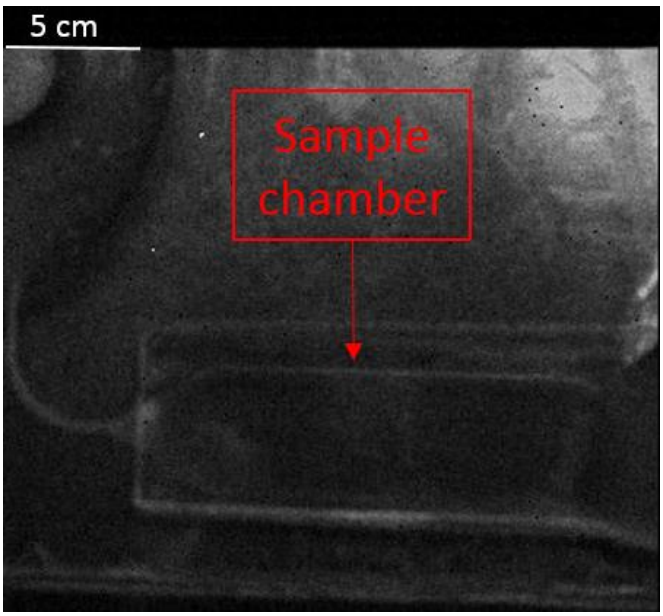

Figure 5-13: The chip was placed inside the light-proof box and under the CCD camera enclosed in a before injecting the reagents.

After that the CL reagents (1:1 ratio of 20 mM luminol and H_2O_2) was pumped into the chip, and then the flow rate was stopped after the sample chamber was filled to let the chemiluminescence reaction occur with the immobilised labelled antibody, where the result that obtained is shown in Figure 5-14.

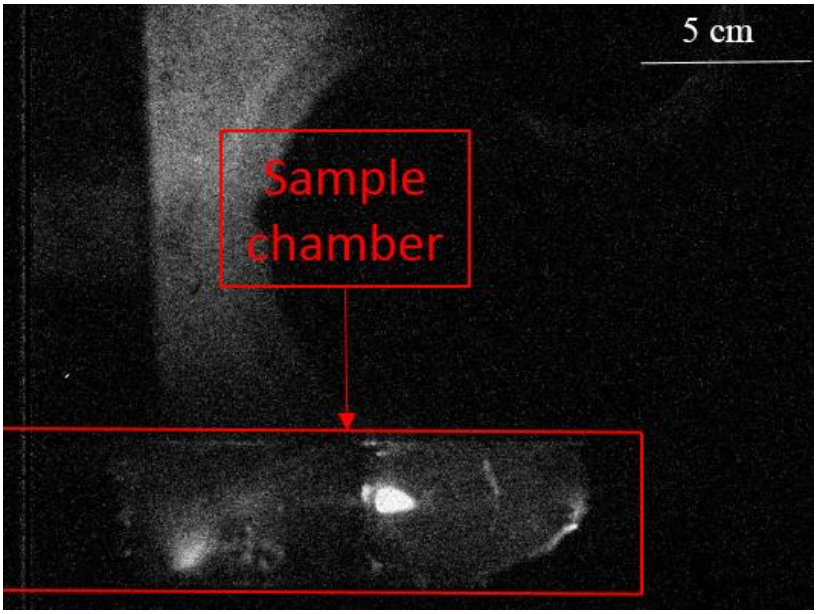

Figure 5-14: Chemiluminescence image upon addition of 20 mM luminol and H_2O_2 for immobilised anti - progesterone on the ITO electrode within the chip. The image was taken under stop –flow conditions.

As one can see in Figure 5-14, the intensity of light was low where the spot of labelled antibody was present as compared to the static system when the reagents were pipetted onto the spot. This result was not expected and could be because the immobilised antibody was scraped off during the insertion of the electrode into the chip, as it had to be a tight fit to prevent leaks. Alternatively, it was possible the concentration of chemiluminescence reagents was not sufficient for the flow system. The total of the sample chamber depth was 0.8 mm. Therefore, the volume of the reagent that contact with labelled antibody was very small, and because the depth of electrode is 0.7 mm, therefore the total volume of the CL reagent interact with labelled antibody is 13.35 µL.

To overcome this issue, the concentration of the reagents was increased to 30mM for luminol and H_2O_2. The concentration of CL reagent can be increased more but with high concentration of reagent the reaction will occur fast and this will produce N_2 gas, which led to form pupils that influence on the CCD image. The result obtained after the reagents concentration increased is present in Figure 5-15.

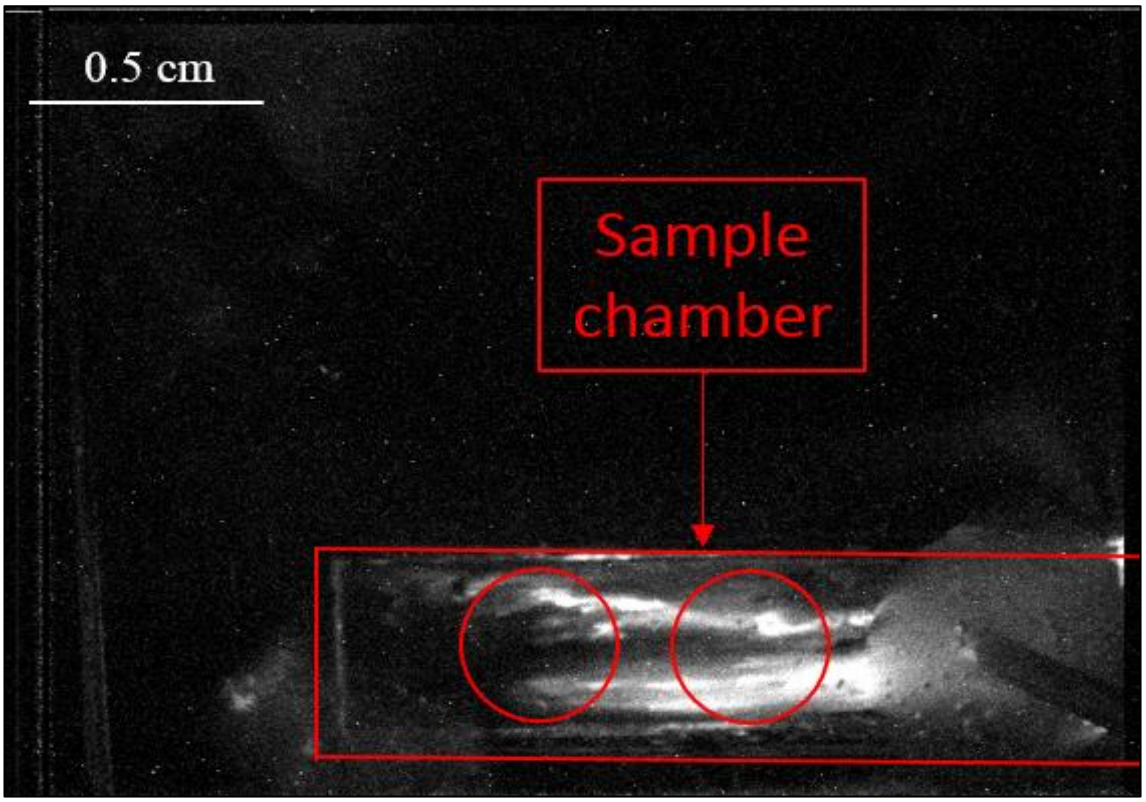

Figure 5-15: chemiluminescence image upon addition of 30 mM luminol and H2O2 for immobilised anti - progesterone on the ITO electrode within the chip. The image was taken under stop - flow conditions.

In Figure 5-15 the light emission can be seen, but it is smeared over one spot where the second spot not is recognised. These may have been due to the presence of some glue from the circular tape surround the spot or the process of inserting the electrode inside the chip that should be carried out with extra care. Moreover, the emission intensity of background increased with increasing concentration of reagents. Many repeats were made where the emission from only one spot appeared or from part of one spot while a few results showed two spots. An example where two CL emission spots were seen from the ITO electrode inside the chip are presented in Figure 5-16.

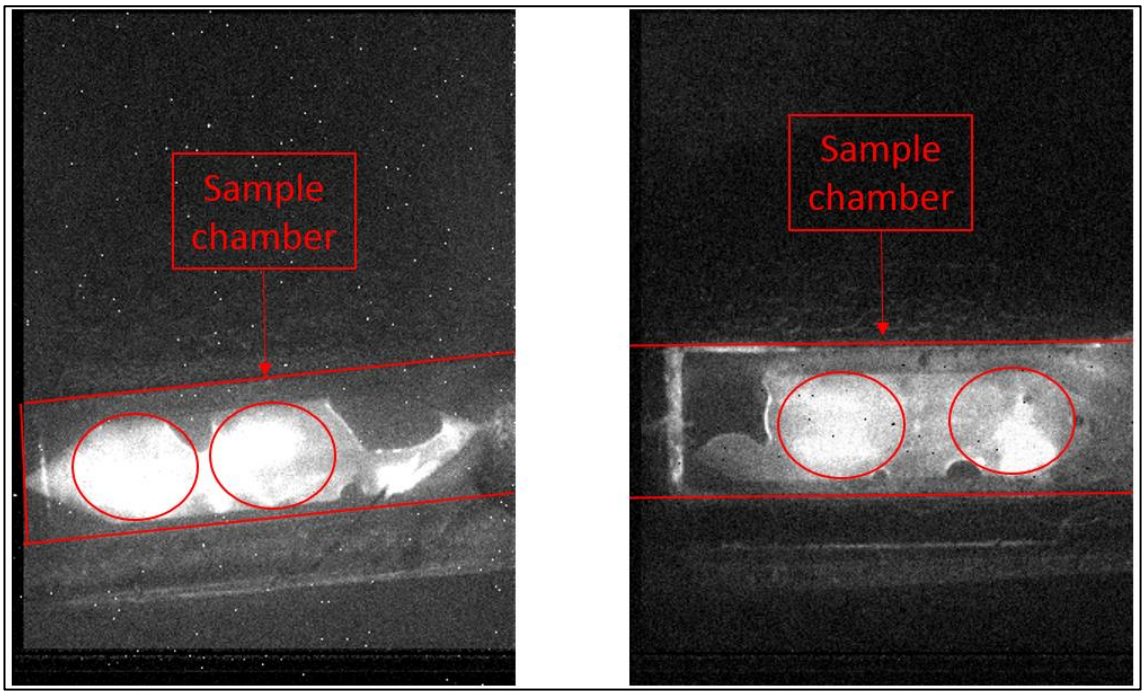

Figure 5-16: Chemiluminescence image upon addition of 30 mM luminol and H_2O_2 for immobilised anti - progesterone on the ITO electrode within the chip. The image was taken under stop – flow conditions.

Figure 5-16 shows two examples of chemiluminescence image inside the plastic chip; the CL emission can be seen over the two spots. However, the light is emitted the entire channel chamber as once the chemiluminescence reaction is catalysed hard to recognise the position of the immobilised labelled antibodies.

Using the COC polymer chip has advantages as it is easy to fabricate and cheap. However, there were many disadvantages with this design, and it was very hard to insert the ITO electrode inside the chip and if often broken and sometimes there was some glue presence on the electrode from the reinforced rings which affected the flow of the chemiluminescence over the electrode. Besides, the channel chamber just covered two spots where the third on was out of the chip, and it became obvious that this design was not suitable with the aim of this project being based on analysis three different types of environmental pollutants.

5.4.2 Glass chip

To overcome the problems faced with cyclic olefin copolymer (COC) polymer chip, a new design of glass chip was fabricated as shown in Figure 2-11. In this design, the ITO electrode was cut to fit inside the channel chamber as explained in section 2.8.2.2. The three different labelled antibodies were immobilised onto the cut electrode and the electrode aligned under the CCD camera to image the chemiluminescence emission under the same condition explained in section 4.1.1.

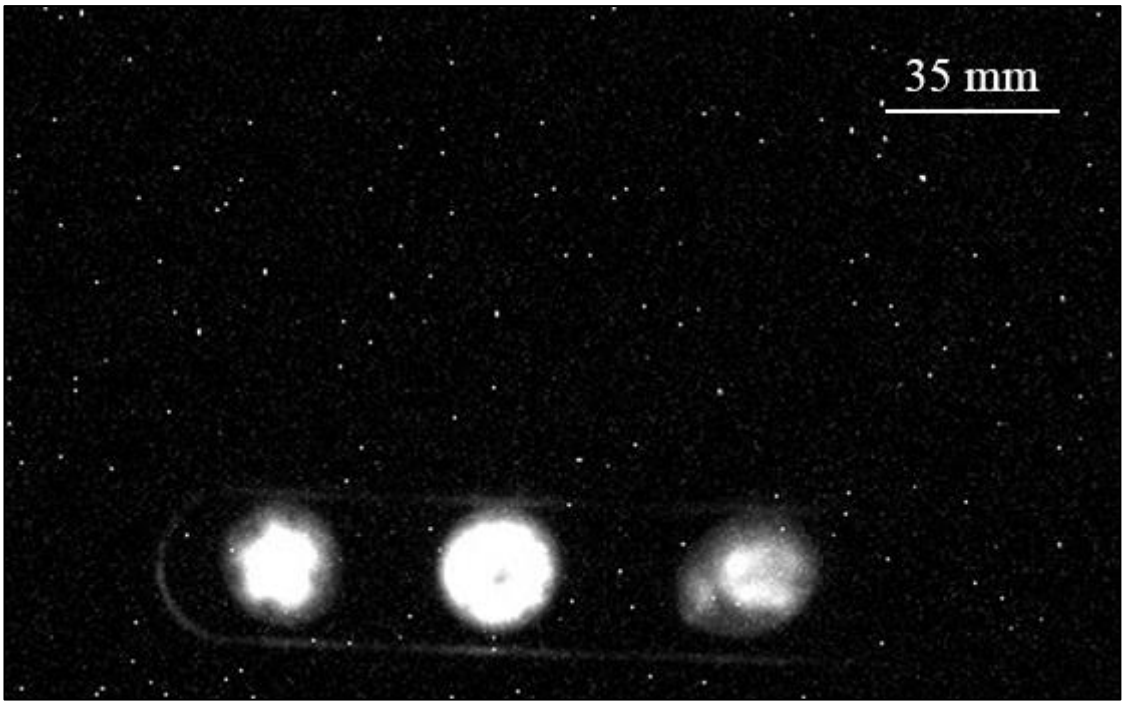

Figure 5-17: chemiluminescence image upon addition of 20 mM luminol and H_2O_2 for three immobilised antibodies on the cut ITO electrode.

Figure 5-17 shows that the reshaping process did not affect the ITO electrode. After that, the ITO electrode was placed inside the chip as described in section 2.8.2.3, and aligned under the CCD camera to examine the chemiluminescence reaction over the electrode. The chemiluminescence reagents were pumped into the chip at flow rate 10 µL min^{-1}until the channel chamber was filled. The first image that obtained for chemiluminescence reaction inside the glass chip is presented in Figure 5-17.

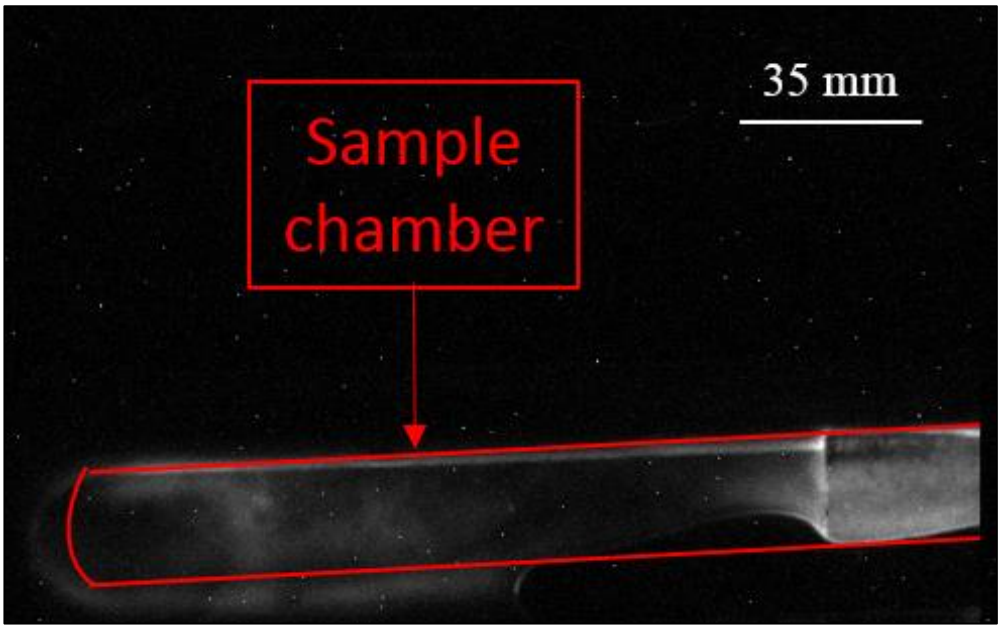

Figure 5-18: Chemiluminescence image upon addition of 20 mM luminol and H_2O_2 for immobilised three types of antibodies on the reshaped ITO electrode inside the glass chip. The image was taken under stop - flow conditions.

The intensity of the light was low where the spot of labelled antibody was present. In addition, the light was centred on the copper foil, and this affected the chemiluminescence measurement, so the concentration of chemiluminescence reagents were increased to 30 mM. This step was repeated many times, and the copper foil was removed in case the copper was catalysing the reaction, and the concentration of chemiluminescence reagents was increased. An example of the CL image obtained from the electrode inside the glass chip is presented in Figure 5-19.

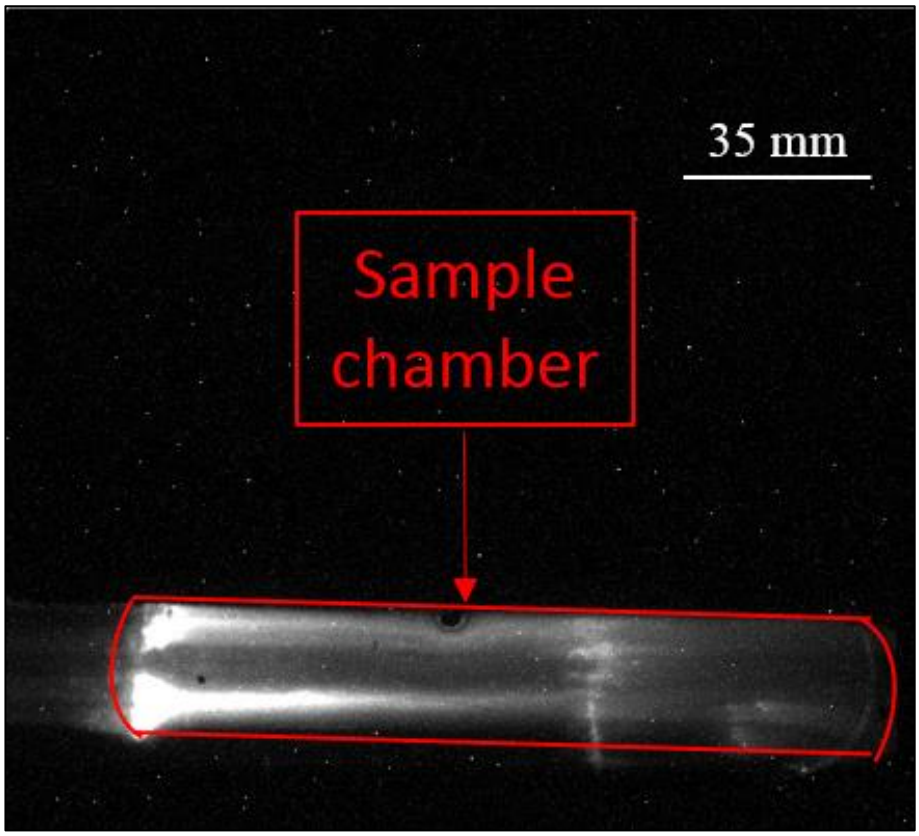

Figure 5-19: Chemiluminescence image upon addition of 30 mM luminol and H_2O_2 for immobilised three types of antibodies on the reshaped ITO electrode inside the glass chip. The image was taken under stop - flow conditions.

Figure 5-19 shows the light at the end of the sample chamber with high intensity, while the rest of light was spread over the electrode, which makes impossible to measure the CL emission intensity for each spot. Although these results look promising, the chip design must be improved to improve the precision and to facilitate detection of each spot. It would help if the depth of the sample chamber increased to allow more volume of the chemiluminescence reagents to cover the electrode. Also instead of having long sample chamber with one inlet it should be replaced with three separate inlets or one inlet branched to three paths which make the reagents come for each spot, where the main problem was with another two design is the interference of the reagents.

5.5 Conclusion

In the chapter the stability of the labelled antibody onto the ITO electrode was evaluated, which showed high stability after oxidation, the ferrocene antibody labelled over three days. In addition, the incubation time and exposure time were investigated, where the incubation time selected to set up at 30 min and the optimum time for exposure was at 200 s. The studies of interference for each type of antibodies shows ineffectual with mixture analyte.

Many different methods based on the immunoassay technique have been applied to detect this analytes and achieved very low LOD, but all of this methods required complicated procedure and consume time. As example of that, Meng *et al.*[240] reported on analysis the benzo (a) pyrene based on the competitive ELISA and LOD of this method was 5.3 pg mL^{-1}. While in the case of progesterone and estradiol, Gaikwad *et al.*[100c] have determined these hormones separately in fish depending on competitive chemiluminescence immunoassay, and the LODs were 3 ng mL^{-1} for progesterone and 2.4 pg mL^{-1} for estradiol. In these work, the mixture of analytes has analysed at the same time, where the calibration curve for the analyte shows LOD at 20.5, 12.95 and 13.97 for estradiol, progesterone and benzo (a) pyrene respectively with a high value of the correlation coefficient which indicated this method provide a high sensitivity and selectivity. The chemiluminescence immunoassay combine with SPE was demonstrated for a mixture of environmental pollutants off – chip was shown work in river water sample. The transfer this approach to microfluidic system device looks promising, however, was not a time to complete this work in the timescale of the project.

Chapter 6. Conclusion and future work

Chemical pollutants analysis in the environmental field can suffer from high cost consume time and chemicals and use complicated techniques. The aim of this thesis was to overcome these difficulties. These were achieved by developing a system that could be portable which combined SPE using a silica monolith material coupled with electrochemical and chemiluminescence immunoassays. In order to attain this target, the research work was divided into three sections:

1. Extraction and pre-concentration of chemical pollutants (progesterone, estradiol and benzo (a) pyrene) from environmental water sample using reverse - phase (C_{18}).
2. Selection of a suitable method to immobilise the antibody to facilitate chemical pollutants detection by chemiluminescence immunoassay.
3. The combination of the SPE methodology with a CL immunoassay to detect the chemical pollutants in river water sample. The conclusions of this work are summarised and discussed in the following sections.

6.1 Development of the silica monolith for chemical pollutants extraction and pre – concentration.

The method of preparation of the inorganic silica monolith using a sol-gel method was investigated.

The internal structure of the silica monolith was found to depend on the chemical composition. Using PEO (200 K) with TMOS and TEOS to fabricate the silica monolith columns were higher surface areas were obtained at 404 ± 1.8 m^2g^{-1} and 324.10 ± 1.2 m^2g^{-1}, respectively. The surface areas obtained in this work was greater than achieved by Fletcher *et al*.[88] which was 201 and 236 m^2g^{-1} for TEOS and TMOS respectively and this

refer to increase the time of hydrothermal treatment process which was 16 hour in Fletcher method and 24 hour in this project. Some commercial SPE monoliths can provide surface area up to 800 $m^2 g^{-1}$. However, these commercial columns are usually available in a particular cartridge shape [52] and the aim of this project is fitted the SPE column inside the microfluidic device.

In fabrication, the hydrothermal treatment step with ammonia was found to be important for increasing the surface area of silica monolith by converting macropores to mesoporous [90-91]. The optimisation of the ammonia concentration, time, and temperature of the thermal decomposition step was vital. It is recommended a further study be undertaken for further increasing the total surface area, though using different type of polymer or mixed to different type of polymer. In addition, the step of the hydrothermal treatment need more study by apply different concentration and changing the time. The method of preparation the silica monolith took almost five days. Any future study would focus on reducing the time of fabrication, however; this method offered high permeability and high surface area.

6.2 Chemical pollutants extraction and pre – concentration

The performance of the silica monolith in extracting and pre - concentration of the interest chemical pollutants was evaluated. The silica monolith was modified with C_{18} for reverse - phase separation. When evaluated by HPLC the C_{18} - TMOS column achieved a high extraction and pre - concentration with recoveries for progesterone, estradiol and benzo (a) pyrene (84.79, 59.61 and 80.93 %[1]) respectively. This method provided several advantages including good selectivity of target chemical pollutants (non – polar compounds) with remove polar compounds that could be effected on the ferrocene on the antibody, and a small volume of solution in the elution step would be enough to complete the process. The total time of this step was around 1 hour.

The method has been shown to work for the extraction and pre - concentration of progesterone, estradiol and benzo (a) pyrene from an environmental water sample (a river water sample) with pre - concentration recoveries at (62.54, 50.13 and 59.51 %), respectively. The HPLC was used to evaluate the process. Continuing work would focus on the extraction and pre - concentration of additional different types of chemical pollutants from more complex environmental samples, such as soil and wastewater sample, by using C_{18} silica monoliths.

6.3 Method of immobilisation of the antibody

The primary step in a heterogeneous immunoassay detection assays is the immobilisation of antibody onto the solid support surface. The immobilisation of the antibody is difficult to achieve, many researchers have demonstrated different protocols for the chemical immobilisation procedure. The antibody orientation and the reproducibility are considered main challenges for chemical immobilisation [142, 164, 208].

Electrochemical modification method was used as discussed in section 4.3 to overcome the drawbacks of chemical methods of immobilisation the antibody onto the solid support surface such as using silane reagent APTMS and GPTMS. In this work the ferrocene labelled antibodies were immobilised onto an ITO electrode to improve and expand its application to a chemiluminescence and electrochemistry based immunoassay. The ITO electrode surface was modified by electrochemical (CV) oxidation with nitrobenzene which converted to phenylamine through electrochemical reduction (CV) to present the NH_2 group on the surface. The activation buffer of EDC and sulfo – NHS was used to immobilise the labelled antibody onto the ITO electrode surface. This method provided a high reproducibility which confirms the antibody orientation has correctly occurred on the ITO surface after modifying the antibody with the ferrocene.

The labelled antibodies with ferrocene could act as a catalyst for chemiluminescence detection. In addition, without adding secondary antibody or antigen-HRP, the reproducibility was improved. This method required a short analysis time with an incubation time of 30 min.

The ITO electrode provided strong bonds between the modified antibody and the electrode surface, with good reproducibility. Also, the electrode showed high stability for over 3 days when storage the electrode in the PBS buffer at 4 ºC before and after oxidation of the ferrocene tag, also, many measurements could be made after washing the electrode from the chemiluminescence reagents with PBS buffer.

6.4 Detection of chemical pollutants from environmental water sample

Square wave voltammetry was the first detection method selected to analyse the mixture of chemical pollutants as it provides high sensitivity, rapid analysis and simple equipment. The drawbacks with this technique was with the cross - reactivity and matrix effect were significantly seen with progesterone and estradiol that interact with ferrocene that labelled the antiboy.

Chemiluminescence was the second detection method applied in this work. This technique is a promising method for portable analysis due to its high sensitivity fast analysis and required a simple instrumentation. A rapid method for detection of the mixture of chemical pollutants has been developed which required 30 min for incubation to complete the antibody and antigen reaction. This approach was achieved using a heterogeneous immunoassay; that is needed only one-step by using the labelled antibody with ferrocene tag on the ITO electrode. Comparing with the traditional immunoassays technique which requires labelled secondary antibody or an HRP enzyme labelled antigen which could lead to increase the analysis time and reduce the reproducibility [124].

The chemiluminescence immunoassay method has been developed to shown that progesterone and estradiol and benzo (a) pyrene can all be monitored successfully off-chip. A LOD was 20.5 pg mL^{-1} and an LLOQ was 63.33 pg mL^{-1} for estradiol while with progesterone the LOD was at 12.95 pg mL^{-1} and LLOQ at 43.16 pg mL^{-1}, the LOD for benzo (A) pyrene was 13.97 pg mL^{-1} and LLOQ was 46.56 pg mL^{-1}. All this result shows the necessary for pre – concentration step to increase the concentration of the analytes in river water sample to be in the range of LOD for each analyte for CLIM technique [229].

6.5 Combine the pre – concentration method with detection of the chemical pollutants of river water.

A successful method for pre – concentration of the mixture of chemical pollutants from river water sample by C_{18} – TMOS and combine with chemiluminescence immunoassays using a small volume of sample and chemiluminescence reagents (10 µL) to complete the analysis process off-chip as explained section 5.3 was achieved in this work. The preliminary results for off-chip detection of progesterone, estradiol and benzo (a) pyrene concentrations were 49, 42 and 31.75 % respectively. These results was less than 50% of the initial concentration (1 pg mL^{-1} in 100 mL), for that the pre – concentration step required more investigation to increase the percentage of recovery through optimising the optimum flow rate at the elution step. The result obtained for off-chip step are at least comparable to those obtained in a conventional laboratory with high sensitivity and selectivity such as HPLC and GC-MS [42], but this method allows to apply for a rapid and portable device with low cost.

6.6 Microfluidic device and future work

In the work two different designs of a microfluidic chip were developed, the first design of the microfluidic device was based on an inexpensive polymer (COC). This microfluidic device system provided a much shorter analysis time (3 min) with a very low volume of both sample and reagent. Unfortunately, the results obtained with this design were highly unreproducible.

The second chip was fabricated using glass, where this design it was required to reshape the ITO electrode to be fitted inside the sample chamber. However, the result showed it difficult to recognise the specific place for each spot where the chemiluminescence emission light was covered whole the electrode.

Future work would consist of further designs of a microfluidic device that could incorporate the ITO electrode as well as giving the CL signal desired for each spot. The preliminary design for the chip is shown in Figure 6-1, where this design provides completely separate between each spot to avoid the mixing between each spot. Nevertheless, this design based on to cut the ITO electrode to a circular motion to be fitted tightly in correct place. Therefore, this design might need more development to fit the ITO electrode directly.

Figure 6-1 shows the polymer chip that will make from COC polymer, which show a high stability with, organic solvent and easy to fabrication. This design will contain to inlet for sample and CL reagents and there is mixing channel to complete the mixing of the reagent before reaching at the electrode place. Also the will be three separate channel for each analyte to be easy analysis the CL emission light, and all of this channel will combine again at the outlet.

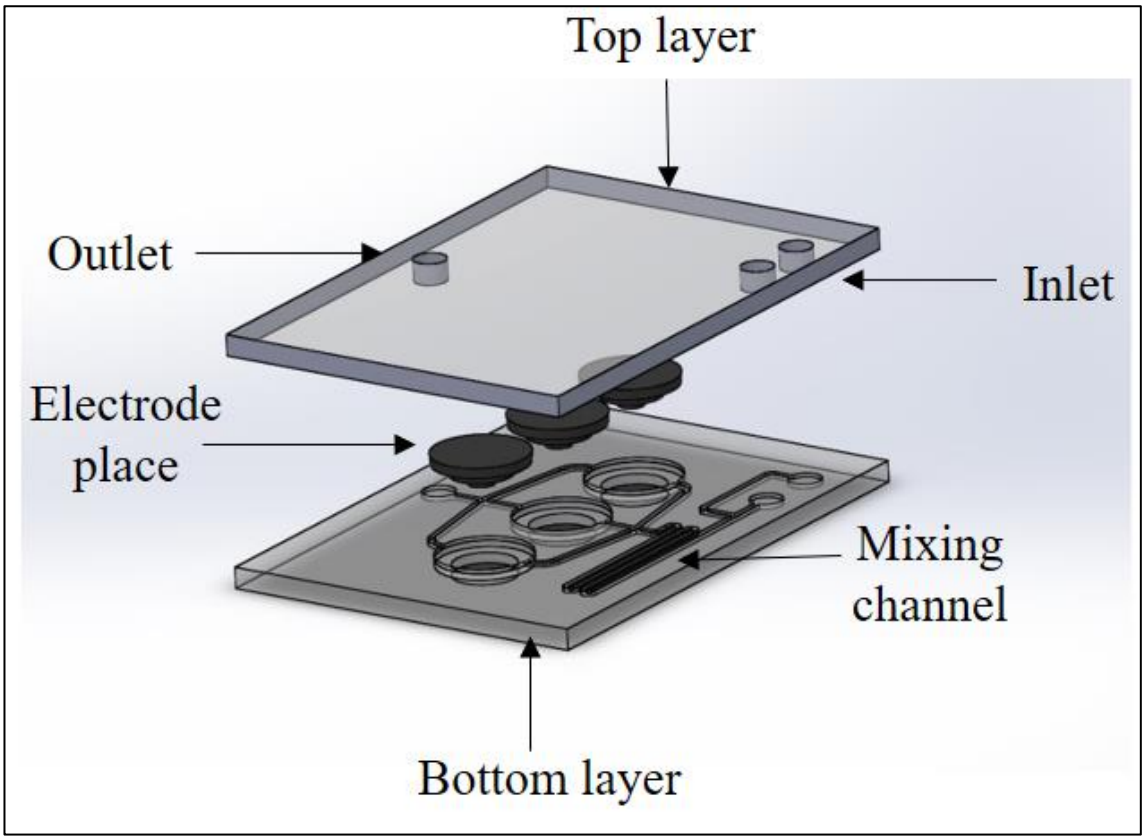

Figure 6-1: The preliminary design of the chip that will use in future work

Chapter 7. References

[1] R. O. Gilbert, *Statistical methods for environmental pollution monitoring*, John Wiley & Sons, **1987**, p.

[2] M. W. Holdgate, *A perspective of environmental pollution*, CUP Archive, **1980**, p.

[3] P. M. Vitousek, H. A. Mooney, J. Lubchenco and J. M. Melillo, *Science* **1997**, *277*, 494-499.

[4] M. K. Hill, *Understanding environmental pollution*, Cambridge University Press, **2010**, p.

[5] U. E. P. tton Agencc, **2006**.

[6] J. H. Seinfeld and S. N. Pandis, *Atmospheric chemistry and physics: from air pollution to climate change*, John Wiley & Sons, **2012**, p.

[7] J. A. Raub, M. Mathieu-Nolf, N. B. Hampson and S. R. Thom, *Toxicology* **2000**, *145*, 1-14.

[8] M. Adon, C. Galy-Lacaux, V. Yoboué, C. Delon, J. Lacaux, P. Castera, E. Gardrat, J. Pienaar, H. A. Ourabi and D. Laouali, *Atmospheric Chemistry and Physics* **2010**, *10*, 7467-7487.

[9] S. Ross, **1994**.

[10] F. R. Troeh and L. M. Thompson, *Soils and soil fertility*, Blackwell Iowa, **2005**, p.

[11] P. Patnaik, *Handbook of environmental analysis: chemical pollutants in air, water, soil, and solid wastes*, CRC Press, **2010**, p.

[12] P. F. Cooper and B. Findlater, *Constructed Wetlands in Water Pollution Control: Proceedings of the International Conference on the Use of Constructed Wetlands in Water Pollution Control, Held in Cambridge, UK, 24–28 September 1990*, Elsevier, **2013**, p.

[13] P. H. Gleick, *Pacific Institute for Studies in Dev., Environment & Security. Stockholm Env. Institute, Oxford Univ. Press. 473p* **1993**, *9*.

[14] T. H. Tietenberg and L. Lewis, *Environmental and natural resource economics*, Addison-Wesley Reading, MA, **2000**, p.

[15] R. P. Schwarzenbach, T. Egli, T. B. Hofstetter, U. Von Gunten and B. Wehrli, *Annual Review of Environment and Resources* **2010**, *35*, 109-136.

[16] D. B. Botkin, E. A. Keller and D. B. Rosenthal, *Environmental science*, Wiley, **2012**, p.

[17] V. K. Gupta, I. Ali, T. A. Saleh, A. Nayak and S. Agarwal, *Rsc Advances* **2012**, *2*, 6380-6388.

[18] P. Dugan, *Biochemical ecology of water pollution*, Springer Science & Business Media, **2012**, p.

[19] U. S. E. P. Agency, *List of Priority Pollutants* **2014**.

[20] M. Lee, *Analytical chemistry of polycyclic aromatic compounds*, Elsevier, **2012**, p.

[21] X.-T. Wang, Y. Miao, Y. Zhang, Y.-C. Li, M.-H. Wu and G. Yu, *Science of the Total Environment* **2013**, *447*, 80-89.

[22] R. Rieger and K. Müllen, *Journal of Physical Organic Chemistry* **2010**, *23*, 315-325.

[23] J. Yan, L. Wang, P. P. Fu and H. T. Yu, *Mutation Research-Genetic Toxicology and Environmental Mutagenesis* **2004**, *557*, 99-108.

[24] P. Boffetta, N. Jourenkova and P. Gustavsson, *Cancer Causes & Control* **1997**, *8*, 444-472.

[25] W. Karcher, *Spectral Atlas of Polycyclic Aromatic Compounds: Including Data on Physico-Chemical Properties, Occurrence and Biological Activity*, Springer Science & Business Media, **2013**, p.

[26] J. L. Gomez-Eyles, T. Sizmur, C. D. Collins and M. E. Hodson, *Environmental Pollution* **2011**, *159*, 616-622.

[27] H. Rubin, *Carcinogenesis* **2001**, *22*, 1903-1930.

[28] W.-C. Tseng, P.-S. Chen and S.-D. Huang, *Talanta* **2014**, *120*, 425-432.

[29] T. Deblonde, C. Cossu-Leguille and P. Hartemann, *International journal of hygiene and environmental health* **2011**, *214*, 442-448.

[30] P. C. von der Ohe, V. Dulio, J. Slobodnik, E. De Deckere, R. Kühne, R.-U. Ebert, A. Ginebreda, W. De Cooman, G. Schüürmann and W. Brack, *Science of the Total Environment* **2011**, *409*, 2064-2077.

[31] R. Rosal, A. Rodríguez, J. A. Perdigón-Melón, A. Petre, E. García-Calvo, M. J. Gómez, A. Agüera and A. R. Fernández-Alba, *Water Research* **2010**, *44*, 578-588.

[32] M. La Farre, S. Pérez, L. Kantiani and D. Barceló, *TrAC Trends in Analytical Chemistry* **2008**, *27*, 991-1007.

[33] S. D. Richardson and T. A. Ternes, *Analytical Chemistry* **2011**, *83*, 4614-4648.

[34] E. Stumm-Zollinger and G. M. Fair, *Journal - Water Pollution Control Federation* **1965**, *37*, 1506-1510.

[35] H.-S. Chang, K.-H. Choo, B. Lee and S.-J. Choi, *Journal of hazardous materials* **2009**, *172*, 1-12.

[36] R. Liu, J. L. Zhou and A. Wilding, *Journal of Chromatography A* **2004**, *1022*, 179-189.

[37] S. Q. Ren, X. Wang, B. J. Tang, G. M. Hu, Z. J. Li, G. N. Chen and J. M. Lin, *Chinese Journal of Analytical Chemistry* **2008**, *36*, 729-734.

[38] X. J. Huang, J. B. Lin, D. X. Yuan and R. Z. Hu, *Journal of Chromatography A* **2009**, *1216*, 3508-3511.

[39] T. Hintemann, C. Schneider, H. F. Schöler and R. J. Schneider, *Water Research* **2006**, *40*, 2287-2294.

[40] Y. Wen, Y. Wang, B. S. Zhou, Y. Xu and Y. Q. Feng, *Chinese Journal of Analytical Chemistry* **2007**, *35*, 681-684.

[41] A. L. Juhasz and R. Naidu, *International biodeterioration & biodegradation* **2000**, *45*, 57-88.

[42] D. Knopp, *Analytical and Bioanalytical Chemistry* **2006**, *385*, 425-427.

[43] N. H. Torres, M. M. Aguiar, L. F. R. Ferreira, J. H. P. Américo, Â. M. Machado, E. B. Cavalcanti and V. L. Tornisielo, *Environmental monitoring and assessment* **2015**, *187*, 1-13.

[44] M. de Fátima Alpendurada, *Journal of Chromatography A* **2000**, *889*, 3-14.

[45] J. R. Dean, *Extraction techniques in analytical sciences*, John Wiley & Sons, **2010**, p.

[46] L. Tavakoli, Y. Yamini, H. Ebrahimzadeh and S. Shariati, *Journal of chromatography A* **2008**, *1196*, 133-138.

[47] L. B. Barber, G. K. Brown and S. D. Zaugg, *ACS Symposium Series* **2000**, pp. 97-123.

[48] C. W. Huck and G. K. Bonn, *Journal of Chromatography A* **2000**, *885*, 51-72.

[49] N. J. Simpson, *Solid-phase extraction: principles, techniques, and applications*, CRC Press, **2000**, p.

[50] S. Mitra, *Sample preparation techniques in analytical chemistry*, John Wiley & Sons, **2004**, p.

[51] H. Sabik, R. Jeannot and B. Rondeau, *Journal of chromatography A* **2000**, *885*, 217-236.

[52] M.-C. Hennion, *Journal of chromatography A* **1999**, *856*, 3-54.

[53] A. Giaquinto, Z. Liu, A. Bach and Y. Kazakevich, *Analytical chemistry* **2008**, *80*, 6358-6364.

[54] H. Minakuchi, K. Nakanishi, N. Soga, N. Ishizuka and N. Tanaka, *Journal of Chromatography A* **1998**, *797*, 121-131.

[55] S. C. Moldoveanu and V. David, *Essentials in modern HPLC separations*, Newnes, **2012**, p.

[56] H. Oberacher and C. G. Huber, *TrAC Trends in Analytical Chemistry* **2002**, *21*, 166-174.

[57] H. Kobayashi, D. Tokuda, J. Ichimaru, T. Ikegami, K. Miyabe and N. Tanaka, *Journal of Chromatography A* **2006**, *1109*, 2-9.

[58] H. Small, *Ion chromatography*, Springer Science & Business Media, **2013**, p.

[59] F. Gritti, W. Piatkowski and G. Guiochon, *Journal of Chromatography A* **2003**, *983*, 51-71.

[60] S. Hjerten, J.-L. Liao and R. Zhang, *Journal of Chromatography A* **1989**, *473*, 273-275.

[61] F. Svec and J. M. Fréchet, *Analytical Chemistry* **1992**, *64*, 820-822.

[62] G. Guiochon, *Journal of Chromatography A* **2007**, *1168*, 101-168.

[63] T. Nema, E. C. Chan and P. C. Ho, *Journal of pharmaceutical and biomedical analysis* **2014**, *87*, 130-141.

[64] F. Svec, *Journal of Chromatography A* **2010**, *1217*, 902-924.

[65] a) E. G. Vlakh and T. B. Tennikova, *Journal of separation science* **2007**, *30*, 2801-2813; b) E. C. Peters, F. Svec and J. M. Frechet, *Advanced Materials* **1999**, *11*, 1169-1181.

[66] S. Xie, F. Svec and J. M. Fréchet, *Chemistry of materials* **1998**, *10*, 4072-4078.

[67] C. Schley, R. Swart and C. G. Huber, *Journal of Chromatography A* **2006**, *1136*, 210-220.

[68] A. Namera, A. Nakamoto, T. Saito and S. Miyazaki, *Journal of separation science* **2011**, *34*, 901-924.

[69] K. Nakanishi and N. Soga, *Journal of non-crystalline solids* **1992**, *139*, 1-13.

[70] B. W. Pack and D. S. Risley, *Journal of Chromatography A* **2005**, *1073*, 269-275.

[71] J. Kirkland, F. Truszkowski and R. Ricker, *Journal of Chromatography A* **2002**, *965*, 25-34.

[72] J. Urban and P. Jandera, *Journal of separation science* **2008**, *31*, 2521-2540.

[73] a) K. Nakanishi, H. Minakuchi, N. Soga and N. Tanaka, *Journal of sol-gel science and technology* **1998**, *13*, 163-169; b) K. Nakanishi, *Journal of Porous Materials* **1997**, *4*, 67-112.

[74] S. M. Fields, *Analytical chemistry* **1996**, *68*, 2709-2712.

[75] M. Niederberger and N. Pinna, *Metal oxide nanoparticles in organic solvents: synthesis, formation, assembly and application*, Springer Science & Business Media, **2009**, p.

[76] A. M Frolova, M. A Chukhlieb, A. V Drobot, A. P Kryshtal, L. P Loginova and A. P Boichenko, *The Open Surface Science Journal* **2009**, *1*.

[77] A.-M. Siouffi, *Journal of Chromatography A* **2003**, *1000*, 801-818.

[78] H. Minakuchi, K. Nakanishi, N. Soga, N. Ishizuka and N. Tanaka, *Analytical chemistry* **1996**, *68*, 3498-3501.

[79] O. Núñez, K. Nakanishi and N. Tanaka, *Journal of Chromatography A* **2008**, *1191*, 231-252.

[80] L. Xu and H. K. Lee, *Journal of Chromatography A* **2008**, *1195*, 78-84.

[81] M. Fardad, *Journal of Materials science* **2000**, *35*, 1835-1841.

[82] D. Wang and G. P. Bierwagen, *Progress in Organic Coatings* **2009**, *64*, 327-338.

[83] T. Coradin, M. Boissiere and J. Livage, *Current medicinal chemistry* **2006**, *13*, 99-108.

[84] K. Sinkó, *Materials* **2010**, *3*, 704-740.

[85] M. Motokawa, H. Kobayashi, N. Ishizuka, H. Minakuchi, K. Nakanishi, H. Jinnai, K. Hosoya, T. Ikegami and N. Tanaka, *Journal of Chromatography A* **2002**, *961*, 53-63.

[86] C. J. Brinker and G. W. Scherer, *Sol-gel science: the physics and chemistry of sol-gel processing*, Academic press, **2013**, p.

[87] S. Shrinivasan, M. C. Breadmore, B. Hosticka, J. P. Landers and P. M. Norris, *Journal of non-crystalline solids* **2004**, *350*, 391-396.

[88] P. D. Fletcher, S. J. Haswell, P. He, S. M. Kelly and A. Mansfield, *Journal of Porous Materials* **2011**, *18*, 501-508.

[89] N. Tanaka, H. Kobayashi, N. Ishizuka, H. Minakuchi, K. Nakanishi, K. Hosoya and T. Ikegami, *Journal of Chromatography A* **2002**, *965*, 35-49.

[90] K. Nakanishi, R. Takahashi, T. Nagakane, K. Kitayama, N. Koheiya, H. Shikata and N. Soga, *Journal of sol-gel science and technology* **2000**, *17*, 191-210.

[91] R. Takahashi, K. Nakanishi and N. Soga, *Faraday Discuss.* **1995**, *101*, 249-263.

[92] C. Milea, C. Bogatu and A. Duta, *Bulletin of TheTransilvania University of Brasov* **2011**, *4*, 53.

[93] a) K. Nakanishi, H. Minakuchi, N. Soga and N. Tanaka, *Journal of Sol-Gel Science and Technology* **1997**, *8*, 547-552; b) N. Ishizuka, H. Minakuchi, K. Nakanishi, K. Hirao and N. Tanaka, *Colloids and Surfaces A: Physicochemical and Engineering Aspects* **2001**, *187*, 273-279; c) G. Puy, R. Roux, C. Demesmay, J.-L. Rocca, J. Iapichella, A. Galarneau and D. Brunel, *Journal of Chromatography A* **2007**, *1160*, 150-159.

[94] D. Smith, G. Scherer and J. Anderson, *Journal of Non-Crystalline Solids* **1995**, *188*, 191-206.

[95] I. Nischang, *Journal of Chromatography A* **2013**, *1287*, 39-58.

[96] F. C. Leinweber and U. Tallarek, *Journal of Chromatography A* **2003**, *1006*, 207-228.

[97] D. Cabooter, K. Broeckhoven, R. Sterken, A. Vanmessen, I. Vandendael, K. Nakanishi, S. Deridder and G. Desmet, *Journal of Chromatography A* **2014**, *1325*, 72-82.

[98] H. Aoki, T. Kubo, T. Ikegami, N. Tanaka, K. Hosoya, D. Tokuda and N. Ishizuka, *Journal of Chromatography A* **2006**, *1119*, 66-79.

[99] I. M. Lazar, L. Li, Y. Yang and B. L. Karger, *Electrophoresis* **2003**, *24*, 3655-3662.

[100] a) M. Kele and G. Guiochon, *Journal of Chromatography A* **2002**, *960*, 19-49; b) C. F. Poole, *Trac Trends in analytical chemistry* **2003**, *22*, 362-373; c) M. GAIKWAD and Y. KHILLARE, *International Journal of Pharma and Bio Sciences* **2015**, *6*, 221-230.

[101] K. Cabrera, G. Wieland, D. Lubda, K. Nakanishi, N. Soga, H. Minakuchi and K. K. Unger, *TrAC Trends in Analytical Chemistry* **1998**, *17*, 50-53.

[102] V. Samanidou, A. Ioannou and I. Papadoyannis, *Journal of Chromatography B* **2004**, *809*, 175-182.

[103] E. Alzahrani and K. Welham, *Analyst* **2012**, *137*, 4751-4759.

[104] C. H. Xie, M. L. Ye, X. G. Jiang, W. H. Jin and H. F. Zou, *Molecular & Cellular Proteomics* **2006**, *5*, 454-461.

[105] J. E. Sandoval and J. J. Pesek, *Analytical Chemistry* **1991**, *63*, 2634-2641.

[106] K. Sing, *Colloids and Surfaces A: Physicochemical and Engineering Aspects* **2001**, *187*, 3-9.

[107] N. Kanellopoulos, *Nanoporous materials: Advanced techniques for characterization, modeling, and processing*, CRC Press, **2011**, p.

[108] P. Jal, S. Patel and B. Mishra, *Talanta* **2004**, *62*, 1005-1028.

[109] J. Goldstein, D. E. Newbury, P. Echlin, D. C. Joy, A. D. Romig Jr, C. E. Lyman, C. Fiori and E. Lifshin, *Scanning electron microscopy and X-ray microanalysis: a text for biologists, materials scientists, and geologists*, Springer Science & Business Media, **2012**, p.

[110] V. Pérez‐Fernández, S. Morante‐Zarcero, D. Pérez‐Quintanilla, M. Á. García, M. L. Marina and I. S. Alonso, *Electrophoresis* **2014**, *35*, 1666-1676.

[111] F. Galán-Cano, V. Bernabé-Zafón, R. Lucena, S. Cárdenas, J. M. Herrero-Martínez, G. Ramis-Ramos and M. Valcárcel, *Journal of Chromatography A* **2011**, *1218*, 1802-1807.

[112] S. Miyazaki, K. Morisato, N. Ishizuka, H. Minakuchi, Y. Shintani, M. Furuno and K. Nakanishi, *Journal of Chromatography A* **2004**, *1043*, 19-25.

[113] J. Sherry, *Chemosphere* **1997**, *34*, 1011-1025.

[114] R. S. Yalow and S. A. Berson, *Nature* **1959**, *184 (Suppl 21)*, 1648-1649.

[115] Ercegovi.Cd, *Advances in Chemistry Series* **1971**, 162-&.

[116] P. J. Delves, S. J. Martin, D. R. Burton and I. M. Roitt, *Roitt's essential immunology*, John Wiley & Sons, **2011**, p.

[117] W. K. Purves, G. H. Orians, D. Sadava and H. C. Heller, *Life: The Science of Biology: Volume III: Plants and Animals*, Macmillan, **2003**, p.

[118] J. P. Gosling, *Immunoassay*, Oxford University Press, **2000**, p.

[119] *Medicine and science in sports and exercise* **2012**, *44*, 1408.

[120] W. Wang, S. Singh, D. L. Zeng, K. King and S. Nema, *Journal of pharmaceutical sciences* **2007**, *96*, 1-26.

[121] G. Köhler and C. Milstein, *nature* **1975**, *256*, 495-497.

[122] L. X. Zhao, L. Sun and X. G. Chu, *Trac-Trends in Analytical Chemistry* **2009**, *28*, 404-415.

[123] U. Dammer, M. Hegner, D. Anselmetti, P. Wagner, M. Dreier, W. Huber and H.-J. Güntherodt, *Biophysical journal* **1996**, *70*, 2437.

[124] A. H. C. Ng, U. Uddayasankar and A. R. Wheeler, *Analytical and Bioanalytical Chemistry* **2010**, *397*, 991-1007.

[125] F. Yu, D. Yao and W. Knoll, *Analytical chemistry* **2003**, *75*, 2610-2617.

[126] H. Akhavan-Tafti, D. G. Binger, J. J. Blackwood, Y. Chen, R. S. Creager, R. de Silva, R. A. Eickholt, J. E. Gaibor, R. S. Handley and K. P. Kapsner, *Journal of the American Chemical Society* **2013**, *135*, 4191-4194.

[127] L. Chen, X. Zhang, G. Zhou, X. Xiang, X. Ji, Z. Zheng, Z. He and H. Wang, *Analytical chemistry* **2012**, *84*, 3200-3207.

[128] D. W. Chan, *Immunoassay: A Practical Guide* **1987**, 1-23.

[129] A. I. Barbosa, A. P. Castanheira, A. D. Edwards and N. M. Reis, *Lab on a Chip* **2014**, *14*, 2918-2928.

[130] A. Bange, H. B. Halsall and W. R. Heineman, *Biosensors and Bioelectronics* **2005**, *20*, 2488-2503.

[131] I. A. Darwish, *Internatonal Jounral Biomedical Science* **2006**, *2*, 217-235.

[132] J. Hou, Y. Yang, B. Gong, S. Li, Z. Ding, S. Wen, S. Li, X. Cheng, L. Cui and Y. Ba, *Zhonghua yu fang yi xue za zhi [Chinese journal of preventive medicine]* **2013**, *47*, 142-146.

[133] M. Pschenitza, R. Hackenberg, R. Niessner and D. Knopp, *Sensors* **2014**, *14*, 9720-9737.

[134] P. J. Wood, *Understanding immunology*, Pearson Education, **2006**, p.

[135] D. R. Shankaran, K. V. Gobi and N. Miura, *Sensors and Actuators B: Chemical* **2007**, *121*, 158-177.

[136] N. Russell, S. Foster, P. Clark, I. Robertson, D. Lewis and P. Irwin, *Australian Veterinary Journal* **2007**, *85*, 487-494.

[137] T. Kreisig, R. Hoffmann and T. Zuchner, *Analytical chemistry* **2011**, *83*, 4281-4287.

[138] Y. H. Dou, S. J. Haswell, J. Greenman and J. Wadhawan, *Electroanalysis* **2012**, *24*, 264-272.

[139] I. Yagi, H. Notsu, T. Kondo, D. A. Tryk and A. Fujishima, *Journal of Electroanalytical Chemistry* **1999**, *473*, 173-178.

[140] X. Pei, B. Zhang, J. Tang, B. Liu, W. Lai and D. Tang, *Analytica Chimica Acta* **2013**, *758*, 1-18.

[141] K. Nakanishi, T. Sakiyama, Y. Kumada, K. Imamura and H. Imanaka, *Current Proteomics* **2008**, *5*, 161-175.

[142] F. Rusmini, Z. Zhong and J. Feijen, *Biomacromolecules* **2007**, *8*, 1775-1789.

[143] J. Křenková and F. Foret, *Electrophoresis* **2004**, *25*, 3550-3563.

[144] N. R. Glass, R. Tjeung, P. Chan, L. Y. Yeo and J. R. Friend, *Biomicrofluidics* **2011**, *5*, 036501.

[145] C. K. Dixit, S. K. Vashist, F. T. O'Neill, B. O'Reilly, B. D. MacCraith and R. O'Kennedy, *Analytical chemistry* **2010**, *82*, 7049-7052.

[146] R. Shi-Qi, W. Xu, T. Bao-Jun, H. Guo-Mao, L. Zhen-Jia, C. Guo-Nan and L. Jin-Ming, *Chinese Journal of Analytical Chemistry* **2008**, *36*, 729-734.

[147] E. W. Young, E. Berthier and D. J. Beebe, *Analytical chemistry* **2012**, *85*, 44-49.

[148] J. M. Goddard and J. Hotchkiss, *Progress in polymer science* **2007**, *32*, 698-725.

[149] Z. Yang, Y. Chevolot, Y. Ataman-Önal, G. Choquet-Kastylevsky, E. Souteyrand and E. Laurenceau, *Sensors and Actuators B: Chemical* **2012**, *175*, 22-28.

[150] L. Brown, T. Koerner, J. H. Horton and R. D. Oleschuk, *Lab on a Chip* **2006**, *6*, 66-73.

[151] G. A. Diaz-Quijada, R. Peytavi, A. Nantel, E. Roy, M. G. Bergeron, M. M. Dumoulin and T. Veres, *Lab on a Chip* **2007**, *7*, 856-862.

[152] J. Raj, G. Herzog, M. Manning, C. Volcke, B. D. MacCraith, S. Ballantyne, M. Thompson and D. W. Arrigan, *Biosensors and Bioelectronics* **2009**, *24*, 2654-2658.

[153] R. Wacker, H. Schröder and C. M. Niemeyer, *Analytical Biochemistry* **2004**, *330*, 281-287.

[154] C. Zheng, J. Wang, Y. Pang, J. Wang, W. Li, Z. Ge and Y. Huang, *Lab on a Chip* **2012**, *12*, 2487-2490.

[155] J. J. Cras, C. A. Rowe-Taitt, D. A. Nivens and F. S. Ligler, *Biosensors and Bioelectronics* **1999**, *14*, 683-688.

[156] Z. Zhang, C. Crozatier, M. Le Berre and Y. Chen, *Microelectronic Engineering* **2005**, *78*, 556-562.

[157] A. Akkoyun and U. Bilitewski, *Biosensors and Bioelectronics* **2002**, *17*, 655-664.

[158] L. Mendoza, R. McQuary, A. Mongan, R. Gangadharan, S. Brignac and M. Eggers, *Biotechniques* **1999**, *27*, 778-779.

[159] L. C. Shriver-Lake, W. B. Gammeter, S. S. Bang and M. Pazirandeh, *Analytica Chimica Acta* **2002**, *470*, 71-78.

[160] G. T. Hermanson, *Bioconjugate techniques*, Academic press, **2013**, p.

[161] H. Zhang and M. E. Meyerhoff, *Analytical chemistry* **2006**, *78*, 609-616.

[162] P. C. Mathias, N. Ganesh and B. T. Cunningham, *Analytical chemistry* **2008**, *80*, 9013-9020.

[163] W. Kusnezow, A. Jacob, A. Walijew, F. Diehl and J. D. Hoheisel, *PROTEOMICS* **2003**, *3*, 254-264.

[164] A. A. Karyakin, G. V. Presnova, M. Y. Rubtsova and A. M. Egorov, *Analytical Chemistry* **2000**, *72*, 3805-3811.

[165] S. K. Vashist, *Diagnostics* **2012**, *2*, 23-33.

[166] Y. Zhang, S. Ge, S. Wang, M. Yan, J. Yu, X. Song and W. Liu, *Analyst* **2012**, *137*, 2176-2182.

[167] J. Yakovleva, R. Davidsson, A. Lobanova, M. Bengtsson, S. Eremin, T. Laurell and J. Emnéus, *Analytical chemistry* **2002**, *74*, 2994-3004.

[168] N.-Y. Lee, Y.-s. Yang, Y.-S. Kim and S.-s. Park, *Bulletin of the Korean Chemical Society* **2006**, *27*, 479-483.

[169] J. P. Gering, L. Quaroni and G. Chumanov, *Journal of Colloid and Interface Science* **2002**, *252*, 50-56.

[170] A. Manz, N. Graber and H. á. Widmer, *Sensors and actuators B: Chemical* **1990**, *1*, 244-248.

[171] X. Zhang and S. Haswell in *Micro-fluidic and lab-on-a-chip technology*, Springer, **2007**, pp. 21-37.

[172] G. M. Whitesides, *Nature* **2006**, *442*, 368-373.

[173] J. R. Anderson, D. T. Chiu, H. Wu, O. Schueller and G. M. Whitesides, *Electrophoresis* **2000**, *21*, 27-40.

[174] S. K. Sia and G. M. Whitesides, *Electrophoresis* **2003**, *24*, 3563-3576.

[175] X. Chen and D.-F. Cui, *Microsystem technologies* **2009**, *15*, 667-676.

[176] T. Rohr, D. F. Ogletree, F. Svec and J. M. Fréchet, *Advanced Functional Materials* **2003**, *13*, 264-270.

[177] B. A. Peeni, M. L. Lee, A. R. Hawkins and A. T. Woolley, *Electrophoresis* **2006**, *27*, 4888-4895.

[178] T. McCreedy, *TrAC Trends in Analytical Chemistry* **2000**, *19*, 396-401.

[179] C. Iliescu, H. Taylor, M. Avram, J. Miao and S. Franssila, *Biomicrofluidics* **2012**, *6*, 016505.

[180] C. W. Price, D. C. Leslie and J. P. Landers, *Lab on a Chip* **2009**, *9*, 2484-2494.

[181] G. S. Fiorini and D. T. Chiu, *BioTechniques* **2005**, *38*, 429-446.

[182] H. Becker and U. Heim, *Sensors and Actuators A: Physical* **2000**, *83*, 130-135.

[183] H. Becker and C. Gärtner, *Electrophoresis* **2000**, *21*, 12-26.

[184] V. Piotter, W. Bauer, T. Benzler and A. Emde, *Microsystem Technologies* **2001**, *7*, 99-102.

[185] J. P. Urbanski, W. Thies, C. Rhodes, S. Amarasinghe and T. Thorsen, *Lab on a Chip* **2006**, *6*, 96-104.

[186] P. Watts and S. J. Haswell, *Current Opinion in Chemical Biology* **2003**, *7*, 380-387.

[187] E. Oosterbroek and A. Van den Berg, *Lab-on-a-chip: miniaturized systems for (bio) chemical analysis and synthesis*, Elsevier, **2003**, p.

[188] S. Haeberle and R. Zengerle, *Lab on a Chip* **2007**, *7*, 1094-1110.

[189] H. A. Stone, A. D. Stroock and A. Ajdari, *Annu. Rev. Fluid Mech.* **2004**, *36*, 381-411.

[190] H.-F. Li and J.-M. Lin, *Analytical and Bioanalytical Chemistry* **2009**, *393*, 555-567.

[191] J. C. Jokerst, J. M. Emory and C. S. Henry, *Analyst* **2012**, *137*, 24-34.

[192] A. G. Crevillén, M. Hervás, M. A. López, M. C. González and A. Escarpa, *Talanta* **2007**, *74*, 342-357.

[193] J. Wang, *TrAC Trends in Analytical Chemistry* **2002**, *21*, 226-232.

[194] J. Tanyanyiwa, E. M. Abad-Villar, M. T. Fernández-Abedul, A. Costa-García, W. Hoffmann, A. E. Guber, D. Herrmann, A. Gerlach, N. Gottschlich and P. C. Hauser, *Analyst* **2003**, *128*, 1019-1022.

[195] R. Daykin and S. Haswell, *Analytica chimica acta* **1995**, *313*, 155-159.

[196] A. D. Beaton, C. L. Cardwell, R. S. Thomas, V. J. Sieben, F.-E. Legiret, E. M. Waugh, P. J. Statham, M. C. Mowlem and H. Morgan, *Environmental Science and Technology* **2012**, *46*, 9548-9556.

[197] B. S. Broyles, S. C. Jacobson and J. M. Ramsey, *Analytical Chemistry* **2003**, *75*, 2761-2767.

[198] E. H. Hansen and M. Miró, *Applied Spectroscopy Reviews* **2008**, *43*, 335-357.

[199] D. A. Skoog and D. M. West, *Principles of instrumental analysis*, Saunders College Philadelphia, **1980**, p.

[200] C. Yi, Q. Zhang, C.-W. Li, J. Yang, J. Zhao and M. Yang, *Analytical and Bioanalytical Chemistry* **2006**, *384*, 1259-1268.

[201] A. M. Garcia-Campana, *Chemiluminescence in Analytical Chemistry*, CRC Press, **2001**, p.

[202] A. Roda, *Chemiluminescence and bioluminescence: past, present and future*, Royal Society of Chemistry, **2011**, p.

[203] D. C. Harris, *Quantitative chemical analysis*, Macmillan, **2010**, p.

[204] W. Baeyens, S. Schulman, A. Calokerinos, Y. Zhao, A. M. G. Campana, K. Nakashima and D. De Keukeleire, *Journal of pharmaceutical and biomedical analysis* **1998**, *17*, 941-953.

[205] A. Garcia-Campana, W. Baeyens, L. Cuadros-Rodriguez, F. Barrero, J. Bosque-Sendra and L. Gamiz-Gracia, *Current Organic Chemistry* **2002**, *6*, 1-20.

[206] H. O. Albrecht, *Zeitschrift für Physikalische Chemie* **1928**, *136*.

[207] C. A. Marquette and L. J. Blum, *Analytical and Bioanalytical Chemistry* **2006**, *385*, 546-554.

[208] R. O'Kennedy, M. Byrne, C. O'Fagain and G. Berns, *Biochemical Education* **1990**, *18*, 136-140.

[209] G. Merényi, J. Lind and T. E. Eriksen, *Journal of Bioluminescence and Chemiluminescence* **1990**, *5*, 53-56.

[210] W. Chen, L. Hong, A.-L. Liu, J.-Q. Liu, X.-H. Lin and X.-H. Xia, *Talanta* **2012**, *99*, 643-648.

[211] *Chemiluminescence and Bioluminescence: Past, Present and Future*, Royal Soc Chemistry, Thomas Graham House, Science Park, Cambridge Cb4 4wf, Cambs, Uk, **2011**, p.

[212] D. R. Crow, *Principles and applications of electrochemistry*, CRC Press, **1994**, p.

[213] G. Liu, J. Wang, J. Kim, M. R. Jan and G. E. Collins, *Analytical Chemistry* **2004**, *76*, 7126-7130.

[214] J. Wang, *Talanta* **2002**, *56*, 223-231.

[215] C. H. Hamann, A. Hamnett and W. Vielstich in *Electrochemistry. 1998, Vol.* Wiley-VCH, **1998**.

[216] D. O. Wipf and R. M. Wightman, *Analytical Chemistry* **1990**, *62*, 98-102.

[217] R. S. Nicholson, *Analytical Chemistry* **1965**, *37*, 1351-1355.

[218] F. Zhao, R. C. Slade and J. R. Varcoe, *Chemical Society Reviews* **2009**, *38*, 1926-1939.

[219] C. Brett, M. O. Brett, A. M. C. M. Brett and A. M. O. Brett, *Electrochemistry: principles, methods, and applications*, **1993**, p.

[220] G. C. Barker and I. L. Jenkins, *Analyst* **1952**, *77*, 685-696.

[221] R. G. Compton and C. E. Banks, *Understanding Voltammetry*, Imperial College Press, **2011**, p.

[222] R. G. Compton, E. Laborda and K. R. Ward, *Understanding voltammetry: simulation of electrode processes*, World Scientific, **2013**, p.

[223] R. L. Pérez and G. M. Escandar, *Environmental Pollution* **2016**, *209*, 114-122.

[224] F. T. Peters, O. H. Drummer and F. Musshoff, *Forensic Science International* **2007**, *165*, 216-224.

[225] J. N. Miller and J. C. Miller, *Statistics and chemometrics for analytical chemistry*, Pearson Education, **2005**, p.

[226] I. Taverniers, M. De Loose and E. Van Bockstaele, *TrAC Trends in Analytical Chemistry* **2004**, *23*, 535-552.

[227] M. Okochi, H. Ohta, T. Tanaka and T. Matsunaga, *Biotechnology and bioengineering* **2005**, *90*, 14-19.

[228] J. Tate and G. Ward, *The Clinical Biochemist Reviews* **2004**, *25*, 105.

[229] M. J. L. de Alda and D. Barcelo, *Journal of Chromatography A* **2001**, *938*, 145-153.

[230] L. Dubois, A. Zdrojewski and J. Monkman, *Microchimica Acta* **1967**, *55*, 834-842.

[231] J. Pan, Y. Huang, W. Shu and J. Cao, *Talanta* **2007**, *71*, 1861-1866.

[232] L.-S. Jang and H.-J. Liu, *Biomedical microdevices* **2009**, *11*, 331-338.

[233] Y.-S. Sohn and Y. K. Lee, *Journal of biomedical optics* **2014**, *19*, 051209-051209.

[234] S.-J. Choi and S.-M. Park, *Advanced Materials* **2000**, *12*, 1547-1549.

[235] F.-Y. Lin, W.-Y. Chen and M. T. Hearn, *Analytical chemistry* **2001**, *73*, 3875-3883.

[236] P. Allongue, C. H. de Villeneuve, G. Cherouvrier, R. Cortes and M.-C. Bernard, *Journal of Electroanalytical Chemistry* **2003**, *550*, 161-174.

[237] H. Alemu, P. Wagana and P. F. Tseki, *Analyst* **2002**, *127*, 129-134.

[238] A. L. Gui, G. Liu, M. Chockalingam, G. Le Saux, E. Luais, J. B. Harper and J. J. Gooding, *Electroanalysis* **2010**, *22*, 1824-1830.

[239] R. Wilson and D. Schiffrin, *Journal of Electroanalytical Chemistry* **1998**, *448*, 125-130.

[240] X. Meng, Y. Li, Y. Zhou, Y. Zhang, L. Yang, B. Qiao, N. Wang, P. Hu, S. Lu and H. Ren, *Analytical biochemistry* **2015**, *473*, 1-6.

Presentation:

Z. O. Oiaidha, and G. M. Greenway," Development of a portable monitoring system for monitoring hormones in the environment, *7th Saudi International Conference* 2014, University of Edinburgh, Edinburgh, UK (2014).

Z. O. Oiaidha, J. D. Wadhawan and G. M. Greenway, "Development portable system device for detecting hormones in the Environment", *Chemistry Colloquium*, University of Hull, UK (2014).

Z. O. Oiaidha, and G. M. Greenway," Development of a portable monitoring system for monitoring hormones in the environment", *The 38th International Symposium on Environmental Analytical Chemistry*, Lausanne, Switzerland (2014).

Z. O. Oiaidha, and G. M. Greenway, "Monitoring of a pollutants in the environment by using a portable system device", *Emerging contaminants in waters and soils*, Royal Society of Chemistry, Sheffield, UK (2015).

Z. O. Oiaidha, N. Pamma and G. M. Greenway, "Development of a portable system device for monitoring toxic organic compounds in environmental sample", *Chemistry Colloquium*, University of Hull, UK (2015).

Z. O. Oiaidha, and G. M. Greenway," Improvement of a portable system device to determination an organic pollutants compounds in the environment", *Euro Analysis*, Bordeaux, France (2015).